

## INFORMATION TO USERS

This manuscript has been reproduced from the microfilm master. UMI films the text directly from the original or copy submitted. Thus, some thesis and dissertation copies are in typewriter face, while others may be from any type of computer printer.

**The quality of this reproduction is dependent upon the quality of the copy submitted.** Broken or indistinct print, colored or poor quality illustrations and photographs, print bleedthrough, substandard margins, and improper alignment can adversely affect reproduction.

In the unlikely event that the author did not send UMI a complete manuscript and there are missing pages, these will be noted. Also, if unauthorized copyright material had to be removed, a note will indicate the deletion.

Oversize materials (e.g., maps, drawings, charts) are reproduced by sectioning the original, beginning at the upper left-hand corner and continuing from left to right in equal sections with small overlaps.

ProQuest Information and Learning  
300 North Zeeb Road, Ann Arbor, MI 48106-1346 USA  
800-521-0600

**UMI<sup>®</sup>**



University of Alberta

Karyopherin-mediated nuclear import: mechanistic insights revealed  
through the characterization of Kap121p and cargoes

by

Deena Marie Leslie



A thesis submitted to the Faculty of Graduate Studies and Research in partial fulfillment of  
the

requirements for the degree of Doctor of Philosophy

Department of Cell Biology

Edmonton, Alberta

Fall 2005



Library and  
Archives Canada

Bibliothèque et  
Archives Canada

Published Heritage  
Branch

Direction du  
Patrimoine de l'édition

0-494-08672-6

395 Wellington Street  
Ottawa ON K1A 0N4  
Canada

395, rue Wellington  
Ottawa ON K1A 0N4  
Canada

*Your file* *Votre référence*

*ISBN:*

*Our file* *Notre référence*

*ISBN:*

**NOTICE:**

The author has granted a non-exclusive license allowing Library and Archives Canada to reproduce, publish, archive, preserve, conserve, communicate to the public by telecommunication or on the Internet, loan, distribute and sell theses worldwide, for commercial or non-commercial purposes, in microform, paper, electronic and/or any other formats.

The author retains copyright ownership and moral rights in this thesis. Neither the thesis nor substantial extracts from it may be printed or otherwise reproduced without the author's permission.

**AVIS:**

L'auteur a accordé une licence non exclusive permettant à la Bibliothèque et Archives Canada de reproduire, publier, archiver, sauvegarder, conserver, transmettre au public par télécommunication ou par l'Internet, prêter, distribuer et vendre des thèses partout dans le monde, à des fins commerciales ou autres, sur support microforme, papier, électronique et/ou autres formats.

L'auteur conserve la propriété du droit d'auteur et des droits moraux qui protègent cette thèse. Ni la thèse ni des extraits substantiels de celle-ci ne doivent être imprimés ou autrement reproduits sans son autorisation.

---

In compliance with the Canadian Privacy Act some supporting forms may have been removed from this thesis.

Conformément à la loi canadienne sur la protection de la vie privée, quelques formulaires secondaires ont été enlevés de cette thèse.

While these forms may be included in the document page count, their removal does not represent any loss of content from the thesis.

Bien que ces formulaires aient inclus dans la pagination, il n'y aura aucun contenu manquant.

  
**Canada**

# University of Alberta

## Library Release Form

**Name of Author:** *Deena Marie Leslie*

**Title of Thesis:** *Karyopherin-mediated nuclear import: mechanistic insights revealed through the characterization of Kap121p and cargoes*

**Degree:** *Doctor of Philosophy*

**Year this Degree Granted:** *2005*

Permission is hereby granted to the University of Alberta Library to reproduce single copies of this thesis and to lend or sell such copies for private, scholarly or scientific research purposes only.

The author reserves all other publication and other rights in association with the copyright in the thesis, and except as herein before provided, neither the thesis nor any substantial portion thereof may be printed or otherwise reproduced in any material form whatsoever without the author's prior written permission.

---

*Signature*

6506 99 A Street  
Grande Prairie, AB,  
Canada  
T8W 2K8

*Sit down before a fact as a little child, be prepared to give up every preconceived notion. Follow humbly wherever and to whatever abysses nature leads, or you shall learn nothing.*

Thomas H. Huxley  
(1825-1895)

# University of Alberta

## Faculty of Graduate Studies and Research

The undersigned certify that they have read, and recommend to the Faculty of Graduate Studies and Research for acceptance, a thesis entitled **Karyopherin-mediated nuclear import: mechanistic insights revealed through the characterization of Kap121p and cargoes** submitted by **Deena Marie Leslie** in partial fulfillment of the requirements for the degree of **Doctor of Philosophy**.

---

John D. Aitchison, Ph.D.

---

Calvin D. Roskelley, Ph.D.

---

Richard A. Rachubinski, Ph.D.

---

Richard W. Wozniak, Ph.D.

---

D. Moira Glerum, Ph.D.

---

Tom C. Hobman, Ph.D.

---

This thesis is dedicated to my parents, Ken and Sheryl Leslie, and my grandparents, George and Anna Sauder, and Mary Leslie and Gordan Pebbles. Without their unconditional love, support and encouragement I would not have had the vision or courage to forge my own path. I would also like to dedicate this thesis to my niece and nephew, Devanna and Kolton Leslie – always ask questions and question answers.

## Abstract

The nuclear envelope divides eukaryotic cells into the nuclear and cytoplasmic compartments. In *Saccharomyces cerevisiae* there are at least 14 soluble nuclear transport receptors, termed karyopherins, which govern the continuous flow of proteins, nucleic acids and small molecules between these two compartments. Knowledge of the cargoes carried by each karyopherin and insight into the mechanisms of transport are fundamental to understanding constitutive and regulated transport, and elucidating how transport impacts normal cellular functions. Yeast Kap121p was studied as a model karyopherin to enhance our understanding of how transport machinery interfaces with its cargoes and how these interactions affect cellular physiology. New *kap121* mutants were generated and proteomics identified 27 candidate Kap121p import cargoes. Two novel phenotypes associated with *kap121* mutants were observed: Defects in mating and pseudohyphal/invasive growth. Ste12p, a transcription factor central to both of these cellular processes, was among the candidate Kap121p cargoes. Characterization of the Kap121p-Ste12p interaction demonstrated that Kap121p interacts directly with Ste12p and that its function is required for Ste12p import. Additionally, mutations within *KAP121* specifically blocked Ste12p-induced transcription and the differentiation pathways it mediates. Together these data clearly demonstrate that seemingly pleiotropic phenotypes associated with *kap* mutants can be directly attributed to the mislocalization of a cargo imported by that  $\beta$ -kap.

Nop1p, Dbp9p and Sof1p were also among the Kap121p-interacting proteins identified and were found to be *bona fide* Kap121p cargoes. Studies characterizing Nop1p import revealed a new class of Kap121p recognized NLS, distinguished by the abundance of arginine and glycine residues (termed rg-NLSs). *KAP104*, a karyopherin that also recognizes rg-NLSs, was shown by several criteria to functionally overlap with Kap121p. Thus, these apparently unrelated transport pathways converge; creating a nuclear transport network that mediates the import of some common cargoes. Additionally, these studies revealed a novel piggy-back mechanism for cargo import; where Nop1p bridges the interaction between Sof1p and Kap121p. These data highlight the complex network of interactions between import karyopherins and their cargoes, and define additional levels of redundancy and flexibility built into nuclear transport pathways to ensure timely cargo delivery.

## Acknowledgements

Completing a Ph.D. is truly a marathon event, and I would not have been able to complete this journey without the aid and support of countless people over the past six years. It is difficult to overstate my gratitude to my supervisor, Dr. John D. Aitchison. With his enthusiasm, encouragement, and great efforts to explain things clearly and simply (and often repeatedly), John has helped to make biology and research fun for me. He has taught me that science rests ultimately upon method. Rather than teaching me the Scientific Method, Steps 1-6, John taught me that the problem we choose, the way we approach it and the way we *communicate* what we find ultimately determines our success as a scientist. I have a long way to go before I master the methods of science, but I owe the direction I'm taking toward this goal to John.

I would like to thank the other members of my supervisory committee, Dr. Richard Rachubinski, Dr. Richard Wozniak and Dr. D. Moira Glerum who have provided me with numerous insights that have guided and challenged my thinking. Finally, I would like to thank Dr. Calvin Roskelley from the University of British Columbia for taking time out from his busy schedule to serve as my external examiner.

I sincerely thank all of the current and former members of the Aitchison lab for their help and friendship over the last six years. I spent a great deal of time at lab and my labmates have become my second family. They are all truly gifted scientists and wonderful friends who have provided me with a fountain of information and have been a source of great emotional support, as well as patient teachers. I am really looking forward to having all of you as colleagues and friends in the years ahead. I would especially like to thank Drs. Jennifer Smith and Marcello Marelli taking the time to read and critique my thesis. You gave me many useful suggestions and I truly appreciate your help.

In science you are never on your own. Therefore, I am grateful for the support of all co-authors who have contributed to my publications and this thesis: Richard W. Wozniak, Michael P. Rout, Wenzhu Zhang, Ben Timney, Brian T. Chait, and Brock Grill.

I wish to thank my family. They have loved, supported and encouraged me to pursue what I enjoyed, even when they didn't understand. Last but not least, I would like to thank Patrick Pedrioli for his unwavering support, patience, and understanding.

# Table of Contents

<b>Chapter 1 - Introduction</b> .....	<b>1</b>
<b>1.1 General introduction to nucleo-cytoplasmic exchange</b> .....	<b>1</b>
<b>1.2 Nucleo-cytoplasmic transport - the stationary phase</b> .....	<b>2</b>
1.2.1 <i>The nuclear envelope</i> .....	2
1.2.2 <i>Structure of the nuclear pore complex (NPC)</i> .....	2
1.2.3 <i>Protein composition of the NPC</i> .....	4
<b>1.3 Passive diffusion versus active nucleo-cytoplasmic transport</b> .....	<b>6</b>
<b>1.4 Nucleo-cytoplasmic transport - the soluble phase</b> .....	<b>9</b>
1.4.1 <i>Signal-mediated transport</i> .....	9
1.4.2 <i><math>\beta</math>-Karyopherins (<math>\beta</math>-Kaps)</i> .....	11
1.4.3 <i>Ran</i> .....	15
<b>1.5 FG nups and the NPC</b> .....	<b>18</b>
1.5.1 <i>FG nups are implicated in passive diffusion</i> .....	19
1.5.2 <i>FG nups are involved in active nucleo-cytoplasmic exchange</i> .....	21
<b>1.6 The mechanism of nucleo-cytoplasmic transport</b> .....	<b>25</b>
<b>1.7 Karyopherin-cargo interactions</b> .....	<b>31</b>
<b>1.8 Regulating nucleo-cytoplasmic exchange</b> .....	<b>34</b>
1.8.1 <i>Post-translational modification of the NPC</i> .....	34
1.8.2 <i>Post-translational modification of cargoes</i> .....	36
<b>1.9 Nucleo-cytoplasmic transport cargoes</b> .....	<b>37</b>
1.9.1 <i>Ste12p</i> .....	37
1.9.2 <i>Nop1p, Sof1p and Dbp9p are required for ribosome biogenesis</i> .....	40
<b>1.10 Goal of this study</b> .....	<b>46</b>
<b>Chapter 2 - Materials and Methods</b> .....	<b>48</b>
<b>2.1 Materials</b> .....	<b>48</b>
2.1.1 <i>Plasmids</i> .....	48
2.1.2 <i>Antibodies</i> .....	48
2.1.3 <i>Oligonucleotides</i> .....	49
2.1.4 <i>Standard buffers and solutions</i> .....	50
<b>2.2 Microorganisms and culture conditions</b> .....	<b>51</b>
2.2.1 <i>Bacterial strains and culture conditions</i> .....	52
2.2.2 <i>S. cerevisiae strains and culture conditions</i> .....	52
2.2.3 <i>Yeast mating</i> .....	55
2.2.4 <i>Sporulation and tetrad dissection</i> .....	55
<b>2.3 Isolation of DNA from microorganisms</b> .....	<b>56</b>
2.3.1 <i>Plasmid DNA isolation from bacteria</i> .....	56
2.3.2 <i>Chromosomal DNA isolation from S. cerevisiae</i> .....	57
2.3.3 <i>Plasmid DNA isolation from S. cerevisiae</i> .....	58
<b>2.4 Standard DNA manipulations</b> .....	<b>58</b>
2.4.1 <i>Amplification of DNA by polymerase chain reaction (PCR)</i> .....	58
2.4.2 <i>Random PCR mutagenesis</i> .....	59
2.4.3 <i>Restriction endonuclease digestion</i> .....	59
2.4.4 <i>Dephosphorylation of 5' ends</i> .....	59
2.4.5 <i>Separation of DNA fragments by agarose gel electrophoresis</i> .....	60
2.4.6 <i>Purification of DNA fragments from agarose gels</i> .....	60
2.4.7 <i>Purification and concentration of DNA from solution</i> .....	61
2.4.8 <i>DNA ligation reactions</i> .....	62
<b>2.5 Introduction of DNA into microorganisms</b> .....	<b>62</b>

2.5.1	Chemical transformation of <i>E. coli</i> .....	63
2.5.2	Electroporation of <i>S. cerevisiae</i> .....	63
<b>2.6</b>	<b>Construction of plasmids for gene expression .....</b>	<b>64</b>
2.6.1	STE12 expression plasmids.....	66
2.6.2	NOP1 expression plasmids.....	68
2.6.3	SOF1 expression plasmids .....	69
2.6.4	DBP9 expression plasmids .....	71
2.6.5	cNLS and PHO4 expression plasmids.....	71
2.6.6	KAP expression plasmids.....	72
<b>2.7</b>	<b>Construction of mutant strains of <i>S. cerevisiae</i>.....</b>	<b>73</b>
2.7.1	Construction of KAP121 null strains .....	73
2.7.2	Construction of kap121 mutant alleles.....	74
2.7.3	Construction of kap95-14 temperature-sensitive strains .....	76
2.7.4	Construction of galactose responsive strains.....	76
2.7.5	Construction of double mutant strains .....	77
<b>2.8</b>	<b>Genomic integration of epitope tags.....</b>	<b>77</b>
2.8.1	Construction of NOP1-A and SOF1-A strains by genomic integration.....	77
2.8.2	Construction of genomically tagged NOP1-GFP and SOF1-GFP strains.....	78
<b>2.9</b>	<b>DNA Sequencing .....</b>	<b>80</b>
<b>2.10</b>	<b>Subcellular fractionation of <i>S. cerevisiae</i>.....</b>	<b>80</b>
2.10.1	Preparation of whole cell lysates for immunoblotting.....	80
2.10.2	Preparation of co-immunopurification whole cell lysates.....	81
2.10.3	Isolation of <i>S. cerevisiae</i> nuclei.....	82
<b>2.11</b>	<b>Overlay Blot Assay.....</b>	<b>83</b>
<b>2.12</b>	<b>Protein analysis and manipulation .....</b>	<b>84</b>
2.12.1	Precipitation co-immunopurification protein eluates .....	84
2.12.2	Determination of protein concentration.....	85
2.12.3	Electrophoretic separation of proteins .....	85
2.12.4	Detection of proteins by gel staining.....	86
2.12.5	Detection of proteins by immunoblotting .....	86
2.12.6	Mass spectrometric protein identification .....	87
<b>2.13</b>	<b>Preparation of Recombinant Proteins.....</b>	<b>87</b>
2.13.1	Synthesis of GST chimeras in <i>E. coli</i> .....	87
2.13.2	Recombinant protein purification and thrombin protease cleavage .....	89
2.13.3	Ran Preparation.....	90
2.13.4	Elution of purified GST chimeras using reduced glutathione.....	91
<b>2.14</b>	<b>Assays.....</b>	<b>91</b>
2.14.1	$\beta$ -galactosidase activity assay.....	91
2.14.2	Pheromone response assay.....	93
2.14.3	Quantitative mating assay.....	93
2.14.4	Invasion assay .....	94
<b>2.15</b>	<b>Co-immunopurifications.....</b>	<b>95</b>
2.15.1	Ex vivo co-immunopurification studies with GST chimeric proteins.....	95
2.15.2	Isolation of Nop1p-pA- and Sof1p-pA-containing Complexes.....	96
<b>2.16</b>	<b>Microscopy.....</b>	<b>97</b>
2.16.1	Analysis of constitutively expressed GFP chimeric proteins .....	97
2.16.2	Visualization of galactose-inducible GFP chimeric proteins.....	97
2.16.3	Temperature shift assays with galactose-inducible GFP chimeric proteins.....	98
2.16.4	Temperature shift assays with genomically tagged GFP gene fusions .....	99
2.16.5	Metabolic poisoning .....	99
<b>2.17</b>	<b>In vitro binding assays .....</b>	<b>100</b>
2.17.1	GST-Ste12p, GST-Dbp9p and GST-Sof1p protein complex formation .....	100
2.17.2	GST-Nop1p protein complex formation .....	100

2.17.3 <i>Ran</i> release.....	101
2.17.4 <i>Sof1p</i> -pA protein complex formation .....	102
2.17.5 <i>In vitro</i> binding challenge assays .....	102
2.17.6 Competition assays .....	103

## **Chapter 3 - Kap121p-mediated nuclear import is required for mating and cellular differentiation in *S. cerevisiae*..... 104**

3.1 Summary.....	104
3.2 <i>KAP121</i> temperature-sensitive mutants .....	105
3.2.1 Generation and characterization of <i>kap121-ts</i> mutants .....	105
3.2.2 Nuclear import of <i>Kap121p</i> cargo in <i>kap121-ts</i> mutants.....	108
3.2.3 <i>kap121-34</i> cells do not respond to pheromone at non-permissive temperatures .....	112
3.3 Identification of <i>Ste12p</i> as a <i>Kap121p</i> -interacting nuclear protein.....	114
3.4 <i>Ste12p</i> is mislocalized in <i>kap121-ts</i> cells .....	119
3.5 Mapping the nuclear localization signal (NLS) of <i>Ste12p</i> .....	122
3.5.1 <i>Kap121p</i> interacts directly with the C terminus of <i>Ste12p</i> .....	122
3.5.2 The <i>Kap121p</i> -interacting domain of <i>Ste12p</i> contains a functional NLS.....	124
3.6 <i>Ran</i> -GTP dissociates the <i>Kap121p</i> - <i>Ste12p</i> complex.....	126
3.7 The C-terminal fragment of <i>Ste12p</i> , amino acid residues 494 to 688, interacts specifically with <i>Kap121p</i> .....	128
3.8 <i>Ste12p</i> induced transcription is severely compromised in <i>kap121-34</i> cells.....	131
3.9 <i>Ste12p</i> -regulated cellular processes are compromised in <i>kap121-34</i> cells .....	134
3.10 Discussion.....	136

## **Chapter 4 - Identification of a unique class of *Kap121p* nuclear import cargoes and a novel nuclear transport network ..... 144**

4.1 Summary.....	144
4.2 <i>Kap121p</i> interacts specifically with a number of ribosome assembly factors .....	145
4.3 <i>Kap121p</i> interacts directly with <i>Nop1p</i> and <i>Dbp9p</i> .....	147
4.4 Development of a regulated <i>in vivo</i> fluorescence-based nuclear import assay.....	149
4.4.1 <i>Nop1p</i> and <i>Dbp9p</i> are tethered in the nucleolus.....	149
4.4.2 Galactose-regulated nuclear import assays demonstrate that <i>Kap121p</i> function is required for <i>Nop1p</i> nuclear import.....	152
4.5 <i>Nop1p</i> contains an N-terminal GAR domain that is similar to rg-NLS sequences.....	155
4.6 Mapping the nuclear localization signal (NLS) of <i>Nop1p</i> .....	156
4.6.1 The RGG-rich N-terminal GAR domain of <i>Nop1p</i> contains a functional NLS.....	156
4.6.2 <i>Kap121p</i> interacts directly with the rg-NLS containing fragment of <i>Nop1p</i> .....	158
4.7 GST- <i>Nop1p</i> (aa1-90)- <i>Kap121p</i> protein complexes are insensitive to <i>RanGTP</i> .....	160
4.8 <i>Kap121p</i> is not able to bind lysine-rich NLS and rg-NLS containing cargoes simultaneously.....	164
4.9 <i>Kap104p</i> mediates <i>Nop1p</i> nuclear import in the absence of <i>Kap121p</i> function.....	165
4.9.1 <i>KAP104</i> and <i>KAP121</i> are synthetically lethal.....	167
4.9.2 <i>Kap104p</i> imports <i>Nop1p</i> in the absence of functional <i>Kap121p</i> .....	169
4.10 <i>Kap121p</i> , and small amounts of <i>Kap104p</i> , co-immunopurify with <i>Nop1p</i> .....	169
4.11 <i>Kap104p</i> interacts directly with <i>Nop1p</i> .....	177
4.12 Discussion.....	175

## **Chapter 5 - Characterization of novel molecular mechanisms of *Kap121p*-mediated nuclear import ..... 183**

5.1 Introduction.....	183
5.2 <i>Kap121p</i> is required for the nuclear import of <i>Sof1p</i> .....	185
5.3 Both <i>Kap121p</i> and <i>Nop1p</i> co-immunopurify with, and interact directly with <i>Sof1p</i> ..	187

5.4 Sof1p is imported by Kap121p using a lysine-rich NLS.....	189
5.4.1 Kap121p binds amino acid residues 381 to 489 of Sof1p .....	189
5.4.2 Amino acids 381 to 489 of Sof1p contain a functional, lysine-rich NLS.....	191
5.5 Tertiary import complexes containing Kap121p, Nop1p and Sof1p assemble in vitro .....	191
5.6 Sof1p can be imported by a piggy-back transport mechanism .....	193
5.7 Discussion.....	197
<b>Chapter 6 - Perspectives .....</b>	<b>201</b>
6.1 Summary.....	201
6.2 Perspectives on the regulation of nucleo-cytoplasmic transport.....	202
6.3 Perspectives on nucleo-cytoplasmic transport and cell physiology .....	205
6.4 Perspectives on nucleo-cytoplasmic transport networks .....	207
6.5 Perspectives on kap-cargo interactions .....	211
6.6 Perspectives on alternative mechanisms of nucleo-cytoplasmic transport.....	214
6.7 Perspectives on cargo delivery.....	217
<b>References .....</b>	<b>220</b>

## List of Tables

Table 1-1 Nucleo-cytoplasmic transport signal sequences.....	10
Table 1-2 NLSs recognized by Kap121p .....	10
Table 2-1 Plasmids .....	48
Table 2-2 Antibodies .....	48
Table 2-3 Oligonucleotides .....	49
Table 2-4 Buffers.....	51
Table 2-5 <i>E. coli</i> strains .....	52
Table 2-6 Bacterial culture media.....	52
Table 2-7 <i>S. cerevisiae</i> strains.....	52
Table 2-8 Yeast culture media .....	54
Table 2.9 Plasmids constructed in this study .....	64
Table 3-1 <i>kap121-34</i> nucleotide and amino acid substitutions .....	111
Table 3-2 Kap121p-interacting nuclear proteins.....	116
Table 4-1 Potential Kap121p-recognized NLSs.....	155

## List of Figures

Figure 1.2.1: Structure of the nuclear pore complex.....	3
Figure 1.2.2: Plot of the position of nucleoporins within the NPC .....	5
Figure 1.4.2: The $\beta$ -karyopherin protein family.....	13
Figure 1.4.3: The RanGTP gradient and nuclear transport.....	16
Figure 1.5.2: Nup subcomplexes in both <i>S. cerevisiae</i> and vertebrate NPCs.....	24
Figure 1.6.1: The “Virtual Gate”: A model describing the mechanism of nucleo-cytoplasmic transport.....	29
Figure 1.9.1: The <i>S. cerevisiae</i> pheromone response and filamentation/invasion response MAPK pathways .....	39
Figure 1.9.2: Pre-rRNA processing pathways in <i>S. cerevisiae</i> .....	44
Figure 3.2.1: <i>kap121-ts</i> mutants.....	107
Figure 3.2.2: Nuclear import of Kap121p cargo in the <i>kap121-ts</i> strains .....	110
Figure 3.2.3: <i>kap121-34</i> cells are unable to respond to a-factor at non-permissive temperatures.....	113
Figure 3.3.1: Kap121p interacts with numerous nuclear proteins.....	116
Figure 3.4.1: Ste12p mislocalizes in <i>kap121-ts</i> at non-permissive temperatures .....	121
Figure 3.5.1: Kap121p interacts directly with the C-terminal portion of Ste12p.....	123
Figure 3.5.2: Amino acid residues 494 to 688 of Ste12p contain a functional Kap121p NLS .....	125
Figure 3.6.1: Ran-GTP dissociates Kap121p-Ste12p(aa494-688) protein complexes.....	127
Figure 3.7.1: The C-terminus of Ste12p specifically enriches Kap121-pA from whole cell lysates.....	130
Figure 3.8.1: Ste12p-induced transcription is compromised in <i>kap121-34</i> cells.....	133
Figure 3.9.1: <i>kap121-34</i> cells are unable to mate or grow invasively.....	135
Figure 4.2.1: Kap121p interacts with numerous nuclear proteins.....	146
Figure 4.3.1: Kap121p interacts directly with Nop1p and Dbp9p.....	148
Figure 4.4.1: Constitutively expressed Nop1p-GFP and Dbp9p-GFP do not mislocalized in <i>kap121-34</i> cells at the restrictive temperature.....	150
Figure 4.4.2: Nop1p does not equilibrate between the nucleus and cytoplasm upon metabolic poisoning .....	153
Figure 4.4.3: Nop1p and Dbp9p mislocalize in <i>kap121-34</i> cells.....	154
Figure 4.5.1: A schematic diagram of Nop1p.....	157
Figure 4.6.1: The RGG-rich GAR domain of Nop1p contains a functional NLS.....	159
Figure 4.6.2: Kap121p interacts directly with the RGG-rich GAR domain of Nop1p.....	161
Figure 4.7.1: RanGTP does not dissociate Kap121p-Nop1p import complexes.....	163

Figure 4.8.1: <b>Kap121p does not interact with cargoes containing lysine-rich NLSs and rg-NLSs concurrently</b> .....	166
Figure 4.9.1: <b><i>kap121-34</i> and <math>\Delta</math><i>kap104</i> are synthetically lethal in combination</b> .....	168
Figure 4.9.2: <b>Overexpression of <i>KAP104</i> rescues the mislocalization of <i>GAL1-Nop1p-GFP</i> in <i>kap121-34</i> cells</b> .....	170
Figure 4.10.1: <b>Kap121p and Kap104p co-immunopurify with Nop1p</b> .....	173
Figure 4.11.1: <b>Kap104p binds directly to Nop1p through its N-terminal, RGG-rich Gar domain</b> .....	174
Figure 4.11.2: <b>Nop1p is correctly localized to the nucleolus in <i>kap104-16</i> cells</b> .....	176
Figure 5.1.1: <b>A schematic diagram of Sof1p</b> .....	184
Figure 5.2.1: <b>Kap121p imports Sof1p</b> .....	186
Figure 5.3.1: <b>Sof1p interacts directly with Kap121p and Nop1p</b> .....	188
Figure 5.4.1: <b>Kap121p interacts directly with amino acids 381-489 of Sof1p</b> .....	190
Figure 5.4.2: <b>Amino acids 381-489 of Sof1p contain a functional NLS</b> .....	192
Figure 5.5.1: <b>Heterotrimeric protein complexes containing Sof1p, Kap121p and Nop1p assemble <i>in vitro</i></b> .....	194
Figure 5.6.1: <b>Sof1p can be imported by piggy-back</b> .....	196

## List of Abbreviations and Symbols

5-FOA .....	5'-fluoroorotic acid
$\alpha$ .....	alpha
ATP .....	adenosine triphosphate
$\beta$ .....	beta
bp .....	base pair
dATP .....	2'-deoxyadenosine 5'-triphosphate
BSA .....	bovine serum albumin
cNLS .....	'classical' nuclear localization signal
dCTP .....	2'-deoxycytidine 5'-triphosphate
D .....	Dalton
dGTP .....	2'-deoxyguanosine 5'-triphosphate
DNA .....	deoxyribonucleic acid
dTTP .....	2'-deoxythymidine 5'-triphosphate
DTT .....	dithiothreitol
ECL .....	enhanced chemoluminescence
ER .....	endoplasmic reticulum
F .....	farad
g .....	gram
<i>g</i> .....	gravitational force
GDP .....	guanosine diphosphate
GFP .....	green fluorescent protein
GST .....	glutathione-S-transferase
GTP .....	guanosine triphosphate
GTPase .....	guanosine triphosphatase
hr .....	hour
HA .....	hydroxyapatite
hnRNP .....	heterogeneous nuclear RNP
HPLC .....	high-pressure liquid chromatography
IgG .....	immunoglobulin G
IPTG .....	isopropyl- $\beta$ -D-thiogalactopyranoside
IVN <sup>+</sup> .....	invasion competent
k .....	kilo
kap .....	karyopherin

m	.....	milli
min	.....	minute
M	.....	moles per litre
mRNA	.....	messenger RNA
n	.....	nano
ncNLS	.....	"non-classical" nuclear localization signal
NE	.....	nuclear envelope
NES	.....	nuclear export signal
NLS	.....	nuclear localization signal
NPC	.....	nuclear pore complex
nup	.....	nucleoporin
O.D.	.....	optical density
ONPG	.....	o-nitrophenyl $\beta$ -D galactopyranoside
ORF	.....	open reading frame
p	.....	pico
PAGE	.....	polyacrylamide gel electrophoresis
PCR	.....	polymerase chain reaction
pH	.....	$-\log[H^+]$
PTM	.....	post-translational modification
RNA	.....	ribonucleic acid
RP	.....	reverse-phase
rRNA	.....	ribosomal RNA
RNP	.....	ribonucleoprotein
SDS	.....	sodium dodecyl sulphate
snoRNA	.....	small nucleolar RNA
snoRNP	.....	small nucleolar RNP
TCA	.....	trichloroacetic acid
ts	.....	temperature-sensitive
U	.....	units of enzyme
UV	.....	ultraviolet light
V	.....	Volts
$\Omega$	.....	ohm
$\mu$	.....	micro
$\psi$	.....	pounds per square inch

## **Chapter 1 – Introduction**

### **1.1 General introduction to nucleo-cytoplasmic exchange**

A characteristic feature of eukaryotic cells is the compartmentalization of cellular processes into distinct, membrane bound environments, termed organelles. Organelles house specialized functions, provide optimal intracellular environments for biochemical reactions, and act as containers that confine potentially harmful reaction byproducts and separate incompatible cellular components from one another. The largest organelle in eukaryotic cells is typically the nucleus, which is contained by the nuclear envelope (NE). The NE physically separates nuclear DNA from the cytoplasm, thereby segregating the sites of gene transcription and ribosome biogenesis from the site of protein synthesis. This barrier provides the cell the ability to strictly coordinate key cellular processes like cell cycle progression, cellular differentiation and gene expression. However, regulating cellular functions in this manner demands that an astonishing number of proteins and RNAs be transported between these two compartments, in a regulated fashion. As such, eukaryotic cell survival depends on bi-directional nucleo-cytoplasmic transport pathways. Operationally, nuclear transport pathways can be divided into two phases: A stationary phase, comprised of the NE and the macromolecular protein complexes called nuclear pore complexes (or NPCs) that are embedded in it; and a soluble (or mobile) phase, which includes nuclear transport receptors, their regulators and the cargoes they translocate.

## **1.2 Nucleo-cytoplasmic transport – the stationary phase**

**1.2.1 The nuclear envelope** – The nuclear envelope is composed of two continuous, topologically distinct phospholipid bilayer membranes, the inner nuclear membrane and the outer nuclear membrane (Figure 1.2.1; (Alberts *et al.*, 2002; Lodish *et al.*, 1999)). The inner nuclear membrane defines the nucleus and in vertebrate cells, but not in yeast cells, is lined with a meshwork of intermediate filaments (termed the nuclear lamina) that is thought to provide the structural support for the NE (Alberts *et al.*, 2002; Lodish *et al.*, 1999). The outer nuclear membrane interfaces with the cytoplasm, is continuous with the endoplasmic reticulum (ER) and, like the membrane of the ER, is studded with ribosomes. The inner and outer nuclear membranes are joined at numerous sites forming circular pores, or aqueous channels, that connect the nucleoplasm and cytoplasm. A third biochemically distinct membrane domain, the pore membrane domain, lines these pores. It is occupied by integral, and peripherally associating proteins that form large octagonally symmetric protein complexes, called nuclear pore complexes (or NPCs), through which all nucleo-cytoplasmic exchange occurs. As such, the NE functions as a selectively permeable barrier between these two cellular environments.

**1.2.2 Structure of the nuclear pore complex (NPC)** – Nuclear pore complexes are evolutionarily conserved ~45-60 MDa macromolecular protein assemblies ~100 nm in diameter (Figure 1.2.1; (Cronshaw *et al.*, 2002; Rout *et al.*, 2000)). NPCs are composed of eight radial spokes and 4 coaxial rings that

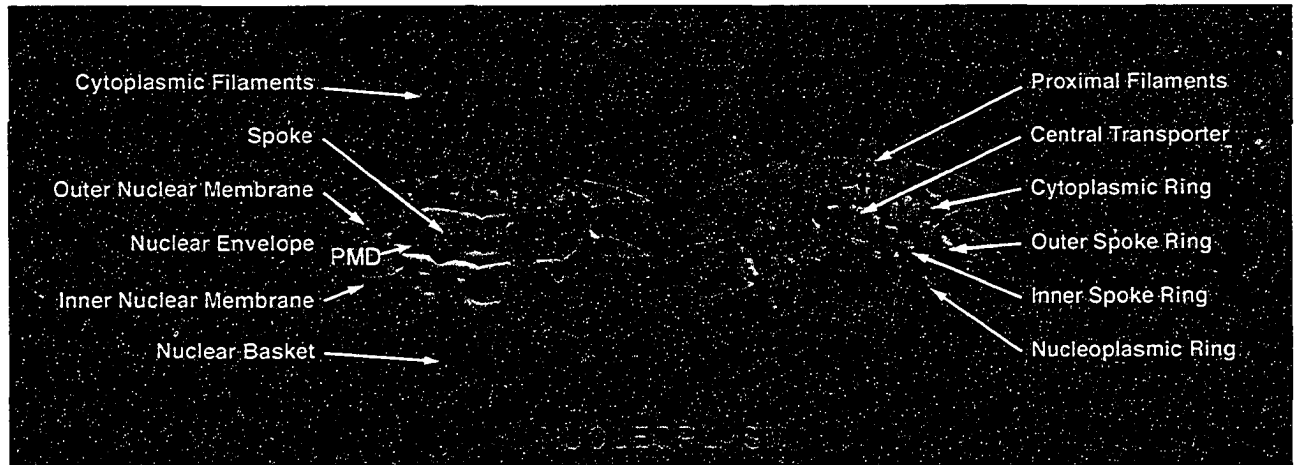


Figure 1.2.1: **Structure of the nuclear pore complex.** Each NPC is a large proteinaceous assembly embedded in the pore membrane domain (PMD) of the nuclear envelope, where the inner and outer nuclear membranes fuse. The NPC contains eight spokes, projecting radially from the wall of the pore membrane and surrounding a central tube called the central transporter. Each spoke is composed of numerous struts and attached to its neighbors by four coaxial rings: an outer spoke-ring in the lumen of the NE adjacent to the pore membrane, a nucleoplasmic ring, a cytoplasmic ring, and an inner spoke-ring surrounding the central transporter (also referred to as the central tube or central channel). A considerable portion of each spoke traverses the pore membrane and resides in the NE lumen. Together these structures comprise the central core. Peripheral elements project from this core toward the nucleoplasm and cytoplasm. These include: numerous proximal filaments on both faces of the cylindrical central core, whose presence (though not directly imaged) is inferred from the large number of symmetrically disposed filamentous nucleoporins; eight cytoplasmic filaments, attached at the cytoplasmic ring; and nuclear filaments originating at the nuclear ring and conjoining distally to form the nuclear basket, which connects with elements of the nucleoskeleton (not shown). Figure adapted from (Rout and Aitchison, 2001).

connect the spokes to each other. These spoke-ring complexes form a central tube or channel (also referred to as the central transporter) that is approximately 30 nm in diameter through which the nucleoplasm and cytoplasm are connected (Rout *et al.*, 2003). The outer spoke ring is embedded in the lumen of the NE, while the cytoplasmic ring, nucleoplasmic ring and inner spoke ring surround the central channel of the NPC. A large portion of each spoke pierces the pore membrane domain and resides within the lumen of the NE. Together, these structures form the cylindrical core of the NPC. This core structure anchors peripheral elements that project towards the cytoplasm and nucleoplasm (Figure 1.2.1). Attached to the cytoplasmic ring are eight fibrils, termed the cytoplasmic filaments that extend into the cytoplasm. Similarly, eight fibrils protrude from the nucleoplasmic ring into the nucleus. But in this instance, they are tethered at their ends by a terminal ring, forming a cage-like structure called the nuclear basket. Based on the high concentration of symmetrically positioned filamentous nucleoporins (see Sections 1.5 and 1.6), numerous proximal filaments are thought to emanate from both faces of the central tube, although they have not been visualized directly (reviewed in Bednenko *et al.*, 2003; Rout and Aitchison, 2001; Rout *et al.*, 2003; Suntharalingam and Wentz, 2003).

**1.2.3 Protein composition of the NPC** – Proteomic studies have revealed that *S. cerevisiae* and mammalian NPCs are compositionally similar and made up of ~30 distinct proteins, termed nucleoporins (or nups) (Figure 1.2.2; (Cronshaw *et al.*, 2002; Rout *et al.*, 2000)). Consistent with the 8-fold symmetry,

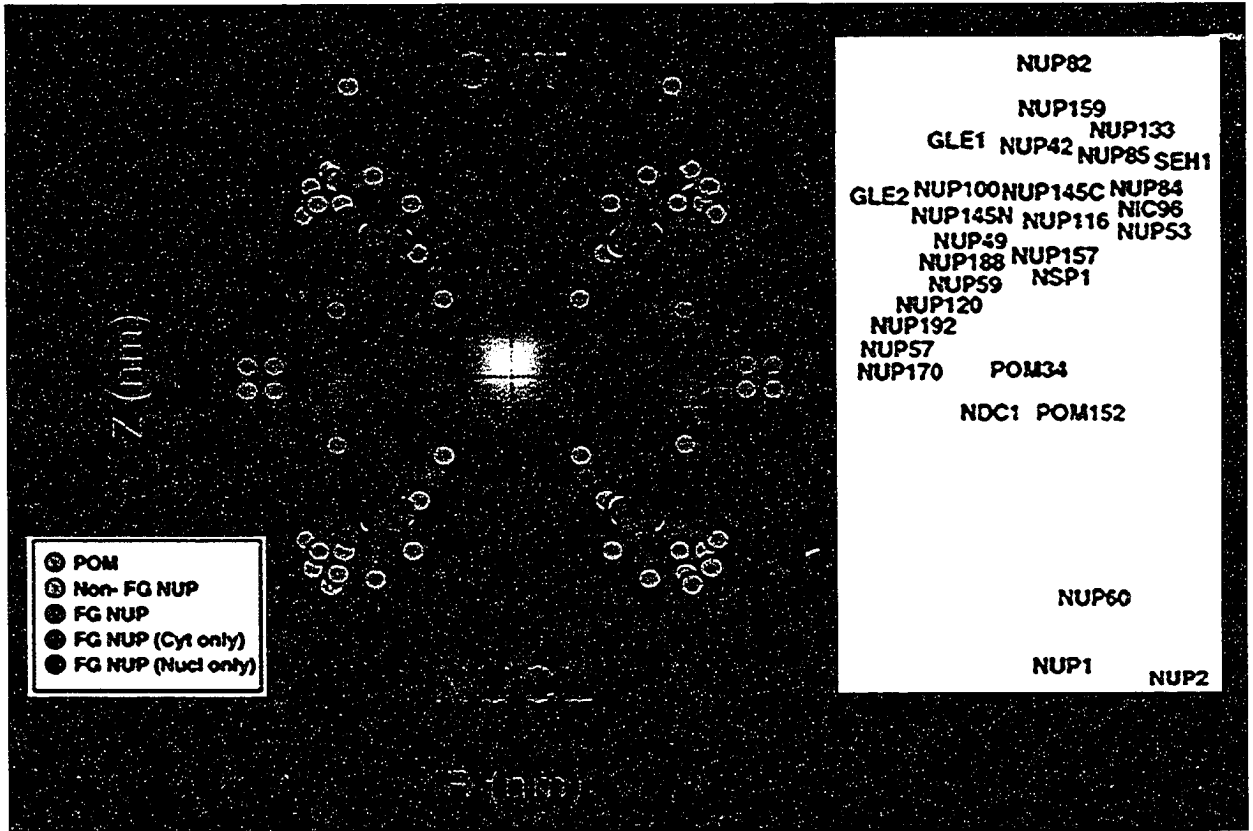


Figure 1.2.2: Plot of the position of nucleoporins within the NPC. Positions are overlaid on a protein density map generated by cryoEM. Green = FG nups that are found on both sides of the NPC; Blue = FG nups asymmetrically localized to the nucleoplasmic face of the NPC; Red = FG nups asymmetrically localized to the cytoplasmic face of the NPC; Grey = non-FG or structural nups; Purple = poms. Figure adapted from (Rout *et al.*, 2000; Rout and Wentz, 1994).

each NPC is predicted to contain 8-48 copies of each nup. The components of the NPC can be divided into three classes (reviewed in Bednenko *et al.*, 2003; Fried and Kutay, 2003; Rout *et al.*, 2003; Suntharalingam and Wente, 2003). The first group of proteins, termed the pore membrane proteins (or poms), contain transmembrane domains that anchor the NPC to the NE. The second class of nups, often referred to as non-FG nups (see below), is believed to function mainly as structural proteins. These nups are thought to provide the positioning scaffold for the third class of nucleoporins (Shulga and Goldfarb, 2003). This third type of nups contains degenerate repeats of the dipeptide phenylalanine-glycine (FG) that are often part of larger FXFG and GLFG repeats (where X represents any amino acid residue and L is leucine). They are collectively termed FG nups. FG repeats are usually clustered and are often separated by hydrophobic spacers that range in length from 5 to 30 amino acid residues (Bednenko *et al.*, 2003). FG nups are thought to line the central channel of the NPC and provide binding sites for soluble nuclear transport factors (reviewed in Bednenko *et al.*, 2003; Fahrenkrog and Aebi, 2003; Rout *et al.*, 2003; Suntharalingam and Wente, 2003).

### **1.3 Passive diffusion versus active nucleo-cytoplasmic transport**

The NPCs, embedded in the NE, function as highly selective, versatile gates that simultaneously restrict the nucleo-cytoplasmic exchange of macromolecules and permit the passive diffusion of small molecules. The segregation of cellular processes to confined organelles has provided eukaryotic

cells with numerous regulatory controls and survival advantages. However, in order for the cell to remain viable the concentrations of many small molecules must be maintained at equilibrium in various compartments of the cell. These equilibriums are maintained by passive diffusion. In theory, NPCs provide little obstruction to the free exchange of any small molecule, like water, ions, metabolites and macromolecules smaller than ~40 KDa (Fried and Kutay, 2003; Rout *et al.*, 2003; Suntharalingam and Wente, 2003), between the nucleus and cytoplasm. In the “virtual gate” model proposed to explain the mechanism of nuclear transport, Rout *et al.* (2000) describe the passive diffusion of these molecules and the factors that constrain movement, in terms of the entropy of the molecule in transit (Rout *et al.*, 2000). In the model, the entropy of a macromolecule is described as the numerous ways the energetic motions of that molecule can be distributed ((Rout *et al.*, 2000); (reviewed in Rout *et al.*, 2003)). In theory, soluble molecules in the cytoplasm move about in a number of ways and have many possible destinations; therefore, their entropy is high. When these molecules enter the restricted space of the central tube of the NPC, the number of possible movements they can make, and remain within the channel, decrease and, consequently, their entropy decreases. Therefore, a molecule freely diffusing between the nucleus and cytoplasm moves from a state of high entropy to one of low entropy, this change is referred to as the “entropic price” (Rout *et al.*, 2003; Rout *et al.*, 2000). If a molecule can afford to pay this “entropic price” – be able to enter the narrow channel of the NPC, withstand its

constraints and remain mobile enough to successfully move from one side to the other – it can traverse the NPC without assistance. But entropy costs increase as the size of the molecule increases. Therefore, according to this model the permeability of the NPC is considered to be inversely proportional to the size of the molecule in transit (Rout *et al.*, 2003).

Active transport mechanisms are, therefore, required to facilitate the translocation of larger molecules, whose diameters can reach 39 nm (Suntharalingam and Wentz, 2003), across the NPC. Moreover, active transport mechanisms also direct the rapid accumulation of many cellular factors in specific organelles, often against significant concentration gradients. These transport mechanisms are frequently used to strictly control when and where a given cellular process or biochemical reaction takes place. Accordingly, cell growth requires macromolecules like transcription factors, ribosomal proteins, *trans*-acting ribosome assembly factors and histones to constitutively, or periodically, concentrate in the nucleus. Concurrently, numerous proteins and ribonucleoprotein particles must also accumulate in the cytoplasm. These facilitated nuclear transport mechanisms are saturable (Goldfarb *et al.*, 1986; Zasloff, 1983), signal-mediated (Dingwall and Laskey, 1991; Fischer *et al.*, 1995; Gerace, 1995) and energy-dependent (Newmeyer *et al.*, 1986; Zasloff, 1983). The translocation process itself is not directly linked to NTP hydrolysis. Instead, the energy is thought to come from a potential energy gradient across the NPC established by the maintenance of distinct pools of GDP- and GTP-bound forms

of the small GTPase Ran (see Section 1.4.3; (Bednenko *et al.*, 2003; Cole and Hammell, 1998; Moore, 1998)). Amazingly, active nucleo-cytoplasmic transport has been estimated to facilitate ~800 individual translocation events of a 100 KDa protein through a single NPC per second (Fried and Kutay, 2003).

## **1.4 Nucleo-cytoplasmic transport – the soluble phase**

**1.4.1 Signal-mediated transport** – The movement of most molecules through the NPC is a highly specific process that is dependent on the recognition of *cis*-acting signal sequences present within these cargo molecules. These targeting signals are recognized by intermediary receptors, or carriers, that interact specifically with the NPC. The soluble transport receptors that recognize these signals are termed karyopherins (or kaps); from the Greek words “karyo” and “pherin”, which are respectively defined as “nut/kernel/nucleus” and “to carry or transfer” (Radu *et al.*, 1995) (they are also known as importins, transportins and exportins) (reviewed in Fried and Kutay, 2003; Mosammaparast and Pemberton, 2004)). Kaps traverse the NPC in association with their substrates, which appear to have no affinity for the NPC in their absence (Mattaj and Englmeier, 1998). Proteins are marked for nuclear import and nuclear export by the presence of nuclear localization signals (NLSs) (Dingwall and Laskey, 1991) or nuclear export signals (NESs) (Fischer *et al.*, 1995; Gerace, 1995), respectively. Several different types of NLSs and NESs have been identified, most of which do not fit a well-defined consensus sequence, but nevertheless are generally recognized by specific kaps (Table 1-1). Moreover, the NLS amino acid residue sequences

present in cargoes that are imported by the same nuclear transport receptor can also vary dramatically (Table 1-2). NLSs and NESs are typically, but not always, short peptides that are located anywhere within the amino acid residue sequence of a cargo and are not cleaved upon translocation. Amino acid residue charge and hydrophobicity appear to be most important; however length and spacing of key residues have also been shown to contribute to signal recognition and subsequent transport (reviewed in Fried and Kutay, 2003; Talcott and Moore, 1999).

**Table 1-1 Nucleo-cytoplasmic transport signal sequences**

Transport signal	Example substrates	Sequence #	Transport receptor(s)	References
Classical mono-partite NLS	SV40 T antigen	PKKKRKVE	Imp $\beta$ /Imp $\alpha$	((Kalderon <i>et al.</i> , 1984a)
Classical bi-partite NLS	nucleoplasmin	KRPAATKKAGQAKKKKLD	Imp $\beta$ /Imp $\alpha$	(Dingwall <i>et al.</i> , 1982; Robbins <i>et al.</i> , 1991)
M9 domain	hnRNPA1	YNDFGNYNQSSNFGPMKGGN FGGRSSGPY	transportin	(Siomi and Dreyfuss, 1995)
BIB domain	rpL23a	VHSHKKKKIRTSPTFRRPKTLRLR RQPKYPRKSAPRRNKLDHY	transportin, Imp5, Imp7, Imp $\beta$	(Jakel and Gorlich, 1998)
RS domain	SR proteins	phosphorylated RS domains	transportin SR2	(Lai <i>et al.</i> , 2001)
Leucine-rich NES	HIV Rev, PKI	consensus: L-X2-3-(L,I,M,F,M)-X2-3- L-X-(L,I,V)	CRM1	(Bogerd <i>et al.</i> , 1999; Bogerd <i>et al.</i> , 1996)
rg-NLS	Nab2p	VDNSQRFTQRGGGAVGKNRRG GRGGNRGGRNNNSTRFNPLAKA LGMAGES	Kap104p	Lee and Aitchison, 1999

Examples of the amino acid residue sequences of common classes of nuclear transport sequences along with the nuclear transport receptor(s) that recognize(s) these signals are presented here. These amino acid residue sequences are written using the standard single letter abbreviations. This table is adapted from Fried and Kutay, 2003.

**Table 1-2 NLSs recognized by Kap121p**

Cargo	Amino Acid Residues	Sequence	Reference
Pho4p	140-166	SANKVTKNKSNSPYLNKRRGKPGPDS	Kaffman <i>et al.</i> , 1998
Spo12p	76-143	KKSTSNLKSSHTTSLNPKKTMFKRDLLKQDPKRKLQLQQ RFASPTDRLVSPCSLKLNEHKVKMFGKKK	Chaves and Blobel, 2001

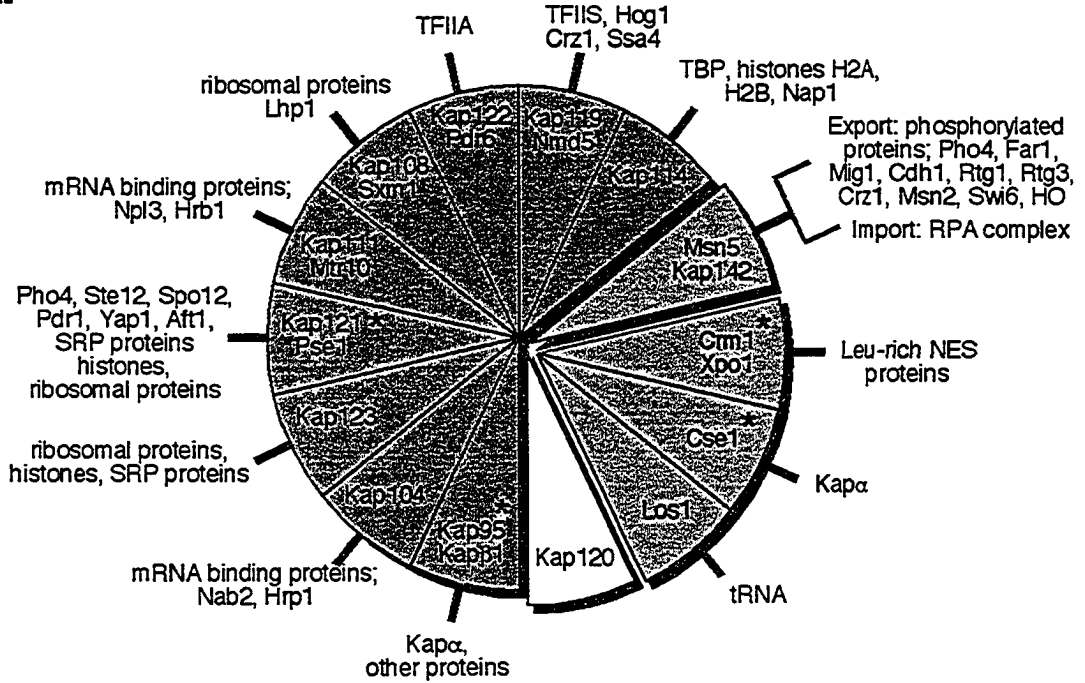
Pdr1p	729-769	WTD MNKILLDFDNDYSVYRSFAHYSISCIILVSQAFSVAEF	Delahodde <i>et al.</i> , 2001
Rpl25p	1-62	MAPSAKATAAKKAVVKG TNGKKALKVRTSATFRLPKTLK LARAPKYASKAVPHYNR LDSYKV	Rout <i>et al.</i> , 1997
Yap1p	5-59	TAKRSLDVVSPGSLAEFEGSKSRHDEIENEHRRTGTRDGE DSEQPKKKGSKTSKK	Isoyama <i>et al.</i> , 2001
histone H2A	1-46	MSGGKGGKAGSAAKASQSRSAKAGLTFFVGRVHLLRRG NYAQRIG	Mosammaparast <i>et al.</i> , 2001
histone H2B	1-52	MSAKAEKKPASKAPA EKKPAAKKTSTSTDGKKRSKARKE TYSSYIYKVLKQT	Mosammaparast <i>et al.</i> , 2001
histone H3	1-28	MARTKQTARKSTGGKAPRKQLASKAARK	Mosammaparast <i>et al.</i> , 2002
histone H4	1-42	MSGRGKGGKGLGKGGAKRHRKILRDNIQGITKPAIRRLA RRGG	Mosammaparast <i>et al.</i> , 2002
Aft1p	198-226 and 332-365	TSSIKPKKKRCVSRFN NCPFRVRATYSL and SKRPLPSVNNTGSINT NNVRRKPKSQCKNKD TLL	Ueta <i>et al.</i> , 2003
Ste12p	494-688	NNMLYPQTATSWNVLP PQA MQPAPTYVGRPYTPNYRSTP GSAMFPYMQSSNSMQWN TAVSPYSSRAPSTTAKNYPPSTF YSQNINQYPRRRTVGM KSSQGNVPTGNKQSVGKSAKISK PLHIKTSAYQKQYKIN LETKARPSAGDEDSAHPDKNKEIS MPTPDSNTLVVQSEEG GAHSLEVD TNRRSDKNLPDAT	Chapter 3
Nop1p	1-90	MSFRPGSRGGSRGGS RGGFGGRGGSRGGARGGSRGGF G GRGGSRGGARGGSRG GFGGRGGSRGGARGGSRGGRRG AAGGARGGAKVVIEP	Chapter 4
Sof1p	381-489	ERSNVKTTREKNKLEY DEKLKERFRHMPEIKRISRHRHVP QVIKKAQEIKNIELSSI KRREANERTRKDMPIYISERKKQI VGTVHKYEDSGRDRKRRKEDDKRDTQEK	Chapter 5

The NLS sequences present of previously characterized Kap121p nuclear import cargoes are presented here. These amino acid residue sequences are written using the standard single letter abbreviations.

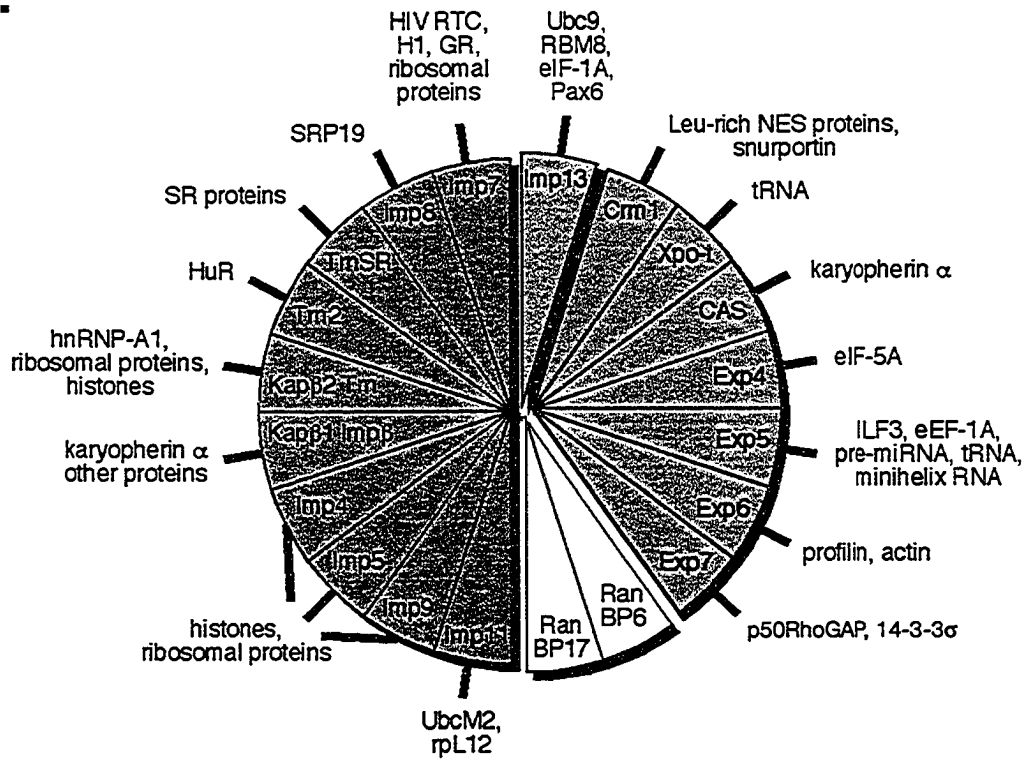
**1.4.2  $\beta$ -Karyopherins ( $\beta$ -Kaps)** – Eukaryotic cells contain two structurally related families of kaps: The  $\beta$ -karyopherins ( $\beta$ -kaps) and the  $\alpha$ -karyopherins ( $\alpha$ -kaps) (reviewed in Chook and Blobel, 2001; Fried and Kutay, 2003; Mosammaparast and Pemberton, 2004; Strom and Weis, 2001). There are 14  $\beta$ -kaps in yeast and more than 20  $\beta$ -kaps in higher eukaryotes (Figure 1.4.2). Members of the  $\beta$ -kap family are large proteins (95-145 KDa) and, while they share little sequence identity (~20%), all are thought to contain 15-20 HEAT repeats (reviewed in Bednenko *et al.*, 2003; Fried and Kutay, 2003; Mosammaparast and Pemberton, 2004). Each HEAT repeat motif is about 50 amino acid residues in length and forms two antiparallel  $\alpha$ -helices that

Figure 1.4.2: **The  $\beta$ -karyopherin protein family.** *A.* Members of the *S. cerevisiae*  $\beta$ -karyopherin protein family. *B.*  $\beta$ -karyopherin proteins in mammals. Alternative names for each kap are also shown. Asterisks denote kaps encoded by essential genes in yeast. Teal = import kaps; Red = export kaps; Purple = kaps that function in both import and export; and Yellow = kaps for which no cargoes have been identified. Figure adapted from (Mosammaparast and Pemberton, 2004).

**A.**



**B.**



are connected by a short turn (Andrade *et al.*, 2001). All  $\beta$ -kaps bind the GTP-bound form of the small GTPase Ran (see Section 1.4.3; (reviewed in Kuersten *et al.*, 2001; Macara, 2001; Quimby and Dasso, 2003; Weis, 2003)) and interact with specific components of the NPC (see Section 1.6).

Many groups in the nuclear transport field have focused their research efforts on identifying the cargoes transported by individual  $\beta$ -karyopherins. Based on these findings,  $\beta$ -kaps can be divided into three categories depending on the direction they transport cargo (Figure 1.4.2). In yeast, the import  $\beta$ -kaps are Kap95p, Kap104p, Kap108p/Sxm1p, Kap111p/Mtr10p, Kap114p, Kap119p/Nmd5p, Kap121p/Pse1p, Kap122p/Pdr6p and Kap123p. The export  $\beta$ -kaps are Kap124p/ Crm1p/Xpo1p, Kap109p/Cse1p and Los1p. Kap142p/Msn5p is capable of moving cargoes both into and out of the nucleus. No cargoes have been identified for Kap120p (reviewed in Chook and Blobel, 2001; Fried and Kutay, 2003; Kuersten *et al.*, 2001; Macara, 2001; Moore, 1998; Mosammaparast and Pemberton, 2004; Strom and Weis, 2001). While only a limited number of substrates have been defined for each  $\beta$ -kap, over 1500 yeast proteins, and multiple RNA species, must be translocated across the NPC in one or both directions during their life-cycle (<https://www.incyte.com/proteome/Retriever/index.html>). Despite this huge transport burden, only 4  $\beta$ -kaps are essential in yeast (Figure 1.4.2), suggesting that overlapping nuclear transport networks provide the redundancy required to sustain growth when the cell becomes compromised.

**1.4.3 Ran** – The small GTPase Ran (Gsp1p in yeast), which cycles between a GTP- and GDP-bound state, is an essential regulator of nucleo-cytoplasmic exchange (reviewed in Kuersten *et al.*, 2001; Mosammaparast and Pemberton, 2004; Quimby and Dasso, 2003; Rout *et al.*, 2003; Suntharalingam and Wentz, 2003; Weis, 2003). A key feature of this Ran GTPase cycle is the spatial separation of GTP loading and hydrolysis: Ran's guanosine nucleotide exchange factor (RanGEF; in metazoans RCC1 and in yeast Prp20p) is confined to the nucleus, while the Ran GTPase-activating protein (RanGAP; RanGAP1 in metazoans and Rna1p in yeast) is restricted to the cytoplasm. The compartmentalization of these two Ran regulators ensures that nuclear Ran is in the GTP-bound state, whereas the GDP-bound form of Ran is concentrated in the cytoplasm. This is referred to as the RanGTP gradient, which is thought to provide kap-cargo complexes with important positional information (Figure 1.4.3A; (Kalab *et al.*, 2002; Weis, 2003)). Thus, import complexes form in the cytoplasm where the concentration of RanGTP is low. They then traverse the NPC and encounter a RanGTP-rich environment on the nucleoplasmic face of the NPC. Here, RanGTP binds to the  $\beta$ -kap, stimulating kap-cargo complex dissociation. Conversely, export karyopherins bind their cargoes cooperatively with Ran-GTP in the nucleus. These nuclear export complexes dissociate once they reach the cytoplasm, where RanGAP induces GTP hydrolysis (Figure

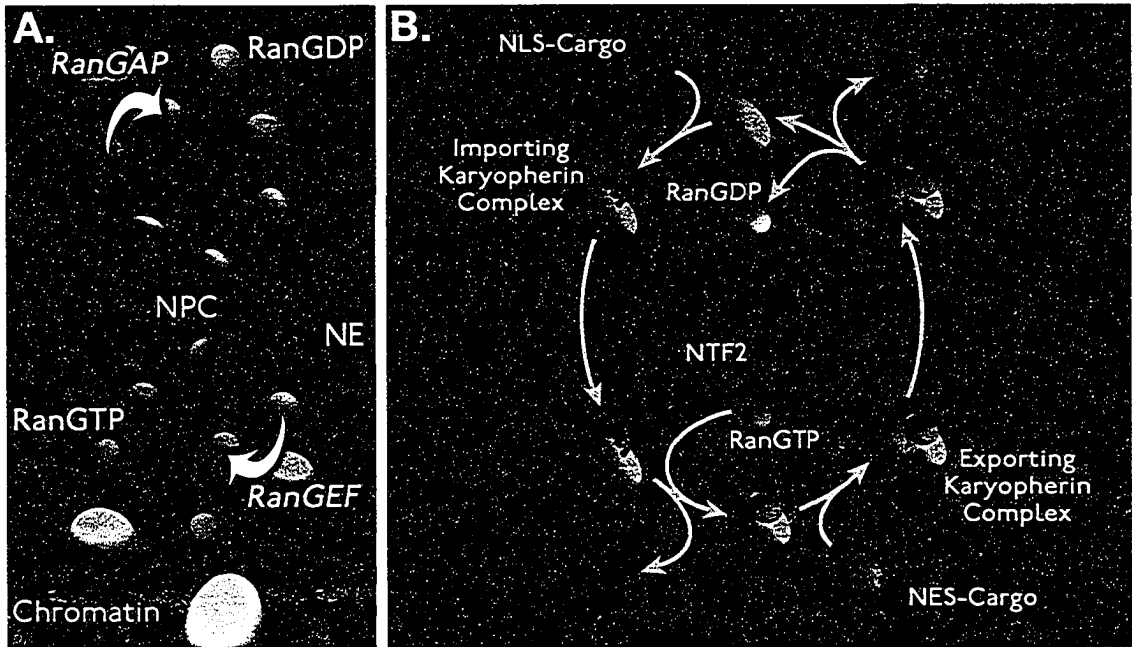


Figure 1.4.3: **The RanGTP gradient and nuclear transport.** *A.* **Setting up the RanGTP gradient across the nuclear envelope (NE).** RanGEF loads Ran with GTP. RanGAP catalyzes GTP hydrolysis by activating the GTPase activity of Ran. RanGEF strongly binds to chromatin and so flags the position of chromatin in the cell. By contrast, RanGAP is found largely in the cytoplasm. The result is that in the vicinity of chromatin (i.e. in the nucleoplasm) one finds mostly Ran bound to GTP whereas cytoplasmic Ran is mainly found in its GDP-bound form. This gradient powers much transport across the nuclear pore complex (NPC). *B.* **The nuclear transport cycle.** An importing karyopherin (kap) binds to its NLS-bearing cargo in the cytoplasm and transits the NPC. On the nucleoplasmic side, RanGTP binds to the kap, causing a conformational change that releases the cargo. In the nucleoplasm, exporting kaps bind their cargos in the presence of RanGTP. Once the exporting complexes are on the cytoplasmic side, RanGTP hydrolysis is stimulated by RanGAP, resulting in the release of cargo. RanGDP is then recycled to the nucleoplasm by NTF2 and is reloaded with GTP to begin another cycle. Figure from (Rout *et al.*, 2003).

1.4.3B; (reviewed in Kuersten *et al.*, 2001; Mosammaparast and Pemberton, 2004; Quimby and Dasso, 2003; Rout *et al.*, 2003; Suntharalingam and Went, 2003; Weis, 2003)).

Other soluble factors are also required to maintain the RanGTP gradient, including coactivators of the Ran cycle, and factors that aid in controlling Ran's interaction with NPC-bound karyopherins (reviewed in Fried and Kutay, 2003; Kuersten *et al.*, 2001; Quimby and Dasso, 2003; Weis, 2003). Without these factors, the continuous outflow of nuclear export complexes and cargo-free  $\beta$ -kaps from the nucleus would quickly deplete the nuclear pool of RanGTP and shutdown signal-mediated transport. One such factor, NTF2, provides an active transport mechanism that rapidly recycles Ran to the nucleus. NTF2 interacts with RanGDP only and is unrelated to members of the  $\beta$ -kap family (Ribbeck *et al.*, 1998; Smith *et al.*, 1998). Another family of Ran-binding proteins (RanBP1 and RanBP2/Nup358 in higher eukaryotes, and Yrb1p in yeast) promotes the dissociation of RanGTP from  $\beta$ -kaps. These factors are required because the interactions between RanGTP,  $\beta$ -kaps, and RanGAP are mutually exclusive (Fried and Kutay, 2003). In the absence of these accessory factors, future rounds of transport would be inhibited because  $\beta$ -kap-RanGTP complexes are extremely stable. The binding of these Ran-binding proteins to export complexes and cargo-free  $\beta$ -kaps promotes the release of RanGTP, enabling RanGAP to bind and activate Ran's GTPase function. Mog1p is another evolutionarily conserved Ran-binding protein that is thought to aid RanGDP release from NTF2

in the nucleus and assist RanGEF-mediated exchange of GDP to GTP (Fried and Kutay, 2003; Weis, 2003). Curiously, factors that dynamically associate with the NPC, namely RanBP3 (Yrb2p in yeast), Nup50p/Npap60p in human cells and Nup2p in yeast cells, have been shown to augment some nuclear transport pathways by regulating the interactions between Ran,  $\beta$ -kaps and the NPC (Denning *et al.*, 2001; Dilworth *et al.*, 2001; Englmeier *et al.*, 2001; Guan *et al.*, 2000; Lindsay *et al.*, 2001; Lindsay *et al.*, 2002).

### 1.5 FG nups and the NPC

Surprisingly, the sequence identity shared by yeast and mammalian nups is generally lower than 20%-25%, with the FG-dipeptide repeats being the most evolutionary conserved domain (Cronshaw *et al.*, 2002; Rout *et al.*, 2000). Yet, many of their functions and/or positions in the NPC have remained evolutionarily conserved. There are ~200 FG nups per NPC, which account for approximately one-half of the total mass of the NPC (Rout *et al.*, 2003). Most of these nups are positioned symmetrically on both the cytoplasmic and nuclear faces of the NPC, a few can, however, be found on one side or the other (Figure 1.2.2; (Cronshaw *et al.*, 2002; Rout *et al.*, 2000)). Current transport models suggest that FG nups gate the passive diffusion of macromolecules between the nucleus and cytoplasm and, simultaneously, facilitate signal-mediated active transport across the NPC by providing binding sites for transport complexes (discussed below; (Bickel and Bruinsma, 2002; Macara, 2001; Ribbeck and Gorlich, 2001, 2002; Rout *et al.*, 2003; Rout *et al.*, 2000; Shulga and Goldfarb, 2003)).

**1.5.1 FG nups are implicated in passive diffusion** – Analysis of the structure of FG-rich repeat regions revealed that these domains adopt an extended conformation with little intrinsic secondary structure (Allen *et al.*, 2000; Buss *et al.*, 1994; Denning *et al.*, 2003). They have also been shown to form filaments and to colocalize with the filamentous structures of the NPC (Allen *et al.*, 2000; Stoffler *et al.*, 1999). These findings are consistent with the idea that FG nups are the main component of the fibril extensions that protrude from both faces of the NPC (reviewed in Bednenko *et al.*, 2003; Rout and Aitchison, 2001; Rout *et al.*, 2003; Suntharalingam and Wente, 2003). In light of these data, FG nups are an integral component of all current models describing nucleo-cytoplasmic transport; all of which suggest that their disordered FG repeat domains restrict the permeability of the NPC (Bickel and Bruinsma, 2002; Macara, 2001; Ribbeck and Gorlich, 2001, 2002; Rout *et al.*, 2003; Rout *et al.*, 2000; Shulga and Goldfarb, 2003).

According to the “virtual gate” model, these FG-rich regions (referred to as “entropic bristles”) are thought to be kept in constant motion by diffusive forces (Hoh, 1998) and, as such, are predicted to fill-up the areas surrounding their anchoring sites in the NPC (Rout *et al.*, 2003; Rout *et al.*, 2000). The model suggests that the constant motion of the “entropic bristles” positioned at the entrances of the NPC guard access to central tube, while the bristles located within the central channel constrain the free space available for molecule diffusion. Therefore, molecules passively diffusing between the nucleus and

cytoplasm would have to continually push these filamentous structures aside while moving through the NPC. This would require energy and add to the entropic price paid by these molecules. Therefore, even when a molecule is small enough to diffuse through the NPC the central channel can still function as a barrier (Rout *et al.*, 2003; Rout *et al.*, 2000).

The “selective-phase” model, proposed by Ribbeck and Gorlich (2001 and 2002), suggests that weak, hydrophobic interactions between the FG repeat domains of loosely folded FG nups generate a hydrophobic meshwork that fills the pore (Ribbeck and Gorlich, 2001, 2002). Thus, the exclusion limit of the NPC is thought to be determined by both the size of the holes in the meshwork and its hydrophobic nature. The high concentration of exposed hydrophobic groups of phenylalanine residues produce an environment that selectively inhibits the diffusion of hydrophilic molecules. At the same time, the sieve-like property of the meshwork permits the diffusion of small inert and hydrophobic molecules, and restricts the flow of larger molecules (Ribbeck and Gorlich, 2001, 2002).

The “oily spaghetti” model proposed by Macara (2001) combines features of the “selective phase” model with the existence of a central open pore ~10 nm in diameter. This model suggests that unstructured, non-interacting FG repeats form extended chains that line the central channel of the NPC like loose “oily spaghetti” (Macara, 2001). Thus, molecules with diameters <10 nm would be able to passively diffuse through the NPC, while the nucleoporin “spaghetti” would hinder the diffusion of the larger molecules (Macara, 2001).

Finally, the “molecular latch” model, recently proposed by Shulga and Goldfarb (2003), suggests that NPCs harbour a diffusion channel with an accessible diameter of 10.7 nm that is gated by molecular latches composed of FG nups and the structural (non-FG) nups that anchor them within the central channel. When closed, these molecular latches restrict diffusion between the nucleus and cytoplasm to molecules smaller than 30 KDa (Shulga and Goldfarb, 2003).

**1.5.2 FG nups are involved in active nucleo-cytoplasmic exchange** – As discussed above, macromolecules traveling between the nucleus and cytoplasm must be able to overcome the “virtual gate” of the NPC and pass through its central tube in order to reach their destinations. Residence within this central channel has been described as a “transition state” for translocation, into which molecules must be encouraged to enter (Rout *et al.*, 2003). Nuclear transport receptors provide these molecules with a way to dynamically interact with the NPC, efficiently enter this “transition state” and efficiently move through the NPC. Genetic and biochemical analyses have demonstrated that every transport factor investigated can bind FG nups, suggesting that these components of the NPC play a direct role in transport (reviewed in Fried and Kutay, 2003; Rout and Aitchison, 2000; Rout *et al.*, 2003; Suntharalingam and Wentz, 2003).

*In vivo*, mutations in several FG nups have been shown to affect import, export or both in yeast and mammalian cells (reviewed in Fried and Kutay, 2003; Stoffler *et al.*, 1999). For example in yeast, strains harbouring mutations in

several of the genes that encode FG nups, including *NUP116*, *NUP1*, *NUP60*, and *NSP1*, display protein and/or RNA transport defects (Denning *et al.*, 2001; Dilworth *et al.*, 2001; Fabre and Hurt, 1997; Hurt *et al.*, 1999; Iovine *et al.*, 1995; Iovine and Wentz, 1997; Stoffler *et al.*, 1999; Strawn *et al.*, 2001). In vertebrates, overexpression of *NUP153* defined a specific role for this protein in mRNA export (Bastos *et al.*, 1996). Similarly, immunodepletion assays have demonstrated that Nup62p is required for nuclear import in *Xenopus* oocytes (Dargemont *et al.*, 1995). RNAi strategies and gene knockout approaches have also shown that depletion of Nup214/CAN leads to a G2 phase cell cycle arrest, and impaired NLS-mediated nuclear import and mRNA export (van Deursen *et al.*, 1996); while loss of Nup98 alters NPC morphology and selectively impairs some nuclear import pathways (Kap  $\beta$ 1/Kap  $\alpha$ - and Kap  $\beta$ 2- (or Transportin) mediated import) (Wu *et al.*, 2001). Together, these findings establish that FG nups are required for efficient nucleo-cytoplasmic exchange.

X-ray crystallography studies have begun to resolve the molecular basis of  $\beta$ -kap-FG nup interactions. They appear to be hydrophobic in nature and are mediated by the phenylalanine of the FG repeat, which is inserted into a hydrophobic pocket formed by the amino acid residue side chains of the transport receptor (reviewed in Bednenko *et al.*, 2003; Chook and Blobel, 2001). While most FG nups have been shown to interact with several  $\beta$ -kaps, the affinity of different transport receptors for specific FG nups varies. For example, overlay blot assays have demonstrated that yeast Kap95p has a higher affinity for Nup1p

and Nsp1p than Kap123p does, which interacts weakly with these nucleoporins (Rout *et al.*, 1997). Kap95p also appears to have a higher affinity for Nup116p, Nup100p and Nup145Np than Kap104p, but both of these  $\beta$ -kaps seem to bind Nup57p with similar strengths (Aitchison *et al.*, 1996). Moreover, co-immunopurification studies demonstrated that Kap121p specifically associates with Nup53p (Marelli *et al.*, 1998).

In addition, immunoelectron microscopy studies have localized nucleoporins to substructures of the NPC (Figures 1.2.2 and 1.5.2; (Fried and Kutay, 2003; Rout *et al.*, 2000; Suntharalingam and Wentz, 2003)), most of which display two-fold symmetry in the plane of the nuclear envelope. Subcomplexes like these are thought to make up the core of the NPC, forming the central tube through which all molecules travel. In contrast, the yeast and vertebrate FG nups Nup159p and Nup42p, and Nup214/CAN and Nup358, respectively, localize exclusively to the cytoplasmic face of the NPC and, as such, are thought to be the main components of the cytoplasmic filaments (Floer and Blobel, 1999; Hurwitz *et al.*, 1998; Kraemer *et al.*, 1994; Rout *et al.*, 2000; Wu *et al.*, 1995). Similarly, the localization of yeast Nup60p and Nup1p, and vertebrate Nup98 and RAE1 localize to the nuclear side of the NPC, suggesting that these FG nups form the nuclear basket. In general, this asymmetric distribution is thought to enhance transport efficiency by providing kap-cargo complexes with additional directional cues and, possibly, high-affinity binding

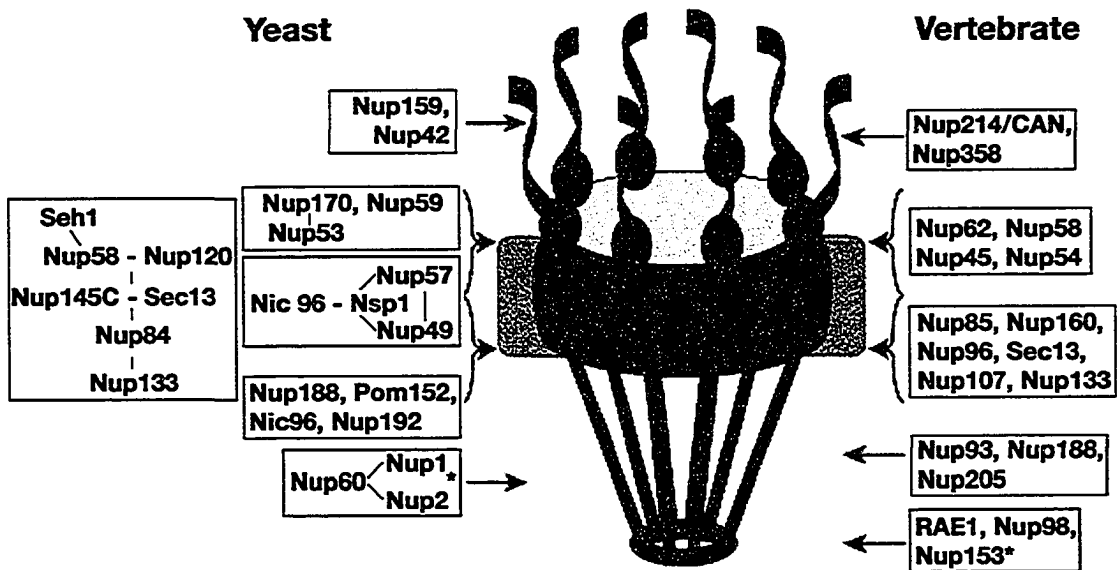


Figure 1.5.2: Nup subcomplexes in both *S. cerevisiae* and vertebrate NPCs. Biochemical and molecular characterization studies have defined a network of nup-nup subcomplexes. The boxes on the left show the reported budding yeast nup subcomplexes. On the right, the vertebrate subcomplexes are shown. Defined nup-nup interactions are indicated by the dashes, whereas commas indicate the association network is not fully known. Their relative surface-accessible localizations are indicated: red or blue boxes indicate asymmetric complexes; green boxes indicate symmetric complexes. Complexes containing dynamic nups are indicated by an asterisk. Figure adapted from (Suntharalingam and Wentz, 2003).

sites (see Section 1.6; (reviewed in Fahrenkrog and Aebi, 2003; Fried and Kutay, 2003; Rout *et al.*, 2003; Suntharalingam and Wentz, 2003)).

Together, these data suggest that FG nups provide multiple docking sites for transport receptors and that specific  $\beta$ -kap-FG nup interactions dictate the distinct, partially overlapping routes that  $\beta$ -kaps follow when traveling through the NPC. The binding sites shared by some of these transport pathways and the varying affinities of  $\beta$ -kap-FG nup interactions could potentially cause competitive interference between import and export complexes traveling through the same NPC. However, its eight-fold symmetry and the high abundance of FG nups, which are thought to provide hundreds of transport factor binding sites per NPC (Rout *et al.*, 2003), are assumed to limit such interference. Thus, enabling different  $\beta$ -kaps to simultaneously occupy different binding sites within a single NPC.

## **1.6 The mechanism of nucleo-cytoplasmic transport**

Early studies characterizing the interactions between nuclear transport complexes and the NPC led researchers to postulate that kap-cargo complexes traverse the NPC by progressively moving from one FG nup to the next, along an interaction gradient of increasing affinity. However, in light of recent studies it is unlikely that they travel through the NPC in this manner. First, architectural and content analysis of both yeast and mammalian NPCs demonstrated that the vast majority of nups, including those that contain  $\beta$ -kap-binding domains, are symmetrically distributed on both the nuclear and cytoplasmic sides of the NPC

((Cronshaw *et al.*, 2002; Rout *et al.*, 2000); (reviewed in Fried and Kutay, 2003; Stoffler *et al.*, 1999; Suntharalingam and Wentz, 2003; Weis, 2003)). Second, while interactions between FG nups and transport receptors are believed to help macromolecules enter the NPC, they also increase the time these complexes spend traversing the channel. Therefore, reasonable transport rates could only be achieved if  $\beta$ -kap-FG nup interactions within the central tube of the NPC are weak. High-affinity interactions have slow off-rates, while fast off-rates are associated with low-affinity interactions. Accordingly, high-affinity interactions within the central tube of the NPC would be counterproductive, as they are predicted to significantly increase the time it takes a transport complex to move from one side of the NPC to the other. On the other hand, low-affinity binding sites are thought to allow transport complexes to traverse this channel without significantly impeding transport rates. Indeed, kinetic studies have demonstrated that the dissociation constants for these  $\beta$ -kap-FG nup interactions are very low, thus their off-rates are fast (Bayliss *et al.*, 1999; Bednenko *et al.*, 2003; Chaillan-Huntington *et al.*, 2000; Ribbeck and Gorlich, 2001). Finally, given the dense concentration of FG repeats in the NPC, it is improbable that kap-cargo complexes sequentially move from the FG repeats of one nup to those of the next. Instead, the  $\beta$ -kap is probably in constant contact with at least one, if not multiple, FG repeats while traversing the NPC. Thus, the avidities of transport receptors for the NPC rather than the affinity of an individual  $\beta$ -kap-FG nup

interaction, most likely provide the mechanism that allows transport complexes to move through this fluid channel.

Nevertheless, high-affinity interactions with FG nups located on either the cytoplasmic or nucleoplasmic faces of the NPC have been observed. For example, co-immunopurification studies have demonstrated that Nup1p and Nup2p (which localize to the nuclear basket of the NPC) co-purify with Kap95p (Dilworth *et al.*, 2001), suggesting that these nups provide high-affinity docking sites for Kap95p import complexes. Similarly, kinetic studies have observed high-affinity interactions between mammalian Kap  $\beta$ 1 nuclear import complexes and an FG nup (Nup153) localized solely to the nuclear basket of the NPC (Ben-Efraim and Gerace, 2001). Studies have also shown that when bound to RanGTP the yeast export factor Crm1p preferentially interacts with the cytoplasmic nucleoporin, Nup214/CAN (Kehlenbach *et al.*, 1999). Accordingly, models describing the mechanism of nuclear transport suggest that these asymmetrically distributed, high-affinity binding sites provide directional cues that increase the efficiency of transport. A recent study supporting this established that while asymmetric FG-rich regions of the NPC are dispensable, these domains are required for the efficient transport of Kap104p, Kap95p and Kap121p cargoes (Strawn *et al.*, 2004).

With these data in mind, several models have been proposed to explain the mechanism of NPC gating and kap-cargo translocation through the NPC. These include the “oily-spaghetti” model (Macara, 2001), the “selective phase”

model (Ribbeck and Gorlich, 2001, 2002), the “molecular latch” model (Shulga and Goldfarb, 2003) and the “virtual gate” model (Rout *et al.*, 2000). While researchers debate the validity of each of these models, most describe three common features: 1.  $\beta$ -kaps reversibly binding at multiple sites within the NPC; 2. Transport through the central channel occurring via facilitated diffusion; 3. Kap-cargo complexes accumulating at selective, high-affinity, rate-limiting sites present in the compartment where Ran activity (either GTP hydrolysis or RanGTP binding) induces their dissociation.

The “virtual gate” model of nucleo-cytoplasmic exchange proposed by Rout *et al.* (2000) speculates that the movement of kap-cargo complexes through the NPC is mainly dependent on two steps, with an optional intermediate step (called “Trapping”) that is thought to increase transport efficiency (Figure 1.6.1; (Rout *et al.*, 2003; Rout *et al.*, 2000)). The first step is referred to as NPC “Gating” and proposes that the passage of macromolecules through the NPC is restricted by the central tube and the Brownian motion of the surrounding filamentous, unstructured FG nups (see Section 1.5.1). The low-affinity binding of  $\beta$ -kaps to numerous FG nups located at the distal edges of the NPC allows transport complexes to overcome this gate and gain access to its central channel. Similar low-affinity interactions would then allow transport complexes to rapidly associate with, and dissociate from, many FG nups. As most of these interactions are with symmetrically distributed FG nups, the karyopherin does not receive any directional cues at this stage of transport. The optional step,

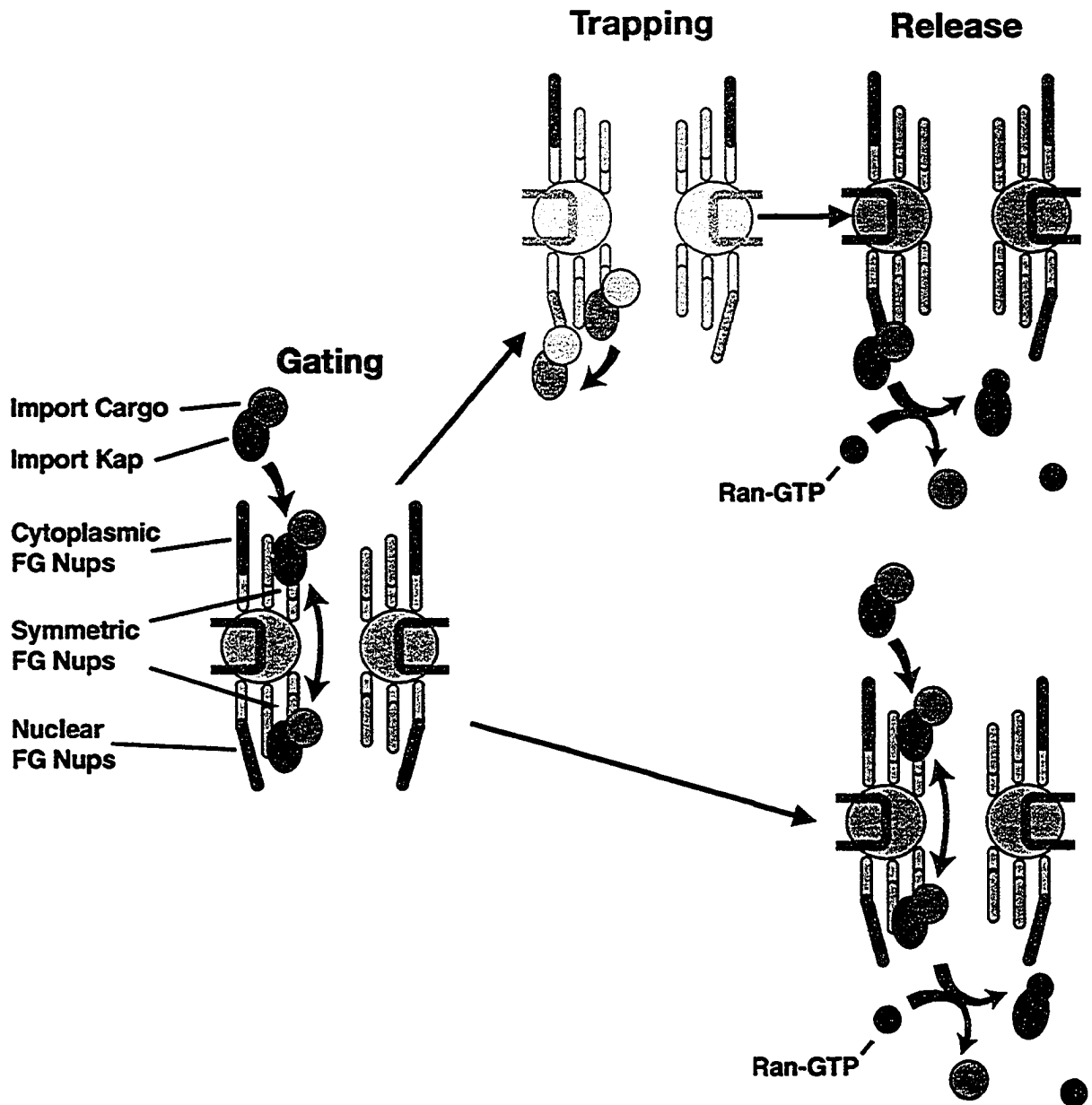


Figure 1.6.1: The “Virtual Gate”: A model describing the mechanism of nucleo-cytoplasmic transport. This cartoon illustrates the movement of a kap-cargo nuclear import complex through the NPC according to the Virtual Gate transport model. See text for details. Figure adapted from (Rout *et al.*, 2000).

described as “Trapping”, involves the preferential binding of kap-cargo complexes to an asymmetric, high-affinity binding site, which is thought to provide transport complexes with a terminal-docking site. This site is present on either the nuclear or cytoplasmic face of the NPC, depending on whether an import  $\beta$ -kap or an export  $\beta$ -kap, respectively, is mediating cargo translocation. Finally, either Ran- GTP binding or GTP hydrolysis (depending on the direction of transport) afford kap-cargo complexes with the terminal directional cue, which triggers the displacement of the cargo from the  $\beta$ -kap and the  $\beta$ -kap from the NPC (Cole and Hammell, 1998; Mattaj and Englmeier, 1998; Moore, 1998). This is the “Release” step and is believed to be irreversible, thereby terminating the transport cycle and establishing the overall direction of transport.

The “selective phase” model, the NPC gate is overcome by the binding of kap-cargo complexes to FG nups, which breaks the hydrophobic FG-repeat meshwork within the interior of the NPC. Dissolution of the meshwork is thought to allow kap-cargo complexes to selectively partition into and through the central channel of the NPC (Ribbeck and Gorlich, 2001, 2002). Similarly, the “oily spaghetti” model suggests that kap-cargo complexes overcome the NPC gate by interacting with FG nups, which allow transport complexes to easily push the loosely packed FG repeats aside. Assuming that transient  $\beta$ -kap-FG nup interactions occur within the central channel, translocation through the NPC is then facilitated by a series of binding and release steps, which coincide with short, random movements within the pore (Macara, 2001). Alternatively, the

“molecular latch” model proposes that translocation through the NPC occurs as a result of a cascade of FG nup-non FG nup partner exchanges within the central channel. These changes are thought to be initiated by the binding of kap-cargo complexes to their cognate FG repeat domains. This induces large conformational changes within the pore that disrupt the molecular latches, which keep the pore in closed. As a result, the central channel opens or dilates, increasing the permeability barrier of the NPC and allowing it to accommodate kap-cargo complexes (Shulga and Goldfarb, 2003). While it is evident that the distinct details of how the NPC is gated and how transport complexes overcome this gate described by each of these models vary, each includes a “Trapping” and “Release” step that is similar to those described in the “virtual gate” model (Macara, 2001; Ribbeck and Gorlich, 2001, 2002; Shulga and Goldfarb, 2003).

### **1.7 Karyopherin-cargo interactions**

In general, nucleo-cytoplasmic transport requires a direct interaction between a given  $\beta$ -kap and its cargo. Translocation of these kap-cargo complexes across the NE is then mediated by direct interactions between  $\beta$ -kaps and FG-nups (see Section 1.5.2). The exception to this trend comes from the Kap  $\beta$ 1/Kap  $\alpha$  (Kap95p/Kap60p in yeast) nuclear import pathway, which was the first import pathway characterized (Rexach and Blobel, 1995). In this instance, members of the  $\alpha$ -kap protein family (Kap60p/Srp1p in yeast and as many as 6 members in metazoan species (<http://www.incyte.com/proteome/Retriever/index.html>)) act as adapters for a  $\beta$ -kap (Kap95p in yeast and Kap  $\beta$ 1 in

mammals):  $\alpha$ -kaps/Kap60p recognize and interact with classical NLS (cNLS)-containing substrates; Kap  $\beta$ 1/Kap95p then binds cargo-bound  $\alpha$ -kap/Kap60p and mediates the movement of this trimeric import complex through the NPC (reviewed in Chook and Blobel, 2001; Fried and Kutay, 2003; Kuersten *et al.*, 2001; Macara, 2001; Moore, 1998; Mosammaparast and Pemberton, 2004; Strom and Weis, 2001).

Knowing whether cargoes for a given  $\beta$ -kap contain similar recognition sequences and if each  $\beta$ -kap contains one or multiple cargo binding pockets are key to understanding how each recognizes and interacts with such structurally diverse substrates. Crystallography studies have solved the structures of mammalian Kap  $\beta$ 1 bound to three different cargoes (Cingolani *et al.*, 2002; Cingolani *et al.*, 1999; Lee *et al.*, 2003). These studies suggest that Kap  $\beta$ 1 uses different interaction interfaces to associate with each of these cargoes. Kap  $\beta$ 1 can simultaneously mediate the nuclear import of non-classical (nc) NLS- and cNLS-containing cargoes by interacting directly or indirectly (via  $\alpha$ -kaps), respectively, with these substrates. This is accomplished using two partially overlapping, non-mutually exclusive cargo binding pockets; an N-terminal set of HEAT repeats (1-11) is used when binding ncNLS cargoes, while HEAT repeats 7 through 19 are used for the interaction with  $\alpha$ -kap-cNLS dimers (Cingolani *et al.*, 2002; Cingolani *et al.*, 1999). In addition, a recent study established that when Kap  $\beta$ 1 is bound to the helix-loop-helix zipper (HLHZ) transcription factor SREBP-2, it adopts a more open conformation to accommodate the HLHZ

domain of this protein and uses more hydrophobic interactions than used when binding  $\alpha$ -kap-cNLS dimers or ncNLS cargoes (Lee *et al.*, 2003). Furthermore, small angle x-ray scattering techniques have demonstrated that all  $\beta$ -kaps do not adopt the same conformations when binding cargo or RanGTP (Fukuhara *et al.*, 2004). Together, these studies suggest that structural flexibility is likely a mechanism employed by all members of the  $\beta$ -kap family and, at least in part, explains how one  $\beta$ -kap can mediate the transport of such structurally and functionally diverse cargoes.

This cargo recognition flexibility has, however, made it difficult for researchers to predict the exact amino acid residues that are required for NLS and NES function, and determine how the  $\beta$ -kap will interact with its substrates. Adding to this complexity, the identification of *bona fide* import and export substrates established that some  $\beta$ -kaps transport common cargoes (Figure 1.4.2). For example, at least four  $\beta$ -kap transport pathways mediate the nuclear import of core histones and ribosomal proteins in yeast and mammalian cells (Jakel and Gorlich, 1998; Mosammaparast *et al.*, 2002b; Mosammaparast *et al.*, 2001; Muhlhauser *et al.*, 2001; Rout *et al.*, 1997; Sydorsky *et al.*, 2003). Notably, these overlapping cargoes are required for essential cellular processes. These data suggest that many  $\beta$ -kap transport pathways will mediate the translocation of proteins whose nuclear functions are required for cell survival. Some interesting issues regarding the regulation of transport are raised by these data, as they suggest that  $\beta$ -kaps might compete for cargoes, or *vice versa*. It is,

therefore, probable that the transport kinetics of a given cargo could be affected by both the presence of other cargoes and the  $\beta$ -kap(s) mediating its import.

## **1.8 Regulating nucleo-cytoplasmic exchange**

Post-translational modification (PTM) of both the soluble and stationary phases of nuclear transport is emerging as a common mechanism employed by the cells to regulate transport. The reversibility and diverse nature of these modifications is thought to allow the cell to inhibit or activate the transport of a specific cargo, or group of cargoes, without globally affecting nucleo-cytoplasmic exchange.

**1.8.1 Post-translational modification of the NPC** – In general, each  $\beta$ -kap is thought to follow a distinct route through the NPC that is dictated by specific kap-nup interactions (reviewed in Fried and Kutay, 2003; Mosammaparast and Pemberton, 2004; Suntharalingam and Wentz, 2003). Furthermore, high-affinity binding sites within the NPC have been identified for some  $\beta$ -kaps (see Sections 1.5.2 and 1.6, and references therein). Most of these sites are differentially localized to either the nuclear or cytoplasmic face of the NPC and are thought to enhance efficient cargo delivery by augmenting kap-cargo complex “Trapping” on the destination face of the NPC. However, these stable docking sites could also be used to specifically regulate gene expression by modifying the nups utilized by a particular nuclear transport receptor. Several groups have demonstrated that post-translational modifications also influence both the architecture and

composition of the NPC (Makhnevych *et al.*, 2003; Matunis *et al.*, 1996; Matunis *et al.*, 1998). These rearrangements are thought to provide the cell with a way to restrain or enhance an individual transport pathway, in a condition-specific manner without dramatically affecting all nucleo-cytoplasmic transport. For example, the mammalian nucleoporin, Nup358, has been shown to be post-translationally modified with SUMO, a small ubiquitin-like modifier, to specifically associate with modified proteins, and to function as a SUMOylating enzyme (Pichler *et al.*, 2002; Vassileva and Matunis, 2004; Zhang *et al.*, 2002). As such, Nup358 is predicted to facilitate nucleo-cytoplasmic transport by altering the modification state of cargoes as they traverse the NPC and aid export complex dissociation on the cytoplasmic face of the NPC.

Similarly, a recent study examining the molecular interactions between the yeast  $\beta$ -kap, Kap121p, and FG nups revealed that Kap121p interacts with a high-affinity binding site in Nup53p that specifically inhibits Kap121p-mediated transport in a cell cycle dependent manner (Makhnevych *et al.*, 2003). At mitosis, coincident with phosphorylation, Nup53p dissociates from Nup170p and interacts with the nearby nucleoporin, Nic96p. This transfer is thought to unmask the high-affinity Kap121p binding site within Nup53p that sequesters Kap121p in the central tube of the NPC and rapidly inhibits Kap121p-mediated import but does not affect other transport pathways. While these findings are specific to an individual  $\beta$ -kap-nup interaction, it is possible that a mechanism such as this could be used by the cell as a general mechanism to regulate nucleo-cytoplasmic

transport. Interestingly, Kap121p interacts with a region of Nup53p that does not contain FG repeats (Lusk *et al.*, 2002), suggesting that regulatory mechanisms such as this are likely mediated by nucleoporin domains that are not FG-rich. It is possible that the use of these non-FG repeat domains to control a specific transport pathway would ensure that the fluidity of the “entropic bristles” within the central tube of the NPC is maintained. Thus, decreasing the potential secondary affects such NPC rearrangements would have on other transport pathways.

**1.8.2 Post-translational modification of cargoes** – Studies have demonstrated that many cellular functions required at precise times during growth and development are regulated by sequestering the kinases, phosphatases and/or transcription factors that control these processes to areas of the cell where they do not function (reviewed in Chen and Greene, 2004; Chook and Blobel, 2001; Fried and Kutay, 2003; Mosammaparast and Pemberton, 2004; Xu and Massague, 2004). When required, these components are then localized to the appropriate cellular compartment. Not surprisingly, mechanisms that activate, or inactivate, the nucleo-cytoplasmic shuttling of these second messengers and transcription factors are often used to regulate their activity. For example, phosphorylation has been shown to regulate the formation of the kap-cargo complexes that mediate the import and/or export of the yeast transcription factors Swi6p, Pho4p and Aft1p (Geymonat *et al.*, 2004; Kaffman *et al.*, 1998a; Kaffman *et al.*, 1998b; Ueta *et al.*, 2003), as well as members of the

NF- $\kappa$ B/REL and FOXO families of transcription factors, histone deacetylases and the tumor suppressor p53 in humans ((McKinsey *et al.*, 2000; Smillie *et al.*, 2004), (reviewed in Chen and Greene, 2004; Liu *et al.*, 1993; Xu and Massague, 2004)). Furthermore, Kap142p/Msn5p functions as the major export receptor for cargoes whose localizations are regulated by their phosphorylation state (Boustany and Cyert, 2002; DeVit and Johnston, 1999; Gorner *et al.*, 2002; Jaquenoud *et al.*, 2002; Kaplun *et al.*, 2003). Studies have also demonstrated that mono- and poly-ubiquitylation, methylation, SUMOylation and acetylation influence the subcellular localization of many signal transducers (Chen and Greene, 2004; Li *et al.*, 2003; Smith *et al.*, 2004; Xu and Massague, 2004).

## **1.9 Nucleo-cytoplasmic transport cargoes**

This study describes the identification and characterization of four novel Kap121p nuclear import cargoes: The yeast transcription factor Ste12p and the ribosome assembly factors Nop1p, Sof1p and Dbp9p. The cellular functions governed by these factors are described below.

**1.9.1 *Ste12p*** – Ste12p is a transcription factor that plays a central role in the signal transduction pathways that transduce environmental stimuli from the plasma membrane to nucleus, which promote yeast cells to mate or become filamentous (form pseudohyphae), change their budding pattern, and invade solid substrates such as agar (Figure 1.9.1; (reviewed in Bardwell, 2004; Elion, 1998, 2000; Gustin *et al.*, 1998; Pan *et al.*, 2000; Schwartz and Madhani, 2004)).

Yeast cells exist as either haploids or diploids, with haploid cells exhibiting one of

two possible mating types, *Mata* or *Mata $\alpha$* . Haploid cells can mate and become diploid when cells of the opposite mating types are cultured together, a process stimulated by the release of mating pheromones. Alternatively, under stressful growth conditions, like nutrient starvation or in the presence of short-chain alcohols (Dickinson, 1996; Lorenz *et al.*, 2000; Pan *et al.*, 2000), haploid yeast cells form pseudohyphae and grow invasively. Although the outcome depends on the cell type and the stimuli they receive, in either case, some of the same signaling elements are involved (Ste20p, Ste11p, Ste7p), and both signal transduction pathways terminate in the phosphorylation and activation of Ste12p (Figure 1.9.1).

**A. Mating** – When the appropriate mating pheromone is present it interacts with plasma membrane receptors resulting in a GDP/GTP exchange on the  $\alpha$  subunit (Gpa1p) of a heterotrimeric G protein (Dietzel and Kurjan, 1987). Ste4p ( $\beta$  subunit) and Ste18p ( $\gamma$  subunit) then stimulate the activation of a mitogen-activated protein (MAP) kinase signal transduction cascade (Whiteway *et al.*, 1988; Whiteway *et al.*, 1989) which terminates in the phosphorylation and activation of Ste12p. Upon activation, Ste12p forms homodimers (Hagen *et al.*, 1991; Johnson, 1995; Roberts and Fink, 1994) or Ste12p-Mcm1p heterodimers (Mead *et al.*, 2002) that bind the pheromone response elements (PREs) found in the promoter regions of ~200 mating specific genes (Roberts *et al.*, 2000) and induces their transcription (Figure 1.9.1, Left). The transcriptional

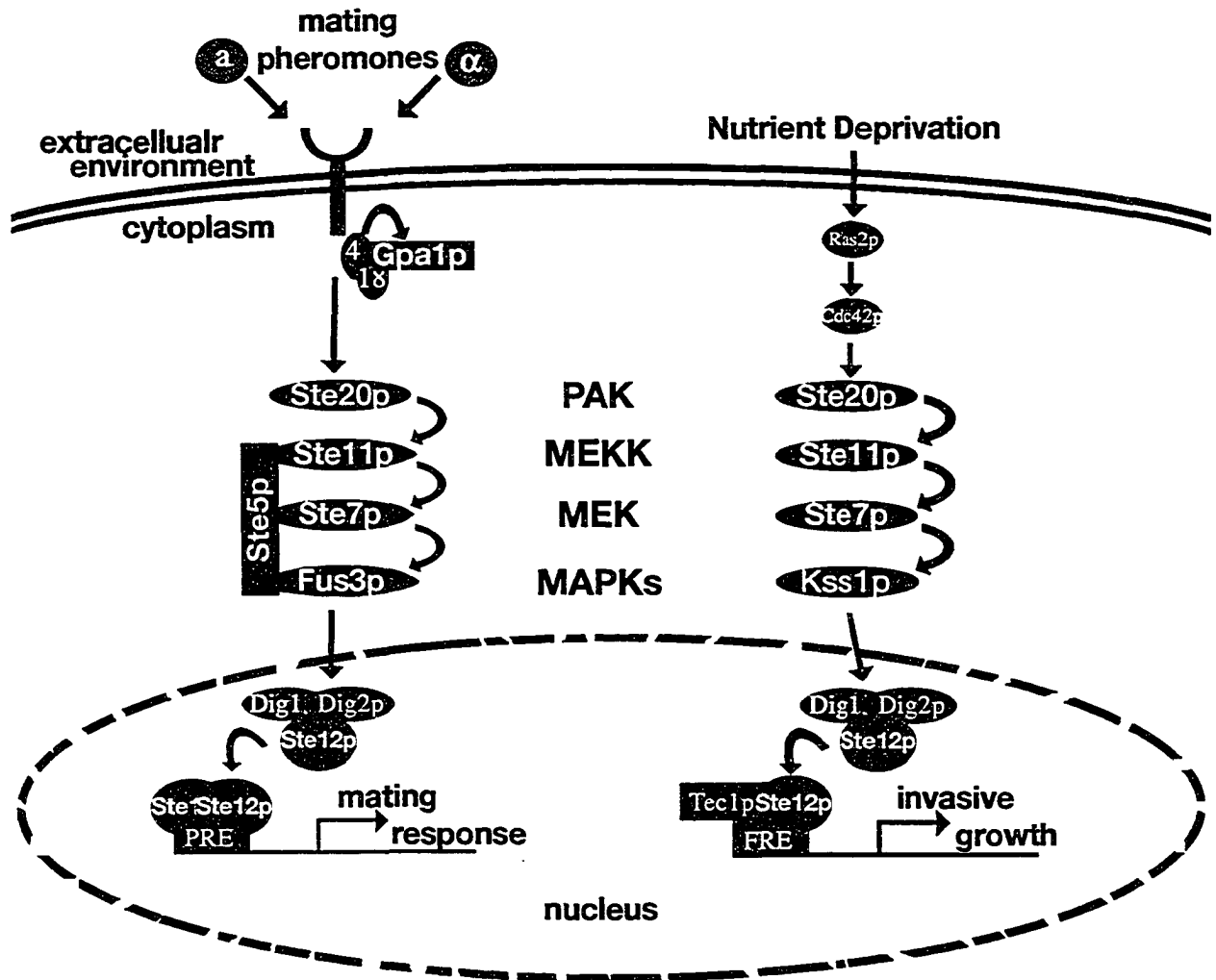


Figure 1.9.1: The *S. cerevisiae* pheromone response and pseudohyphal/invasive growth response mitogen-activated protein (MAP) kinase pathways. Schematic cartoons of selected elements of the MAPK signaling cascade that regulates the yeast pheromone response (Left cascade) and the filamentation/invasion growth transition (Right cascade). Figure adapted from (Bardwell, 2004; Schwartz and Madhani, 2004).

activation of these genes triggers a number of cellular responses that include polarized growth or shmooing, cell cycle arrest in G<sub>1</sub>, and the increased expression of proteins required for cell adhesion, cell fusion, and nuclear fusion.

**B. Invasive Growth** – During the invasive growth transition, nutrient deprivation stimulates the activation of two signaling pathways: The MAP kinase pathway required for mating (reviewed in Bardwell, 2004; Schwartz and Madhani, 2004) and the nutrient sensing PAK pathway (not discussed here, see Pan et al., 2000). Activated Ste12p forms a heterodimer with a second transcription factor, Tec1p (Figure 1.9.1, Right; (Madhani and Fink, 1997; Mosch and Fink, 1997). This protein complex then interacts with promoters containing PREs in close proximity to Tec1p binding sites (collectively termed filamentation/invasion response elements or FREs) and this induces the transcription of *FLO11*. Flo11p is required for many of the critical processes that enable yeast invasion. These include adhesion of mother-daughter cells, maintenance of pseudohyphal filaments and agar invasion (Bardwell, 2004; Pan *et al.*, 2000; Prinz *et al.*, 2004; Schwartz and Madhani, 2004).

### **1.9.2 *Nop1p, Sof1p and Dbp9p are required for ribosome biogenesis* –**

Mature eukaryotic ribosomes contain one copy of each of the four ribosomal RNAs (rRNAs) and approximately 78 ribosomal proteins (r-proteins) (reviewed in Aitchison and Rout, 2000; Fatica and Tollervey, 2002; Kressler *et al.*, 1999;

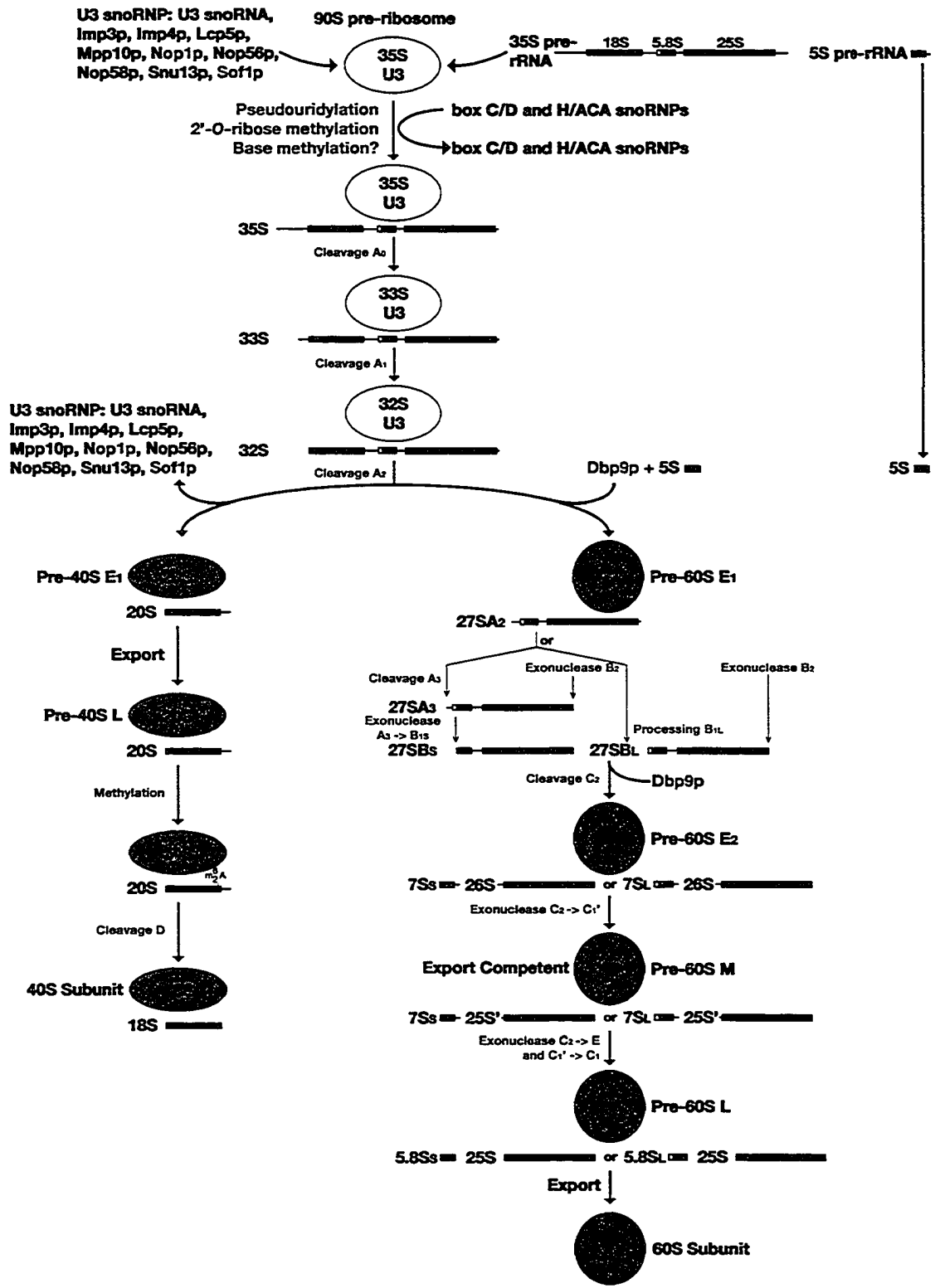
Venema and Tollervey, 1999). Synthesis of mature ribosomal subunits requires three major processing events that occur concurrently: 1. Methylation and pseudouridylation of pre-rRNA and mature rRNA species; 2. Cleavage of pre-rRNA to mature 18S, 5.8S, and 25S rRNAs; and 3. The assembly of r-proteins onto mature rRNA species (Figure 1.9.2). In addition, numerous *cis*-acting factors, namely small nucleolar RNAs (snoRNAs), are also required for the covalent processing of pre-rRNAs (reviewed in Bachellerie *et al.*, 2002). snoRNAs can be divided into two groups based on conserved sequence and structural features; box C/D snoRNAs direct site-specific 2'-O-ribose methylation, while box H/ACA snoRNAs select the sites of pseudouridine formation (Figure 1.9.2). The experimental, or predicted, enzymatic functions of *trans*-acting ribosome assembly factors, as well as their physical or functional association with snoRNA, have demonstrated that they can be grouped into sub-families based on common functions (Kressler *et al.*, 1999; Venema and Tollervey, 1999). These sub-families include components of small nucleolar ribonucleoprotein particles (snoRNPs) rRNA modifying enzymes, endo- and exonucleases and putative RNA helicases.

One of the significant metabolic burdens of a rapidly growing yeast cell is that imposed by ribosomal biosynthesis. It is estimated that under exponential growth conditions yeast allocate ~60% of the total transcription, ~50% of RNA polymerase II transcription and ~90% of mRNA splicing activities to ribosome synthesis (Warner, 1999). rRNA transcription and ribosomal subunit assembly

take place within a specialized domain of the nucleus, termed the nucleolus. As a result, the NE physically separates these processes from the site of protein synthesis. While the segregation of these assembly and operational processes is thought to provide numerous quality control checkpoints, they also demand that all components of the ribosome be correctly sorted to the appropriate compartment of the cell. Accordingly, ~150,000 ribosomal proteins must be imported into the nucleus per minute where they are assembled by over 60 different *trans*-acting nuclear factors into ~4,000 ribosomal subunits (Warner, 1999). These subunits are then exported to the cytoplasm where they are assembled on mRNA species into ~2,000 translation-competent ribosomes (Warner, 1999). Therefore, it is not surprising that eukaryotic cells dedicate a sizeable portion of their energy pools to this process and have evolved intricate mechanisms to ensure that ribosomes are synthesized flawlessly.

Members of the DEAD-box RNA helicase family are required for rRNA metabolism and, as a result, ribosome biogenesis (Venema and Tollervey, 1999). Dbp9p is an essential DEAD-box RNA helicase required for the processing of 27S rRNA precursors to mature 25S and 5.8S rRNAs (Figure 1.9.2; (Daugeron *et al.*, 2001; Kikuma *et al.*, 2004)). DEAD-box RNA helicases are thought to not only be required for the ATP-dependent dissociation of RNA-RNA substrates, but also modulate specific RNA-protein and protein-protein interactions (Lorsch and Herschlag, 1998a, b). The structural rearrangements that they govern ensure efficient and accurate ribosome biogenesis. Indeed, in the absence of Dbp9p

Figure 1.9.2: **Pre-rRNA processing pathways in *S. cerevisiae*.** An outline of ribosome synthesis, including a simplified version of the processing events required for rRNA maturation. The 90S pre-ribosome is proposed to contain the 35S pre-rRNA and the U3 snRNA. The primary RNA pol I transcript is processed at its 3' end to yield the 35S rRNA. The early rRNA cleavages at A<sub>0</sub> to A<sub>2</sub> lead to the separation of the pre-40S and pre-60S particles. In both pathways a series of predicted intermediates are drawn, which are designated early (E), middle (M) and late (L) according to their position in the proposed pathway. The processing steps associated with each of these complexes are indicated, as is the likely time of export to the cytoplasm. The 20S pre-rRNA is matured by endonucleolytic cleavage at site D. The 27SA<sub>2</sub> precursor is processed by two alternative pathways. In the major pathway, about 85% of 27SA<sub>2</sub> pre-rRNA is cleaved at site A<sub>3</sub> and then 5'→3' exonucleolytically digested to site B<sub>1S</sub>. In the minor pathway, about 15% of the 27SA<sub>2</sub> molecules are processed at site B<sub>1L</sub>. While processing at site B<sub>1</sub> is completed, the 3' end of mature 25S rRNA is generated by processing at site B<sub>2</sub>. The subsequent ITS2 processing of both 27SB species appears to be the same. Cleavage at sites C<sub>1</sub> and C<sub>2</sub> releases the mature 25S rRNA and the 7S pre-rRNA. The latter undergoes 3'→5' exonucleolytic digestion to the 3' end of the mature 5.8S rRNA. The 5S pre-rRNA is processed at its 3' end to generate the mature 5S rRNA. Nop1p, Sof1p and Dbp9p are shown at the stages of rRNA maturation where they function. Figure adapted from Kressler *et al.*, 1999 and Fatica and Tollervey, 2002.



function half-mer polysomes accumulated in the cell (Daugeron *et al.*, 2001). This terminal phenotype is indicative of early pre- ribosomal particle instability, which was highlighted by the data demonstrating that these cells were unable to process 27S rRNA precursors.

Numerous studies have focused on characterizing the components of snoRNP particles and the specific roles they play in ribosome biogenesis. Among these are Nop1p (nucleolar protein) and Sof1p (suppressor of fibrillarin), both of which are components of box C/D snoRNPs (reviewed in Fatica and Tollervey, 2002; Kressler *et al.*, 1999; Venema and Tollervey, 1999). Nop1p is encoded by an essential, evolutionarily conserved house-keeping gene that is approximately 70% identical to its human homologue fibrillarin (Aris and Blobel, 1991; Jansen *et al.*, 1991). Characterization of *nop1* temperature-sensitive mutants revealed that mutations clustered in the core of a methyltransferase-like motif (s-adenosyl-L-methione-(AdoMet)-binding domain) specifically inhibited rRNA methylation (Tollervey *et al.*, 1993), marking Nop1p as the most likely box C/D methyltransferase candidate. A recent study demonstrated that Nop1p provided a snoRNP complex, containing Nop1p, Nop58p, Nop56p and Snu13p, with the methyltransferase activity required for 2'-O-ribose methylation of rRNA *in vitro* (Galardi *et al.*, 2002). Consequently, as each eukaryotic ribosome contains ~50-100 2'-O-ribose methylation sites it appears as though all ribosome-related post-transcriptional processing events are dependent on Nop1p (Figure 1.9.2).

Sof1p was originally characterized based on its ability to suppress the temperature-sensitive phenotype of yeast *NOP1* deletion mutants expressing human fibrillarin (Jansen *et al.*, 1993). This study demonstrated that a single amino acid residue substitution in Sof1p (encoded by *sof1-56*) significantly improved growth and restored pre-rRNA processing in this strain. This substitution resides within the central domain of Sof1p that contains a G  $\beta$ -like repeat (or WD) domain also found in other nuclear factors required for ribosome biogenesis. Both Nop1p and U3 snoRNA co-purified with Sof1p-pA. In addition, *in vivo* depletion of Sof1p was found to impair pre-rRNA processing and inhibition of 18S rRNA production (Jansen *et al.*, 1993). Together, these findings characterized Sof1p as a new component of U3 snoRNP rRNA processing machinery. However, the precise molecular function Sof1p governs during rRNA processing has not yet been defined. Moreover, it is still unclear how the amino acid residue substitution within the G  $\beta$ -like motif of this protein affects its interaction with fibrillarin/Nop1p and suppresses the temperature-sensitive phenotype of this *nop1* mutant strain.

### **1.10 Goal of this study**

To enhance our general understanding of the molecular mechanisms of nucleo-cytoplasmic exchange, I have focused on characterizing how nuclear transport machinery interfaces with its cargoes and how these interactions affect cellular physiology. The goal of this study was to identify novel nuclear import cargoes for the typical yeast  $\beta$ -karyopherin, Kap121p, and characterize the

molecular mechanisms that facilitate their translocation. Temperature-sensitive mutations in *KAP121* were generated and the phenotypes associated with these mutants investigated. Potential Kap121p import cargoes were then identified using a protein A (pA) tagged version of Kap121p as a probe in overlay blot assays of yeast nuclear proteins. A combination of *ex vivo*, *in vitro* and *in vivo* techniques were then used to ascertain whether these substrates were *bona fide* Kap121p cargoes and characterize the molecular interactions required for efficient nuclear import.

## Chapter 2 - Materials and Methods

### 2.1 Materials

**2.1.1 Plasmids** – The plasmids used for cloning and those kindly provided by colleagues are described in Table 2-1.

**Table 2-1 Plasmids**

Name	Components	Source/Reference
p104-LYS	<i>Amp<sup>R</sup> CEN6/ARSH4 fl ori lacZ LYS2 KAP104</i>	Aitchison <i>et al.</i> , 1996
p12-GFP2-NLS (pKW431)	<i>Amp<sup>R</sup> 2μ P<sub>ADHI</sub> URA3 NLS nes 2xGFP</i>	Stade <i>et al.</i> , 1997
pBxAHIS5	<i>Amp<sup>R</sup> ori BioXProteinA spHIS5</i>	Aitchison <i>et al.</i> , 1995
pGEX-4T-3	<i>Amp<sup>R</sup> lacIq P<sub>uvr</sub> pBR322ori glutathione S-transferase (GST)</i>	Amersham Pharmacia Biotech
pGFP-HIS5	<i>Amp<sup>R</sup> ori GFP spHIS5</i>	Dilworth <i>et al.</i> , 2001
pHL3	<i>Cap<sup>R</sup> his3::LEU2</i>	Cross, F. R., 1997
pRpl25NLS-GFP	<i>Amp<sup>R</sup> fl 2μ P<sub>TP1</sub> ColE1ori LEU2 yEGFP3 RPI_25NLS</i>	Benjamin Timney
pRS314	<i>Amp<sup>R</sup> CEN6/ARSH4 fl ori lacZ TRP1</i>	Sikorski and Hieter, 1989
pRS315	<i>Amp<sup>R</sup> CEN6/ARSH4 fl ori lacZ LEU2</i>	Sikorski and Hieter, 1989
pRS316	<i>Amp<sup>R</sup> CEN6/ARSH4 fl ori lacZ URA3</i>	Sikorski and Hieter, 1989
pRS317	<i>Amp<sup>R</sup> CEN6/ARSH4 fl ori lacZ LYS2</i>	Sikorski and Hieter, 1989
pRS426	<i>Amp<sup>R</sup> 2μ ori fl lacZ URA3</i>	Christianson <i>et al.</i> , 1992
pSB234	<i>Amp<sup>R</sup> 2μ P<sub>TRZ1</sub> lacZ URA3</i>	Trueheart <i>et al.</i> , 1987
pUH7	<i>Amp<sup>R</sup> ura3::HIS3</i>	Cross, 1997
pYES2	<i>Amp<sup>R</sup> fl 2μ P<sub>GALJ</sub> CYC<sub>TT</sub> pUCori URA3</i>	Invitrogen, Carlsbad, CA
pYX242-GFP	<i>Amp<sup>R</sup> fl 2μ P<sub>TP1</sub> ColE1ori LEU2 yEGFP3</i>	Rosenblum <i>et al.</i> , 1998

**2.1.2 Antibodies** – The primary and secondary antibodies used in this study are described in Table 2-2.

**Table 2-2 Antibodies**

Antibody Specificity	Type <sup>a</sup>	Name	Dilution	Source/Reference
<i>Aequoria victoria</i> GFP <sup>c</sup>	rb-pc	α-GFP	1:2500	Dr. Michael Rout
Bacterial β-galactosidase	m-mc	α-β-Gal	1:1,000	Roche Applied Science
horseradish peroxidase- conjugated α-mouse IgG	dk	α-mouse-HRP	1:5,000	Amersham Pharmacia
horseradish peroxidase- conjugated α-rabbit IgG	dk	α-rabbit-HRP	1:5,000	Amersham Pharmacia
<i>S. aureus</i> protein A (pA)	rb-pc	Affinity-purified rabbit α-mouse IgG	1:5,000	ICN Biomedicals/Cappel

<i>S. cerevisiae</i> Gsp1p <sup>c</sup>	rb-pc	α-Gsp1p	1:5,000	Dwayne Weber
<i>S. cerevisiae</i> Kap104p <sup>b,c</sup>	rb-pc	α-Kap104p	1:2500	Dwayne Weber
<i>S. cerevisiae</i> Kap108p <sup>b,c</sup>	rb-pc	α-Kap108p	1:1,000	Rosanna Baker
<i>S. cerevisiae</i> Kap121p <sup>c</sup>	rb-pc	α-Kap121p	1:2,000	Marelli et al., 1998
<i>S. cerevisiae</i> Kap123p	m-pc	α-Kap123p	1:500	Rout et al., 1997
<i>S. cerevisiae</i> Nop1p	m-mc	mAb D77	1:500	Aris and Blobel, 1991

<sup>a</sup> rb, rabbit; m, mouse; dk, donkey; pc, polyclonal; mc, monoclonal.

<sup>b</sup> elicited against GST-purified Kap108p or Kap104p for Dr. Aitchison as previously described (Marelli *et al.*, 1998).

<sup>c</sup> these antibodies cross-react with glutathione S-transferase and *Staphylococcus aureus* protein A

### 2.1.3 Oligonucleotides – The oligonucleotides used in this study were

synthesized either by Sigma or IDT. These oligonucleotides are listed in Table 2-

3.

**Table 2-3 Oligonucleotides**

Name	Sequence <sup>a</sup>	Application
DBP9 5'	GCCCGGAATTC AAAATGAGCTATGAGAAAAAGTCT	pDBP9GFP and pGST-Dbp9p
DBP9 3'	GCCGTCGACTAGGATCCCTTTGAAGTTCTTCAACGGGTC	
NOP1 5'	GGCGCGAATTC AAAATGTCATTGACACCAGGTAGC	pNOP1GFP
NOP1 3'	GCCGAATCCAAAGCTTTGATTCTTCAAACCGCTTCTCAT	
NOP1-Sec#1 5'	GGCGAATTC AAAGCTTATGTCATTGACACCAGGTAGC	pGAL1-Nop1(aa1-90)-GFP and pGST-Nop1(aa1-90)
NOP1-Sec#1 3'	GCCGAATTC TGGTTCAATAACGACCTTGGC	
NOP1-Sec#2 5'	GGCGAATTC AAAGCTTATGGGTCATAGACATGCCGGTGTTAC	pGAL1-Nop1(aa91-327)-GFP and pGST-Nop1(aa91-327)
NOP1-Sec#3 5'	GGCGAATTC AAAGCTTATGGCAAAGAAGACCTAAT	
NOP1-Sec#3 3'	GCCGAATTC TTTCTTCAAACCGCTTCTCAT	pGAL1-Nop1(aa210-327)-GFP and pGST-Nop1(aa210-327)
NOP1cNLS 5'	GGCAAGCTTTGGGAGTGAACCAAGACTGGAC	pRS315-NOP1cNLS and pRS315-NOP1
NOP1cNLS 3'	GGCAAGCTTTGAATTC TACTCGACCTTCGGCTTCTTCTTGGCCCTTCTTCAAACCGCTTCTCAT	
NOP1-cNLS 3'	GGCAAGCTTTTCTTCTTCAAACCGCTTCTCAT	pRS315-NOP1
Nop1p-pA 5'	CCATATGAAAGAGACCATTGTATCGTCGTTGGTAGATACATGAGAAGCGGTTTGAAGAAAATTGAAGGTAGAGGTGAAGCTCAAAA	NOP1 genomic tagging
Nop1p-pA 3'	CGAGGGTTACAAAACTCAAATAGGAAGTGAAACTGATGGGGGAAATATATATAAACGGCTGACGGTATCGATAAGCTT	
PHO4NLS 5'	GCCGGATCCAGGCGATTGTTTCAGTGA	pGST-Pho4pNLS
PHO4NLS 3'	GCGAATTC CGCTTAGGCCGGCCCAAATGG	
SOF1 5'	GCCCGGAATTC AAAATGAAGATTAAGACCATTAAA	pSOF1GFP
SOF1 3'	GCCGTCGACTAGGATCCCTTTTCTTGTAGTATCACGTTT	
SOF1N 5'	GCCCGGAATTC AAAATGAAGATTAAGACCATTAAA	pGAL1-Sof1p(aa1-130)-GFP and pGST-Sof1p(aa1-130)
SOF1N 3'	GCCGTCGACTAGGATCCCAAATCTGGCTTCTTGTATG	
SOF1WD 5'	GCCCGGAATTC AAAATGAAGAGCCAAAATTTATG	pGAL1-Sof1p(aa131-380)-GFP and pGST-Sof1p(aa131-380)
SOF1WD 3'	GCCGTCGACTAGGATCCCAAAGCTTTACTTCTCCATAG	
SOF1C 5'	GCCCGGAATTC AAAATGGAGAGGTCTAATGTCAA	pGAL1-Sof1p(aa381-489)-GFP and pGST-Sof1p(aa381-489)
SOF1C 3'	GCCGTCGACTAGGATCCCTTTTCTTGTAGTATCACGTTT	
SOF1NLS 5'	GCCCGGAATTC AAAATGAAAAGAATCAGTAGACAT	pGAL1-Sof1p(aa411-450)-GFP and pGST-Sof1p(aa411-450)
SOF1NLS 3'	GCCGTCGACTAGGATCCCATCCTTTCTAGTACGCCCTTC	

Sof1p-pA 5'	GATTCAGGAAGAGATAGGAAAAGAAGAAAGGAAGAT GACAAACGTGATACTCAAGAAAAGATTGAAGGTAGAG GTGAAGCTCAAAAA	<i>SOF1</i> genomic tagging
Sof1p-pA 3'	AATGGTAATTTTAATTTAACGGGACTGGCGTGAACATT TATCAAATACATGTGAATTAAGCTGACGGTATCGATA AGCTT	<i>SOF1</i> genomic tagging
STE12 5'	GCCCGGAATTCCAAATGAAAGTCCAAATAACCAAT	pSTE12GFP
STE12 3'	GCCAAGCTTCGGTTGCATCTGGAAGGTTTTT	
STE12-Sec#1 5'	GGCGAATTCCAAAGCTTATGAAAGTCCAAATAACCAAT	pSte12p(aa1-252)-GFP and pGST-Ste12p(aa1-252)
STE12-Sec#1 3'	GCCGAATTCGAGGGCCACGCCTAAAAGCGG	
STE12-Sec#2 5'	GGCGAATTCCAAAGCTTATGGATGACGATGCGCCAGAA	pSte12p(aa253-493)-GFP and pGST-Ste12p(aa253-493)
STE12-Sec#2 3'	GCCGAATTCATTGTTATCACATCCTTCTGG	
STE12-Sec#3 5'	GGCGAATTCCAAAGCTTATGCTGTATCCACAAACTGCA	pSte12p(aa494-688)-GFP and pGST-Ste12p(aa494-688)
STE12-Sec#3 3'	GGCGAATTCGGTTGCATCTGGAAGGTTTTT	
STE12/MCP 5'	GGCAAGCTTTATGAACTCTAGAGTGTTCATAATTTGAA	pRS426-STE12 and pRS316- STE12cNLS
STE12/MCP 3'	GCCCTCGAGTTAACTATTATGAMCATCGATGCCTTCACC	
STE12cNLS 3'	GCCGAATTCAGAGCTCGACCTTCCGCTTCTTCTGGGC CCGGTTGAATCTGGAAGGTTTTT	pRS316-STE12cNLS
T7	AATACGACTCACTATAGGG	Marker Swap
T3	ATTAACCTCACTAAAGGG	
M13 forward	GTAAAACGACGGCCAG	Marker Swap
M13 reverse	CAGGAACAGCTATGAC	
YES2-KAP123 5'	GCCGAGCTCAAAAATGGATCAACAATTTCTAAGT	pGAL1-KAP123-LEU2
YES2-KAP123 3'	GCCTCTAGAGGGCAGGTGCCTAAGATTGGGTGG	
YES2-KAP108 5'	GCCGAGCTCAAAAATGGTACAAGAACAGGCCAATT	pGAL1-KAP108-LEU2
YES2-KAP108 3'	GCCTCTAGAGGGCTGATCCGGTTAAGTCGGAGG	
LEU2/pYES2 5'	GGCGGCGCTAGCATCAAAATTCGATGACTGGAAA	pYES2-LEU2
LEU2/pYES2 3'	GGCGGCGGGCCCTTAAGCAAGGATTTTCTTAAC	
F854	AGTTATCGAAGTTCGGAG	<i>KAP121</i> sequencing
F1237	CCCTTCTCGAAGCTTAT	
F1632	GTGAGTGGTCCAAGTTAG	
F2036	GACCACGCTCGTCAAGCT	
F2443	CGCTCCGAAGGATATTC	
F2830	CCGAATTCTGGGTGATGA	
F3235	GTTGTGGCATAAAGCTTC	
F3641	GTAGTTATTGGTGACTTG	
F4058	CGCCAATTGTGTGTGCTC	
R1191	GCAACTGTTGTATCTGGGAG	
R1599	GCCGTAAGTGCAGCAATT	
R2015	CATCGGTATCGTCAGATT	
R2402	GAACTCTTGAGGTGCATT	
R2799	GATCTGAGCGCATCATCT	
R3210	CCGGTGGCTGCAAGTAAA	
R3602	GGAAATGTGTTTATCATAG	
R4015	GGCAGCTTCTTTGTCAGT	
R4403	CGCTATTACCACCGGTAA	

<sup>a</sup> Restriction endonuclease recognition sites are underlined.

**2.1.4 Standard buffers and solutions** – The buffers and solutions used in this study are described in Table 2-4.

**Table 2-4 Buffers**

Solution	Composition	Reference
6 x sample dye	30% glycerol, 0.25% bromophenol blue, 0.25% xylene cyanole	Maniatis <i>et al.</i> , 1982
6X SDS sample buffer	375 mM Tris-HCl (pH 6.8), 60 mM DTT, 60% glycerol, 12% SDS and 0.006% bromophenol blue	Ausubel <i>et al.</i> , 1994
amido black stain	40% (v/v) methanol, 10% (v/v) acetic acid, 0.1% Naphthol Blue Black	Ausubel <i>et al.</i> , 1994
binding buffer	20 mM HEPES-KOH pH 6.8, 2 mM MgOAc <sub>2</sub> , 150 mM KOAc	Rexach and Blobel, 1995
blocking buffer	TBS-T, 5% skim milk powder	Ausubel <i>et al.</i> , 1994
breakage buffer	10 mM Tris-HCl (pH 8.0), 100 mM NaCl, 1 mM EDTA, 2% Triton X-100, 1% SDS	Ausubel <i>et al.</i> , 1994
Coomassie blue stain	0.1% Coomassie Brilliant Blue R-250, 10% (v/v) acetic acid, 35% (v/v) methanol	Ausubel <i>et al.</i> , 1994
destain	10% (v/v) acetic acid, 35% (v/v) methanol	Ausubel <i>et al.</i> , 1994
elution buffer	20 mM HEPES-KOH pH 7.5, 0.05% Tween 20	Dilworth <i>et al.</i> , 2001
glutathione elution buffer	20 mM reduced glutathione, 100 mM Tris-HCl pH 8.0, 120 mM NaCl	Leslie <i>et al.</i> , 2004
loading buffer	Binding Buffer + (30 mM EDTA, 4 mM DTT, 3 mM GTP or GDP)	Rexach and Blobel, 1995
magic A	1 M unbuffered Tris, 13% SDS	
magic B	0.2 M DTT, 30% glycerol, 0.002% bromophenol blue	
PVP solution	8% PVP, 20 mM potassium phosphate (pH 6.5), 0.75 M MgCl <sub>2</sub>	Rout and Blobel, 1993
running buffer	50 mM Tris, 0.4 M glycine, 1% SDS	Ausubel <i>et al.</i> , 1994
solution P	0.4 mg/ml pepstatin A, 18 mg/ml phenylmethylsulfonyl fluoride	Aitchison <i>et al.</i> , 1996
STE	100 mM NaCl, 10 mM Tris-HCl pH 7.5, 1 mM EDTA	Ausubel <i>et al.</i> , 1994
0.5X TBE	44.5 mM Tris, 44.5 mM boric acid, 0.5 mM EDTA	Maniatis <i>et al.</i> , 1982
TBE	89 mM Tris, 89 mM Boric Acid, 1 mM EDTA	Maniatis <i>et al.</i> , 1982
TBS-T	100 mM Tris-HCl (pH 7.5), 150 mM NaCl, 0.1% Tween 20	Huynh <i>et al.</i> , 1985
TE	10 mM Tris-HCl (pH 7.0-8.0, as required), 1 mM EDTA	Maniatis <i>et al.</i> , 1982
transfer buffer	25 mM Tris base, 192 mM glycine, 0.1% SDS, 20% (v/v) methanol	Towbin <i>et al.</i> , 1979; Burnette <i>et al.</i> , 1981
10X transport buffer (10X TB)	200 mM Hepes-KOH, 1.1 M KOAc, 20 mM MgCl <sub>2</sub> , 10 μM ZnCl <sub>2</sub> , 10 μM CaCl <sub>2</sub> , 10 mM DTT, 1% Tween 20, pH 7.5	Aitchison <i>et al.</i> , 1996
transport buffer (TB)	20 mM Hepes-KOH, 110 mM KOAc, 2 mM MgCl <sub>2</sub> , 1 μM ZnCl <sub>2</sub> , 1 μM CaCl <sub>2</sub> , 1 mM DTT, 0.1% Tween 20, pH 7.5	Aitchison <i>et al.</i> , 1996
transport buffer 2 (TB2)	TB plus, 0.2% casamino acids, ~40 ng/μl BSA	Leslie <i>et al.</i> , 2004
wash buffer (WB)	150 mM NaCl, 0.1 mM MgCl <sub>2</sub> , 0.1% Tween-20, 50 mM Tris-HCl, pH 7.5	Dilworth <i>et al.</i> , 2001

## 2.2 Microorganisms and culture conditions

**2.2.1 Bacterial strains and culture conditions** – *E. coli* strains and culture media used in this study are described in Tables 2-5 and Tables 2-6, respectively. Unless otherwise stated, bacteria cultures were grown at 37°C. Cultures of 3 mL or less were grown in 16 x 150mm glass tubes in an orbital shaker at 200 rpm. Cultures greater than 3 mL were grown in flasks and did not exceed 25% of the flask volume.

**Table 2-5 *E. coli* strains**

Strains	Genotype	Source
DH5 $\alpha$	F <sup>-</sup> $\phi$ 80d <i>lacZ</i> $\Delta$ M15 $\Delta$ ( <i>lacZYA-argF</i> )U169 <i>deoR recA1 endA1 hsdR17</i> ( $\tau_k$ , $m_k$ <sup>+</sup> ) <i>phoA supE44 <math>\lambda</math>-thi-1 gyrA96 relA1</i>	Gibco/BRL or BioLine
Bl21(DE3)pLysS	F <sup>-</sup> <i>ompT hsdS<sub>B</sub></i> ( $\tau_B$ $m_B$ ) <i>gal dem</i> (DE3) pLysS (CamR)	Invitrogen

**Table 2-6 Bacterial culture media**

Medium	Composition	Reference
LB <sup>a,b</sup>	1.0% tryptone, 0.5% yeast extract, 1% NaCl	Maniatis <i>et al.</i> , 1982
SOB	2% tryptone, 0.5% yeast extract, 10 mM NaCl, 2.5 mM KCl	Maniatis <i>et al.</i> , 1982
SOC	SOB + (10 mM MgCl <sub>2</sub> , 10 mM MgSO <sub>4</sub> , 0.36% glucose)	Maniatis <i>et al.</i> , 1982
Terrific Broth (TBr) <sup>a</sup>	1.27% tryptone, 2.55% yeast extract, 0.57% glycerol, 44 mM potassium phosphate (pH 6.4)	Maniatis <i>et al.</i> , 1982

<sup>a</sup> For plasmid selection ampicillin or chloramphenicol was added to 100  $\mu$ g/mL or 34  $\mu$ g/mL, respectively, as necessary.

<sup>b</sup> Agar was added to 2% for solid media.

**2.2.2 *S. cerevisiae* strains and culture conditions** – The *S. cerevisiae* strains used in this study are described in Table 2-7. Yeast culture media are described in Table 2-8. Cultures of 5 mL or less were grown in 16 x 150 mm glass tubes in either an orbital shaker at 180-200 rpm or in a rotating wheel. Cultures of greater volume were grown in flasks and culture volumes did not exceed 50% of the flask volume.

**Table 2-7 *S. cerevisiae* strains**

Strains	Genotype	Reference/Source
DF5	<i>Mata/Mat<math>\alpha</math> ura3-52/ura3-52 his3<math>\Delta</math>200/his3<math>\Delta</math>200 trp1-1/trp1-1 leu2-3, 112/leu2-3, 112 lys2-801/lys2-801</i>	Aitchison <i>et al.</i> , 1996

<i>Δkap104</i>	<i>Matα ura3-52 his3Δ200 trp1-1 leu2-3, 112 hys2- 801 kap104::ura3::HIS3 pKAP104-URA3</i>	Aitchison <i>et al.</i> , 1996
<i>Δkap108</i>	<i>Matα ura3-52 his3Δ200 trp1-1 leu2-3, 112 hys2- 801 kap108::ura3::his3::LEU2 pKAP108-URA3</i>	Rosanna Baker
<i>Δkap121/pKAP121-URA3</i>	<i>Mata ura3-52 his3Δ200 trp1-1 leu2-3, 112 hys2- 801 kap121::ura3::HIS3 pKAP121-URA3</i>	Section 2.7.1
<i>Δkap121LEU2/pKAP121-URA3<sup>i</sup></i>	<i>Mata ura3-52 his3Δ200 trp1-1 leu2-3, 112 hys2- 801 kap121::ura3::his3::LEU2 pKAP121-URA3</i>	Section 2.7.1
<i>Δkap121LEU2<sup>ΔN11</sup>/pKAP121-URA3<sup>i</sup></i>	<i>Mata ura3<sup>c</sup> his<sup>d</sup> trp1<sup>c</sup> leu2<sup>e</sup> hys2<sup>s</sup> kap121::ura3::his3::LEU2 pKAP121-URA3</i>	Section 2.14.4
<i>Δkap121LEU2<sup>ΔN13</sup>/pKAP121-URA3<sup>i</sup></i>	<i>Mata ura3<sup>c</sup> his<sup>d</sup> trp1<sup>c</sup> leu2<sup>e</sup> hys2<sup>s</sup> kap121::ura3::his3::LEU2 pKAP121-URA3</i>	Section 2.14.4
<i>Δkap121LEU2<sup>ΔN7</sup>/pKAP121-URA3<sup>i</sup></i>	<i>Mata ura3<sup>c</sup> his<sup>d</sup> trp1<sup>c</sup> leu2<sup>e</sup> hys2<sup>s</sup> kap121::ura3::his3::LEU2 pKAP121-URA3</i>	Section 2.14.4
<i>kap104-16<sup>i</sup></i>	<i>Matα ura3<sup>a</sup> his3<sup>b</sup> trp1-1 leu2-3, 112 hys2- 801 kap104::ura3::HIS3 pkap104-16 Gal<sup>R</sup></i>	Section 2.7.4
<i>kap104-16</i>	<i>Matα ura3-52 his3Δ200 trp1-1 leu2-3, 112 hys2- 801 kap104::ura3::HIS3 pkap104-16</i>	Aitchison <i>et al.</i> , 1996
<i>KAP104-A</i>	<i>Matα ura3-52 his3Δ200 trp1-1 leu2-3, 112 hys2- 801 KAP104-pA/HIS5</i>	Aitchison <i>et al.</i> , 1996
<i>KAP108-A</i>	<i>Mata ura3-52 his3Δ200 trp1-1 leu2-3, 112 hys2- 801 KAP108-pA/HIS5</i>	Rosanna Baker
<i>kap121-18</i>	<i>Mata ura3-52 his3Δ200 trp1-1 leu2-3, 112 hys2- 801 kap121::ura3::HIS3 pkap121-18</i>	Section 2.7.2
<i>kap121-26</i>	<i>Mata ura3-52 his3Δ200 trp1-1 leu2-3, 112 hys2- 801 kap121::ura3::HIS3 pkap121-26</i>	Section 2.7.2
<i>kap121-34<sup>i</sup></i>	<i>Matα ura3<sup>a</sup> his3<sup>b</sup> trp1-1 leu2-3, 112 hys2- 801 ade2-1 kap121::ura3::HIS3 pkap121-34 Gal<sup>R</sup></i>	Section 2.7.4
<i>kap121-34</i>	<i>Mata ura3-52 his3Δ200 trp1-1 leu2-3, 112 hys2- 801 kap121::ura3::HIS3 pkap121-34</i>	Section 2.7.2
<i>kap121-34, Δkap108/pKAP108-URA3</i>	<i>Mata ura3-52 his3Δ200 trp1-1 leu2-3, 112 hys2- 801 kap108::ura3::his3::LEU2 kap121::ura3::HIS3 pkap121-41 pKAP108-URA3</i>	Section 2.7.5
<i>kap121-34LEU2<sup>ΔN7</sup></i>	<i>Mata ura3<sup>c</sup> his<sup>d</sup> trp1<sup>c</sup> leu2<sup>e</sup> hys2<sup>s</sup> kap121::ura3::his3::LEU2 pkap121-34</i>	Section 2.14.4
<i>kap121-34LEU2, Δkap104/pKAP104-URA3<sup>i</sup></i>	<i>Mata ura3-52 his3Δ200 trp1-1 leu2-3, 112 hys2- 801 kap121::ura3::his3::LEU2 kap104::ura3::HIS3 pkap121-41 pKAP104-URA3</i>	Section 2.7.5
<i>kap121-41</i>	<i>Mata ura3-52 his3Δ200 trp1-1 leu2-3, 112 hys2- 801 kap121::ura3::HIS3 pkap121-41</i>	Section 2.7.2
<i>KAP121-A<sup>h</sup></i>	<i>Mata ura3-52 his3Δ200 trp1-1 leu2-3, 112 hys2- 801 KAP121-pA/HIS5</i>	Rout <i>et al.</i> , 1997
<i>kap121-34LEU2<sup>i</sup></i>	<i>Mata or Matα ura3-52 his3Δ200 trp1-1 leu2-3, 112 hys2- 801 kap121::ura3::his3::LEU2 pkap121-34</i>	Section 2.7.2
<i>KAP123-A</i>	<i>Mata ura3-52 his3Δ200 trp1-1 leu2-3, 112 hys2- 801 KAP123-pA/HIS5</i>	Rout <i>et al.</i> , 1997
<i>kap95-14</i>	<i>Matα ura3-52 his3Δ200 trp1-1 leu2-3, 112 hys2- 801 kap104::ura3::HIS3 pkap95-14</i>	Leslie <i>et al.</i> , 2002
<i>KAP95-A</i>	<i>Mata ura3-52 his3Δ200 trp1-1 leu2-3, 112 hys2- 801 KAP95-pA/HIS5</i>	Rout <i>et al.</i> , 1997
<i>NOP1-A</i>	<i>Matα ura3-52 his3Δ200 trp1-1 leu2-3, 112 hys2- 801 NOP1-pA/HIS5</i>	Section 2.8.1
<i>NOP1-GFP</i>	<i>Matα ura3-52 his3Δ200 trp1-1 leu2-3, 112 hys2- 801</i>	Section 2.8.2

	NOP1-GFP/HIS5	
NOP1-GFP, $\Delta kap121$ LEU2/pKAP121- URA3 <sup>i</sup>	Mata <i>ura3-52 his3<math>\Delta</math>200 trp1-1 leu2-3, 112 lys2-801</i> NOP1-GFP/HIS5 <i>kap121::ura3::his3::LEU2 pKAP121- URA3</i>	Section 2.8.2
NOP1-GFP, <i>kap121- 34</i> LEU2/LYS2 <sup>h</sup>	Mata <i>ura3-52 his3<math>\Delta</math>200 trp1-1 leu2-3, 112 lys2-801</i> NOP1-GFP/HIS5 <i>kap121::ura3::his3::LEU2 pkap121-34- LYS2</i>	Section 2.8.2
NOP1-GFP, <i>kap121- 34</i> LEU2/LYS2, <i>kap104-16</i> <sup>f</sup>	Mata <i>ura3-52 his3<math>\Delta</math>200 trp1-1 leu2-3, 112 lys2-801</i> NOP1-GFP/HIS5 <i>kap121::ura3::his3::LEU2</i> <i>kap104::ura3::HIS3 pkap121-34-LYS2 pkap104-16</i>	Section 2.8.2
SK1	Mata <i>bo::LYS2 lys2 ura3 leu2::hisG trp1::hisG arg4-Bgl his4b</i>	Lydall <i>et al.</i> , 1996
SOF1-A	Mata <i>ura3-52 his3<math>\Delta</math>200 trp1-1 leu2-3, 112 lys2-801</i> SOF1-pA/HIS5	Section 2.8.1
SOF1-GFP	Mata <i>ura3-52 his3<math>\Delta</math>200 trp1-1 leu2-3, 112 lys2-801</i> SOF1-GFP/HIS5	Section 2.8.2
SOF1-GFP, $\Delta kap121$ LEU2/pKAP121- URA3 <sup>i</sup>	Mata <i>ura3-52 his3<math>\Delta</math>200 trp1-1 leu2-3, 112 lys2-801</i> SOF1- GFP/HIS5 <i>kap121::ura3::his3::LEU2 pKAP121-URA3</i>	Section 2.8.2
SOF1-GFP, <i>kap121- 34</i> LEU2/LYS2 <sup>h</sup>	Mata <i>ura3-52 his3<math>\Delta</math>200 trp1-1 leu2-3, 112 lys2-801</i> SOF1- GFP/HIS5 <i>kap121::ura3::his3::LEU2 pkap121-34-LYS2</i>	Section 2.8.2
SOF1-GFP, <i>kap121- 34</i> LEU2/LYS2, <i>kap104-16</i> <sup>f</sup>	Mata <i>ura3-52 his3<math>\Delta</math>200 trp1-1 leu2-3, 112 lys2-801</i> SOF1- GFP/HIS5 <i>kap121::ura3::his3::LEU2 kap104::ura3::HIS3</i> <i>pkap121-34-LYS2 pkap104-16</i>	Section 2.8.2
W303	Mata/Mata <i>ade2-1/ade2-1 ura3-1/ura3-1 his3-11, 15/his3-11, 15 trp1-1/trp1-1 leu2-3, 112/leu2-3, 112 can1-100/can1-100</i>	Rout <i>et al.</i> , 1997

<sup>a</sup> *ura3-52* or *ura3-1*.

<sup>b</sup> *his3 $\Delta$ 200* or *his3-11*.

Gal<sup>R</sup> galactose-responsive, these strains are underlined.

<sup>c</sup> *ura3* or *ura3-52*.

<sup>d</sup> *his3 $\Delta$ 200* or *his4b*.

<sup>e</sup> *trp1-1* or *trp1::hisG*.

<sup>f</sup> *leu2-3, 112* or *leu2::hisG*.

<sup>g</sup> *lys2-801* or *lys2*.

<sup>h</sup> originally termed *PSE1-A*.

<sup>i</sup> all derivatives of  $\Delta kap121$ , *kap121-34* or *kap104-16* strains are referred to as  $\Delta kap121$ , *kap121-34* or *kap104-16* in Chapters 3 and 4. Consult the sections below for exact strain used in each experiment.

**Table 2-8 Yeast culture media**

Medium	Composition <sup>a, b</sup>	Reference
YEPD	1% yeast extract, 2% peptone, 2% glucose	Ausubel <i>et al.</i> , 1994
YEPGal	1% yeast extract, 2% peptone, 2% galactose	Ausubel <i>et al.</i> , 1994
Sporulation Media	1% potassium acetate, 0.1% yeast extract, 0.05% glucose	Ausubel <i>et al.</i> , 1994
CSMD	0.17% YNB-AA/AS, 0.5% (NH <sub>4</sub> ) <sub>2</sub> SO <sub>4</sub> , CSM dropout powder (minus the appropriate amino acids and nucleotides) according to manufacturer, 2% glucose	Ausubel <i>et al.</i> , 1994
CSMGal	0.17% YNB-AA/AS, 0.5% (NH <sub>4</sub> ) <sub>2</sub> SO <sub>4</sub> , CSM dropout powder (minus the appropriate amino acids and nucleotides) according to manufacturer, 2% galactose	Ausubel <i>et al.</i> , 1994
5-fluoro-orotic acid (5-FOA)	0.1% 5-FOA, 0.13% CSM-Ura dropout powder, 0.17% YNB-AA/AS, 0.5% (NH <sub>4</sub> ) <sub>2</sub> SO <sub>4</sub> , 2% dextrose, 12 $\mu$ g/mL uracil	Ausubel <i>et al.</i> , 1994

<sup>a</sup> For solid media, agar was added to 2%.

<sup>b</sup> Glucose and galactose were added from stock solutions after autoclaving.

**2.2.3 Yeast mating** – *S. cerevisiae* strains were mated using a nutritional complementation method (Ausubel *et al.*, 1994). Freshly grown haploid strains of different mating types were patched individually and mixed on the surface of a YEPD agar plate. The plates were incubated at room temperature for 5 hrs. The haploid strains and the mating mixture were then restreaked onto a CSMD plate lacking the appropriate amino acids and nucleotides to select for the desired diploid strain and incubated at 23°C for three to five days.

**2.2.4 Sporulation and tetrad dissection** – *S. cerevisiae* diploid strains were sporulated in liquid culture as previously described (Ausubel *et al.*, 1994). Diploid strains were grown to saturation in the appropriate selection medium. Cells from 1 mL of the culture were harvested, washed with sterile water, resuspended in 5 mL YEPA and incubated at 23°C for 5 hrs. Cells from 1 mL of this culture were harvested, resuspended in 1mL sporulation media, incubated at 23°C for 2-5 days and monitored for the formation of tetrads.

Tetrads were prepared for dissection using a modified version of the Zymolyase 100T protocol described in Ausubel *et al.* (1994). Cells (consisting of a mixture of tetrads and single cells) from 100 µL of the sporulation culture were harvested and washed twice with 500 µL sterile water. The pellet was resuspended in 500 µL sterile water, diluted 1/10 with sterile water and Zymolyase 100T added to a final concentration of 10 µg/µL. Following a 15 to 30 min incubation at 23°C, 10 µL of the cell suspension were plated on YEPD agar

and the tetrads were dissected using a Nikon Eclipse E400 microscope equipped with a manual micromanipulation stage. The dissection plates were incubated at 23°C for 5 days and the desired haploid strains selected based on their ability to grow on the appropriate selection media.

## **2.3 Isolation of DNA from microorganisms**

Unless otherwise stated, reactions were in 1.7 mL microcentrifuge tubes and microcentrifugation was performed at 16,000 x *g*.

**2.3.1 Plasmid DNA isolation from bacteria** – Single bacterial colonies were inoculated into 3 mL of LB (Table 2-6) containing ampicillin and grown overnight. Plasmid DNA was isolated from the culture by alkaline lysis (Maniatis *et al.*, 1982) or by using a QIAprep Miniprep Kit (Qiagen).

For the alkaline lysis method, cells were harvested by microcentrifugation and resuspended in 100 µL 50 mM Tris-HCl (pH 7.5), 10 mM EDTA containing 100 µg of RNase A/mL. Samples were gently mixed by inversion with 200 µL of 0.2 M NaOH containing 1% SDS and incubated on ice for 10 min. 150 µL of 1.25 M KOAc, 7% glacial acetic acid was added, the samples mixed by inversion and incubated on ice for 10 min. The precipitate was pelleted by microcentrifugation for 5 min at 4°C. The supernatant was extracted with an equal volume of phenol/chloroform/isoamyl alcohol (25:24:1) extraction. The supernatant was recovered and extracted again with chloroform/isoamyl alcohol (24:1). The DNA was precipitated from the aqueous phase by the addition of ethanol as described

in Section 2.4.7 and resuspended in 40  $\mu$ L of TE (pH 8.0) (Table 2-4) containing 20  $\mu$ g of RNase A/mL.

Plasmid DNA isolation using the QIAprep Miniprep Kit was performed according to the manufacturer's instructions. This is essentially an alkaline lysis method. Following lysis and protein precipitation, plasmid DNA was adsorbed onto a silica gel membrane. Chaotropic salts were passed over the column to remove contaminating proteins; these residual salts were then removed by washing with Qiagen wash buffer (Buffer PE) and plasmid DNA was eluted in 50  $\mu$ L of 10 mM Tris-HCl (pH 7.5).

**2.3.2 Chromosomal DNA isolation from *S. cerevisiae*** – Chromosomal DNA was isolated from yeast by a rapid isolation procedure (Ausubel *et al.*, 1994). Yeast cells were grown overnight in 5 mL of YEPD or the appropriate CSMD. Cells were harvested by centrifugation, washed twice with 5 mL of water, transferred to a 1.7 mL microcentrifuge tube and washed once with breakage buffer (Table 2-4). To simultaneously break yeast cells and separate nucleic acids from proteins, cells were mixed with 200  $\mu$ L each of breaking buffer, acid-washed glass beads (Sigma) and phenol/cholorform/isoamyl alcohol (25:24:1). The samples were vortexed for 3 min at 4<sup>o</sup>C. 200  $\mu$ L of TE (pH 8.0) were added, the mixture was vortexed briefly, and the aqueous and organic layers separated by centrifugation for 5 min. DNA was purified and precipitated from the aqueous solution as described in Section 2.4.7. To remove excess salts, the recovered nucleic acids were resuspended in 100  $\mu$ L of water, ethanol precipitated a

second time and resuspended in 100  $\mu$ L of TE (pH 8.0) containing 20  $\mu$ g of RNase A/mL.

**2.3.3 Plasmid DNA isolation from *S. cerevisiae*** – Plasmid borne *kap121* temperature-sensitive (ts) alleles were recovered using a modified version of the method described in Section 2.3.2. *kap121-ts* strains were grown overnight in CSMD medium lacking the appropriate amino acids and nucleotides at 23°C and isolated nucleic acids were resuspended 20  $\mu$ L of water. The recovered plasmid DNA was amplified by transformation into *E. coli* (Section 2.5.1) followed by plasmid DNA isolation (Section 2.3.1).

## 2.4 Standard DNA manipulations

Unless otherwise stated, reactions were in 1.7 mL microcentrifuge tubes and microcentrifugation was performed at 16,000 x *g*.

**2.4.1 Amplification of DNA by polymerase chain reaction (PCR)** – PCR was used to introduce mutations within a specific gene, amplify specific DNA sequences and facilitate cloning. All PCR reactions discussed in this work were performed using the Expand Long Template PCR system (Roche) following the manufacturer's instructions. Reactions were performed in 0.6 mL microcentrifuge tubes and typically contained 10 U of Expand DNA polymerase, 0.5  $\mu$ g of template DNA, 100 pmol of each primer, 20 mM of each of dATP, dCTP, dGTP and dTTP in 100  $\mu$ L of reaction buffer. Reactions were overlaid with mineral oil, and, in general, the DNA was denatured at 95°C for 1 min,

renatured at temperatures between 55°C and 65°C, depending on the primers use, for 45 sec and elongated at 68°C for 3 min. Samples were cycled under these conditions 30 times in a Robocycler 40 (Stratagene) or a PTC-200 (MJ Research).

**2.4.2 Random PCR mutagenesis** – Mutagenesis PCR reactions were performed as previously described (Muhlrad *et al.*, 1992) in 0.6 mL microcentrifuge tubes. Reactions contained 0.1 U of Taq DNA polymerase/ $\mu\text{L}$ , 0.05  $\mu\text{g}$  of template DNA/ $\mu\text{L}$ , 1 pmol of each primer/ $\mu\text{L}$ , 100  $\mu\text{M}$  dGTP, 100  $\mu\text{M}$  dCTP, 100  $\mu\text{M}$  dTTP, and 5  $\mu\text{M}$  dATP and carried out as described above.

**2.4.3 Restriction endonuclease digestion** – DNA was digested according to the manufacturer's instructions. For diagnostic and preparative digests, approximately 0.5  $\mu\text{g}$  and 3-5  $\mu\text{g}$  of DNA, respectively, were digested for 2-16 hrs. Double digests were carried out according to the instructions supplied in the NEB or Fermentas catalogs.

**2.4.4 Dephosphorylation of 5' ends** – Prior to ligation, plasmids digested with one restriction endonuclease were dephosphorylated to prevent self-ligation. Immediately after plasmid digestion, 5 U of CIAP was added to the reaction and incubated at 37°C for 30 min. Dephosphorylation reactions were terminated by the addition of EDTA to a final concentration of 10 mM, followed by a 1 hr incubation at 72°C. The dephosphorylated plasmids were phenol/chloroform/

isoamyl alcohol (25:24:1) and chloroform/isoamyl alcohol (24:1) extracted, and precipitated as described in Section 2.4.7.

**2.4.5 Separation of DNA fragments by agarose gel electrophoresis** – 6 x sample dye (Maniatis *et al.*, 1982) was added to the DNA in solution at a ratio of 1:5 and the DNA fragments were separated in agarose gels containing 0.5 µg ethidium bromide/mL in TBE (Table 2-4). Fragments of 300 bp or less were separated in 2% agarose gels; larger DNA fragments were separated in 0.8% agarose gels. DNA was visualized using a BioRad ultra-violet transilluminator (Hercules, CA).

**2.4.6 Purification of DNA fragments from agarose gels** – DNA fragments were isolated from SeaKem GTG agarose (Cambrex) gels by electroelution using a unidirectional eluter. Briefly, the eluter was filled with 0.5X TBE, a gel slice containing the DNA fragment of interest was placed in the platform slot and 80 µL of 7.5 M ammonium acetate containing 0.25% bromophenol blue was placed in the V-channel collection tube. The DNA fragment was transferred from the gel slice to the salt solution at 100 V for 30 to 60 min. The salt/DNA mixture (~300 µL) was removed from the V-channel, the DNA was precipitated by the addition of 2.5 vol of EtOH and 1 µg glycogen, and resuspended in 10 µL of water.

Alternatively, DNA fragments were isolated from agarose gel slices using a QIAquick Gel Extraction Kit (Qiagen) according to the manufacturer's instructions. The gel slice containing the DNA fragment of interest is dissolved

and the DNA adsorbed onto a silica-gel surface. Contaminants were then removed by washing with Qiagen wash buffer (Buffer PE) and the DNA fragments were eluted in 20  $\mu$ L of 10 mM Tris-HCl (pH 7.5).

#### **2.4.7 Purification and concentration of DNA from solution –**

Phenol/chloroform/isoamyl alcohol extraction and precipitation with ethanol or a QIAquick PCR Purification Kit were used to concentrate DNA and remove contaminants (small oligonucleotides, salt, dyes ethidium bromide, nucleotide triphosphates and proteins). Purification and concentration of DNA using the QIAquick PCR Purification Kit was performed according to the manufacturer's instructions. DNA fragments (100 bp to 10 kbp) were adsorbed onto a silica-gel surface, contaminants were removed by washing with Qiagen wash buffer (Buffer PE), and the DNA fragments were eluted in 20 to 50  $\mu$ L of Tris-HCl (pH 8.5).

Alternatively, DNA in 100 to 300  $\mu$ L of aqueous solution was purified by phenol/chloroform/isoamyl alcohol extraction. Samples were vortexed with an equal volume of phenol/chloroform/isoamyl alcohol (25:24:1), and the organic and aqueous phases were separated by microcentrifugation for 3 min. The aqueous layer was extracted against an equal volume of chloroform/isoamyl alcohol (24:1) as described above. The aqueous phase was recovered and the DNA was precipitated by adding 0.1 volume of 3 M NaOAc and 2.5 volumes of ice-cold absolute ethanol, followed by incubation at  $-20^{\circ}\text{C}$  for 30 min. The precipitate was pelleted by microcentrifugation for 20 min and the salts were removed by washing the pellet with 70% ethanol. The pellet was dried and

dissolved in a minimal volume of water. No additional salt was added to the precipitation reaction if the DNA solution contained a high concentration of salt (> 0.3 M). Finally, if the DNA concentration was low (< 100 ng), 1 µg glycogen was added to the precipitation reactions as a carrier.

**2.4.8 DNA ligation reactions** – T4 DNA ligase (Roche or Fermentas) was used to construct the hybrid DNA plasmids described in this study (Section 2.6). The DNA fragments to be ligated were obtained by restriction endonuclease digestion (Section 2.4.3). Prior to ligation the 5' ends of singly digested plasmids were dephosphorylated to prevent intramolecular ligation (Section 2.4.4). DNA fragments to be ligated were purified by agarose gel electrophoresis (Section 2.4.5 and 2.4.6). The appropriate purified DNA fragments were combined and treated with T4 DNA ligase according to the manufacturer's specifications in ligase buffer containing 1 mM ATP, with the final reaction volume being 10 µL. The final concentration of DNA in each ligation reaction was approximately 60 mM. The DNA fragments were pooled at fragment to plasmid molar ratios between 3:1 and 7:1, and the reactions were incubated at 16°C for ~18 hrs. 3 µL of the ligation reaction was introduced into *E. coli* (Section 2.5.1). Plasmids were isolated (Section 2.3.1) and the desired recombinant plasmids identified by restriction endonuclease digestion.

## **2.5 Introduction of DNA into microorganisms**

DNA was introduced into *E. coli* via chemical transformation and transformants were identified by antibiotic selection. DNA was introduced into *S. cerevisiae* by electroporation and the transformants were identified by auxotrophic selection.

**2.5.1 Chemical transformation of *E. coli*** – Plasmid DNA was introduced into commercially available transformation-competent DH5 $\alpha$  (subcloning efficiency) or BL21(DE3)pLysS (Table 2-5) as instructed by the manufacturer. Generally, 3  $\mu$ L of a ligation reaction, or  $\sim$ 0.5  $\mu$ g of plasmid DNA, were added to 25 to 50  $\mu$ L of cells. The mixture was incubated on ice for 30 min, subjected to heat shock at 42 $^{\circ}$ C (for DH5 $\alpha$ ) or 37 $^{\circ}$ C (for BL21(DE3)pLysS) for 30 or 45 sec, respectively, and then returned to ice for 2 min. 1 mL of SOC (Table 2-6) was added and the cells were allowed to recover in a 37 $^{\circ}$ C water bath shaker for 1 hr. The cells were concentrated by centrifugation at 2500 x *g* for 5 min and spread onto LB agar plates containing ampicillin (Table 2-6) for antibiotic selection and incubated at 37 $^{\circ}$ C for  $\sim$ 18 hrs. When necessary, 60  $\mu$ L of 2% X-gal and 10  $\mu$ L 1M isopropyl- $\beta$ -D-thiogalactopyranosid (IPTG) were spread onto plates prior to plating of cells.

**2.5.2 Electroporation of *S. cerevisiae*** – Electro-competent yeast cells were prepared as described in Ausubel *et al.* (1994). Yeast strains were grown overnight in 5 mL of YEPD (Table 2-8) at 30 $^{\circ}$ C (for wild-type strains) or 23 $^{\circ}$ C (for temperature-sensitive strains). 1 mL of the culture was added to 50 mL of YEPD

and the cells were grown to an OD<sub>600</sub> of ~0.8. Cells were harvested by centrifugation at 4,000 x *g* for 5 min, resuspended in TE (pH 7.5) (Table 2-4) containing 10 mM lithium acetate and incubated for 30 min at 30°C with gentle agitation. 1 M dithiothreitol (DTT) was added to a final concentration of 20 mM and the cells were incubated at 30°C with agitation for an additional 15 min. Cells were harvested by centrifugation 4,000 x *g*, washed twice with 1 mL ice cold water, twice with ice cold 1 M sorbitol and resuspended in a minimal volume of 1 M sorbitol. 0.5 to 1 µg of plasmid DNA, or ~200 ng of linear DNA, were mixed with 40 µL of these electro-competent cells and pulsed in a pre-chilled 2 mm gap width BioRad electroporation cuvette at 16kV, 25 µF, 200 Ω using a BioRad Gene Pulser. 100 µL of ice-cold 1 M sorbitol were immediately added to the cells and the suspension was plated onto appropriate selective media agar plates. Plates were incubated at 23°C or 30°C, depending upon the strain. Transformed colonies were generally visible within 2-5 days.

## 2.6 Construction of plasmids for gene expression

The plasmids generated throughout the course of this study are listed in Table 2-9. See below for cloning details.

**Table 2.9 Plasmids constructed in this study**

Name	Backbone <sup>a</sup>	Cloning Cassette
p <i>STE12GFP</i>	pYX242-GFP	<i>STE12</i>
pSte12p(aa1-252)-GFP	pKW431	<i>STE12</i> nt 1-759
pSte12p(aa253-493)-GFP	pKW431	<i>STE12</i> nt 760-1485
pSte12p(aa494-688)-GFP	pKW431	<i>STE12</i> nt 1486-2064
pGST-Ste12p(aa1-252)	pGEX-4T-3	<i>STE12</i> nt 1-759
pGST-Ste12p(aa253-493)	pGEX-4T-3	<i>STE12</i> nt 760-1485

pGST-Ste12p(aa494-688)	pGEX-4T-3	STE12 nt 1486-2064
pRS426-STE12	pRS426	STE12 +/-500 nt
pRS316-STE12cNLS	pRS316	STE12 -500nt, SV40cNLS
pNOP1GFP	pYX242-GFP	NOP1
pGAL1-NOP1GFP	pYES2	NOP1, yEGFP3
pGAL1-Nop1(aa1-90)-GFP	pYES2	NOP1 nt 1-270, yEGFP3
pGAL1-Nop1(aa91-327)-GFP	pYES2	NOP1 nt 271-981, yEGFP3
pGAL1-Nop1(aa210-327)-GFP	pYES2	NOP1 nt 658-981, yEGFP3
pGST-Nop1p	pGEX-4T-3	NOP1
pGST-Nop1p(aa1-90)	pGEX-4T-3	NOP1 nt 1-270
pGST-Nop1p(aa91-327)	pGEX-4T-3	NOP1 nt 271-981
pGST-Nop1p(aa210-327)	pGEX-4T-3	NOP1 nt 658-981
pRS315-NOP1cNLS	pRS315	NOP1 +700 nt, SV40cNLS
pRS315-NOP1	pRS315	NOP1 +500 nt
pSOF1GFP	pYX242-GFP	SOF1
pGAL1-SOF1GFP	pYES2	SOF1, yEGFP3
pGAL1-Sof1p(aa1-130)-GFP	pYES2	SOF1 nt 1-390, yEGFP3
pGAL1-Sof1p(aa131-380)-GFP	pYES2	SOF1 nt 391-1140, yEGFP3
pGAL1-Sof1p(aa381-489)-GFP	pYES2	SOF1 nt 1141-1467, yEGFP3
pGAL1-Sof1p(aa411-450)-GFP	pYES2	SOF1 nt 1231-1350, yEGFP3
pGST-Sof1p(aa1-130)	pGEX-4T-3	SOF1 nt 1-390
pGST-Sof1p(aa131-380)	pGEX-4T-3	SOF1 nt 391-1140
pGST-Sof1p(aa381-489)	pGEX-4T-3	SOF1 nt 1141-1467
pGST-Sof1p(aa411-450)	pGEX-4T-3	SOF1 nt 1231-1350
pDBP9GFP	pYX242-GFP	DBP9
pGAL1-DBP9GFP	pYES2	DBP9, yEGFP3
pGST-Dbp9p	pGEX-4T-3	DBP9
pGAL1-cNLSGFP	pYES2	cNLS, nes, 2xGFP
pGST-Pho4p(aa140-166)	pGEX-4T-3	PHO4 nt
pKAP121-URA3	pRS316	KAP121 +/-1,000 nt
pKAP121-TRP1	pRS314	KAP121 +/-1,000 nt
pKAP121-LEU2	pRS315	KAP121 +/-1,000 nt
pYES2-LEU2	pYES2	LEU2 -200 nt
pGAL1-KAP104-LEU2	pYES2-LEU2	KAP104
pGAL1-KAP108-LEU2	pYES2-LEU2	KAP108 +138 nt
pkap121-18	pRS314	kap121-18 +/-1,000 nt
pkap121-26	pRS314	kap121-26 +/-1,000 nt
pkap121-34	pRS314	kap121-34 +/-1,000 nt
pkap121-41	pRS314	kap121-41 +/-1,000 nt
pkap121-34-LYS2	pRS317	kap121-34 +/-1,000 nt

<sup>a</sup> Detailed descriptions of these plasmid backbones can be found in Table 2-1.

**2.6.1 STE12 expression plasmids** – To construct an *STE12* fusion gene encoding Ste12p fused in frame at its carboxy (C) terminus to green fluorescent protein (GFP), the *STE12* open reading frame (ORF) was amplified by PCR (Section 2.4.1) from yeast genomic DNA using *STE12* 5' and *STE12* 3' oligonucleotides (Table 2-3). This product was digested with *EcoRI* and *HindIII*, and ligated into the corresponding sites of pYX242-GFP (Table 2-1 (Rosenblum *et al.*, 1998)). The resulting recombinant plasmid was termed p*STE12GFP*.

Fragments of the *STE12* gene, nucleotides (nt) 1-759, nt 760-1485, or nt 1486-2064) were fused in frame at their amino terminus to glutathione S-transferase (GST) or at their carboxy terminus to GFP. These fragments of the *STE12* coding sequence were amplified by PCR (Section 2.4.1) from yeast genomic DNA using oligonucleotides *STE12*-Sec#1 5' and *STE12*-Sec#1 3', *STE12*-Sec#2 5' and *STE12*-Sec#2 3', and *STE12*-Sec#3 5' and *STE12*-Sec#3 3'. When constructing GST fusions, these PCR products were digested with *EcoRI* and ligated into the corresponding site of pGEX-4T-3 (Table 2-1). Desired recombinant plasmids were identified by restriction endonuclease digestion and termed pGST-Ste12p(aa1-252), pGST-Ste12p(aa253-493), and pGST-Ste12p(aa494-688), respectively. GFP fusions were constructed by digesting the same PCR fragments of *STE12* with *EcoRI* and *HindIII* and ligating them into the corresponding restriction endonuclease sites of p12-GFP2-NLS (Table 2-1: pKW431 (Stade *et al.*, 1997); a gift from K. Weis, University of California at San Francisco, CA). In each case, this resulted in the removal of the cassette

encoding the NLS of Simian Virus 40 (SV40) large T antigen (a prototypical cNLS) from p12-GFP2-NLS plasmid and replacing it with *STE12* fragment coding sequences. Thereby, generating in frame fusion genes containing the desired fragments of *STE12*, a mutant (p12) NES and two GFP coding sequences (2xGFP). The resulting plasmids were termed pSte12p(aa1-252)-GFP, pSte12p(aa253-493)-GFP and pSte12p(aa494-688)-GFP.

Overexpression of *STE12* was achieved by inserting the *STE12* gene cassette into a multicopy plasmid, pRS426 (Table 2-1(Christianson *et al.*, 1992)). *STE12*, including 500 nt upstream and downstream of the ORF (nt +1 corresponds to the A of the initiator codon, ATG), was amplified by PCR (Section 2.4.1) from yeast genomic DNA using oligonucleotides STE12/MCP 5' and STE12/MCP 3' (Table 2-3). The resulting PCR product was digested with *HindIII* and *XhoI* and ligated into the corresponding restriction endonuclease sites of pRS426. The resulting plasmid was termed pRS426-*STE12*.

A modified *STE12* gene encoding Ste12p fused at its carboxy terminus with a cNLS was made by inserting the SV40 large T antigen NLS coding sequence (Kalderon *et al.*, 1984b) in frame at its 3' end. The *STE12cNLS* fusion was constructed by PCR amplification (Section 2.4.1) of the *STE12* gene, including 500 nucleotides upstream of the ORF, using oligonucleotides STE12/MCP 5' and STE12cNLS 3' (which contains the SV40 large T antigen NLS coding sequence). The PCR product was digested with *HindIII* and *EcoRI* and ligated into the corresponding restriction endonuclease sites of pRS316

(Table 2-1 (Sikorski and Hieter, 1989)). The resulting plasmid was termed pRS316-*STE12cNLS*.

**2.6.2 NOP1 expression plasmids** – To construct p*NOP1GFP*, the ORF of *NOP1* was amplified from yeast genomic DNA by PCR (Section 2.4.1) using oligonucleotides NOP1 5' and NOP1 3' (Table 2-3). The resulting PCR product was digested with *EcoRI* and *HindIII* and ligated into the corresponding restriction endonuclease sites of pYX242-GFP (Table 2-1 (Rosenblum *et al.*, 1998)). To place the *NOP1GFP* gene fusion under control of a galactose-regulated promoter (*GAL1*) the fusion was excised from pYX242-GFP using the 5' *EcoRI* and the 3' *XhoI* restriction endonuclease sites and subcloned into the corresponding restriction endonuclease sites of pYES2 (Table 2-1; Invitrogen, Carlsbad, CA). The resulting plasmid was termed p*GAL1-NOP1GFP*.

*NOP1* fragment constructs were produced by PCR (Section 2.4.1) using oligonucleotides designed to amplify segments containing nucleotides (nt) 1-270 (*NOP1*-Sec#1 5' and *NOP1*-Sec#1 3'), nt 211-981 (*NOP1*-Sec#2 5' and *NOP1*-Sec#3 3'), or nt 658-981 (*NOP1*-Sec#3 5' and *NOP1*-Sec#3 3') (Table 2-3) of *NOP1* with 5' *EcoRI* and *HindIII* and 3' *EcoRI* restriction sites. *HindIII* and *EcoRI* digested PCR products were first cloned into p12-GFP2-NLS (pKW431) as described above. The resulting GFP gene fusions were then excised from p12-GFP2-NLS using the 5' *HindIII* and the 3' *XhoI* restriction endonuclease sites, and subcloned into the corresponding restriction endonuclease sites of pYES2 (Table 2-1). The plasmids were termed p*GAL1-Nop1p(aa1-90)*-GFP, p*GAL1-*

Nop1p(aa91-327)-GFP and pGAL1-Nop1p(aa210-327)-GFP. The same PCR products, as well as a full-length *NOP1* PCR product (which was amplified as described above using oligonucleotides NOP1-Sec#1 5' and NOP1-Sec#1 3' (Table 2-3)), were digested with *EcoRI* and ligated into the *EcoRI* site of pGEX-4T-3. All positive clones were restriction endonuclease digested to identify the desired recombinants, which were termed pGST-Nop1p, pGST-Nop1p(aa1-90), pGST-Nop1p(aa90-327) and pGST-Nop1p(aa210-327), respectively.

The *NOP1cNLS* gene fusion was produced by PCR amplification (Section 2.4.1) of *NOP1* from yeast genomic DNA using oligonucleotides NOP1cNLS 5' and NOP1cNLS 3' (Table 2-3). These oligonucleotides were designed to generate a gene cassette encoding *NOP1* including 700 nucleotides upstream of the ORF fused in frame at its 3' end to the SV40 large T antigen NLS coding sequence (Kalderon *et al.*, 1984b). This PCR product was digested with *HindIII*, ligated into the corresponding restriction endonuclease site of pRS315 and termed pRS315-*NOP1cNLS*. As a control, a *NOP1* cassette, including 700 nt upstream of the ORF but lacking the in-frame cNLS fusion, was also amplified from yeast genomic DNA using oligonucleotides NOP1cNLS 5' and NOP1-cNLS 3' (Table 2-3). This *NOP1* PCR fragment was similarly cloned into the *HindIII* restriction endonuclease site of pRS315 and the termed pRS315-*NOP1*.

**2.6.3 *SOF1* expression plasmids** – p*SOF1GFP* was constructed in essentially the same manner as p*NOP1GFP*. The *SOF1* ORF was amplified (Section 2.4.1) using oligonucleotides *SOF1* 5' and *SOF1* 3' (Table 2-3), and the resulting PCR

product was cloned into the *EcoRI* and *BamHI* restriction endonuclease sites of pYX242-GFP (Rosenblum *et al.*, 1998). The resulting *SOF1GFP* gene fusion was excised from pYX242-GFP using the 5' *EcoRI* and the 3' *XhoI* restriction endonuclease sites and placed under control of the *GAL1* promoter by subcloning it into pYES2 (Table 2-1). The resulting plasmid was termed p*GAL1-SOF1GFP*.

*SOF1* fragment constructs were produced in the same manner as described above for *NOP1* using oligonucleotides designed to amplify segments of *SOF1* containing 5' *EcoRI* and 3' *BamHI* and *Sall* restriction endonuclease sites: nt 1-390 (*SOF1N* 5' and *SOF1N* 3'); nt 391-1140 (*SOF1WD* 5' and *SOF1WD* 3'); nt 1141-1467 (*SOF1C* 5' and *SOF1C* 3'); or nt 1231-1350 (*SOF1NLS* 5' and *SOF1NLS* 3') (Table 2-3). Galactose-inducible GFP gene fusions were constructed by first ligating *EcoRI* and *BamHI* digested *SOF1* fragment PCR products into the corresponding restriction endonuclease sites of pYX242-GFP (Table 2-1). The resulting GFP gene fusions were excised from pYX242-GFP by digesting these plasmids with *EcoRI* and *XhoI* and subcloning the recovered DNA fragments into the corresponding restriction endonuclease sites of pYES2 (Table 2-1). The resulting plasmids were termed p*GAL1-Sof1p(aa1-130)*-GFP, p*GAL1-Sof1p(aa131-380)*-GFP, p*GAL1-Sof1p(aa381-489)*-GFP and p*GAL1-Sof1p(aa411-450)*-GFP. N-terminal GST gene fusions containing the fragments of the *SOF1* were constructed by digesting the same PCR products (*SOF1* (nt 1-390), *SOF1* (nt 391-1140), *SOF1* (nt 1141-1467) and

*SOF1* (nt 1231-1350)) with *EcoRI* and *SaII* and ligating them into the corresponding restriction endonuclease sites of pGEX-4T-3. These plasmids were termed pGST-Sof1p(aa1-130), pGST-Sof1p(aa131-380), pGST-Sof1p(aa381-489) and pGST-Sof1p(aa411-450).

**2.6.4 DBP9 expression plasmids** – The ORF of *DBP9* was amplified from yeast genomic DNA as described above using primers DBP9 5' and DBP9 3' (Table 2-3). The resulting PCR product was digested with *EcoRI* and *BamHI* and ligated into the corresponding restriction endonuclease sites of pYX242-GFP and termed p*DBP9GFP*. This GFP chimera was then excised from p*DBP9GFP* using *EcoRI* and *XhoI* and subcloned into the corresponding restriction endonuclease sites of pYES2. The resulting plasmid was termed p*GAL1-DBP9GFP*. The same *DBP9* PCR product was also digested with *EcoRI* and *SaII*, ligated into the corresponding restriction endonuclease sites of pGEX-4T-3 and the resulting plasmid was termed pGST-Dbp9p.

**2.6.5 cNLS and PHO4 expression plasmids** - p*GAL1-cNLSGFP* was generated by subcloning a *HindIII/XhoI cNLSnes-2xGFP* fragment restriction endonuclease digested from p12-GFP2-NLS (Table 2-1) into the corresponding restriction endonuclease sites of pYES2 (Table 2-1).

The nucleotides encoding the NLS of *PHO4*, amino acid residues 140 to 166 (Kaffman *et al.*, 1998b), were amplified from yeast genomic DNA by PCR using oligonucleotides PHO4NLS 5' and PHO4NLS 3'. This PCR product was digested with *BamHI* and *EcoRI* restriction endonucleases, ligated into the

corresponding restriction endonuclease sites of pGEX-4T-3 and the resulting plasmid was termed pGST-Pho4p(aa140-166).

**2.6.6 KAP expression plasmids<sup>1</sup>** – To facilitate complementation of  $\Delta kap121$  haploid strains (Section 2.7.1) and the generation of *kap121* mutant alleles (Section 2.7.2), the *KAP121* gene, including 1,000 nucleotides upstream and downstream of the ORF, was cloned into the *SacI* restriction endonuclease site of pRS316, pRS315 and pRS314 (Table 2-1) to yield p*KAP121-URA3*, p*KAP121-LEU2* and p*KAP121-TRP1*, respectively.

Overexpression of *KAP104* and *KAP108* was achieved by placing these ORFs under the control of the *GAL1* promoter present in pYES2 (Table 2-1). First, for selection purposes, the *URA3* gene of pYES2 was replaced with the *S. cerevisiae LEU2* gene. To this end, the *S. cerevisiae LEU2* gene, plus 200 bp upstream of the start codon, was amplified from yeast genomic DNA by PCR using oligonucleotides LEU2/pYES2 5' and LEU2/pYES2 3' (Table 2-3) and digested with *NdeI* and *Apal*. pYES2 was also digested with *NdeI* and *Apal*, thereby removing nt 1-599 of the *URA3* gene, and the *NdeI/Apal* digested *LEU2* PCR product was ligated in place of the excised *URA3* fragment. The resulting plasmid was termed pYES2-*LEU2*. Next, the ORF of *KAP104* was amplified from p104-LYS (Table 2-1 (Aitchison *et al.*, 1996)) by PCR (Section 2.4.1) and digested with *SacI*. The resulting *KAP104* fragment was ligated into the *SacI* restriction endonuclease site of pYES2-*LEU2*. The desired recombinants were

---

<sup>1</sup> p*KAP121-URA3*, p*KAP121-LEU2* and p*KAP121-TRP1* were constructed by Dr. John Aitchison at the Rockefeller University.

identified by restriction endonuclease digestion and termed pGAL1-KAP104-LEU2. Similarly, the ORF of *KAP108* was amplified from yeast genomic DNA by PCR using primers YES2-KAP108 5' and YES2-KAP108 3'. The PCR product was digested with *SacI* and *XbaI* and ligated into the corresponding restriction endonuclease sites of pYES2-LEU2 and termed pGAL1-KAP108-LEU2.

## 2.7 Construction of *S. cerevisiae* mutant strains

**2.7.1 Construction of KAP121 null strains<sup>2</sup>** – The *kap121* null strain, and derivatives there of, were derived from DF5 (Table 2-7). The heterozygous *kap121::URA3/KAP121* strain was constructed in DF5 diploid cells by direct integration of a PCR product containing the *URA3* gene (Rothstein, 1991) and nucleotides –60-3 and 3177-3230 of *KAP121* as previously described (Aitchison *et al.*, 1995), thereby replacing the *KAP121* ORF with *URA3*. Genomic DNA was isolated from Ura<sup>+</sup> diploids (Section 2.3.2) and PCR amplification (Section 2.4.1) used to confirm deletion of *KAP121*. For selection purposes, the *URA3* gene was then replaced with a *HIS3* cassette by homologous recombination of a *ura3::HIS3* cassette using a previously described “marker swap” technique (Cross, 1997). Briefly, a *ura3::HIS3* cassette (comprised of an inactive *URA3* gene containing the *HIS3* gene inserted into the intragenic *StuI* site of *URA3*) was amplified from pUH7 (Table 2-1) using M13 forward and reverse primers (Table 2-3), which anneal to their corresponding sequences that flank the *ura3::HIS3* cassette present in pUH7. This PCR product was concentrated

---

<sup>2</sup> Performed by Brock Grill at the University of Alberta.

(Section 2.4.7), transformed into the *kap121::URA3/KAP121* diploid strain (Section 2.5.2) and transformants were selected on CSMD-His agar plates. The desired Ura<sup>-</sup>, His<sup>+</sup> strains were identified based on their ability to grow on CSMD-His but not on CSMD-Ura agar plates, the resulting strains were designated *kap121::ura3::HIS3/KAP121*. *kap121::ura3::HIS3/KAP121* cells were transformed with *pKAP121-URA3* (Section 2.5.2). The transformants were sporulated (Section 2.2.4), tetrads dissected (Section 2.2.4), and *kap121::ura3::HIS3/pKAP121-URA3* haploids were selected by growth on CSMD-His-Ura agar plates. The resulting strain was designated *Δkap121/pKAP121-URA3*. For additional selection purposes, the *HIS3* gene of *Δkap121/pKAP121-URA3* was replaced with the *LEU2* gene via homologous recombination of a *his3::LEU2* cassette as described above. This *his3::LEU2* cassette was amplified by PCR from pHL3 (Table 2-1 (Cross, 1997)) using oligonucleotides T3 and T7 (Table 2-3), which anneal to their corresponding sequences that flank the *his3::LEU2* cassette present in pHL3. The resulting His<sup>-</sup> Leu<sup>+</sup> *Mata* and *Mataα* strains were termed *Δkap121LEU2/pKAP121-URA3*.

**2.7.2 Construction of *kap121* mutant alleles<sup>3</sup>** – *kap121* mutant alleles were generated using the gapped plasmid repair method (Muhlrad *et al.*, 1992). Briefly, the *KAP121* gene, including 1,000 nucleotides upstream and downstream of the ORF, was amplified under mutagenic PCR conditions as described above (Section 2.4.2). The *pKAP121-TRP1* gapped plasmid was constructed by

---

<sup>3</sup> Performed by Brock Grill at the University of Alberta.

digesting *pKAP121-TRP1* with *BalI* and *NdeI*, followed by gel purification (Section 2.4.6) and isolation of an ~ 7.5 kb DNA fragment containing pRS314 and nt -1,000 to -1 and 2,393 to +1,000 of *KAP121*. The *KAP121* mutagenic PCR product and the *pKAP121-TRP1* gapped plasmid were cotransformed into *Δkap121/pKAP121URA3* cells (Section 2.5.2) at a molar ratio of 10:1. The transformants were plated on CSMD-Ura-Trp agar plates and incubated at 23°C for 3 to 4 days.

Plasmid shuffling was then used to select for *kap121* mutants that were able to grow at 23°C but not at 37°C (Muhlrad *et al.*, 1992). Briefly, colonies were replica plated onto 5-fluoroorotic acid (5-FOA)-containing medium (Boeke *et al.*, 1984) and incubated at 23°C and 37°C to select cells lacking *pKAP121-URA3*. Mutants that grew well at 23°C but failed to grow at 37°C were characterized further. To confirm that the temperature-sensitive (*ts*) phenotype was not the result of nutritional requirements, these colonies were replica-plated to YEPD and incubated at 23°C and 37°C. Finally, mutants were tested for their ability to be complemented with a wild-type copy of *KAP121*, *pKAP121-URA3*. Four colonies were isolated that fulfilled all of these requirements. These strains were classified as *kap121-ts* strains and designated *kap121-18*, *kap121-26*, *kap121-34*, and *kap121-41*.

The plasmids encoding these *ts* alleles were isolated (Section 2.3.3), termed *pkap121-18*, *pkap121-26*, *pkap121-34*, and *pkap121-41*, and the *kap121-34* and *kap121-41* alleles sequenced as described below (Section 2.8). For

additional selection purposes, the *kap121-34* allele was excised from pRS314 using *SacI* and ligated into the corresponding site of pRS317. This plasmid was termed *pkap121-34-LYS2*. Furthermore,  $\Delta$ *kap121LEU2/pKAP121-URA3 Mata* and *Mata $\alpha$*  strains were also transformed with the *pkap121-34* plasmid, plated on 5-FOA containing agar plates as described above to isolate *kap121-34LEU2* strains.

**2.7.3 Construction of *kap95-14* temperature-sensitive strains<sup>4</sup>** – The *kap95-14* temperature-sensitive strain (Leslie *et al.*, 2002) is a derivative of DF5 and was produced as previously described (Aitchison *et al.*, 1996).

**2.7.4 Construction of galactose-responsive strains** – Galactose-responsive *kap121-34* and *kap104-16* strains were generated by crossing *kap121-34* or *kap104-16* haploids (Aitchison *et al.*, 1996) with W303 haploids (Table 2-7 (Aitchison *et al.*, 1995)), a strain that grows well on galactose-containing media. The resulting diploids were sporulated and the tetrads dissected (Section 2.2.4). *kap121-34* and *kap104-16* haploid strains were selected based on their ability to grow on the appropriate selective media, in the presence of galactose as the sole carbon source, in a temperature-sensitive manner as described above (Section 2.7.2). Strains that grew well on galactose at 23°C but did not grow at 37°C were selected for further experiments and are referred to as *kap121-34* and *kap104-16*.

---

<sup>4</sup>The *kap95-14* strain was produced by Dr. John Aitchison at the Rockefeller University.

**2.7.5 Construction of double mutant strains** – Strains used to analyze genetic interactions between *KAP121* and *KAP104* or *KAP108* were constructed by crossing *kap121-34LEU2* or *kap121-34* to  $\Delta$ *kap104* (Aitchison *et al.*, 1996) or  $\Delta$ *kap108* (Sydorsky *et al.*, 2003) null mutants containing wild-type copies of *KAP104* (p*KAP104-URA3*) or *KAP108* (p*KAP108-URA3*), respectively. The resulting diploids were sporulated and the tetrads dissected as described above (Section 2.2.4). The desired double mutant haploids were selected by growth on the CSMD-His-Leu-Trp-Ura agar plates and termed *kap121-34LEU2, Δkap104/pKAP104-URA3* and *kap121-34LEU2, Δkap108/pKAP108-URA3*.

## 2.8 Genomic integration of epitope tags

### 2.8.1 Construction of NOP1-A and SOF1-A strains by genomic integration –

Genomic copies of *NOP1* and *SOF1* were tagged by homologous recombination as previously described (Aitchison *et al.*, 1995) by integrating a gene cassette encoding the IgG binding domains of *Staphylococcus aureus* protein A (pA) in-frame at the 3' ends of these ORFs. Briefly, the protein A gene and adjacent *HIS5* gene were amplified by PCR (Section 2.4.1) from the plasmid pBxA-HIS5 (Table 2-1 (Aitchison *et al.*, 1995)) using oligonucleotides Nop1p-pA 5' and Nop1p-pA 3', or Sof1p-pA 5' and Sof1p-pA 3' (Table 2-3). These primers were designed as follows: The sense (5') primer encodes the C terminus of Nop1p (nt 922-981) or Sof1p (nt 1408-1467) (up to, but not including the stop codon) and continues into the first 21 nucleotides of pA. The antisense primer contains the untranslated regions of *NOP1* (nt 1051-1110) or *SOF1* (nt 1531-1590)

downstream of their stop codons, and the reverse complement of the last 24 nucleotides of the *Schizosaccharomyces pombe* *HIS5* ORF. The resulting PCR products encode the 3' ends of the *NOP1* or *SOF1* ORFs fused in-frame to the 700 bp pA sequence followed by the *S. pombe* *HIS5* cassette and sequences complementary to the untranslated regions of *NOP1* or *SOF1*. These PCR products were purified (Section 2.4.7), transformed into DF5 haploid strains by electroporation (Section 2.5.2) and the integrants selected on CSMD-His agar plates. To identify cells that synthesized Nop1p-pA or Sof1p-pA, 5 mL overnight cultures of His<sup>+</sup> transformants were grown up in CSMD-His medium, 1.5 mL of each culture was harvested and whole cells lysates were produced as described below (Section 2.10.1). Transformants expressing pA chimeras of the correct predicted relative molecular masses were identified by immunoblotting with affinity-purified rabbit  $\alpha$ -mouse IgG and  $\alpha$ -rabbit-HRP antibodies (Table 2-2), and detected using enhanced chemiluminescence (ECL) reagents as described in Section 2.12.5. The desired recombinant strains were designated *NOP1-A* or *SOF1-A*.

**2.8.2 Construction of genomically tagged *NOP1*-GFP and *SOF1*-GFP strains** – Chromosomal *NOP1* and *SOF1* were tagged with *Aequoria victoria* green fluorescent protein (GFP) in  $\Delta kap121LEU2/pKAP121-URA3$  and DF5 *Mata* $\alpha$  haploid cells via homologous recombination as described above and previously (Dilworth *et al.*, 2001). His<sup>+</sup> transformants expressing GFP fusions that localized to the nucleolus were identified and confirmed by  $\alpha$ -GFP immunoblot detection of

appropriately sized Nop1p-GFP and Sof1p-GFP chimeric proteins.  $\Delta kap121LEU2/pKAP121-URA$  strains expressing *NOP1-GFP* or *SOF1-GFP* were termed *NOP1-GFP*,  $\Delta kap121LEU2/pKAP121-URA3$  and *SOF1-GFP* $\Delta kap121/pKAP121-URA3$ , while the DF5 strains were designated *NOP1-GFP* and *SOF1-GFP*. *NOP1-GFP*,  $\Delta kap121LEU2/pKAP121-URA3$  and *SOF1-GFP*,  $\Delta kap121LEU2/pKAP121-URA3$  strains were then transformed with *pkap121-34-LYS2*, the transformants were plated on 5-FOA-containing medium and incubated at 23°C to select cells lacking *pKAP121-URA3*. The resulting strains were termed *NOP1-GFP*, *kap121-34LEU2/LYS2* and *SOF1-GFP*, *kap121-34LEU2/LYS2*.

To generate *kap121-34*, *kap104-16* double mutants containing *NOP1-GFP* or *SOF1-GFP*, the *NOP1-GFP*,  $\Delta kap121LEU2/pKAP121-URA3$  and *SOF1-GFP*,  $\Delta kap121LEU2/pKAP121-URA3$  strains described above were crossed with *kap104-16* (Table 2-7 (Aitchison *et al.*, 1996)), and the resulting diploids sporulated to generate *NOP1-GFP*,  $\Delta kap121LEU2/pKAP121-URA3$ , *kap104-16* and *SOF1-GFP*,  $\Delta kap121LEU2/pKAP121-URA3$ , *kap104-16* haploid strains. Because the *NOP1-GFP*, *SOF1-GFP* and  $\Delta kap104$  cassettes are His<sup>+</sup>, the desired haploids were selected from tetrads that segregated the His<sup>+</sup> phenotype at 3:1 or 2:2 ratios. Expression of *NOP1-GFP* or *SOF1-GFP* was confirmed as described above and the resulting His<sup>+</sup>Leu<sup>+</sup>Ura<sup>+</sup>Trp<sup>+</sup>GFP<sup>+</sup> strains were transformed with *pkap121-34-LYS2*. These transformants were plated on 5-FOA-containing agar plates and incubated at 23°C to select cells lacking

*pKAP121-URA3*. The resulting double mutants were designated *NOP1-GFP*, *kap121-34LEU2/LYS2*, *kap104-16* and *SOF1-GFP*, *kap121-34LEU2/LYS2*, *kap104-16*.

## 2.9 DNA Sequencing

The DNA Core Services Laboratory at the University of Alberta sequenced the *kap121-34* and *kap121-41* mutant alleles using the dideoxynucleotide chain-termination method (Sanger *et al.*, 1977) with fluorescently labeled DNA. Oligonucleotide primers were designed to sequence ~400bp overlapping DNA fragments of *KAP121* from both the coding and complementary strands, with the overlapping sequences being approximately 50 bp in length. Automated sequencing reactions were performed on *pkap121-34* or *pkap121-41* plasmid DNA using a Beckman Coulter CEQ2000XL sequencing machine. The resulting *kap121-34* DNA sequences were compared to *KAP121* using the DNASTAR (DNASTAR Inc., Madison WI) Lasergene software MegAlign (Wilbur-Lipman: ktuple, 3; gap penalty, 3; window, 20 (Lee and Aitchison, 1999)). Nucleotide substitutions were deemed *bona fide* if they appeared in both the coding and complementary strand sequences.

## 2.10 Subcellular fractionation of *S. cerevisiae*

**2.10.1 Preparation of whole cell lysates for immunoblotting** – When assaying protein levels and screening His<sup>+</sup> colonies for appropriate integration of either the *pA/HIS5* or the *GFP/HIS5* gene cassettes whole cell lysates were

generated via chemical lysis of yeast cells. Typically, the strain of interest was grown overnight in 5 mL of YEPD or the appropriate selection media. Cells were harvested by centrifugation at 3,000 x *g* for 5 min at room temperature, transferred to a 1.7 mL eppendorf tube and washed twice with 1 mL of sterile water. The cell pellet was resuspended in 240  $\mu$ L 1.85 M NaOH, 7.4% (v/v)  $\beta$ -mercaptoethanol and incubated on ice for 10 min. The polypeptides were precipitated by addition of an equal volume of 50% trichloroacetic acid (TCA), followed by incubation on ice for 10 min and collected by centrifugation at 15,000 x *g* for 10 min at 4°C. The supernatant was aspirated, the pellet was washed with sterile water and resuspended in 50  $\mu$ L magic A (Table 2-4). An equal volume of magic B (Table 2-4) was added, the mixture was vortexed briefly and heated at 65°C for 15 min. Proteins in these samples were separated by SDS-PAGE (Section 2.12.3), and analyzed by immunoblotting and enhanced chemiluminescence (Section 2.12.5) (ECL, Pierce).

**2.10.2 Preparation of co-immunopurification whole cell lysates** – For co-immunopurification studies whole cell lysates were prepared using a French press chamber (SLM-Aminco model 2,000 $\psi$ , Spectronics Instruments, Rochester, NY) or a microfluidizer (Model M-110S, Microfluidics International Corp., Newton, MA,) as previously described (Leslie *et al.*, 2004; Marelli *et al.*, 1998). The *S. cerevisiae* strain of interest was grown to an OD<sub>600</sub> of 1.0 in 2L YEPD at 30°C, harvested by centrifugation at 4,000 x *g* in a Beckman JS 4.2 rotor for 5 min, washed with 50 mL ice cold transport buffer (TB) plus 1/100

solution P (Table 2-4) and resuspended in 25 mL of the same buffer. The cell suspension was passed through a pre-chilled French press chamber at least three times or through the microfluidizer at least six times with the coil immersed in ice water. Cell lysis was monitored by microscopy. An equal volume of ice cold TB containing 1/100 solution P, 2% Triton X-100, 40% dimethyl sulfoxide (DMSO) was added and the lysate was clarified by centrifugation at 4,000 x g in a Beckman JS 4.2 rotor for 30 min at 4°C. The protein concentration of the resulting lysate was determined using the Bradford method as described in Section 2.12.2 and the lysate was stored at -80°C in 5 mL aliquots.

**2.10.3 Isolation of *S. cerevisiae* nuclei<sup>5</sup>** - Nuclei were isolated as previously described (Strambio-de-Castillia *et al.*, 1995). Yeast cells were grown to an OD<sub>600</sub> of 1.0 in 2 L YEPD. The cells were harvested by centrifugation, washed and resuspended in 2 mL of 1.1 M sorbitol/g of cells. The cells were converted to spheroplasts by addition of 1/100 1% zymolyase 20T and 1/10 glucosylase and incubation at 30°C with agitation. The resulting spheroplasts were washed thoroughly and lysed by homogenizing three times with a Polytron (Polytron Inc. Tallahassee, FL) in 20 mL of polyvinylpyrrolidone (PVP) solution containing 2 mM DTT, 0.025% Triton X-100, and 1/100 solution P. The lysates were separated into crude nuclei and cytosolic fractions by centrifugation at 14,700 x g in a Beckman JS 13.1 rotor for 20 min at 4°C. The resulting supernatant (corresponding to the cytosolic fraction) was stored at -80°C and diluted at a

---

<sup>5</sup> Performed by Drs. John Aitchison and Michael Rout at the Rockefeller University.

ratio of 1:4 with TB for overlay blot assays. The crude nuclei were resuspended in 10 mL of 1.8 M sucrose in PVP solution (Table 2-4) and overlaid onto a four-step sucrose gradient (consisting of 9 mL each of 1.60 M sucrose, 2.15 M sucrose, 2.25 M sucrose, and 2.52 M sucrose all in PVP solution and containing 1/100 solution P). The gradients were centrifuged in a Beckman SW28 rotor at 103,000 x *g* for 6 hrs at 4°C and the purified nuclei were collected from the 2.25 M/2.52 M sucrose interface.

### **2.11 Overlay Blot Assay<sup>6</sup>**

Yeast nuclei were prepared as described above (see Section 2.10.3 and Rout and Blobel, 1993). The proteins were denatured in SDS and fractionated by hydroxyapatite (HA) high-pressure liquid chromatography (HPLC). Pooled HA/HPLC column fractions were further separated by standard formic acid HPLC separation (Rout and Blobel, 1993; Wozniak *et al.*, 1994) and each of the resulting column fractions were concentrated by TCA precipitation. 1/10 volume of TCA was added to each fraction, incubated on ice for 30 min and collected via centrifugation at 20,000 x *g* for 30 min. Precipitated protein pellets were washed twice with acetone, resuspended in equal volumes of magic A and magic B (Table 2-4), and heat denatured at 65°C for 15 min. Each fraction was then separated by SDS-PAGE in Novex SDS-polyacrylamide gels and transferred to nitrocellulose membranes. Nitrocellulose membranes were blocked with TB containing 1/100 solution P and probed with diluted cytosolic fractions (Section

---

<sup>6</sup> Performed by Drs. John Aitchison and Michael Rout at the Rockefeller University.

2.10.3) isolated from yeast cells expressing protein A-tagged Kap121p or Kap123p via incubation on an orbital shaker for 18 hrs at 4°C (Aitchison *et al.*, 1996; Rout *et al.*, 1997). Binding of the protein A tagged fusions was detected by immunoblotting with affinity-purified rabbit  $\alpha$ -mouse IgG and  $\alpha$ -rabbit-HRP, followed by ECL as described below (Section 2.12.5). Bands of interest were identified in replicate Novex SDS-polyacrylamide gels and excised for identification by mass spectrometry as described in Section 2.12.6 (Qin *et al.*, 1997; Rout *et al.*, 2000).

## **2.12 Protein analysis and manipulation**

**2.12.1 Precipitation co-immunopurification protein eluates** – To precipitate the eluates derived from the MgCl<sub>2</sub> step gradient, all eluate volumes were brought to 1 mL with ice cold sterile water. Sodium deoxycholate and TCA were added to each of the fractions to final concentrations of 0.012% and 7.7% (v/v), respectively, and incubated on ice for 1 hr. The precipitated proteins were collected by centrifugation at 20,000 x *g* for 30 min at 4°C, the supernatant aspirated and the precipitates were resuspended in 100  $\mu$ L of water. 900  $\mu$ L of acetone was added to each and the samples were incubated at –20°C for 2 hrs. The resulting precipitates were collected by centrifugation at 20,000 x *g* for 30 min at 4°C, the pellets were dried and resuspended in 50  $\mu$ L of magic A and 50  $\mu$ L magic B (Table 2-4).

**2.12.2 Determination of protein concentration** – Protein concentration was determined by the method of Bradford (Bradford, 1976) using the BioRad protein assay dye reagent. To create a standard curve, six 10  $\mu$ L samples of water containing 0 to 20  $\mu$ g of BSA (Sigma) were added to 1 mL of reagent, vortexed briefly and incubated at room temperature for 5 min. The OD<sub>595</sub> of each sample was measured and plotted against protein concentration. Dilutions of the samples to be tested were prepared and measured in the same manner. Protein concentrations were estimated from samples with absorbances in the linear range of the standard curve.

**2.12.3 Electrophoretic separation of proteins** – Proteins were separated by sodium dodecyl sulphate-polyacrylamide gel electrophoresis (SDS-PAGE) by the method of Laemmli (1970) as described in Ausubel *et al.* (1994). 6 x SDS sample buffer (Table 2-4) was added to protein samples in solution to yield a final buffer concentration of 62.5 mM Tris-HCl (pH 6.8), 10 mM DTT, 10% glycerol, 2% SDS and 0.001% bromophenol blue. Alternatively, precipitated protein samples were resuspended in equal volumes of magic A and magic B (Table 2-4). Samples were then denatured by heating in a 65°C water bath for 15 min. Proteins were separated by electrophoresis on discontinuous slab gels. Stacking gels contained 3% acrylamide/*N,N'*-methylene-bis-acrylamide (37.5:1), 15% sucrose, 60 mM Tris-HCl (pH 6.8), 0.1% SDS, 0.1% (v/v) *N,N,N,N* - Tetramethyl-Ethylenediamine (TEMED), 0.1% (w/v) ammonium persulphate (APS). Resolving gels contained a continuous gradient of 7 to 15%

acrylamide/*N,N'*-methylene-bis-acrylamide (37.5:1) and 0 to 15% sucrose in 370 mM Tris-HCl (pH 8.8), 0.1% SDS, 0.1% (v/v) TEMED, 0.042% (w/v) ammonium persulphate. Electrophoresis was performed using a mini-Protean II electrophoresis system (BioRad) according to the manufacturer's instructions in SDS-PAGE running buffer (Table 2-4).

**2.12.4 Detection of proteins by gel staining** – Proteins resolved in polyacrylamide gels were visualized by staining with Coomassie blue stain (Table 2-4) for at least 30 min and the unbound dye was removed by incubating gels in destain (Table 2-4). Gels were dried on a vacuum drier (BioRad) or using gel drying film (BioRad).

**2.12.5 Detection of proteins by immunoblotting** – Proteins separated by SDS-PAGE were transferred to nitrocellulose at room temperature for 3 to 18 hrs at 400 mA or 50 mA, respectively, in transfer buffer (Table 2-4 (Burnette, 1981; Towbin *et al.*, 1979)) in a mini Trans-Blot electrophoresis transfer cell (BioRad). Proteins bound to nitrocellulose were visualized by staining with amido black stain (Table 2-4) and then incubated with gentle agitation in blocking buffer (Table 2-4) to prevent non-specific binding of the antibodies. Membranes were then incubated with agitation at room temperature for 1.5 hrs with primary antibody in blocking buffer and then with the appropriate secondary antibody labeled with horseradish peroxidase (HRP) in blocking buffer for 30 min. After each antibody incubation, unbound antibodies were removed by washing the blots at room temperature three times for 10 min each in TBS-T. Antigen-

antibody complexes were detected by incubating the blot in a 1:1 mixture of the two detection reagents supplied in the ECL Supersignal detection kit (Pierce) and exposing the blot to X-Omat X-K1 film.

**2.12.6 Mass Spectrometric Protein Identification<sup>7</sup>** – The method used for in-gel tryptic digestion of proteins separated by SDS-PAGE was as previously described (Zhang and Chait, 2000). Matrix-assisted Laser Desorption/Ionization (MALDI)-time-of-flight (TOF) MS was carried out using a commercial instrument (Perseptive Biosystems STR, Framington, MA) operated in the delayed-extraction reflector mode (FWHM resolution ~5,000). Protein identification was carried out using the protein search engine "ProFound", which employs a Bayesian algorithm to identify proteins from protein databases using mass spectrometric peptide mapping data (Zhang and Chait, 2000). Proteins were ranked in order of their probabilities. When the probability for the first-ranked protein was close to unity and there was a large probability transition ( $\geq 10^3$ ) from the first to second candidate, the identification of the top ranked protein was considered to be highly confident (Zhang and Chait, 2000).

## **2.13 Preparation of Recombinant Proteins**

**2.13.1 Synthesis of GST chimeras in E. coli** – Plasmids pGEX-4T-3 and those containing gene fusions encoding GST chimeras were introduced into the protease-deficient *E. coli* strain BL21(DE3)pLysS (Table 2-5; Novagen, Madison,

---

<sup>7</sup> Performed by Wenzhu Zhang in Dr. Brian T. Chait's laboratory at the Rockefeller University.

WI). Small-scale induction experiments were performed on a number of transformants to confirm synthesis of full-length GST chimeric proteins. Typically, transformants were grown overnight in 5 mL of LB (Table 2-6) containing ampicillin and chloramphenicol, the cultures were diluted in duplicate 1 in 5 into fresh LB containing antibiotics and cultured for 30 min. One culture of each strain was induced to express the GST chimeric protein via addition of 2 mM IPTG and incubated at 37°C for an additional 5 hrs. Whole cell lysates from both the induced and the uninduced cultures were generated as described above (Section 2.10.1). The proteins present in these lysates were resolved by SDS-PAGE (Section 2.12.3) and visualized by Coomassie blue staining (Section 2.12.4). GST chimeric proteins were identified based on the presence of a protein band of the predicted relative molecular mass in the IPTG induced samples.

Transformants containing abundant GST chimeras were then induced to express these chimeric genes on a larger scale using a super GST expression protocol (C. Patrick Lusk, personal communication). To this end, 30 mL cultures of each strain were grown for ~18 hrs at 37°C in Terrific Broth (TBm; Table 2-6) containing antibiotics, the cells were harvested by centrifugation at 4,000 x *g* in a Beckman JS 4.2 rotor, resuspended in 50 mL of TBm containing antibiotics and incubated in 250 mL flask for 8 hrs. The cells were harvested as described above, resuspended in 1 L of TBm containing antibiotics and incubated in a 6 L flask for 5 hrs at 250 rpm. GST chimeric protein synthesis was then induced by

the addition of IPTG to a final concentration of 2 mM and incubating the cultures at 30°C for 16 hrs. Cells were harvested by centrifugation 4,000 x *g* in a Beckman JS 4.2 rotor, washed with sterile water, resuspended in STE containing 1/100 solution P and flash frozen in a dry ice/ethanol bath or liquid nitrogen. Suspensions were thawed at room temperature, Triton X-100 was added to a final concentration of 1% and the cells lysed by sonication. Lysates were clarified by centrifugation at 17,500 x *g* in a Beckman JA17 rotor for 20 minutes at 4 °C and stored at –80°C in 1 mL aliquots.

**2.13.2 Recombinant protein purification and thrombin protease cleavage –** *E. coli* protein lysates, produced as described above, were thawed, and incubated with 50 to 200 µL of pre-equilibrated glutathione (GT)-Sepharose (Amersham Pharmacia Biotech) for 1 hr at 4°C with rotation. GT-Sepharose was pre-equilibrated by washing the beads three times with 1 mL of transport buffer (TB) and incubating them in 1 mL of TB with rotation for 30 min at room temperature. All subsequent steps were carried out on ice and the buffers contained 1/100 solution P, unless otherwise stated, and all washing steps were performed with 1 mL of buffer. The beads were pelleted by centrifugation as recommended by the manufacturer and washed three times with TB, once with TB containing 500 mM NaCl, and three times with TB. For immobilized GST-Nop1p chimeric proteins, the beads were washed three times with TB, once with TB containing 1 M NaCl, incubated in TB containing 100 µM ATP with gentle

agitation for 2 min and washed three additional times with TB. The beads were resuspended in 100  $\mu$ L TB lacking solution P.

Proteins were cleaved from the beads by the addition of thrombin (Sigma) to a final concentration of 0.3 U/ $\mu$ L and incubation either at room temperature for 30 to 60 min, or at 4°C for 3 to 16 hrs, with rotation. Thrombin was inactivated by the addition of 3 U of hirudin (Sigma). Cleaved proteins were collected through a Micro Bio-Spin chromatography column (BioRad) and cleared of any residual GST proteins by incubation with 20  $\mu$ L of pre-equilibrated GT resin at 4°C for 30 min. These samples were collected a second time through a fresh Micro Bio-Spin chromatography column and stored in small aliquots at –80°C.

**2.13.3 Ran Preparation** –Yeast Ran (Gsp1p) was synthesized as a GST chimera in *E. coli* as described above (Section 2.13.1). GST-Ran was purified and cleaved with thrombin as described above, except binding buffer (Table 2-4) was used in place of transport buffer. Purified Ran was then loaded with either GTP or GDP as described previously (Rexach and Blobel, 1995). Briefly, Ran samples were divided into two equal fractions and an equal volume of loading buffer (Table 2-4), containing either GTP or GDP, added. The samples were incubated with rotation at room temperature for 90 min. The loading reaction was quenched by the addition of magnesium acetate to a final concentration of 30 mM and incubation with rotation at 4°C for 15 min. The samples were stored in small aliquots at –80°C.

**2.13.4 Elution of purified GST chimeras using reduced glutathione** – GST chimeras were purified and eluted from the GT-Sepharose beads as follows: Approximately 0.5 mg of each chimera protein was purified and the beads were washed as described above (Section 2.13.2). The chimeras were eluted from the beads by incubation in 100  $\mu$ L of glutathione elution buffer (Table 2-4) at room temperature for 2 hrs and the supernatants (which contain the desired GST chimeras) were collected through a Micro Bio-Spin chromatography column (Section 2.13.2). The protein concentrations of the resulting eluates were adjusted to 10 to 20 ng/ $\mu$ L using 10X TB, 1% casamino acids and 1  $\mu$ g of BSA/ $\mu$ L to yield TB2 buffer concentrations.

## 2.14 Assays

**2.14.1  $\beta$ -galactosidase activity assay** – DF5 *Mata* and *kap121-34 Mata* cells were transformed with a plasmid encoding the *fus1-lacZ* chimeric gene (pSB234, Table 2-1 (Trueheart *et al.*, 1987)). Transformants were grown to an OD<sub>600</sub> of 0.200 and divided into two equal aliquots. Cultures were treated with 5  $\mu$ M  $\alpha$ -factor and incubated at 23°C, 30°C, or 37°C. Samples were taken upon initial addition of  $\alpha$ -factor, and at 1 hr and 3 hrs intervals post-pheromone treatment. These samples were divided in half and prepared for immunoblot analysis or  $\beta$ -galactosidase activity assays. For western blot analysis, whole cell protein lysates were prepared (Section 2.12.1), separated by SDS-PAGE (Section 2.12.3) and transferred to nitrocellulose membranes (Section 2.12.4). The  $\beta$ -

galactosidase chimera or Gsp1p were detected with  $\alpha$ - $\beta$ -Gal or  $\alpha$ -Gsp1p (Table 2-2), respectively, and visualized as described above (Section 2.12.5).

The  $\beta$ -galactosidase activity of each sample was assayed by monitoring the cleavage of o-nitrophenyl  $\beta$ -D galactopyranoside (ONPG), a  $\beta$ -galactosidase substrate, as described in the Yeast Protocols Handbook (Clonetechn Laboratories, 2001). Briefly, the OD<sub>600</sub> of each culture was determined, the cells were harvested by centrifugation at 4,000 x *g* for 5 min at room temperature, washed with Z buffer (Table 2-4 (Clonetechn Laboratories, 2001)) and resuspended in 100 mL of the same buffer. The cells were lysed by 3 freeze-thaw cycles in which the cell suspensions were flash frozen in liquid nitrogen, followed by quick thawing in a 37°C water bath. 700 $\mu$ L 0.27%  $\beta$ -mercaptoethanol containing 0.56 mg of ONPG was added to each sample and incubated with agitation at 30°C for 3 minutes. Reactions were neutralized by the addition of 400  $\mu$ L 1 M Na<sub>2</sub>CO<sub>3</sub>, vortexed briefly, and clarified by centrifugation at 15,000 x *g* for 10 min at room temperature. The supernatants were transferred to 2 mL disposable cuvettes and the OD<sub>420</sub> of each sample was determined using a spectrophotometer. Units of  $\beta$ -galactosidase activity were calculated using the following formula: (1,000 x OD<sub>420</sub> of centrifuged reaction mixture)/(OD<sub>600</sub> of culture x volume of culture x minutes of assay) (Trueheart *et al.*, 1987). The standard deviations from the means were calculated from three separate experiments.

**2.14.2 Pheromone response assay** – The pheromone response assay was carried out as described previously (Sprague, 1991). Briefly, *kap121-34 Mata* and DF5 (WT) *Mata* cultures were grown to an OD<sub>600</sub> of ~0.3 at 23°C in YEPD and the number of budded and unbudded cells in each culture was determined using a hemacytometer and phase contrast microscopy. The cultures were separated into two equal aliquots, one aliquot of each strain was treated with 2.5 μM α-factor (Sigma) while the other aliquot was left untreated. Both the treated and untreated cultures were then incubated at 23°C, 30°C or 37°C. Samples of each culture were taken at 1 hr intervals post-pheromone treatment and fixed with 3.7% (v/v) formaldehyde in 7.5 mM NaCl. The number of budded and unbudded/shmooed cells in each sample were determined as described above. The standard deviations from the means were calculated from three separate experiments.

**2.14.3 Quantitative mating assay** – Quantitative mating assays were performed as previously described (Sprague, 1991). Briefly, actively growing cultures of α-mating types of the strains to be tested (*kap121-34*, *Δkap121/pKAP121-URA3*, *kap121-34/pRS426-STE12*, *kap121-34/pRS316-STE12cNLS*) and a-mating types of a wild-type tester strain (transformed with pRS315 for selection purposes; (DF5/pRS315)) were grown at 23°C in the appropriate selection medium.  $2 \times 10^6$  *kap121-34*, *kap121Δ/KAP121*, *kap121-34/pRS426-STE12*, or *kap121-34/pRS316-STE12cNLS* cells were mixed with  $\sim 10^7$  DF5/pRS315 cells. The mating mixtures were incubated in 250 μL of YEPD

at 30°C for 5 hrs and plated in a 1:1,000 dilution onto CSMD-His-Trp-Leu or CSMD-His-Trp-Ura-Leu agar plates to select for diploids. To determine the number of viable haploid cells of the strain being tested, the mating mixtures were also plated in a 1:1,000 dilution onto CSMD-His-Trp (for *kap121-34*), CSMD-His-Ura (for  $\Delta kap121/pKAP121-URA3$ ) or CSMD-His-Trp-Ura (for *kap121-34/pRS426-STE12* and *kap121-34/pRS316-STE12cNLS*) agar plates to select haploids. The resulting haploid and diploid colonies were counted after 3 days of growth at 23°C. The mating efficiency was expressed as a percentage of the input haploids of the strain being tested that formed diploid colonies (Kunzler *et al.*, 2001). The standard deviations from the means were calculated from three separate experiments.

**2.14.4 Invasion assay** – To obtain invasion competent *kap121* temperature-sensitive strains  $\Delta kap121LEU2/pKAP121-URA3$  haploids were crossed with SK1 (*Mata*) (Lydall *et al.*, 1996), an invasion-competent *S. cerevisiae* strain. The resulting diploids were sporulated and tetrads were dissected as described above (Section 2.2.4).  $\Delta kap121LEU2/pKAP121-URA3$  haploids were identified by growth on CSMD-Leu-Ura agar plates, patched on YEPD agar plates and incubated at 23°C for 2 days. The plates were then washed with a gentle stream of deionized water to rinse all cells from the agar surface and reveal invasion competent strains (Roberts and Fink, 1994). Three invasion competent  $\Delta kap121LEU2/pKAP121-URA3$  strains were isolated and designated  $\Delta kap121LEU2^{nv7}/pKAP121-URA3$ ,  $\Delta kap121LEU2^{nv11}/pKAP121-URA3$  and

$\Delta kap121LEU2^{inv13}/pKAP121-URA3$ .  $\Delta kap121LEU2^{inv7}/pKAP121-URA3$  was then transformed with  $pkap121-34$ , the transformants were replica plated to 5-FOA-containing agar plates to isolate isogenic strains containing only a temperature-sensitive copy  $kap121$  ( $kap121-34$ ) or a wild-type copy of  $KAP121$ . The resulting strain was called  $kap121-34LEU2^{inv7}$ .  $kap121-34LEU2^{inv7}$  was also transformed with  $pRS426-STE12$  and  $pRS316-STE12cNLS$ . All of the resulting invasion competent strains were patched to YEPD plates with a toothpick, incubated at 30°C for 2 days and assayed for invasion as described above. While only one colony from each of the  $pRS426-STE12$  and  $pRS316-STE12cNLS$  transformations is shown in Chapter 3, the invasive properties of three colonies from each transformation were tested and all were found to behave similarly.

## 2.15 Co-immunopurifications

### 2.15.1 Ex vivo co-immunopurification studies with GST chimeric proteins –

The GST chimeric proteins containing fragments of Ste12p or Nop1p were purified from *E. coli* lysates as described above (Section 2.13.2). Clarified whole cell lysates were prepared as described above (Section 2.10.2) from yeast strains synthesizing Kap95-pA (Aitchison *et al.*, 1996; Rout *et al.*, 1997), Kap104p-pA (Aitchison *et al.*, 1996), Kap121p-pA (Rout *et al.*, 1997), or Kap123p-pA (Rout *et al.*, 1997). The protein concentration of these lysates was determined as described above (Section 2.12.2) and brought to a final concentration of 1 mg/mL with TB. 5 mL of each lysate was incubated with the immobilized GST chimeras for 18 hrs at 4 °C with rotation. Immobilized protein

complexes were washed four times with wash buffer (WB) plus 1:1,000 solution P and successively eluted with WB containing 500 mM, 1 M, and 2 M MgCl<sub>2</sub> and finally with 0.5 M acetic acid. The proteins in each fraction were precipitated as described above (Section 2.12.1), and prepared for SDS-PAGE using magic A and B. Protein samples were separated in SDS-polyacrylamide gels (Section 2.12.3), and stained with Coomassie blue (Section 2.12.4) or transferred to nitrocellulose (Section 2.12.5). To detect protein A-tagged chimeras immunoblots were performed as described above (Section 2.12.5) using affinity-purified rabbit  $\alpha$ -mouse IgG and  $\alpha$ -rabbit-HRP antibodies (Table 2-2).

### **2.15.2 Isolation of Nop1p-pA- and Sof1p-pA-containing complexes –**

Lysates were prepared from *NOP1-A* and *SOF1-A* yeast cells using a microfluidizer as described above (Section 2.10.2). These lysates were incubated overnight on a rotator at 4°C with 75  $\mu$ L of pre-equilibrated (Section 2.13.2) IgG-coupled magnetic beads from a  $2.0 \times 10^6$  bead/mL slurry (DynaL Biotech). The beads were collected using a magnet, washed four times with 5 mL TB and the bound proteins were eluted with increasing concentrations (50mM, 100mM, 250mM, 500mM, 1M, 2M and 4M) of MgCl<sub>2</sub> in elution buffer (Table 2-4). Proteins in each eluate fraction were precipitated with TCA as described above (Section 2.12.1). The precipitated protein fractions were prepared for SDS-PAGE using magic A and B, electrophoretically separated (Section 2.12.3) and transferred to nitrocellulose membranes (Section 2.12.5). As necessary, immunoblotting was performed with  $\alpha$ -Kap121p,  $\alpha$ -Kap108p,  $\alpha$ -

Kap104p and  $\alpha$ -Kap123p antibodies (Table 2-2) as described above (Section 2.12.5).

## **2.16 Microscopy**

All fluorescence microscopy experiments were performed using either a Zeiss Axioskop 2 or a Zeiss Axiophot equipped for fluorescence, and images were captured using a Spot camera (Diagnostic Instruments Inc.) or a CoolSNAP camera (Photometrics).

**2.16.1 Analysis of constitutively expressed GFP chimeric proteins** – DF5 *Mata*, *kap121-ts*, *kap95-14* and *kap121-ts/pKAP121* strains were transformed with pYX242-GFP plasmids containing *STE12*, *NOP1*, *SOF1*, *DBP9* or plasmids containing *STE12* gene fragments as indicated, as well as p12-GFP2-NLS (Table 2-1 (Stade *et al.*, 1997) and 2-8). These strains were grown in CSMD supplemented with appropriate amino acids and nucleotides to mid-logarithmic phase at 23°C. Direct fluorescence microscopy was then used to determine the cellular localization of each GFP chimera. Where temperature shifts were required, cultures were grown to mid-logarithmic phase at 23°C as described above and the localization of the GFP chimeric proteins was established by direct fluorescence microscopy. The cultures were then shifted to 30°C or 37°C for the indicated time and examined again as described above.

**2.16.2 Visualization of galactose-inducible GFP chimeric proteins** – To identify the regions of Nop1p and Sof1p that contain functional NLSs, *kap121-34*

cells were transformed with plasmids encoding the galactose-inducible *NOP1* or *SOF1* deletion fragment GFP-chimeras (Table 2-8). These strains were grown to mid-logarithmic phase at 23°C in CSMGal lacking the appropriate amino acids and nucleotides and visualized directly by fluorescence microscopy.

**2.16.3 Temperature shift assays with galactose-inducible GFP chimeric proteins** – *kap121-34* and *kap104-16* haploid strains containing *GAL1*-inducible GFP chimeric proteins (*pGAL1-NOP1GFP*, *pGAL1-SOF1GFP*, *pGAL1-DBP9GFP*, *pGAL1-cNLSGFP*, *pGAL1-Nop1p(aa1-90)-GFP*, *pGAL1-Sof1p(aa381-489)-GFP* or *pGAL1-Sof1p(aa411-450)-GFP* (Table 2-8)), and *pKAP121-URA3* or *pKAP104-URA3* (as indicated), were grown overnight at 23°C in CSMD medium lacking the appropriate amino acids and nucleotides. The cultures were divided in half and incubated at 23°C or 37°C for 2 hrs. The cells were harvested, washed with sterile water and resuspended in CSMGal lacking the appropriate amino acids and nucleotides (Table 2-8) to induce expression of the gene fusions. These cultures were incubated at 23°C or 37°C for an additional 2-3 hrs and the cellular distributions of the GFP chimeras were established using direct fluorescence microscopy.

*pRS315-NOP1* and *pRS315-NOP1cNLS* were transformed into *kap121-34/pGAL1-SOF1GFP* cells and the localization of Sof1p-GFP was analyzed after its induction as described above.

For *KAP104* and *KAP108* regulated expression, *kap121-34/pGAL1-NOP1GFP* and *kap121-34/pGAL1-SOF1GFP* strains were transformed with

pGAL1-KAP104-LEU2 or pGAL1-KAP108-LEU2. The expression of the GFP chimeras and *KAP104* or *KAP108* were induced as described above. The cellular localization of each GFP chimera was analyzed by direct fluorescence microscopy. To confirm overexpression of *KAP104* or *KAP108*, whole cell lysates from 1.5 mL of each culture were prepared as described above (Section 2.10.1) and analyzed by immunoblotting with  $\alpha$ -GFP,  $\alpha$ -Kap104p,  $\alpha$ -Kap108p, and mAb D77 antibodies (Table 2-2).

**2.16.4 Temperature shift assays with genomically tagged GFP gene fusions** – When analyzing the cellular localization of genomically GFP-tagged *NOP1* (eNop1p-GFP) or *SOF1* (eSof1p-GFP), strains containing the *NOP1-GFP* or *SOF1-GFP* genomic tags (Table 2-7) were grown to mid-logarithmic phase at 23°C and visualized by direct fluorescence microscopy (T=0). These cultures were then shifted to 37°C and the cellular localization of eNop1p-GFP or eSof1p-GFP was monitored at the indicated time intervals as described above.

**2.16.5 Metabolic poisoning** – Metabolic poisoning assays were performed as previously described (Shulga *et al.*, 1996). Briefly, 5 mL cultures of *kap121-34* cells transformed with p*NOP1GFP*, p*SOF1GFP*, or p12-GFP-NLS were grown to mid-logarithmic phase at 23°C in CSM-D-His-Trp-Ura and the localizations of these GFP chimeras analyzed as described above. 1.5 mL of each culture was harvested and the cells washed with CSM-His-Trp-Ura. Cells were resuspended in CSM-His-Trp-Ura containing 10 mM sodium azide and 10 mM 2-

deoxyglucose, incubated on ice for 2 hrs and the localizations of Nop1p-GFP and cNLS-GFP monitored at the indicated time points.

## **2.17 *In vitro* binding assays**

### **2.17.1 *GST-Ste12p, GST-Dbp9p and GST-Sof1p protein complex formation***

– For *in vitro* binding reactions involving GST-Ste12p, GST-Dbp9p and the fragments of GST-Sof1p, initial purification was carried out as described above (Section 2.13.2). Purified Kap121p was incubated with the GT-Sepharose immobilized chimeric proteins for 1 hr at 4 °C with rotation. The beads were collected by centrifugation as recommended by the manufacturer, the unbound protein fractions were collected and prepared for SDS-PAGE using 6X SDS sample buffer (Table 2-4) as described above (Section 2.12.3). The bound protein complexes were washed three times with TB, once with TB containing 500 mM NaCl and three additional times with TB. The beads were loaded onto a microcentrifuge chromatography column (BioRad) and 60  $\mu$ L 1X SDS sample buffer passed over the beads twice to release the bead-bound proteins. Both the bound and unbound fractions were heat denatured as described above (Section 2.12.3) and an equal volume of each sample was separated by SDS-PAGE (Section 2.12.3) and visualized by Coomassie blue staining.

**2.17.2 *GST-Nop1p protein complex formation*** – GST-chimeras containing full-length Nop1p, the deletion fragments of Nop1p or GST alone were immobilized on GT-Sepharose as described above (Section 2.13.2) and

incubated with purified recombinant Kap121p, Kap104p or Kap108p (Section 2.13.2) in TB for 3 hrs at 4°C. The beads were collected by centrifugation and the unbound protein fractions were collected and prepared for SDS-PAGE as described above. The beads were washed three times with 1mL TB and collected as described above (Section 2.17.1) SDS-PAGE and Coomassie blue staining were used to analyze equal volume of each of these fractions.

**2.17.3 Ran release** – GST-Ste12p(aa494-688)/Kap121p, GST-Nop1p(aa1-90)/Kap121p and GST-Dbp9p/Kap121p protein complexes were formed as above (Section 2.17.1 and 2.17.2) and separated into three equal aliquots. Ran-GTP, Ran-GDP, or GTP-loading buffer alone were added and incubated with rotation at room temperature for 30 min. The beads were collected by centrifugation, and each unbound protein fraction was collected and prepared for SDS-PAGE. The bound protein complexes were washed three times with TB and released from the beads as described above (Section 2.17.1). Proteins in the resulting fractions were separated by SDS-PAGE and visualized by Coomassie blue staining. The amounts of Kap121p present in each lane of the gel were quantified using ImageQuant as previously described (Lee and Aitchison, 1999). The quantity of Kap121p released from the complex was represented graphically as a percentage of total Kap121p ( $\frac{\text{released}}{\text{released} + \text{bound}} \times 100\%$ ). The standard deviations from the means were calculated from three separate experiments.

**2.17.4 Sof1p-pA protein complex formation** – Sof1p-pA was isolated from a yeast whole cell lysate. 100  $\mu$ L of IgG-coupled magnetic beads, from a  $2.0 \times 10^6$  bead/mL slurry, were pre-equilibrated by washing the beads three times with 1 mL TB. The beads were then blocked by incubation with TB containing 0.4  $\mu$ g of BSA/ $\mu$ L and 0.2% casamino acids (Difco) at room temperature for 30 min. The beads were added to 10 mL of a *SOF1-A* yeast whole cell lysate (Section 2.10.2) and incubated with rotation at 4°C for 2-16 hrs. The beads were collected using a magnet and the unbound fraction was aspirated slowly and discarded. The beads were washed three times with 5 mL TB and three times with 5 mL of elution buffer containing 1 M  $MgCl_2$  to remove Sof1p-interacting proteins. The sample was then divided into 4 equal fractions, 400 to 800 ng of the indicated purified recombinant proteins were added to individual fractions of the immobilized Sof1p-pA and incubated at 4°C for 2 hrs. The beads were collected and the unbound protein fractions were prepared for SDS-PAGE. Immobilized protein fractions were washed three times with 1mL TB and prepared for SDS-PAGE as described above. The samples were separated by SDS-PAGE, transferred to nitrocellulose membranes and immunoblotted with  $\alpha$ -Kap121p (which recognizes GST, protein A and Kap121p (Marelli *et al.*, 1998)).

**2.17.5 In vitro binding challenge assays** – For Sof1p-pA-GST-Nop1p and Sof1p-pA-Kap121p complex challenge assays, the complexes were assembled as described above (Section 2.17.4) and divided into five equal fractions. The bead-bound proteins from one of these fractions were released from the beads

with 1X SDS sample buffer. The remaining fractions of beads were incubated with either recombinant Kap121p (in TB2), GST-Nop1p (in TB2), GST (in TB2) or TB2 alone, as indicated, for 2 hrs at 4°C. The beads were collected using a magnet and the unbound protein fractions prepared for SDS-PAGE. The beads were washed two times with 1mL TB and the bead-retained proteins were collected as described above. All samples were separated by SDS-PAGE and transferred to nitrocellulose membranes. Immunoblotting using  $\alpha$ -Kap121p was used to analyze the unbound and bound fractions.

**2.17.6 Competition assays** – Nop1p-pA was purified from *NOP1-A* cell lysates as described above (Section 2.17.4). The immobilized chimera was incubated with ~400 ng of purified Kap121p (in TB2) at 4°C for 3 hrs and the beads washed three times with 1mL TB containing 500 mM NaCl. The Nop1p-Kap121p complexes were then challenged with the indicated GST-NLS chimeric protein (in TB2 plus 500 mM NaCl), GST (in TB2 plus 500 mM NaCl), or TB2 plus 500 mM NaCl for 3 hrs at 4°C. All unbound and bead-bound fractions were analyzed by immunoblotting as described above (Section 2.17.4).

## Chapter 3 – Kap121p-mediated nuclear import is required for mating and cellular differentiation in *S. cerevisiae*<sup>8</sup>

### 3.1 Summary

The prototypical Kap121p nuclear import pathway was used as a model to enhance our general understanding of how regulated nucleo-cytoplasmic transport events influence cellular physiology. This chapter describes the identification and characterization of Ste12p, a transcription factor required for both the mating response and pseudohyphal or invasive growth, as a Kap121p nuclear import cargo. While generating *kap121* temperature-sensitive (ts) mutants, two previously unreported phenotypes associated with *kap121* mutants were detected: defects in mating and in the transition from the normal yeast form to the pseudohyphal, invasive form. Using Kap121p as a probe in overlay blot assays of yeast nuclear proteins, Ste12p was identified among 27 potential Kap121p cargoes. Together, these preliminary studies suggested that these mutant phenotypes could result from an inability to import Ste12p. Indeed, *in vivo* fluorescence microscopy studies showed that Ste12p mislocalized to the cytoplasm upon temperature inactivation of Kap121p in *kap121-ts* mutant strains. Co-immunopurification and *in vitro* binding studies demonstrated that Kap121p interacted specifically with Ste12p, and that this interaction was sensitive to Ran-GTP. The Kap121p-specific NLS of Ste12p was found to reside within the C

---

<sup>8</sup> The data presented in this Chapter were published in Leslie, D.M., B. Grill, M.P. Rout, R.W. Wozniak, and J.D. Aitchison. 2002. Kap121p-mediated nuclear import is required for mating and cellular differentiation in yeast. *Mol Cell Biol.* 22:2544-55.

terminus of Ste12p. Furthermore, overexpressing *STE12* or expressing a *STE12cNLS* gene fusion in *kap121-ts* haploid cells suppressed both the invasive growth and mating defects of this strain. Together, these data established that Ste12p is imported into nuclei by Kap121p, and that the mating and cellular differentiation defects associated with *kap121-ts* mutants are attributable, at least in part, to the mislocalization of Ste12p. This chapter emphasizes how employing parallel experimental approaches when initially identifying potential nuclear transport cargoes provides valuable insight that can link the phenotypes associated with *kap* mutants to their transport substrates.

### **3.2 *KAP121* temperature-sensitive mutants**

**3.2.1 *Generation and characterization of kap121-ts mutants*** – Previous studies have demonstrated that *KAP121* is an essential gene (Rout *et al.*, 1997; Seedorf and Silver, 1997). To understand the essential role Kap121p plays in cellular fitness and aid in the identification of Kap121p-specific cargoes, a random PCR mutagenesis approach (Muhlrad *et al.*, 1992) was used to isolate temperature-sensitive mutant alleles of *KAP121*. Four temperature-sensitive clones were isolated based on their ability to grow on rich solid medium at 23 °C but not at 37°C (Figure 3.2.1A)<sup>9</sup>. To characterize the growth rates of these mutant clones in liquid culture, their growth was monitored over a 12 hour period at either 23°C or 37°C and growth curves were generated from these data for each strain (Figure 3.2.1B). When compared to a wild-type strain

---

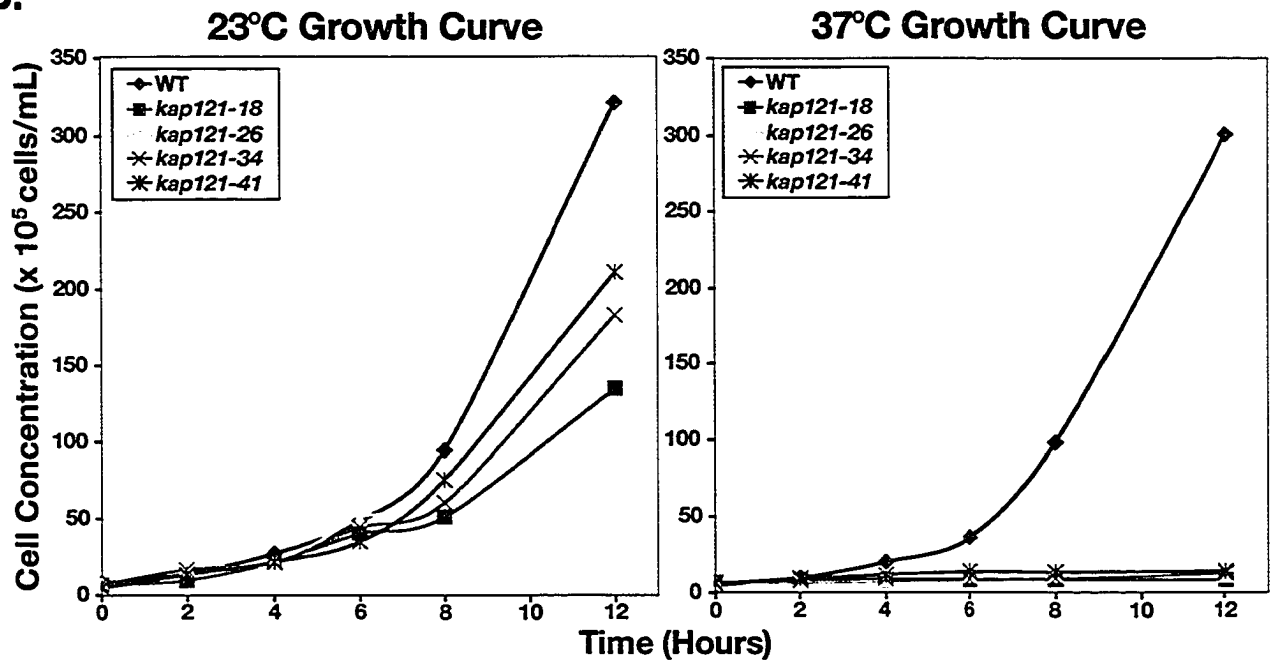
<sup>9</sup> *kap121-ts* strains were isolated by Brock Grill.

Figure 3.2.1: *kap121-ts* mutants. *A.* Parental (PT) DF5 cells,  $\Delta kap121/pKAP121-URA3$  (WT), and the *kap121-ts* yeast strains were streaked on to YEPD agar plates and incubated for 2 days at 23°C or 37°C. When incubated at 23°C, all strains grew, but the growth of the temperature-sensitive strains (*kap121-18*, *kap121-26*, *kap121-34*, and *kap121-41*) was dramatically inhibited at 37°C. *B.* WT ( $\Delta kap121/pKAP121-URA3$ ) and *kap121-ts* strains were inoculated into YEPD liquid medium at a concentration of  $5 \times 10^5$  cells/mL and incubated at either 23°C or 37°C. Aliquots were removed from each culture at the indicated times and the cell concentration of each culture was determined using a hemacytometer. Culture concentrations are plotted against time (hours). *C.* WT ( $\Delta kap121/pKAP121-URA3$ ) and *kap121-ts* strains were inoculated into YEPD liquid medium at a concentration of  $\sim 1 \times 10^6$  cell/ml and incubated at 37°C. Cells were harvested from these cultures at the indicated times and whole cell lysates were generated. An equal amount of protein from each sample was separated by SDS-PAGE, transferred to nitrocellulose and probed with  $\alpha$ -Kap121p and  $\alpha$ -Gsp1p (loading control) antibodies (Table 2-2).

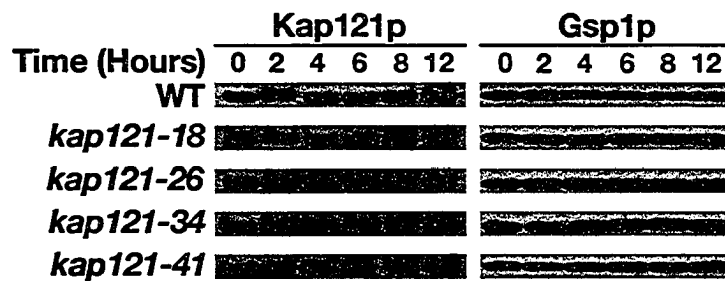
**A.**



**B.**



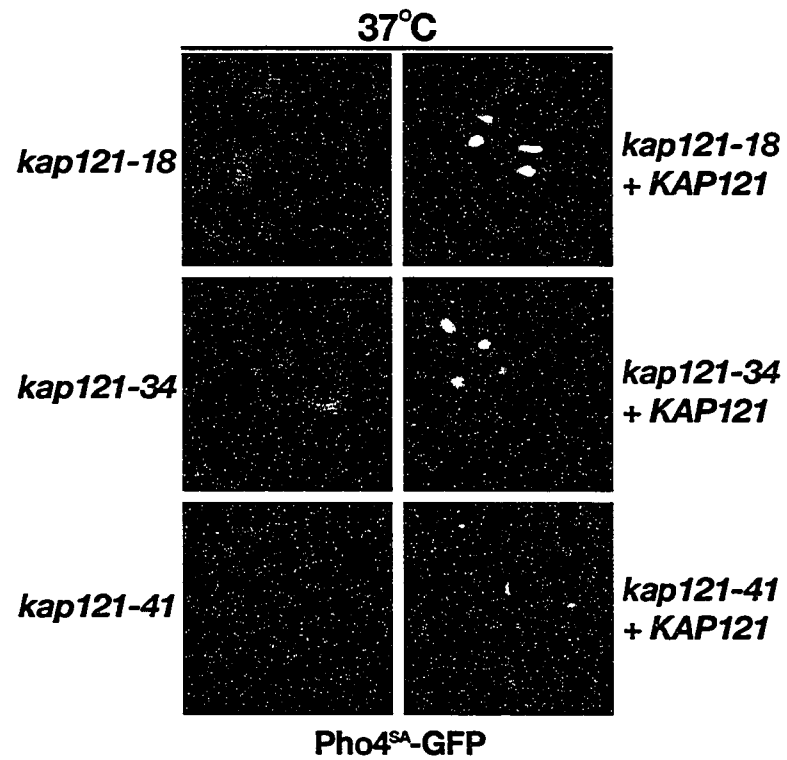
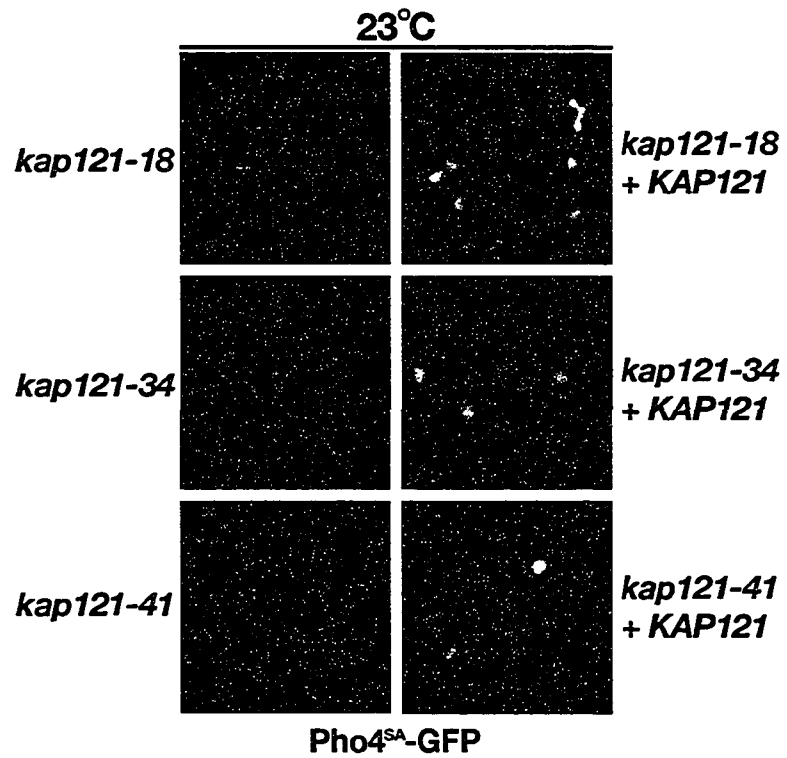
**C.**



( $\Delta kap121/pKAP121-URA3$ ), all of the mutant strains grew slower at the permissive temperature (23°C) and displayed dramatic growth defects at the non-permissive temperature (37°C). Immunoblotting whole cell lysates obtained from both the wild-type and temperature-sensitive strains during a similar temperature shift time course with  $\alpha$ -Kap121p antibodies (Table 2-2) demonstrated that each mutant allele produced proteins of the same molecular mass as wild-type Kap121p (Figure 3.2.1C), indicating that Kap121p was present but not functional at the non-permissive temperature (37°C).

**3.2.2 Nuclear import of Kap121p cargo in *kap121-ts* mutants** – To determine if the *kap121-ts* alleles isolated contained mutations that impaired Kap121p mediated nuclear import, the cellular localization of a Pho4<sup>SA</sup>-GFP fusion (Kaffman *et al.*, 1998b) was monitored in the *kap121-18*, *kap121-34*, and *kap121-41* strains. As previously observed with other *kap121* mutants (*pse1-1* (Kaffman *et al.*, 1998b) and *kap121-41* (Marelli *et al.*, 1998)), this GFP chimera was predominantly mislocalized to the cytoplasm of each strain at the permissive temperature (23°C) and was completely mislocalized at the non-permissive temperature (37°C) (Figure 3.2.2). When a wild-type allele of *KAP121* was added back to each strain, Pho4<sup>SA</sup>-GFP relocalized to the nucleus at both 23°C and 37°C (Figure 3.2.2), demonstrating that these mutant alleles of *KAP121* specifically impaired the Kap121p transport pathway in the similar manner as the *pse1-1* allele. As differences in import among the three *kap121-ts* strains examined (Figure 3.2.2 and below) were not obvious, and not specifically

Figure 3.2.2: **Nuclear import of Kap121p cargo in the *kap121-ts* strains.** The Pho4<sup>SA</sup>-GFP gene fusion (Kaffman *et al.*, 1998b) was expressed in the indicated *kap121-ts* strains, as well as the same strains also expressing a wild-type *KAP121* allele. The cultures were grown to mid-logarithmic phase at 23°C and the GFP chimera detected using fluorescence microscopy (Top). These cultures were then incubated at 37°C for 3 hours and localization of Pho4<sup>SA</sup>-GFP determined as described above. Note that when expressed in the *kap121-ts* mutants at 23°C the GFP fusion was predominantly mislocalized to the cytoplasm and completely mislocalized to the cytoplasm of these cells when incubated at 37°C.



explored, I chose to focus on characterizing the mutant phenotypes of one of these strains, *kap121-34*. DNA sequence analysis of the *kap121-34* allele identified 20 point mutations, which resulted in 13 amino acid residue changes throughout the length of the protein (Table 3-1).

**Table 3-1 *kap121-34* nucleotide and amino acid residue substitutions**

Nucleotide Change	Position	Amino Acid Residue Change	Position
A -> C	305	I -> T	102
A -> G	977	D -> G	326
T -> C	1087	Y -> H	363
A -> G	1274	Q -> R	425
A -> T	1336	T -> S	446
A -> G	1630	K -> E	544
T -> G	2042	L -> R	681
A -> G	2105	E -> G	702
T -> C	2317	S -> P	773
A -> T	2566	N -> Y	856
C -> T	2732	S -> F	911
T -> C	3068	V -> A	1023
A -> G	3109	I -> V	1037

*kap121-34* DNA coding sequence was determined in both the forward and reverse orientation, and the resulting *kap121-34* DNA sequences were compared to *KAP121* using MegAlign. Nucleotide substitutions that appeared in both the forward and reverse orientation sequences were incorporated into the full-length *KAP121* sequence and translated using EditSeq. The resulting *kap121-34p* amino acid residue sequence was compared with wild-type Kap121p using MegAlign and amino acid residue substitutions recorded. The nucleotide substitutions that resulted in amino acid residue changes are presented here.

As demonstrated above, initial analysis of *kap121-34* cells showed that this strain grew more slowly than the wild-type strain at all temperatures tested (Figure 3.2.1B). However, closer examination of *kap121-34* cells revealed that these cells accumulated late in cell division as large-budded cells after 4 hours of growth at 37°C<sup>10</sup> (Marelli *et al.*, 1998). Furthermore, when crossed with other strains, this strain did not mate as well as other laboratory strains (see below; Figure 3.9.1). This mating deficiency suggested that Kap121p might mediate the

<sup>10</sup> Similar, independent observations were made by Dr. Marcello Marelli and Dr. C. Patrick Lusk when working with the *kap121-41* strain .

nuclear import of proteins required for mating; a pheromone response assay was, therefore, used to further characterize this phenotype.

**3.2.3 *kap121-34* cells do not respond to pheromone at non-permissive temperatures** – When haploid cells are treated with the appropriate pheromone a number of physiological changes occur that are indicative of mating responses, including cell cycle arrest (evidenced by the accumulation of unbudded cells) and shmoo formation, which can be assayed using differential phase contrast microscopy (Figure 3.2.3A; (Sprague, 1991)). To this end, *kap121-34 Mata* and wild-type (DF5) *Mata* cultures were grown to mid-logarithmic phase at 23°C and were found to contain 40-50% unbudded cells, a characteristic typical of actively growing cultures (Figure 3.2.3B). These cultures were then treated with 2.5 μM α-factor, incubated at 23°C, 30°C or 37°C, and assayed for shmoo formation and cell cycle arrest at 1 hour intervals post-pheromone treatment. In WT (DF5) cultures, the number of unbudded and shmooed (unbudded/shmooed) cells increased to ~75% after 3 hours of pheromone treatment at 23°C, ~85% at 30°C and 75% at 37°C. The number of unbudded and shmooed cells increased to ~70% at both 23°C and 30°C in *kap121-34* cultures, indicating that these cells were also able respond to α-factor at permissive temperatures (Figure 3.2.3B). However, at the non-permissive temperature *kap121-34* cells did not respond to pheromone treatment. The number of unbudded and shmooed cells remained constant at ~40% under these conditions (Figure 3.2.3A/B). These data supported our qualitative observation that wild-type Kap121p was important for

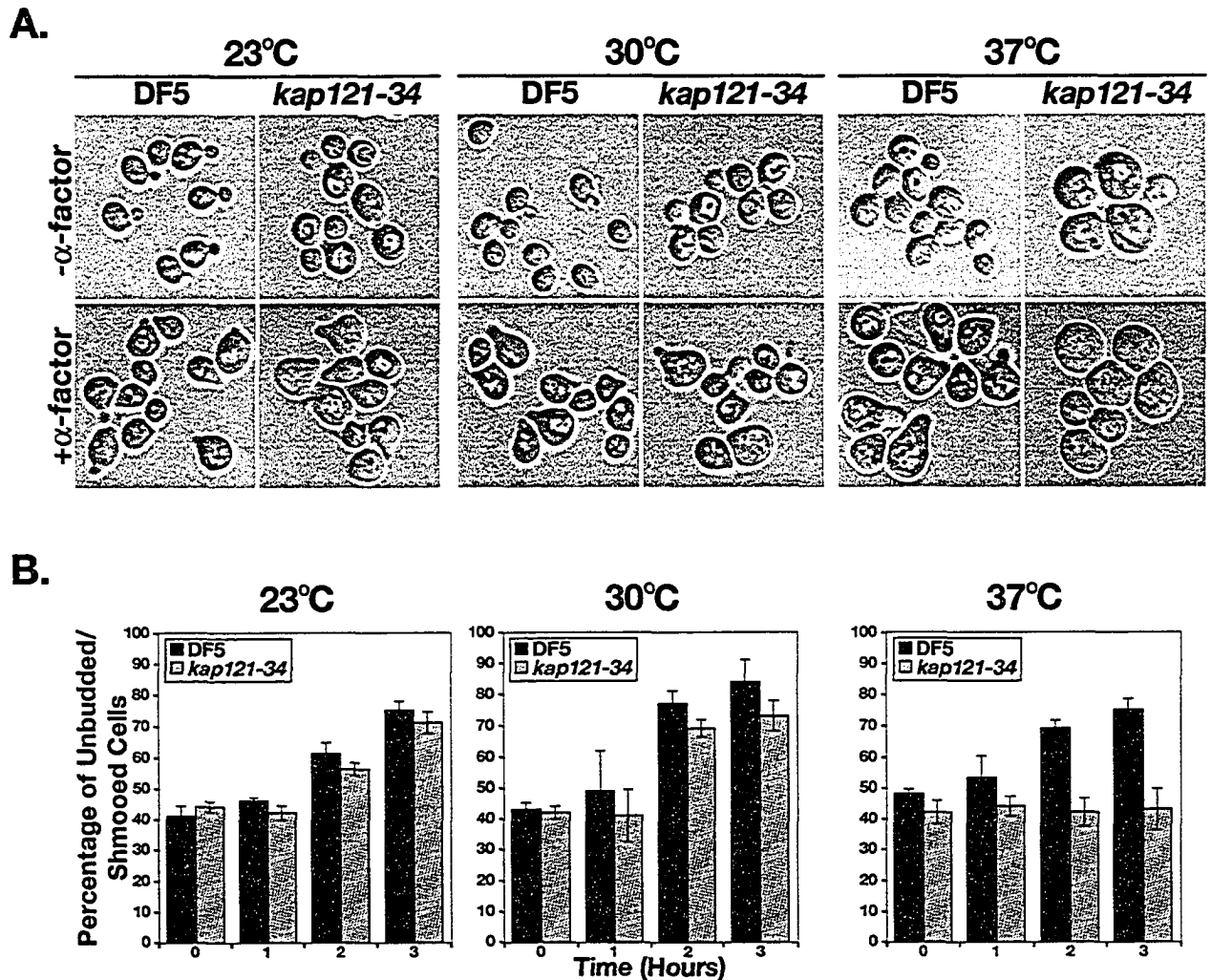


Figure 3.2.3: *kap121-34* cells are unable to respond to  $\alpha$ -factor at non-permissive temperatures. Exponentially growing DF5 *Mata* and *kap121-34 Mata* cultures were treated with 2.5  $\mu$ M  $\alpha$ -factor and incubated at 23°C, 30°C or 37°C. Samples were taken from each culture at 1 hour intervals post-pheromone treatment and fixed with 3.7% formaldehyde in 7.5 mM NaCl. *A.* The cultures were assayed using differential phase contrast microscopy for cell cycle arrest (the accumulation of unbudded cells) and shmoo formation. Note that shmoos were not detected in the *kap121-34* cultures when incubated at 37°C. *B.* The number of budded cells was compared to the number of unbudded/shmooed cells in each culture. Plotted are the percentages of unbudded/shmooed cells in the presence of pheromone. The standard deviations from the means were calculated from three separate experiments. Note the lack of response to pheromone by *kap121-34* cells at 37°C.

the mating response. I, therefore, hypothesized that an essential factor required for yeast mating responses was normally imported into the nucleus by Kap121p. While previous studies had identified a number of Kap121p nuclear import cargoes, including Pho4p (Kaffman *et al.*, 1998b), Spo12p (Chaves and Blobel, 2001), Pdr1p (Delahodde *et al.*, 2001) and Yap1p (Isoyama *et al.*, 2001), the cellular processes governed by these substrates are not specifically related to the mating process. Thus, overlay blot assays of yeast nuclear proteins were used to identify Kap121p cargoes; some of which may be implicated in this specific differentiation program.

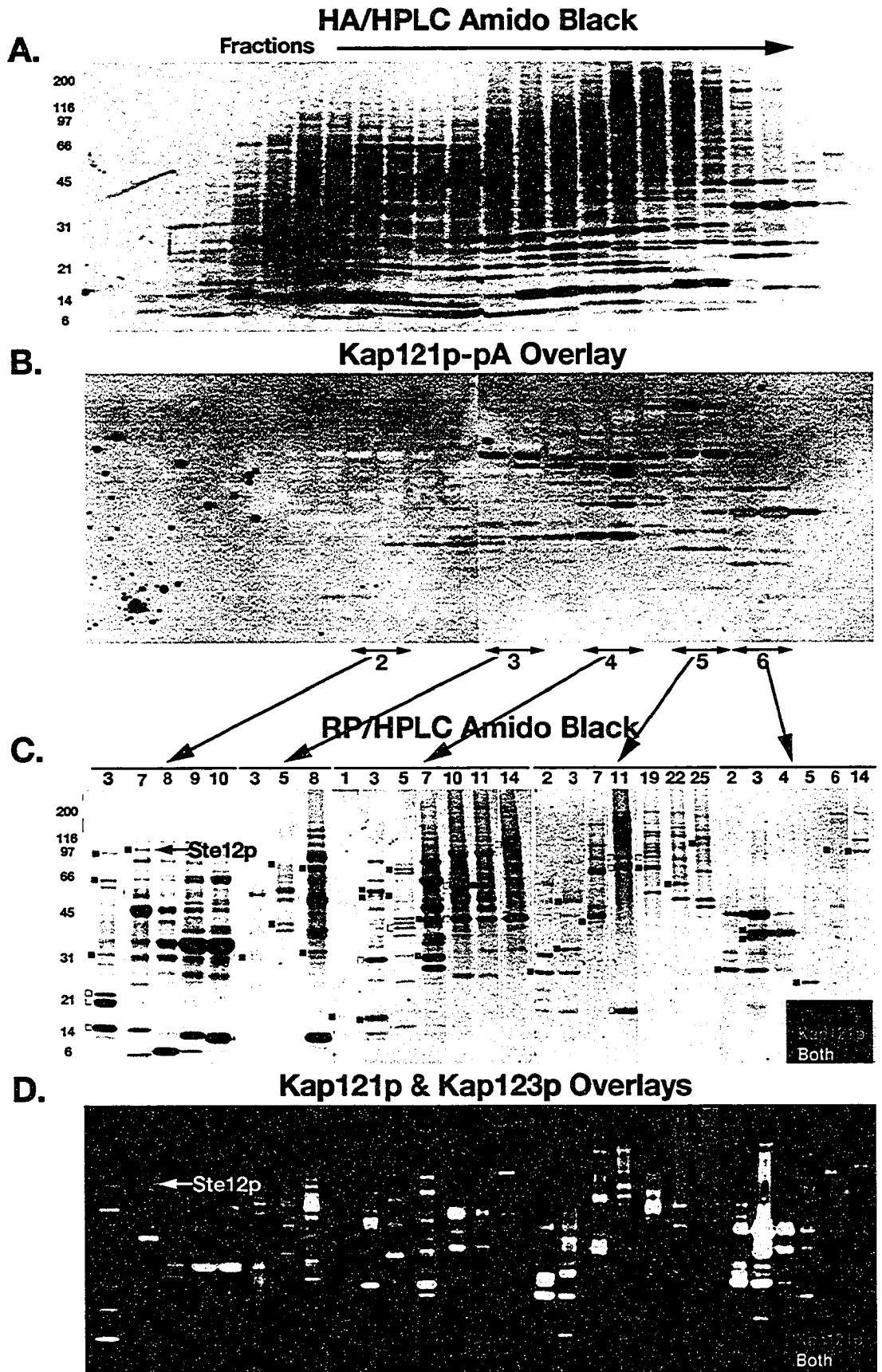
### **3.3 Identification of Ste12p as a Kap121p-interacting nuclear protein**

A protein A (pA)-tagged Kap121p chimera (Kap121-pA) was used in an overlay assay to detect nuclear proteins that interact with Kap121p<sup>11</sup>. Yeast nuclei were purified, the proteins fractionated using hydroxyapatite HPLC (HA/HPLC), separated by SDS-PAGE, and transferred to nitrocellulose membranes (Figure 3.3.1A). The membranes were incubated with cytosols from yeast cells expressing Kap121p-pA, and the bound chimera was detected with rabbit IgG and enhanced chemiluminescence (Figure 3.3.1B). Because Kap121p and Kap123p are functionally similar and it is well established that they bind to many of the same cargoes (Rout *et al.*, 1997), the overlay blot assay was repeated using protein A-tagged Kap123p (Kap123p-pA) as a control. Fractions enriched with Kap121p-interacting proteins were pooled and further fractionated

---

<sup>11</sup> Overlay blot assays were performed by Drs. John Aitchison and Michael Rout.

Figure 3.3.1: **Kap121p interacts with numerous nuclear proteins.** *A.* Yeast nuclear proteins were purified, fractionated by hydroxyapatite HPLC (HA/HPLC), separated by SDS-PAGE, transferred to nitrocellulose membranes and detected by amido-black staining. *B.* These membranes were then probed with cytosols from cells expressing either Kap121p-pA or Kap123p-pA and the bound chimeras were detected with horse-radish peroxidase-conjugated rabbit IgG and ECL. The Kap121p-pA overlay blot is shown here. *C.* Fractions enriched with Kap121p interacting proteins were pooled as indicated and further fractionated by reverse-phase HPLC (RP/HPLC). The resulting fractions were separated by SDS-PAGE, transferred to nitrocellulose membranes and detected by amido-black staining. *D.* These membranes were separately probed with cytosols containing Kap121p-pA or Kap123p-pA as described above and the bound chimeras detected as before. Shown are overlaid, colorized images of each blot (red = Kap123p-pA; green = Kap121p-pA; yellow = both). Karyopherin-interacting proteins were identified by mass spectrometry of the same protein bands in an identical gel. The protein bands corresponding to the identified proteins are marked with red, green or yellow squares (indicating their interaction specificity) on the RP/HPLC amido black-stained membrane. The band corresponding to Ste12p is labeled in panels *C* and *D*. (Overlay blot assays were performed by Drs. John Aitchison and Michael Rout.)



by reverse-phase HPLC (RP/HPLC), separated by SDS-PAGE and transferred to nitrocellulose membranes (Figure 3.3.1C). These membranes were again separately probed with Kap121-pA and Kap123-pA cytosols. The resulting Kap121p-pA and Kap123p-pA profiles were compared (Figure 3.3.1D) and all karyopherin-interacting proteins were identified by MALDI-TOF mass spectrometry of the same bands in Coomassie blue-stained SDS-polyacrylamide gels<sup>12</sup>.

Twenty-seven Kap121p-interacting proteins were identified (Table 3-2). In agreement with previous studies, many of these proteins, including ribosomal proteins, also interacted with Kap123p; however, 11 proteins favored Kap121p over Kap123p under these conditions. Among these was Ste12p (Figure 3.3.1), a transcription factor that regulates mating responses and cellular differentiation. The central role that Ste12p plays in regulating mating responses (Gustin *et al.*, 1998; Liu *et al.*, 1993; Roberts and Fink, 1994), together with the data demonstrating that *kap121-34* mutants were unable to respond to  $\alpha$ -factor at elevated temperatures prompted further characterization of the Kap121p-Ste12p interaction.

**Table 3-2 Kap121p-interacting nuclear proteins**

YPD Name	a.k.a	MW	Binding Preference	Function	#Peptides	% Coverage	P(top)/P(next)	Band #
YBR031W	Rpl4Ap	39124	Kap121p/ Kap123p	Ribosomal protein L4 (yeast L2; YL2; r2; Xenopus L1; Drosophila L1; rat L4), nearly identical to Rpl4Bp	11	49	1 x 10 <sup>(15)</sup>	26
YBR079C	Rpg1p; Tif32p	110329	Kap121p/ Kap123p	Translation initiation factor eIF3, p110 subunit	12	18	1 x 10 <sup>(10)</sup>	34
YBR142W	Mak5p	87051	Kap121p/ Kap123p	Probable RNA-helicase of the DEAD box family, involved in maintenance of M double-stranded RNA (dsRNA) killer plasmid, required for 60S	16	26	2 x 10 <sup>(25)</sup>	41

<sup>12</sup> Wenzhu Zhang in Dr. Brian Chait's laboratory at the Rockefeller University performed MALDI-TOF mass spectrometry experiments and subsequent protein identifications.

				ribosomal subunit biogenesis				
YCR016W		33594	Kap121p	Protein of unknown function	11	41	5 x 10(4)	17
YDL014W	Nop1p	34487	Kap121p	Fibrillarin, required for 35S rRNA processing and methylation, methyltransferase component of box C/D snoRNPs which function in 2'-O-methylation of ribosomal RNAs, and component of U3 snoRNP, which is required for 18S rRNA biogenesis	9	45	5 x 10(7)	49,50,52
YDL208W	Nhp2p	18883	Kap121p/ Kap123p	Nucleolar protein required in association with H/ACA snoRNAs for ribosomal RNA pseudouridylation	6	32	1 x 10(10)	7,42
YDR012W	Rpl4Bp	39094	Kap121p/ Kap123p	Ribosomal protein L4 (yeast L2; YL2; rp2; Xenopus L1; Drosophila L1; rat L4), nearly identical to Rpl4Ap	10	44	1 x 10(12)	26
YER082C	Utp7p; Kre31p	62333	Kap121p	Component of U3 snoRNP (also called small subunit processome), which is required for 18S rRNA biogenesis, has one WD (WD-40) domain	15	31	2 x 10(25)	25
YER126C	Nsa2p; Kre32p	29751	Kap121p	Nuclear protein involved in ribosome biogenesis	12	41	2 x 10(10)	36
YHR084W	Ste12p	77853	Kap121p	Transcription factor that binds to pheromone response element (PRE) to regulate genes required for mating, also functions with Tec1p to regulate genes required for pseudohyphal growth	14	32	8 x 10(21)	12
YHR203C	Rps4Bp	29431	Kap121p/ Kap123p	Ribosomal protein S4 (yeast S7; YS6; rp5; rat and human S4), identical to Rps4Ap	24	66	1 x 10(50)	28
YJR145C	Rps4Ap	29431	Kap121p/ Kap123p	Ribosomal protein S4 (yeast S7; YS6; rp5; rat and human S4), identical to Rps4Bp	23	62	1 x 10(49)	28
YKR024C	Dbp7p	83328	Kap121p/ Kap123p	Protein involved in 60S ribosomal large subunit biogenesis, member of DEAD-box family of putative ATP-dependent RNA helicases	8	16	1 x 10(7)	40
YLL011W	Sof1p	56804	Kap121p	Protein component of U3 snoRNP (also called small subunit processome), which is required for 18S rRNA biogenesis, contains seven WD (WD-40) repeats	17	49	1 x 10(23)	38
YLR175W	Cbf5p	54717	Kap121p/ Kap123p	Ribosomal RNA pseudouridine synthase, associated with H/ACA class small nucleolar RNAs (snoRNAs)	14	36	5 x 10(19)	32,33
YLR276C	Dbp9p	68076	Kap121p	Member of the DEAD-box RNA helicase family, functions in rRNA processing to the precursor of 60S ribosomal subunits, interacts with Dbp6p	16	39	3 x 10(26)	44
YLR448W	Rpl6Bp	20004	Kap121p/ Kap123p	Ribosomal protein L6 (yeast L17B; YL16B; human L6), nearly identical to Rpl6Ap	8	50	2 x 10(3)	8
YML069W	Pob3p	62960	Kap121p	Protein that binds to DNA polymerase I (Poll) that is involved in both transcription and replication	9	24	5 x 10(3)	18
YML073C	Rpl6Ap	19980	Kap121p/ Kap123p	Ribosomal protein L6 (yeast L17A; YL16A; human L6), nearly identical to Rpl6Bp	8	50	2 x 10(3)	8
YNL002C	Rlp7p; Rix9p	36569	Kap121p/ Kap123p	Protein with similarity to ribosomal proteins including Rpl7p (Rpl7Ap and Rpl7Bp), involved in processing of precursor rRNAs	14	45	1 x 10(17)	30
YNL075W	Imp4p	33486	Kap121p	Component of U3 snoRNP (also called small subunit processome), which is required for pre-18S rRNA processing, member of superfamily of proteins with a sigma70-like motif	15	53	3 x 10(13)	17
YOL041C	Nop12p	51962	Kap121p	Protein important for the synthesis of 25S pre-rRNA	10	25	6 x 10(12)	24
YOL090W	Msh2p	108860	Kap121p/ Kap123p	Component with Msh3p and Msh6p of DNA mismatch binding factor, involved in repair of single base mismatches and short insertions/deletions	12	21	5 x 10(16)	43
YOL127W	Rpl25p	15775	Kap121p/ Kap123p	Ribosomal protein L25 (YL25; rp61L; E. coli L23; rat L23a), required for efficient pre-rRNA processing, including early cleavage steps and processing of internal transcribed spacer 2 (ITS2)	9	60	1 x 10(7)	6
YOL145C	Ctr9p	124639	Kap121p/ Kap123p	Protein required for normal expression of G1 cyclins CLN1 and CLN2, has tetratricopeptide (TPR) repeats and binds triplex DNA, may be involved in transcription elongation	6	9	5 x 10(2)	34

YOR063W	Tcm1p	43796	Kap121p/ Kap123p	Ribosomal protein L3 (YL1; rp1; rat L3), responsible for trichodermin resistance and involved in maintenance of dsRNA viruses	22	49	1 x 10 <sup>(31)</sup>	37,51
YPL012W	Rrp12p	137501	Kap121p	Protein possibly involved in rRNA processing, has high similarity to uncharacterized <i>C. albicans</i> Orf6.7937p	36	44	1 x 10 <sup>(35)</sup>	45

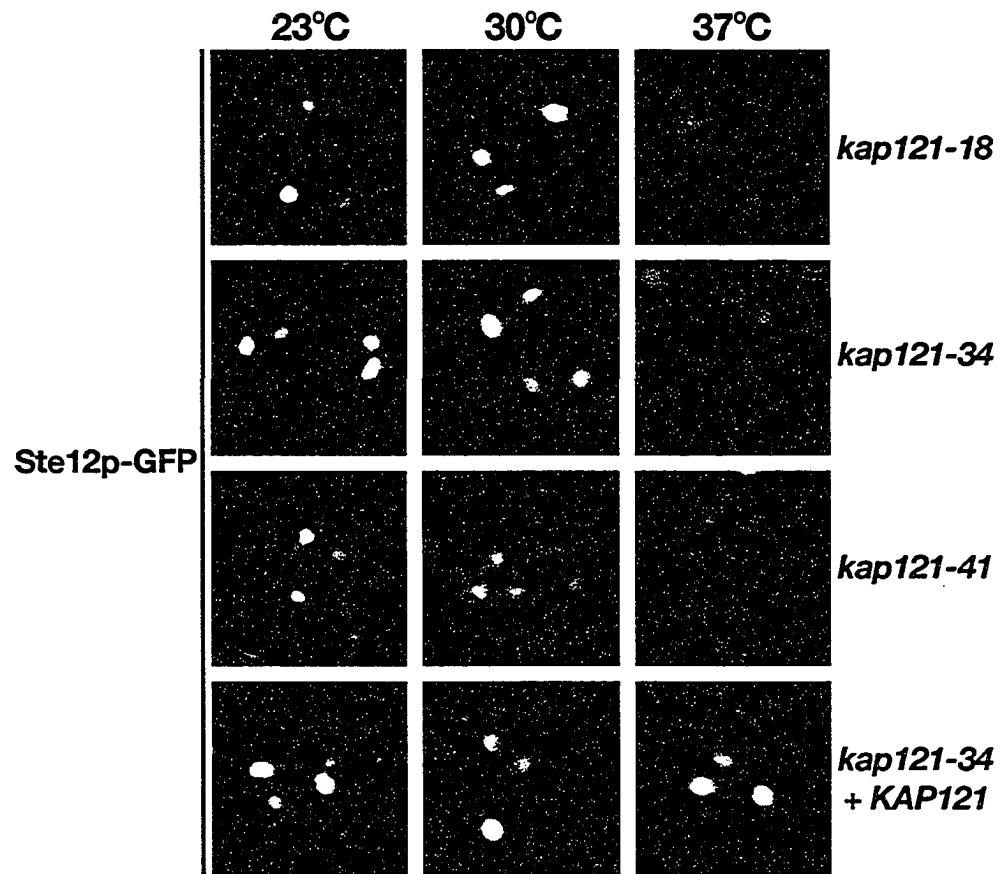
Proteins identified by Kap121p-pA and Kap123p-pA overlays are listed as their open reading frame identifier and their common names. Calculated molecular masses (MW) are shown. Binding preference indicates whether the protein bound specifically to Kap121p or showed little specificity between the Kap121p-pA and Kap123p-pA. Functions are listed as annotated in YPD (Yeast Proteome Database; Incyte Genomics; <https://www.incyte.com>). The number of peptides identified, percent coverage of the protein and the ratio of the probability of the first-ranked protein to the second-ranked protein as determined by the protein search engine "ProFound" is shown. For ratios  $\geq 10^3$  the identification of the top-ranked protein is considered to be highly confident.

### 3.4 Ste12p is mislocalized in *kap121-ts* cells

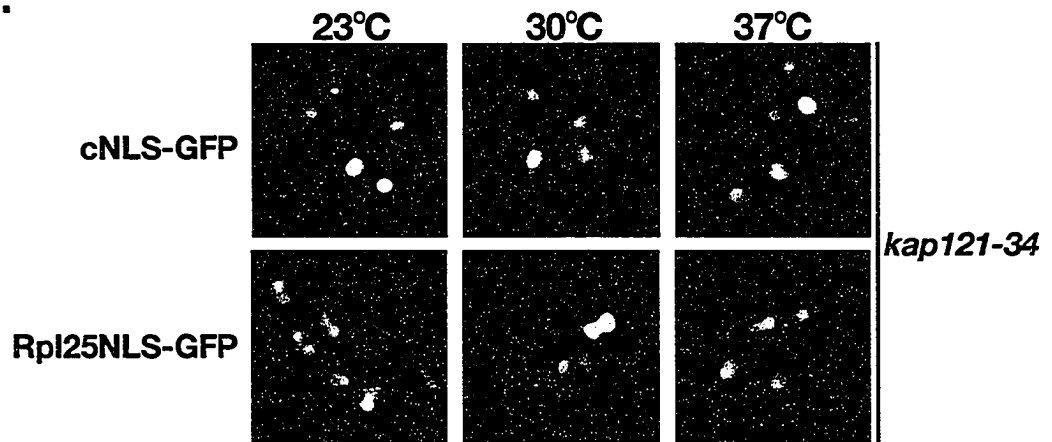
To determine if Ste12p is a cargo of the Kap121p-mediated transport pathway, Ste12p was C-terminally tagged with green fluorescent protein (GFP) and its cellular localization examined in *kap121-18*, *kap121-34* and *kap121-41* cells (Figure 3.4.1A). At 23°C, Ste12p-GFP was predominantly nuclear but also detectable in the cytoplasm of *kap121-ts* cells. After 3 hours at 30°C the cytoplasmic pool of Ste12p-GFP increased and at 37°C Ste12p mislocalized to the cytoplasm, with little or no defined nuclear signal (Figure 3.4.1A). When a functional copy of *KAP121* was added back to *kap121-34* cells, Ste12p-GFP remained nuclear at all temperatures. Similar observations were made when a wild-type copy of *KAP121* was added back to *kap121-18* and *kap121-41* cells. These data demonstrated that partial or total loss of Kap121p function caused the redistribution of Ste12p to the cytoplasm, while the presence of a functional copy prevented this mislocalization. As controls, the cellular localizations of GFP fusion proteins containing the cNLS of SV40 large T antigen and the NLS of Rpl25p (Rpl25NLS), whose import into the nucleus are mediated by

Figure 3.4.1: **Ste12p mislocalizes in *kap121-ts* at non-permissive temperatures.** *A.* Ste12p was expressed as a GFP chimera in the indicated *kap121-ts* haploid cells, as well as *kap121-34* cells expressing a wild-type copy of *KAP121*. Cultures were grown to mid-logarithmic phase at 23°C and GFP detected using direct fluorescence microscopy. In each case, the GFP fusion localized predominantly to the nucleus. Each culture was then shifted to 30 °C or 37 °C for 3 hours prior to microscopy analysis. Note that after the temperature shift to 30°C the cytoplasmic pool of Ste12p-GFP increased and at 37°C this chimera was primarily mislocalized to the cytoplasm. *B.* The cNLS of SV40 large T-antigen and the NLS of Rpl25p (Rpl25NLS) were expressed as GFP chimeras in *kap121-34* cells under the conditions described above and their cellular localizations monitored as before.

**A.**



**B.**



Kap95p/Kap60p and Kap123p, respectively (Rexach and Blobel, 1995; Rout *et al.*, 1997), were monitored in the *kap121-34* strain. Both of these GFP chimeras localized to the nucleus at all temperatures tested (Figure 3.4.1B), indicating that Ste12p mislocalization was specific to the Kap121p transport pathway.

### 3.5 Mapping the nuclear localization signal (NLS) of Ste12p

**3.5.1 Kap121p interacts directly with the C terminus of Ste12p** – Both the overlay assay and the *in vivo* import data suggested that Kap121p interacts with Ste12p and mediates its nuclear import. *In vitro* binding studies were used to determine whether Kap121p interacts directly with Ste12p. A GST chimera containing full-length Ste12p was constructed and expressed in *E. coli*, however this chimera was highly susceptible to proteolysis. Deletion fragments of Ste12p were, therefore, generated to further characterize this interaction and concomitantly identify the region of Ste12p that contains its NLS. Ste12p contains a number of domains that are essential for its function as a transcription factor (Pi *et al.*, 1997; Yuan and Fields, 1991), but the presence of an obvious NLS was not clear. Visual analysis of the amino acid residue sequence of Ste12p revealed a few regions located in both the N-terminal and C-terminal portions of Ste12p that could function as NLS sequences based on the high concentration of basic amino acid residues within these areas (Figure 3.5.1A). GST chimeras containing amino acid residues 1-252, 253-493, 494-688 (GST-Ste12p(aa1-252), GST-Ste12p(aa253-493) and GST-Ste12p(aa494-688), respectively) and GST alone were expressed in *E. coli*, immobilized

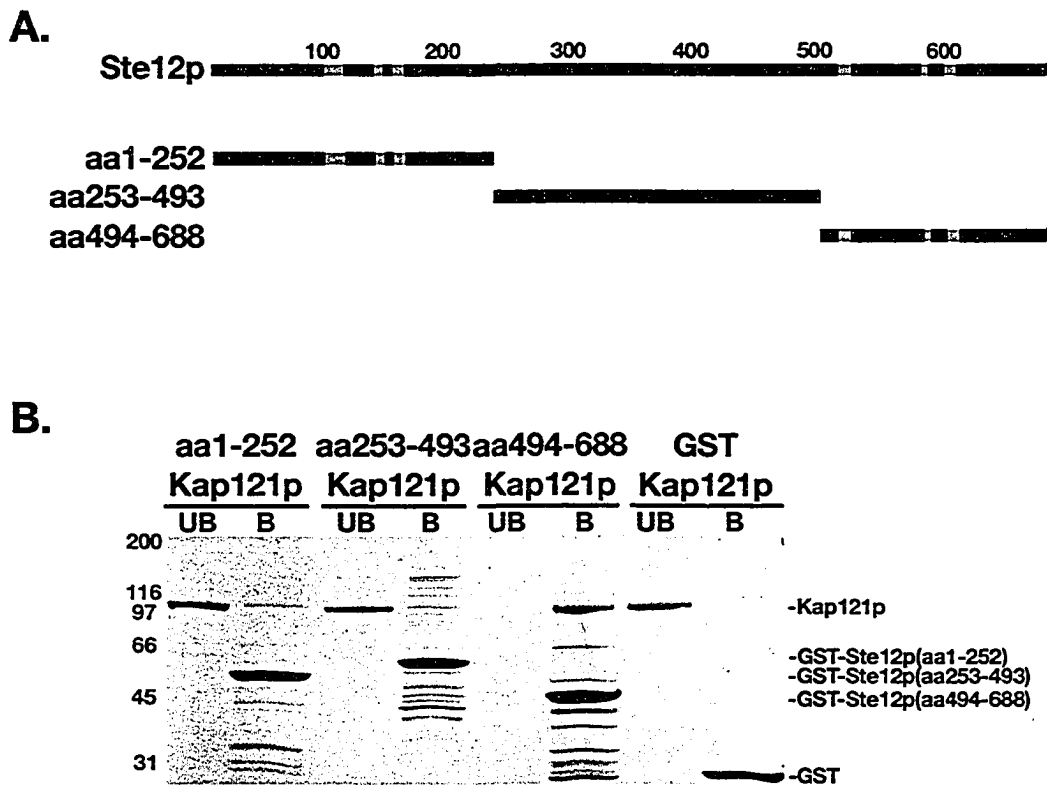


Figure 3.5.1: **Kap121p** interacts directly with the C-terminal portion of **Ste12p**. *A.* The schematic diagram illustrates the fragments of **Ste12p** expressed as GST fusions, with the regions in gray highlighting basic regions that were considered as potential NLS sequences. *B.* GST alone (~400 ng) and the fragments of **Ste12p** (~400 ng) were expressed as GST-chimeric proteins in *E. coli* and immobilized on GT-Sepharose. The immobilized chimeras were incubated with recombinant **Kap121p** (~200 ng). After extensive washing, bound protein fractions were released from the GT resin by incubation with 1x SDS sample buffer. Equal amounts of both the unbound (UB) and bound (B) protein fractions were analyzed by SDS-PAGE and Coomassie blue staining.

on GT-Sepharose and incubated with recombinant Kap121p. Kap121p bound directly to the C-terminal fragment of Ste12p (amino acid residues 494-688), but failed to bind to either the N-terminal (amino acid residues 1-252) or central portions (amino acid residues 253-493) of the protein or GST alone (Figure 3.5.1B).

### **3.5.2 The Kap121p-interacting domain of Ste12p contains a functional NLS**

– To evaluate the potential of each fragment of Ste12p to be imported into nuclei *in vivo*, these fragments were C-terminally fused to a tandem repeat of two GFPs (2xGFP), expressed under control of the *ADH1* promoter and visualized directly by fluorescence microscopy in wild-type (DF5) yeast cells. In agreement with the *in vitro* binding studies, only the C-terminal, Kap121p-interacting fragment of Ste12p (amino acid residues 494-688) was targeted to the nucleus, while the other fragments were diffusely localized throughout the cell (Figure 3.5.2A). Furthermore, the import of Ste12p(aa494-688)-GFP was found to be dependent on Kap121p function. In *kap121-34* cells, Ste12p(aa494-688)-GFP was localized predominantly to nuclei at 23°C but mislocalized to the cytoplasm at 37°C (Figure 3.5.2B). Moreover, the nuclear import of this GFP chimera was rescued by introducing a wild-type copy of *KAP121* into this strain. As a control, we also monitored the localization of Ste12p(aa494-688)-GFP in a *kap95* temperature-sensitive strain (*kap95-14*). In this strain, the atypical yeast  $\beta$ -karyopherin (Kap95p) is mutated and, consequently, cNLS-containing reporters are mislocalized to the cytoplasm at restrictive temperatures. Under these

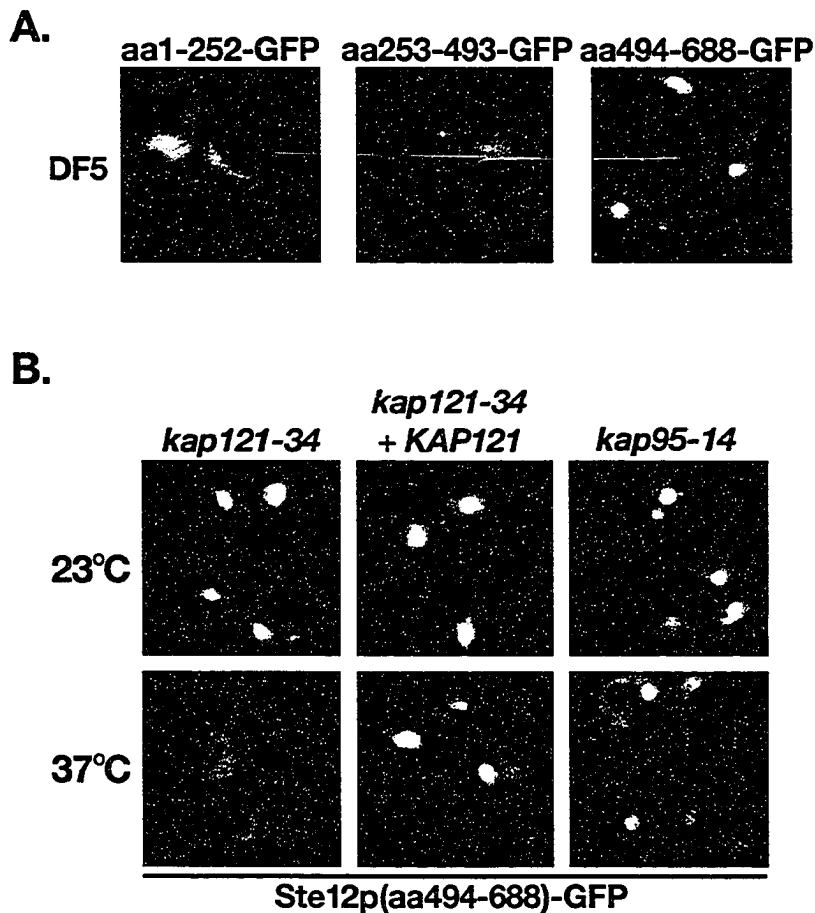


Figure 3.5.2: Amino acid residues 494 to 688 of Ste12p contain a functional Kap121p NLS. *A.* Ste12p deletion constructs were expressed as GFP chimeras in haploid DF5 cells. Cultures were grown to mid-logarithmic phase at 23°C, and the localization of these GFP chimeras determined using direct fluorescence microscopy. Note the nuclear localization of the C-terminal portion of Ste12p. *B.* The C-terminal GFP chimera (Ste12p(aa494-688)-GFP) was expressed in *kap121-34*, *kap121-34* containing a wild-type copy of *KAP121* (*kap121-34* + *KAP121*) and *kap95-14* cells. Cultures were grown to mid-logarithmic phase at 23°C, and the GFP chimeras detected as described above or incubated at 37°C for 3 hours prior microscopy analysis. Note the cytoplasmic accumulation of Ste12p(aa494-688)-GFP in *kap121-34* after the temperature shift.

conditions, the Ste12p(aa494-688)-GFP chimera remained nuclear at both the permissive and non-permissive temperatures (Figure 3.5.2B). Taken together, these data demonstrated that Kap121p mediates the nuclear import of Ste12p through a direct interaction with an, as yet undefined, NLS present between amino acid residues 494 and 688 of Ste12p.

### **3.6 RanGTP dissociates the Kap121p-Ste12p complex**

RanGTP is a key regulator and a driving force of nucleo-cytoplasmic transport (Clarke and Zhang, 2001; Cole and Hammell, 1998; Macara, 2001; Moore, 1998; Strom and Weis, 2001). Previous studies have shown that the binding of Ran-GTP to import-bound  $\beta$ -karyopherins; including Kap95p (Rexach and Blobel, 1995), Kap104p (Lee and Aitchison, 1999), Kap123p (Schlenstedt *et al.*, 1997), and Kap121p (Kaffman *et al.*, 1998b; Schlenstedt *et al.*, 1997), contributes, to varying degrees, to the displacement of import substrates. To test if RanGTP affected Kap121p-Ste12p(aa494-688) import complexes in a similar manner, this complex was immobilized on GT-Sepharose as described above and incubated with RanGTP, RanGDP, or GTP-loading buffer. The unbound and bound protein fractions were analyzed by SDS-PAGE and visualized by Coomassie blue staining (Figure 3.6.1A). Addition of RanGTP to the complex resulted in the release of Kap121p into the unbound protein fraction. By comparison when the complex was challenged with RanGDP or GTP-loading buffer, Kap121p remained predominantly in the bound fraction. Quantification of the amount of Kap121p released in three separate experiments revealed that

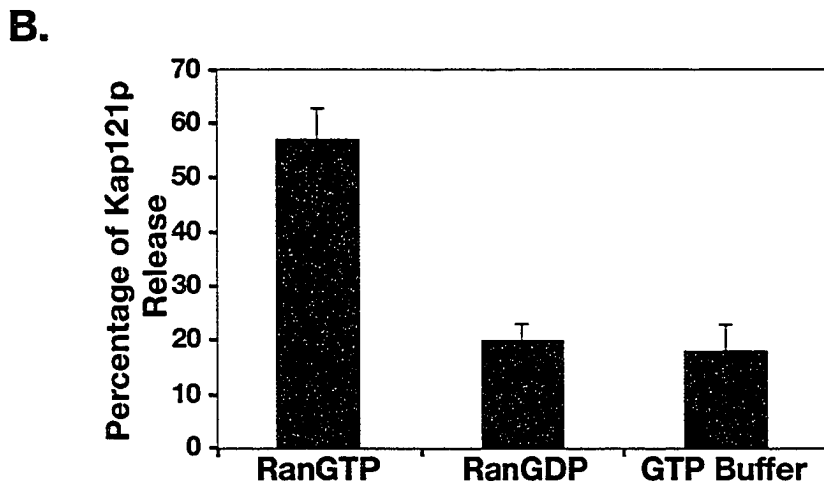
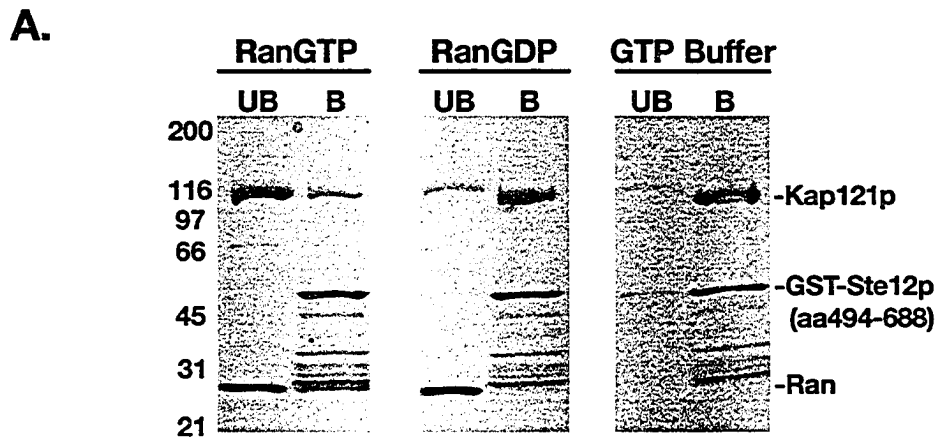


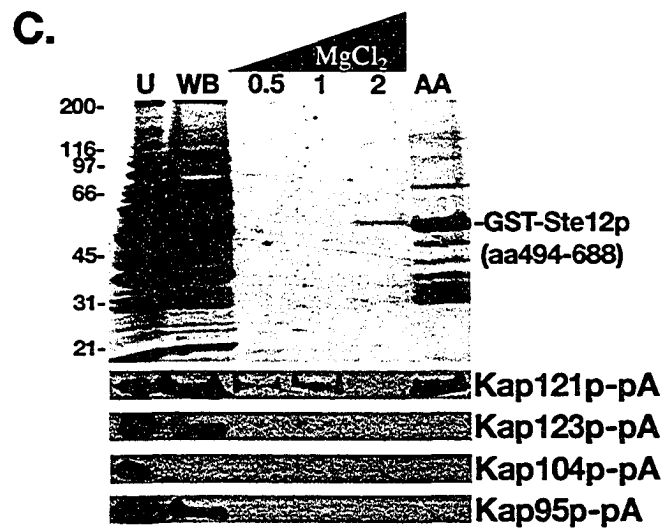
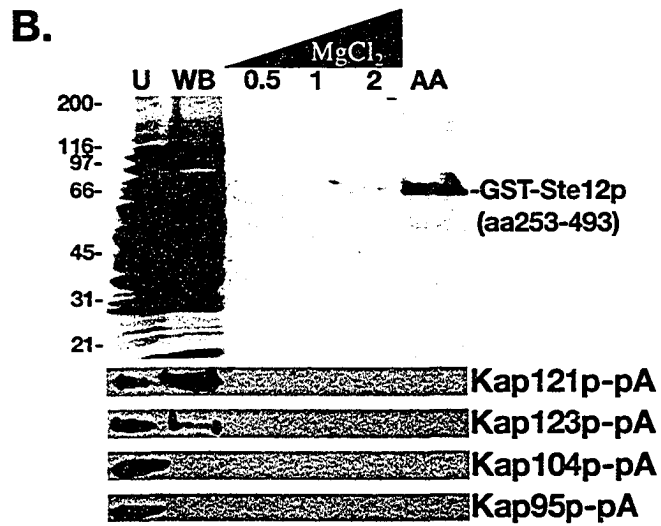
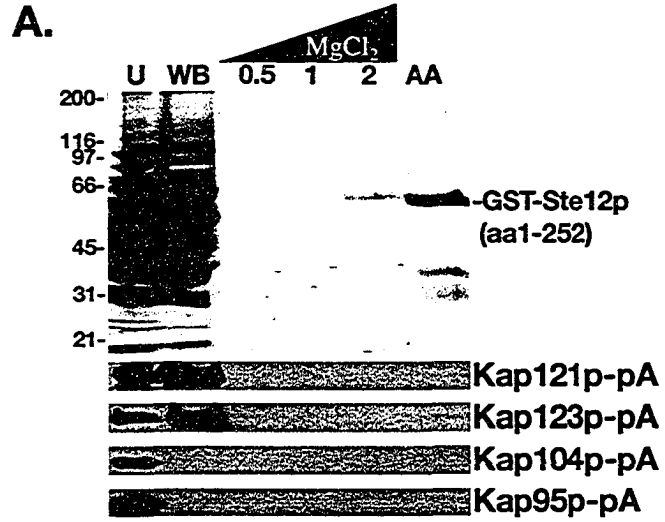
Figure 3.6.1: **Ran-GTP dissociates Kap121p-Ste12p(aa494-688) protein complexes.** *A.* GT-Sepharose immobilized GST-Ste12p(aa494-688)-Kap121p complexes were incubated with RanGTP (~120 ng), RanGDP (~120 ng), or GTP-loading buffer, as indicated, for 30 min at room temperature. The unbound (UB) protein fractions were collected and the proteins remaining bound to the resin (B) were released by incubation in 1x SDS sample buffer. Equal amounts of each protein fraction were analyzed by SDS-PAGE and Coomassie blue staining. *B.* The results from three separate experiments were quantified as described in Section 2.17.3. The graph represents the percentage of Kap121p that was released by each treatment. The standard deviations from the means were calculated from three separate experiments. Note that Kap121p was preferentially released when the protein complex was incubated with RanGTP.

RanGTP stimulated the dissociation of this import complex approximately 3-fold over that of either RanGDP or buffer alone (Figure 3.6.1B). The specific dissociation of Kap121p-Ste12p(aa494-688) protein complexes by RanGTP is similar to other nuclear import carrier/cargo interactions and is thought to mimic the conditions these complexes encounter as they enter the nucleus *in vivo* (Isoyama *et al.*, 2001; Kaffman *et al.*, 1998b; Lee and Aitchison, 1999; Rexach and Blobel, 1995; Rout *et al.*, 1997; Schlenstedt *et al.*, 1997).

### **3.7 The C-terminal fragment of Ste12p, amino acid residues 494 to 688, interacts specifically with Kap121p**

Previous studies suggest that the Kap121p and Kap123p transport pathways overlap and are capable of mediating the nuclear import of some common substrates (Isoyama *et al.*, 2001; Rout *et al.*, 1997). To investigate the specific role that Kap121p plays in the nuclear import of Ste12p, immunopurification studies were used to determine whether the recombinant, *E. coli* expressed Ste12p GST chimeras could interact with other  $\beta$ -karyopherins. Each GST-Ste12p chimera was immobilized on GT-Sepharose and incubated with lysates derived from yeast strains expressing protein A (pA)-tagged copies of Kap95p, Kap104p, Kap121p, and Kap123p. Bound proteins were eluted from the column with increasing concentrations of MgCl<sub>2</sub> and lastly with 0.5 M acetic acid. Coomassie blue staining and immunoblotting (Figure 3.7.1) demonstrated that of the four karyopherins tested, only Kap121p specifically enriched with the C terminus of Ste12p. Together, the immunopurification data, the overlay blot

Figure 3.7.1: **The C terminus of Ste12p specifically enriches Kap121-pA from whole cell lysates.** Recombinant GST-Ste12p(aa1-252) (A), GST-Ste12p(aa253-493) (B), and GST-Ste12p(aa494-688) (C) chimeras were immobilized on GT-Sepharose and incubated with whole cell lysates from strains expressing protein A (pA) chimeras of kaps. Bound protein complexes were washed with wash buffer (WB), followed by increasing concentrations of MgCl<sub>2</sub> (MgCl<sub>2</sub> in M is indicated) and finally with 0.5 M acetic acid (AA). Proteins from each fraction were separated by SDS-PAGE. **Top Panel** shows the Coomassie blue-stained gel resulting from incubating the Ste12p GST-chimeras with lysates derived from cells expressing Kap121p-pA. **Bottom Panel** shows immunoblots detecting the pA chimeras in the unbound lysate (U), the first wash buffer fraction (WB) and eluate fractions from each experiment. Note the only detected interaction was between Kap121p and the C-terminal portion of Ste12p.

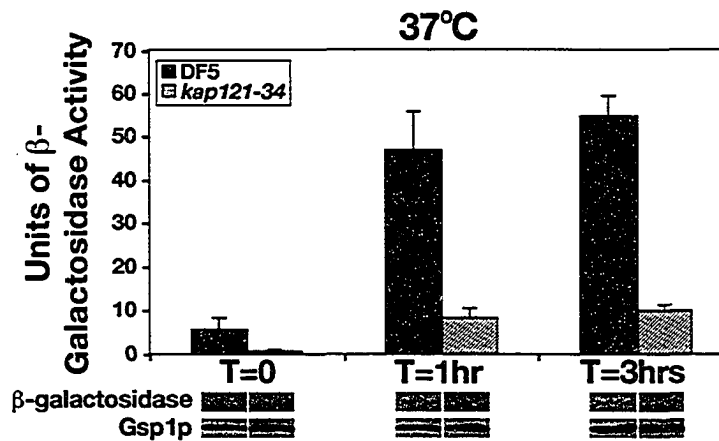
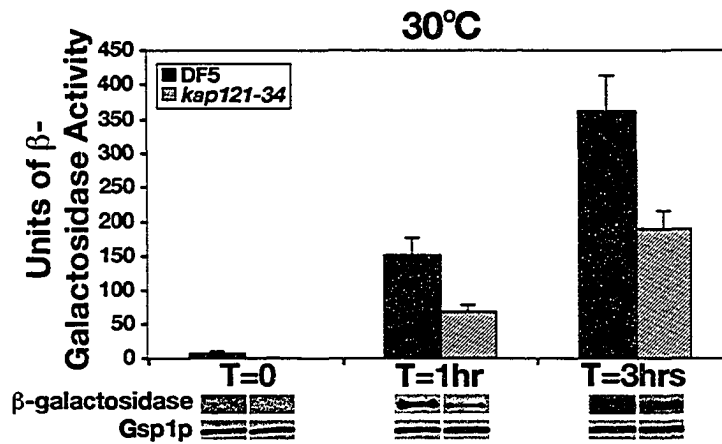
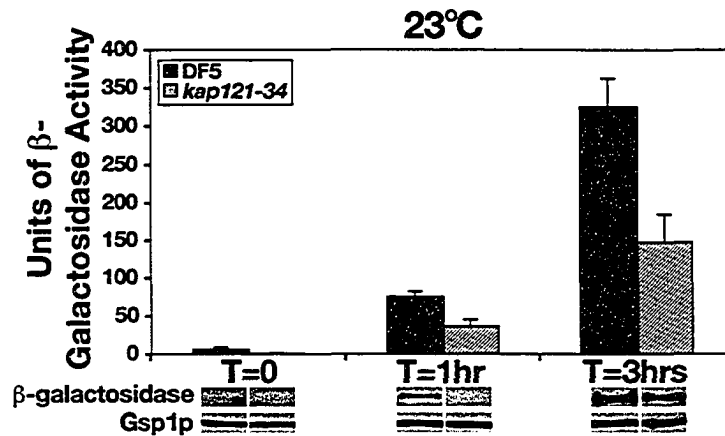


assays and the *in vitro* binding studies provide complementary evidence demonstrating that Kap121p interacts exclusively with Ste12p in a RanGTP sensitive manner via direct binding with the NLS-containing C terminus of this protein.

### **3.8 Ste12p-induced transcription is severely compromised in *kap121-34* cells.**

The data presented above suggest that *kap121-34* cells are unable to respond to mating pheromones at elevated temperatures because, under these conditions, Ste12p is mislocalized to the cytoplasm of these cells. Therefore, I hypothesized that Ste12p-induced transcription would also be affected in *kap121-34* cells. A well-characterized Ste12p-dependent  $\beta$ -galactosidase reporter, *fus1-LacZ* (Trueheart *et al.*, 1987) was used to monitor Ste12p-induced transcription in *kap121-34 Mata* and wild-type (DF5) *Mata* cells in response to the mating pheromone,  $\alpha$ -factor. These strains were grown to mid-logarithmic phase, treated with 5  $\mu$ M  $\alpha$ -factor and incubated at 23°C, 30°C and 37°C. Samples were obtained from each culture prior to pheromone treatment, and at 1 hour and 3 hours post-pheromone treatment.  $\beta$ -galactosidase activity assays and immunoblotting were used to determine the transcriptional activity of Ste12p under these conditions. In both strains,  $\beta$ -galactosidase activity peaked at 3 hours post-pheromone treatment, but at all temperatures tested *kap121-34* cells displayed significantly less Ste12p transcriptional activity than that observed in wild-type cells. This effect was more pronounced at 37°C (Figure 3.8.1).

Figure 3.8.1: **Ste12p-induced transcription is compromised in *kap121-34* cells.** *kap121-34 Mata* and wild-type (DF5) *Mata* cells containing a *fus1-LacZ* fusion were induced with 5  $\mu$ M  $\alpha$ -factor and incubated at 23°C, 30°C, or 37°C. Samples were taken at the indicated intervals post-pheromone treatment and prepared for immunoblot analysis or  $\beta$ -galactosidase activity assays. Units of  $\beta$ -galactosidase activity were determined as described in Materials and Methods (Section 2.14.1) and represented graphically, the error was calculated from three separate experiments. Immunoblots detecting the  $\beta$ -galactosidase and Gsp1p (loading control) were from whole cell lysates obtained from the same experiment represented graphically. The standard deviations from the means were calculated from three separate experiments. Note the  $\beta$ -galactosidase activity and the amount of  $\beta$ -galactosidase protein produced by *kap121-34* cells were significantly less than that produced by wild-type cells at all temperatures.



It should also be noted that the overall enzymatic activity was decreased in both wild-type and mutant cells at 37°C. The reasons for this are unclear, but may involve a heat shock response and may partially explain a poor mating efficiency of even wild-type cells at 37°C (Reid and Hartwell, 1977).

### **3.9 Ste12p-regulated cellular processes are compromised in *kap121-34* cells**

The fact that, coincident with its mislocalization to the cytoplasm, Ste12p activity is apparently compromised at permissive temperatures provided the opportunity to assay both mating and invasive growth efficiencies under permissive growth conditions. To address this, quantitative mating and invasive growth assays were performed with *kap121-34* mutants at 23°C and 30°C. Quantitative mating assays showed that the mating efficiency of *kap121-34* cells was at least 3-fold less than that observed for wild-type cells (Figure 3.9.1A). Furthermore, the invasive growth assay demonstrated that invasion-competent cells (Gustin *et al.*, 1998) carrying a WT copy of *KAP121* displayed characteristic haploid invasive growth, but otherwise isogenic cells containing the *kap121-34* allele were unable to invade agar at either 23°C or 37°C (Figure 3.9.1B). Taken together, these data further supported the findings presented above which established that Kap121p mediates the nuclear import of Ste12p and, as a result, limited Kap121p function affected the cellular differentiation reactions regulated by nuclear Ste12p.

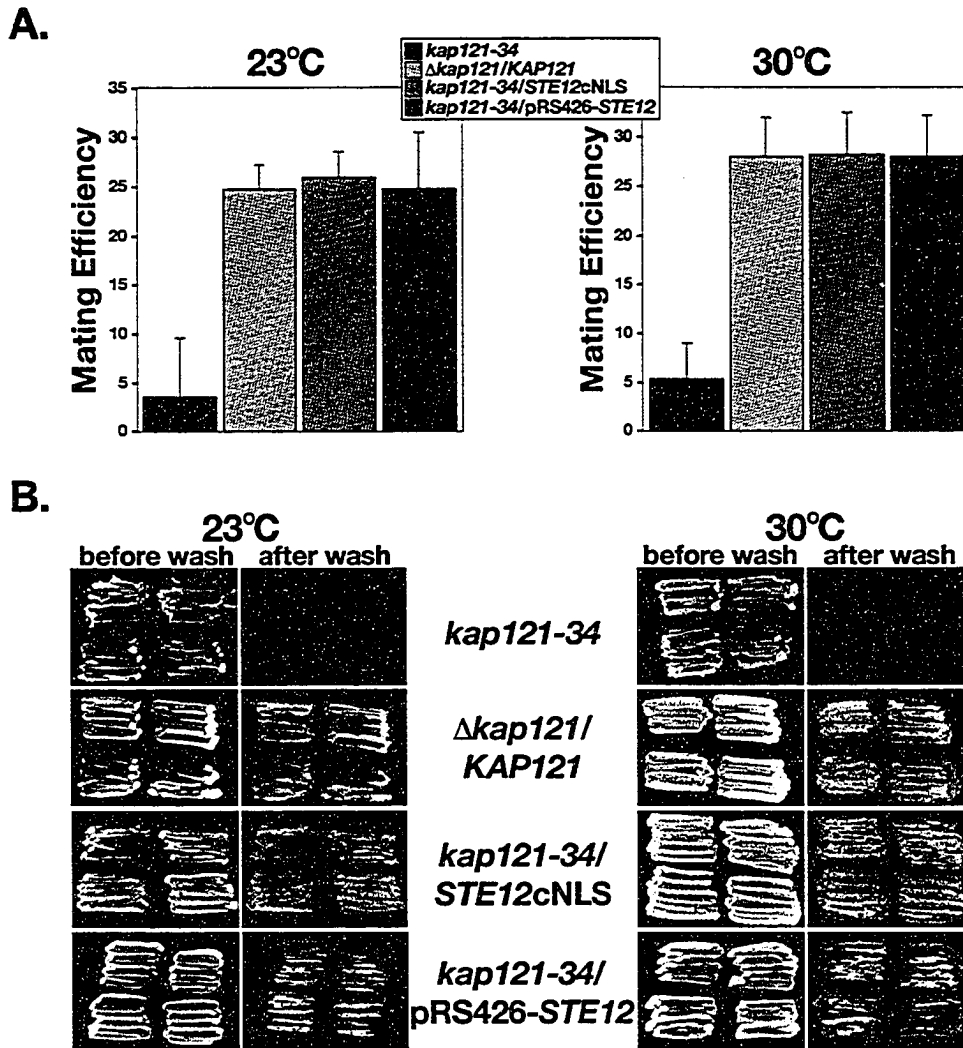


Figure 3.9.1: *kap121-34* cells do not mate efficiently or grow invasively. *A.* Exponentially growing *kap121-34*,  $\Delta$ *kap121*/p*KAP121*-*URA3*, *kap121-34*/pRS426-*STE12*, *kap121-34*/pRS316-*STE12cNLS* and wild-type tester strains were grown at 23°C,  $2 \times 10^6$  cells of the strain being tested were mixed with  $10^7$  cells of the tester strain and incubated at 23°C or 30°C for 5 hours. The mating mixtures were plated on the appropriate selection media to select for diploids, as well as haploid cells of the strain being tested, and the resulting colonies counted. The standard deviations from the means were calculated from three separate experiments. Mating efficiency is expressed as a percentage of the input haploids of the strain being tested that formed diploid colonies. *B.* Invasion-competent *kap121-34* cells,  $\Delta$ *kap121*/p*KAP121*-*URA3* cells and *kap121-34* cells containing either wild-type *STE12* on a multicopy plasmid (pRS426-*STE12*) or the *STE12cNLS* fusion (pRS316-*STE12cNLS*) were patched onto YEPD media and incubated at 23°C or 30°C for 2 days. The plates were then washed with a gentle stream of deionized water to reveal invasive growth (Roberts and Fink, 1994). Note that *kap121-34* cells were unable to grow invasively; but that  $\Delta$ *kap121*/p*KAP121*-*URA3* cells and *kap121-34* cells expressing multiple copies of *STE12*, or the *STE12cNLS* fusion were able to invade the agar.

However because Kap121p likely imports many cargoes, we wished to evaluate whether these phenotypes primarily resulted from inefficient Ste12p import. To address this, invasion-competent *kap121-34* cells were transformed with a multicopy plasmid encoding *STE12*, effectively resulting in the overexpression of *STE12*. Under these conditions, the *kap121-34* mating and invasive growth defects were rescued (Figure 3.9.1A,B). Previous studies have demonstrated that overexpression of *STE12* suppressed many mating defects (Dolan and Fields, 1990; Schrick *et al.*, 1997) and stimulated pseudohyphal/invasive growth (Lorenz and Heitman, 1997; Treisman, 1996). It was therefore possible that additional components required for these differentiation processes may be similarly mislocalized in *kap121-34* cells and that overexpression of *STE12* could mask their mislocalization. To address the specific role Ste12p plays in the development of these *kap121-34* mutant phenotypes, *STE12* was fused in frame to the SV40 large T antigen cNLS sequence (Kalderon *et al.*, 1984b); thereby allowing it to be imported by the Kap95p/Kap60p import pathway. Expression of this chimera in *kap121-34* cells, from its endogenous promoter, rescued both mating and invasion mutant phenotypes (Figure 3.9.1A/B). Together, these findings clearly demonstrated that the observed Ste12p-induced transcription deficiency in *kap121-34* cells and subsequent inability of these cells to mate or grow invasively were directly related to the inefficient nuclear import of Ste12p in this mutant strain.

### 3.10 Discussion

To expand our understanding of the mechanisms of nuclear transport, this study focused on unraveling the web of interactions for a typical karyopherin, Kap121p. Kap121p is an essential yeast protein (Rout *et al.*, 1997; Seedorf and Silver, 1997) that was initially characterized as a  $\beta$ -kap based on its similarity to Kap95p and Kap123p (Rout *et al.*, 1997). Kap121p was then found to be functionally homologous to Kap123p; both  $\beta$ -kaps mediated the nuclear import of many common cargoes (Isoyama *et al.*, 2001; Mosammaparast *et al.*, 2002b; Mosammaparast *et al.*, 2001; Rout *et al.*, 1997). However, each also appears to have its own set of cargoes. Studies have shown that Kap121p imports Pho4p (Kaffman *et al.*, 1998b), Pdr1p (Delahodde *et al.*, 2001), Spo12p (Chaves and Blobel, 2001), and Aft1p (Ueta *et al.*, 2003), transcription factors that regulate phosphate homeostasis, multidrug resistance, sporulation, iron homeostasis and cell size regulation, respectively. A two-pronged approach was used to further characterize Kap121p: New *kap121* temperature-sensitive mutants were generated; and overlay blot assays were used to initiate the identification of novel Kap121p nuclear import cargoes.

This approach proved to be very fruitful; four *kap121* temperature-sensitive alleles were isolated and 27 Kap121p-interacting proteins were identified (Figures 3.2.1 and 3.3.1). Kap123p also bound some of Kap121p-interacting proteins, supporting the previously reported redundancy between these two  $\beta$ -kaps (Isoyama *et al.*, 2001; Mosammaparast *et al.*, 2001; Rout *et al.*, 1997). However, 11 proteins preferentially interacted with Kap121p (Table 3-2).

Given that approximately one third of all yeast proteins are imported into the nucleus, I believe that this list represents a subset of all Kap121p cargoes. Indeed, only one of the twelve previously characterized Kap121p cargoes, Rpl25p, was among these 27 proteins (Chaves and Blobel, 2001; Delahodde *et al.*, 2001; Isoyama *et al.*, 2001; Kaffman *et al.*, 1998b; Mosammaparast *et al.*, 2002b; Mosammaparast *et al.*, 2001; Ueta *et al.*, 2003). This was not surprising, as the nature of this approach, using a karyopherin as the probe to identify cargoes, demands that the cargoes be sufficiently abundant in order to detect these interactions. In the past, Kap121p cargoes were identified by monitoring the cargo's (Yap1p, Pdr1p, Pho4p, Aft1p and histones H2A, H2B, H3, and H4) cellular localization in different *kap* mutants or when Kap121p co-immunopurified with the cargo of interest (Spo12p). The majority of the  $\beta$ -kap-interacting proteins (23 of the 27) identified here are abundant cellular factors that are required for ribosome biogenesis. Therefore, these proteins are likely to represent some of the more abundant Kap121p cargoes in the cell.

Intriguingly, two previously unreported phenotypes associated with the *kap121* temperature-sensitive mutants were also observed here: defects in the mating response and the transition to the pseudohyphal, invasive form (Figures 3.2.3 and 3.9.1). These two, apparently distinct, differentiation programs are activated by different external stimuli and utilize different MAP kinases to convey their signals to the nucleus. However, both pathways share some signaling elements (Ste20p, Ste11p and Ste7p) and converge on a single nuclear

transcription factor, Ste12p – a protein that specifically interacted with Kap121p in the overlay assays (reviewed in Bardwell, 2004; Pan *et al.*, 2000; Schwartz and Madhani, 2004). Depending on the MAP kinase activated, the phosphorylation state of Ste12p, and its interaction partners, different transcriptional programs are activated (see Section 1.9.1). These specific gene expression patterns induce either the mating response or pseudohyphal/invasive growth. Indeed, based on what is currently known about these two cellular responses, Ste12p is unique among characterized nuclear proteins whose mislocalization could specifically disable both of these differentiation programs.

Thus, *in vivo* fluorescence studies were used to test if the nuclear import of Ste12p was dependent on Kap121p. Analysis of Ste12p-GFP chimeras demonstrated that Ste12p was not efficiently imported into nuclei of *kap121-ts* cells, and remained cytoplasmic at the non-permissive temperature (Figure 3.4.1). When a functional copy of *KAP121* was added back to these cells, Ste12p import was restored, establishing that functional Kap121p is required for Ste12p nuclear import. Furthermore, although Kap121p function has previously been shown to overlap with that of Kap123p, Ste12p is a Kap121p-specific nuclear import cargo. In agreement with the overlay assays, immunopurification studies showed that of the  $\beta$ -kaps tested (Kap95p, Kap104p, Kap121p and Kap123p) only Kap121p specifically purified with Ste12p (Figure 3.7.1). Additionally, *in vivo* fluorescence localization studies demonstrated that a

temperature-sensitive mutation in *KAP95* did not affect Ste12p nuclear import (Figure 3.5.2).

A combination of *in vivo* fluorescence localization and *in vitro* binding studies determined that amino acid residues 494-688 of Ste12p contain a functional Kap121p-specific NLS (Figures 3.5.2). Furthermore, these studies demonstrated that, as with other cargoes for this  $\beta$ -kap (Isoyama *et al.*, 2001; Kaffman *et al.*, 1998b; Ueta *et al.*, 2003), Kap121p interacts directly with Ste12p in a RanGTP-sensitive manner (Figure 3.5.1 and 3.6.1). While I have not attempted to more precisely define the amino acid residues that are necessary and sufficient for NLS activity, amino acid residue sequence alignment studies have predicted a number of domains within this fragment of Ste12p that could function in this capacity. Alignments between the NLS of Pho4p and full-length Ste12p identified two short domains, amino acid residues 521-534 and 638-657, which are 28.6% and 35% similar to the Pho4p NLS, respectively. Moreover, an independent amino acid residue sequence alignment study between the Kap121p-interacting domains of Nup53p, Pho4p, Yap1p, Spo12p and Ste12p identified a larger domain, amino acid residues 606 to 651 (Lusk *et al.*, 2002). Interestingly, the parallels between these  $\beta$ -kap-interacting domains fall into two distinct regions that are separated by a spacer of variable length – a characteristic reminiscent of the bipartite NLS sequences found in some Kap95p/Kap60p nuclear import cargoes. Mutational and structural analysis of

Ste12p will fully illustrate which, if any, of these potential NLS domains in this C-terminal fragment frame the minimal NLS required for Kap121p interaction.

Ste12p is constitutively expressed and localized to the nucleus (Bardwell, 2004; Hung *et al.*, 1997), therefore in the absence of appropriate external stimuli its activity must be repressed. This is accomplished by the binding of Dig1p and Dig2p, which function as negative regulators of Ste12p. Upon stimulation, phosphorylation of Ste12p, and/or Dig1p and Dig2p alters the ability of these regulators repress Ste12p activity (Olson *et al.*, 2000). Given that Ste12p activity is restricted to the nucleus (Bardwell, 2004; Pan *et al.*, 2000), it is likely that mutations affecting its nuclear import would impair mating, and pseudohyphal/invasive growth to the same extent as complete loss of this transcription factor. Therefore, a role for Kap121p in Ste12p import suggests that the cytoplasmic mislocalization of Ste12p in *kap121* cells is the primary cause of the observed mating and invasive growth defects. Indeed, Ste12p-induced transcription was severely compromised in these cells at all temperatures tested (Figure 3.8.1). Moreover, expression of a *STE12cNLS* fusion or overexpression of *STE12* suppressed both mutant phenotypes. Together, these data suggest that, although other Kap121p cargoes are mislocalized in *kap121-34* cells, the phenotypes observed under these conditions are linked directly to Ste12p.

A number of other mutant phenotypes have also been associated with *kap121* temperature-sensitive mutants. These include the nuclear accumulation of small ribosomal subunits (Moy and Silver, 1999), drug sensitivity (Delahodde

*et al.*, 2001), sporulation defects (Chaves and Blobel, 2001) and cell cycle progression defects (Makhnevych *et al.*, 2003; Marelli *et al.*, 1998), as well as the accumulation of mRNA in nuclei of *kap121/kap123* (*pse1-1/kap123Δ*) double mutants (Seedorf and Silver, 1997). Studies have directly attributed the drug sensitivity and inefficient sporulation to the mislocalization of Kap121p import cargoes (Chaves and Blobel, 2001; Delahodde *et al.*, 2001). But direct roles for Kap121p or Kap123p in mRNA and/or ribosomal subunit export have not been shown. However, the studies presented here and previously have demonstrated that these  $\beta$ -kaps, as well as Kap108p/Sxm1p and Kap119p/Nmd5p, mediate the nuclear import of ribosomal proteins and ribosome assembly factors (see Chapter 4 and 5, and Rout *et al.*, 1997; Sydorsky *et al.*, 2003). Ribosome subunit assembly is extremely complex and requires the coordinated activity of numerous nuclear proteins. Thus, the accumulation of these subunits in nuclei of *kap* mutants could be a downstream consequence of the inability to efficiently import proteins required for their assembly or subsequent export. Indeed, a recent study by Sydorsky *et al.* (2003) demonstrated that the nuclear accumulation of pre-60S ribosomal subunits in *rai1/kap123* double mutant strains was partially due to the inefficient Kap123p-mediated import of Nmd3p, a factor required for the pre-60S subunit export. Together, these findings underscore the validity of our parallel approaches and provide a framework for future studies aimed at linking seemingly pleiotropic phenotypes (like the nuclear accumulation

of mRNA and ribosomal subunits) associated with *kap* mutants to their transport cargoes.

## Chapter 4 – Identification of a unique class of Kap121p nuclear import cargoes and a novel nuclear transport network<sup>13</sup>

### 4.1 Summary

This chapter focuses on the identification of two novel Kap121p transport cargoes, Nop1p and Dbp9p. Nop1p is a nucleolar protein encoded by an essential yeast housekeeping gene required at the early stages of ribosome biogenesis. Dbp9p is an essential DEAD-box helicase that is also required for 60S ribosome assembly. *In vivo* fluorescence microscopy studies demonstrated that Nop1p and Dbp9p accumulated in the cytoplasm of *kap121-ts* mutant cells at the restrictive temperature. Furthermore, *in vitro* binding studies showed that Kap121p interacts directly with both of these cargoes. Additional characterization of the Kap121p-Nop1p protein-protein interaction demonstrated that, in addition to lysine-rich nuclear localization signals (NLS), Kap121p recognizes a unique class of NLS sequences, termed rg-NLSs that are distinguished by the abundance of arginine and glycine residues. In contrast to previous studies, which have shown that Kap121p-lysine-rich NLS nuclear import complexes are sensitive to RanGTP, Nop1p-Kap121p nuclear import complexes were stable in the presence of RanGTP. These findings suggest that separate molecular mechanisms are used to terminate Kap121p-mediated import cycles. Moreover, *in vitro* competition binding assays established that Kap121p does not

---

<sup>13</sup> The majority of the data presented in this Chapter were published in Leslie, D.M., W. Zhang, B.L. Timney, B.T. Chait, M.P. Rout, R.W. Wozniak, and J.D. Aitchison. 2004. Characterization of karyopherin cargoes reveals unique mechanisms of Kap121p-mediated nuclear import. *Mol Cell Biol.* 24:8487-503.

interact with these two types of cargo concurrently. I also discovered a functional relationship between Kap121p and Kap104p, a kap that also recognizes rg-NLSs, and demonstrated that Kap104p can compensate for loss of functional Kap121p. These findings established for the first time that these seemingly unrelated nucleo-cytoplasmic transport pathways converge; giving rise to a nuclear transport network in which different karyopherins mediate the import of some common cargoes, highlighting the complex network of interactions between import karyopherins and their cargoes.

#### **4.2 Kap121p interacts specifically with a number of ribosome assembly factors**

As described above (Section 3.3), overlay blot assays were used to identify interactions between Kap121p and nuclear proteins by probing three dimensionally separated yeast nuclear proteins with cytosols isolated from strains expressing protein A tagged Kap121p (Kap121p-pA) or Kap123p (Kap123p-pA) (Figure 3.3.1). The sections of these overlay blots that are relevant to this chapter are shown in Figure 4.2.1. Twenty-seven Kap121p-interacting proteins were identified (Table 3-2) and further studies demonstrated that this procedure could successfully be used to identify direct interactions between  $\beta$ -kaps and cargoes. These interactions included Ste12p, which was confirmed to be an authentic import cargo of Kap121p (see Chapter 3 and Leslie *et al.*, 2002), and numerous ribosomal cargoes of Kap123p (Rout *et al.*, 1997). The successful preliminary identification of a novel Kap121p nuclear import

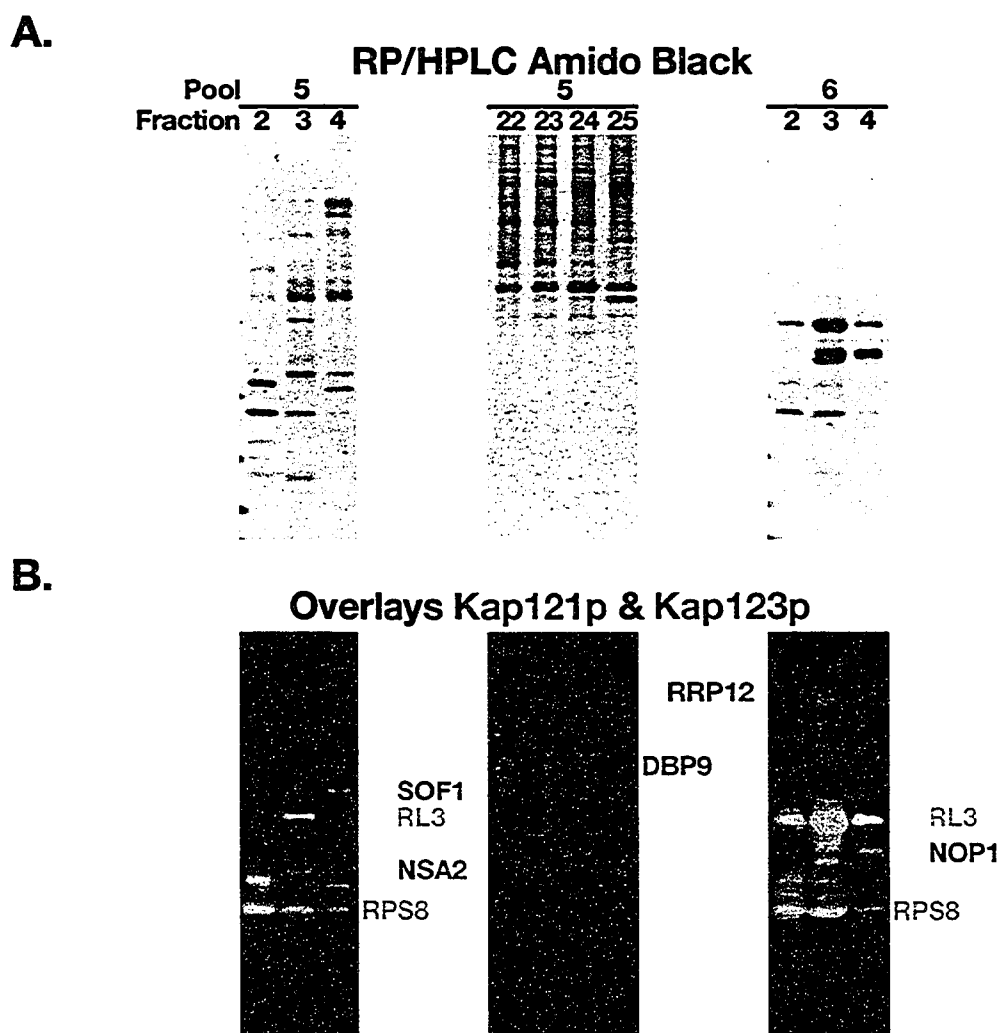


Figure 4.2.1: **Kap121p** interacts with numerous nuclear proteins. *A.* Yeast nuclear proteins were purified, fractionated and probed with cytosols from cells expressing either Kap121p-pA or Kap123p-pA as described previously (See Sections 2.11 and 3.3, and Figure 3.3.1). Fractions enriched with Kap121p-pA-interacting proteins were pooled as shown in Figure 3.3.2 and the proteins fractionated further using RP/HPLC. These samples were then separated by SDS-PAGE, transferred to nitrocellulose membranes, and detected by amido black staining. *B.* Membranes were separately probed with cytosols from cells expressing Kap121p-pA or Kap123p-pA and bound chimeras were detected as described above. Shown are overlaid, colorized images of each blot (red = Kap121p-pA; blue = Kap123p-pA). Karyopherin-interacting proteins were identified by mass spectrometry of the corresponding protein bands in an identical gel.

cargo, Ste12p, using this approach prompted further characterization of the Kap121p interactions identified here.

Previous studies have demonstrated that  $\beta$ -kaps often transport cargoes that mediate similar tasks in the cell (e.g. transcription factors) or that function together (e.g. ribosome proteins). Interestingly, the majority of the proteins that interacted specifically with Kap121p in the overlay blot assay function as *trans*-acting ribosome assembly factors. Together, these data suggest that Kap121p could function as the primary transport receptor for this class of essential cellular factors. Two of the most prominent Kap121p-interacting proteins identified in the overlay blot assays were Nop1p and Dbp9p. I, therefore, chose to further characterize the Kap121p-Dbp9p and Kap121p-Nop1p interactions.

### **4.3 Kap121p interacts directly with Nop1p and Dbp9p**

Previous studies have demonstrated that Kap121p mediates the nuclear import of its cargoes by interacting directly with them. Solution binding assays were, therefore, used to determine whether Kap121p was also capable of binding directly to Nop1p and Dbp9p. GST fusion proteins containing full-length Nop1p or Dbp9p were synthesized in *E. coli*, immobilized on GT-Sepharose and incubated with recombinant Kap121p. As observed with previously identified Kap121p cargoes, Kap121p interacted directly with both GST-Nop1p and GST-Dbp9p (Figure 4.3.1). Given that  $\beta$ -kaps, including Kap121p, typically mediate nuclear transport by interacting directly with their substrates, these findings presented here suggest that Kap121p mediates the nuclear import of these

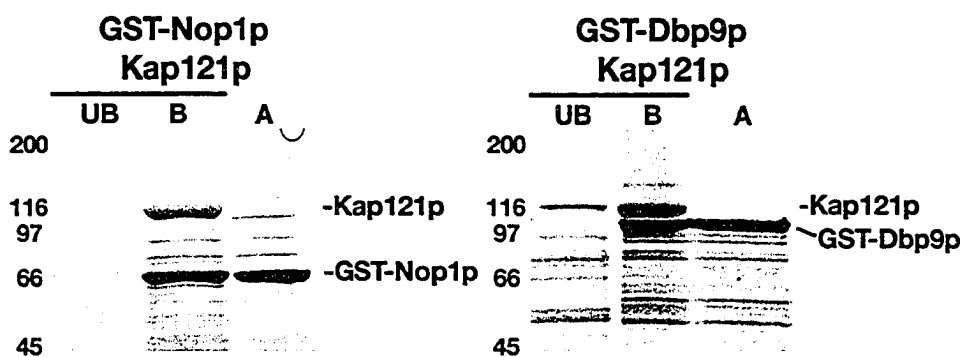


Figure 4.3.1: **Kap121p interacts directly with Nop1p and Dbp9p.** *E. coli* synthesized GST chimeras containing Nop1p or Dbp9p (~400 ng) were immobilized on GT-Sepharose and incubated with recombinant Kap121p (~300 ng). The unbound protein fractions (UB) were collected and after extensive washing, 1x SDS sample buffer was passed over the GT-resin to release the bead-bound proteins (B). Equal amounts of both the bound and unbound protein fractions, as well as the GST-fusion proteins alone (A), were analyzed using SDS-PAGE and Coomassie blue staining.

*trans*-acting ribosome assembly factors into the nucleus.

#### 4.4 Development of a regulated *in vivo* fluorescence-based nuclear import assay

**4.4.1 *Nop1p* and *Dbp9p* are tethered in the nucleolus** – To determine whether Nop1p and Dbp9p are authentic Kap121p nuclear import cargoes, these proteins were C-terminally tagged with the green fluorescent protein (GFP)<sup>14</sup>. The cellular localization of Nop1p-GFP and Dbp9p-GFP were examined in the *kap121-34* temperature-sensitive strain at permissive (23°C) and non-permissive temperatures (37°C) by direct fluorescence microscopy. In agreement with previous studies, both Nop1p-GFP (Aris and Blobel, 1991) and Dbp9p-GFP (Daugeron *et al.*, 2001) localized exclusively to the nucleolus at 23°C, but surprisingly both proteins remained nucleolar after a 3 hour incubation at 37°C (Figure 4.4.1A). This is in contrast to Ste12p (see Chapter 3; Figure 3.4.1) and other previously characterized Kap121p cargoes (Chaves and Blobel, 2001; Delahodde *et al.*, 2001; Kaffman *et al.*, 1998b; Mosammaparast *et al.*, 2001; Rout *et al.*, 1997; Ueta *et al.*, 2003), which redistribute from the nucleus to the cytoplasm under similar non-permissive and semi-permissive conditions.

I was concerned that plasmid expression of these GFP chimeras may be well above endogenous levels, which could mask the mislocalization of endogenous Nop1p (or Dbp9p), therefore *NOP1* was genomically tagged with

---

<sup>14</sup> Benjamin Timney, in Dr. Michael Rout's laboratory, constructed the plasmids constitutively expressing these *NOP1GFP* and *DBP9GFP* chimeric genes.

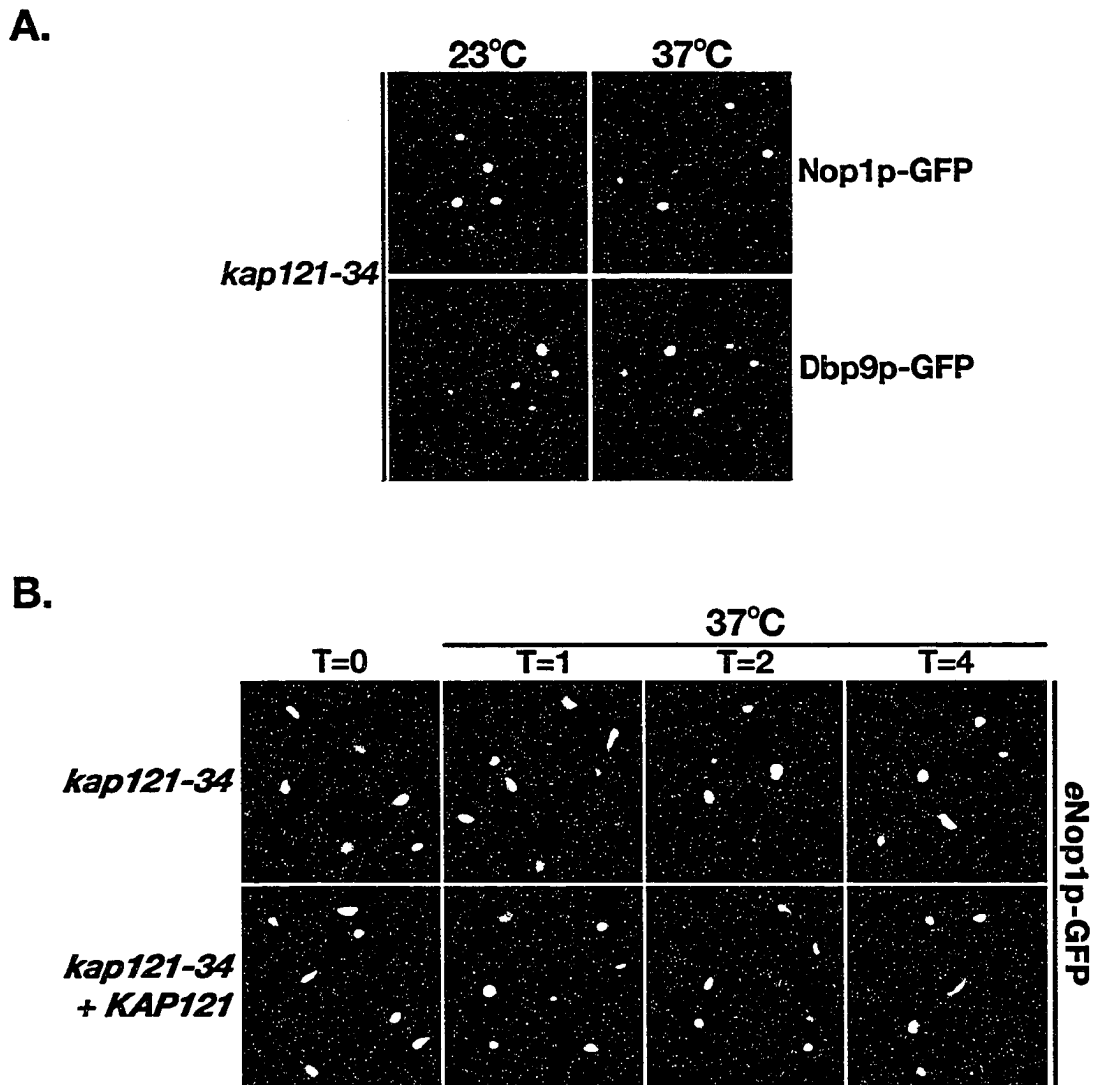


Figure 4.4.1: Constitutively expressed Nop1p-GFP and Dbp9p-GFP do not mislocalize in *kap121-34* cells at the restrictive temperature. *A.* The cellular distribution of constitutively expressed Nop1p-GFP (pNOP1GFP) and Dbp9p-GFP (pDBP9GFP) were monitored by direct fluorescence microscopy in *kap121-34* cells. Cells expressing these GFP chimeras were visualized after growth to mid-logarithmic phase at the permissive temperature (23°C) and after a 3 hour incubation at the restrictive temperature (37°C). Both Nop1p-GFP and Dbp9p-GFP remained exclusively nucleolar after 3 hours at 37°C. *B.* NOP1-GFP, *kap121-34* haploid cells were grown at 23°C (T=0). The cultures were then shifted to 37°C and the distribution of *eNop1p-GFP* was observed at 1 hour (T=1), 2 hours (T=2) and 4 hours (T=4) post-temperature shift by direct fluorescence microscopy. As a control, a wild-type copy of *KAP121* (pKAP121-URA5) was added back to this strain. Note, under these conditions *eNop1p-GFP* remained entirely nucleolar.

GFP in the *kap121-34* strain. These cells were grown to mid-logarithmic phase at 23°C and the localization of endogenous Nop1p-GFP (eNop1p-GFP) was determined as described above (Figure 4.4.1B; T=0). Cultures were then incubated at 37°C and the cellular localization of eNop1p-GFP was monitored periodically. Surprisingly, under these conditions eNop1p-GFP remained exclusively nucleolar (Figure 4.4.1B). These data suggested one of two possibilities: 1. Another member of the  $\beta$ -karyopherin protein family is mediating the nuclear import of Nop1p; or 2. Mechanisms such as binding and retention within the nucleolus keep Nop1p (and Dbp9p) in the nucleus after Kap121p inactivation.

A previously described *in vivo* nuclear import assay (Shulga *et al.*, 1996) was used to test the nucleolar retention hypothesis. This assay utilizes the metabolic poisons azide and deoxyglucose, which reduce the cellular levels of RanGTP (Schwoebel *et al.*, 2002), to induce the redistribution of the soluble contents of the nucleus between the nucleus and cytoplasm. As mentioned in Chapter 1, the RanGTP gradient is required for all aspects of nucleo-cytoplasmic transport; including nuclear import cargo dissociation, nuclear export complex assembly and the recycling of nuclear import  $\beta$ -kaps to the cytoplasm (reviewed in Fried and Kutay, 2003; Mosammaparast and Pemberton, 2004; Rout *et al.*, 2003). Thus, treating cells with azide and deoxyglucose results in the nucleo-cytoplasmic equilibration of soluble nuclear transport cargoes (Shulga *et al.*, 1996). To this end, *kap121-34* cells were poisoned (treated with 10 mM

deoxyglucose and 10 mM sodium azide, and incubated on ice) and the cellular localizations of Nop1p-GFP and cNLS-GFP monitored. The cNLS-GFP fusion equilibrated between the nucleus and cytoplasm in a manner similar to that previously reported (Shulga *et al.*, 1996), however these conditions failed to induce the equilibration Nop1p-GFP (Figure 4.4.2). Together, these findings suggest that Nop1p is not a soluble nucleoplasmic protein and that during Kap121p inactivation its nuclear concentration is maintained by mechanisms such as binding and retention within the nucleolus.

#### **4.4.2 Galactose-regulated nuclear import assays demonstrate that**

##### ***Kap121p function is required for Nop1p nuclear import*** – In light of the data

presented above I imagined that if Nop1p and Dbp9p are *bona fide* Kap121p nuclear import cargoes, inducing their expression after inactivation of Kap121p would reveal whether this transport pathway is required for their nuclear import.

*NOP1GFP* and *DBP9GFP* were, therefore, placed under the control of a galactose-inducible promoter (*GAL1*). The expression of these GFP fusions was induced after temperature inactivation of *kap121-34p* and their cellular distributions were examined by direct fluorescence microscopy. After 3 hours of growth under inducing conditions at 37°C, both Nop1p-GFP and Dbp9p-GFP accumulated in the cytoplasm of *kap121-34* cells, but were appropriately localized to at 23°C or when a wild-type copy of *KAP121* was present (Figure 4.4.3). By comparison, when synthesized under the same conditions (under control of the *GAL1* promoter) cNLS-GFP remained nuclear at both the

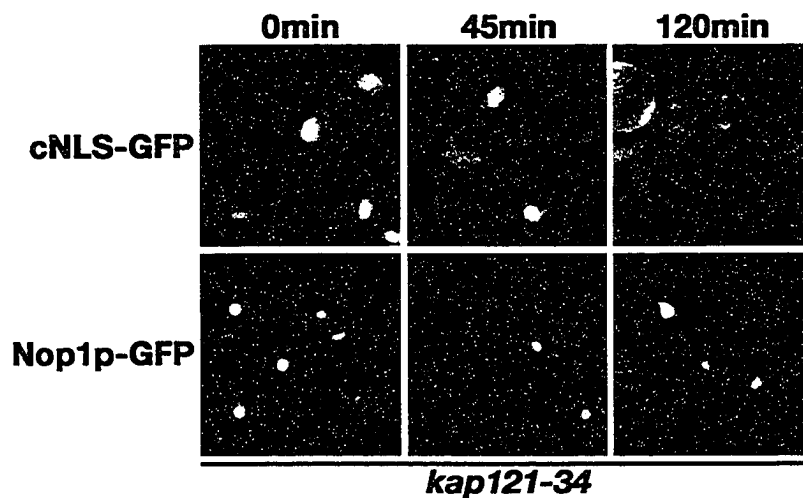


Figure 4.4.2: **Nop1p does not equilibrate between the nucleus and cytoplasm upon metabolic poisoning.** *kap121-34* cells containing pNOP1GFP (Nop1p-GFP) or p12-GFP2-NLS (cNLS-GFP) were grown to mid-logarithmic phase at 23°C (0 min). Cells were then washed, placed in media containing 10 mM sodium-azide and 10 mM 2-deoxyglucose, and incubated on ice. The cellular distributions of these GFP chimeras were documented by direct fluorescence microscopy at the indicated times. Note, the cNLS-GFP equilibrated between the nucleus and the cytoplasm while Nop1p-GFP remained exclusively nucleolar.

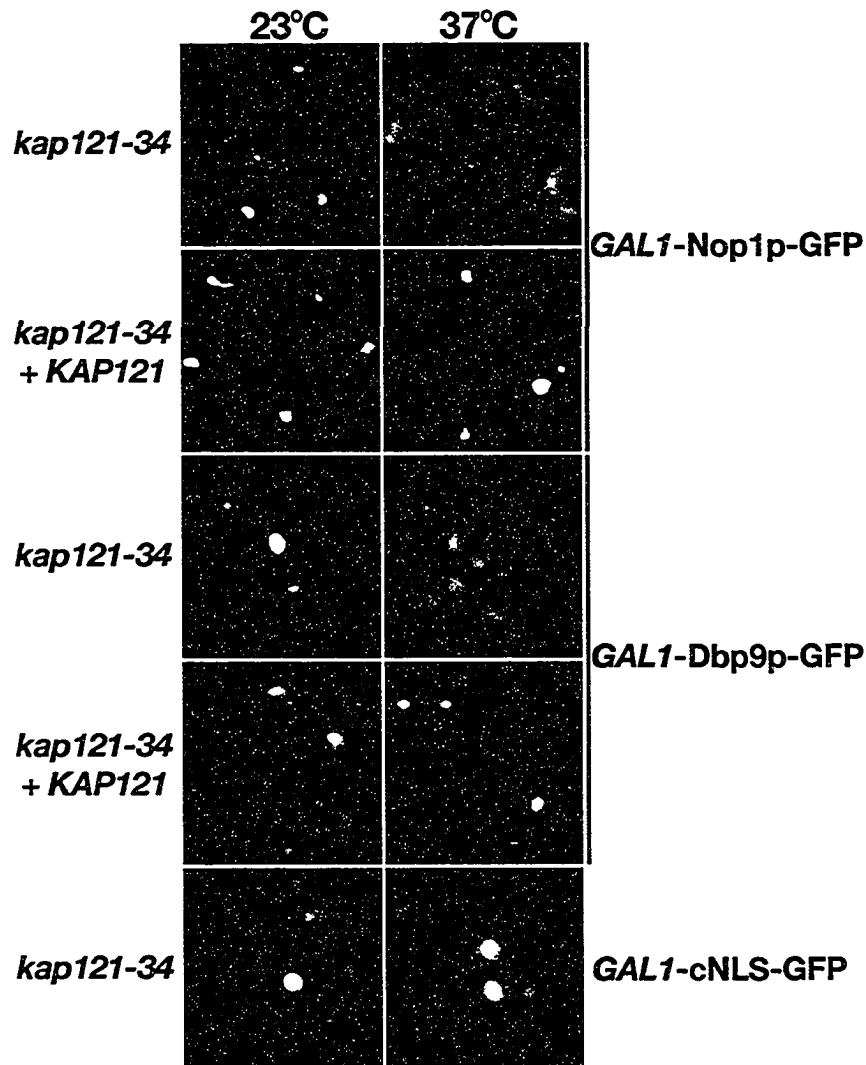


Figure 4.4.3: Nop1p and Dbp9p mislocalize in *kap121-34* cells. The cellular distributions of galactose-inducible *NOP1GFP* (*GAL1-Nop1p-GFP*) and *DBP9GFP* (*GAL1-Dbp9p-GFP*) gene fusions were monitored by direct fluorescence microscopy in *kap121-34* cells. These chimeras were expressed at either 23°C or 37°C. Note, both *GAL1-Nop1p-GFP* and *GAL1-Dbp9p-GFP* accumulated in the cytoplasm of *kap121-34* cells when expressed at the non-permissive temperature. This contrasts with control *kap121-34* cells containing a wild-type copy of *KAP121* (*pKAP121-URA3*) or *kap121-34* cells expressing a *GAL1-cNLS-GFP* chimera.

permissive and non-permissive temperatures. These data indicate that Kap121p is required for the efficient nuclear import of Nop1p and Dbp9p.

#### 4.5 Nop1p contains an N-terminal GAR domain that is similar to rg-NLS sequences

The NLS regions of previously characterized Kap121p cargoes are generally rich in lysine residues (Table 1-2), and in this sense resemble the cNLSs or the NLSs of ribosomal proteins. Similarly, visual inspection of the amino acid residue sequences of Dbp9p and Nop1p, as well as the other 9 potential Kap121p-specific cargoes identified in the overlay blot assay revealed that each contains at least one lysine-rich region that could represent functional Kap121p NLS sequences (Table 4-1).

**Table 4-1 Potential Kap121p-recognized NLSs**

YPD Name	a.k.a	Predicted lysine-rich NLS	Location
YCR016W		KSSTKKGKRVSKPGTKKKEKLSKDEKNSKKNKILK	aa61-98
YDL014W	Nop1p	FSHRPGRELISMAKKRPNIIP	aa199-219
YER082C	Utp7p; Kre31p	KPDVKGKNSGLRSFLRKK	aa487-504
YER126C	Nsa2p; Kre32p	KLTGWKGGKQFAKKR RIIRPSALRQKK	aa41-54 aa170-181
YHR084W	Ste12p	GRPYTPNYRSTPGS PRRRTVGMKSSQGNVPTGNKQSVGKSAKISKPLHIK	aa521-564 aa582-616
YLL011W	Sof1p	KRISRHRHVPQVIKKAQEIKNIELSSIKRREANERRTR KDMPYISERKKQ	aa411-450
YLR276C	Dbp9p	KKPSKKKKVQVKKDK RGNGTKVKFVPPHNAKKR	aa365-379 aa554-571
YML069W	Pob3p	YKDKLKKQYDAKTHI	aa342-355
YNL075W	Imp4p	RVVCILKHLFNAGPKK	aa200-216
YOL041C	Nop12p	KNKSAVRKICSNLNAVVFQDHHLR	aa 342-365
YPL012W	Rp12p	LKLLRWSHEH TGHFKAKVKH	aa971-990

The amino acid residue sequences of the regions of the potential Kap121p-specific import cargoes that were found to be similar to the NLSs of previously identified Kap121p lysine-rich NLS are presented here. These amino acid residue sequences are written using the standard single letter abbreviations.

This was also true for Nop1p; a potential lysine-rich Kap121p NLS is located between amino acid residues 199 and 219 (Table 4-1; Figure 4.5.1). However, Nop1p also contains an N-terminal GAR (glycine/arginine-rich) domain. This domain is very similar to the arginine-glycine rich RNA binding domains of Nab2p and Nab4p/Hrp1p (Figure 4.5.1), which in *S. cerevisiae*, are also nuclear import signals (rg-NLSs) recognized by the karyopherin, Kap104p (Lee and Aitchison, 1999). Moreover, localization studies of Nop1p homologues identified the evolutionarily conserved N-terminal domain as possessing nuclear localization activity. In the case of human Nop1p (fibrillarin), this domain was required, but not sufficient, for nuclear import (Snaar *et al.*, 2000). In *Arabidopsis* the GAR domain of AtFbr1 was both necessary and sufficient to target this protein to nucleoli (Pih *et al.*, 2000). These data strongly suggested that if Kap121p mediates the nuclear import of Nop1p it could do so by interacting with an NLS that is different from those previously characterized for Kap121p cargoes.

#### **4.6 Mapping the nuclear localization signal (NLS) of Nop1p**

**4.6.1 The RGG-rich N-terminal GAR domain of Nop1p contains a functional NLS** – As described above, two potential NLSs were identified for Nop1p: an RGG-rich NLS within the N-terminal GAR domain of this protein and a lysine-rich domain (aa 199-219) that is similar to previously characterized Kap121p NLSs (Table 4-1 and Figure 4.5.1). To determine if either of these sequences contain a functional Kap121p NLS, three fragments encoding amino acid residues 1-90,



91-327 and 210-327 of Nop1p were fused to the 5' end of a tandem repeat of two GFPs (Figure 4.6.1A). The expression of these Nop1p-(2xGFP) chimeras was regulated using the *GAL1* promoter in *kap121-34* cells as described above and their cellular localizations determined by fluorescence microscopy at 23°C (Figure 4.6.1B). Nop1p(aa1-90)-GFP, the fragment containing the RGG- rich GAR domain, was targeted to the nucleus, whereas Nop1p(aa91-327)-GFP and Nop1p(aa210-327)-GFP were diffusely distributed throughout the cell. Notably, Nop1p(aa1-90)-GFP lacks the aforementioned lysine-rich region most closely related to other Kap121p NLSs (Chaves and Blobel, 2001; Delahodde *et al.*, 2001; Kaffman *et al.*, 1998b; Lusk *et al.*, 2002; Mosammaparast *et al.*, 2002b; Mosammaparast *et al.*, 2001; Ueta *et al.*, 2003). Moreover, the import of Nop1p(aa1-90)-GFP was found to be dependent on Kap121p function. When the expression of Nop1p(aa1-90)-GFP was induced at 37°C in *kap121-34* cells it mislocalized to the cytoplasm, but appropriately localized to the nucleolus when expressed at the permissive temperature (23°C) (Figure 4.6.1C). Introduction of a wild-type copy of *KAP121* rescued this nuclear import defect at the non-permissive temperature. These findings suggested that Kap121p mediates the nuclear import of Nop1p via an atypical rg-NLS.

**4.6.2 *Kap121p* interacts directly with the rg-NLS containing fragment of *Nop1p*** – To confirm that Kap121p is capable of interacting directly with the RGG-rich GAR domain of Nop1p, GST fusion proteins containing the Nop1p deletion fragments described above were constructed. These chimeric proteins

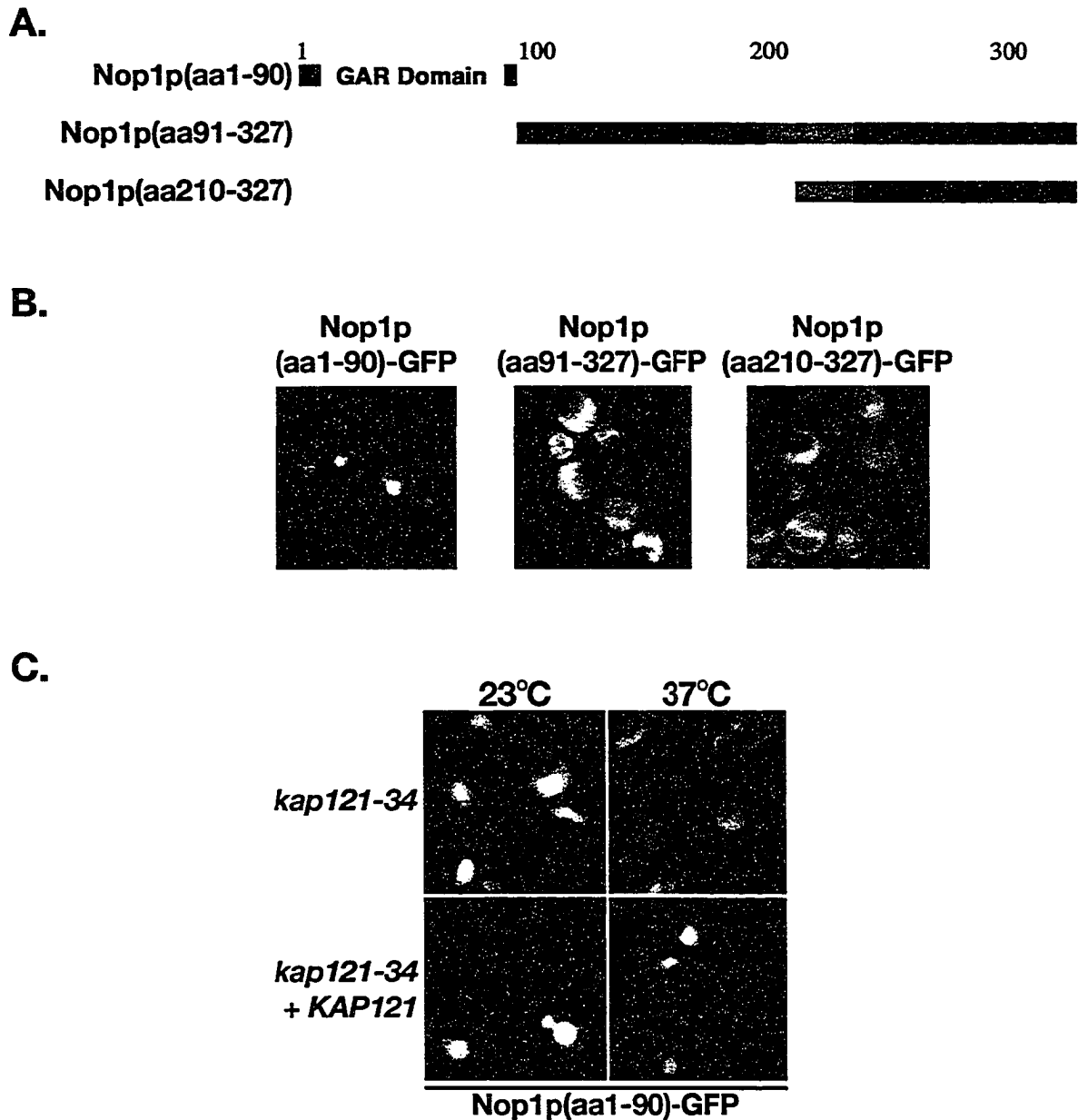


Figure 4.6.1: **The RGG-rich GAR domain of Nop1p contains a functional NLS.** *A.* A schematic diagram representing the fragments of Nop1p expressed as GST- and GFP-fusion proteins. The GAR domain and the lysine-rich domain, which is similar to other Kap121p NLSs (aa199-219; gray), are highlighted. *B.* Galactose-inducible GFP chimeras containing these three fragments of Nop1p were synthesized at 23°C in *kap121-34* cells and localized using direct fluorescence microscopy. Note the nuclear localization of Nop1p(aa1-90)-GFP. *C.* Nop1p(aa1-90)-GFP was synthesized at either 23°C and 37°C in *kap121-34* and *kap121-34 + KAP121* cells, and localized as described above. Note, Nop1p(aa1-90)-GFP mislocalized to the cytoplasm of in *kap121-34* cells at 37°C.

were synthesized in *E. coli*, immobilized on GT-Sepharose and incubated with recombinant Kap121p. In agreement with the *in vivo* localization studies, Kap121p bound directly to GST-Nop1p(aa1-90), but failed to interact to any appreciable extent with either GST-Nop1p(aa91-327), GST-Nop1p(aa210-327) or GST alone (Figure 4.6.2). The weak binding to GST-Nop1p(aa91-327) may reflect the presence of the basic region (aa199-219) similar to other Kap121p NLSs, but which, as shown above, is inactive as an NLS *in vivo* (Figure 4.6.1B). Taken together, these data show that Kap121p interacts directly with an rg-NLS sequence present in the N-terminal GAR domain of Nop1p, which is both necessary and sufficient for its Kap121p-mediated import. Furthermore, these findings also establish that this  $\beta$ -kap mediates the nuclear import of two distinct types of cargoes: those containing lysine-rich NLSs and those with rg-NLSs.

#### **4.7 GST-Nop1p(aa1-90)-Kap121p protein complexes are insensitive to RanGTP**

Previous studies have shown that the binding of nuclear RanGTP to Kap121p-cargo complexes specifically induces the dissociation of these complexes (see Chapter 3 and Isoyama *et al.*, 2001; Kaffman *et al.*, 1998b; Ueta *et al.*, 2003). To test if RanGTP also displaces Kap121p from GST-Nop1p(aa1-90), GST-Nop1p(aa1-90)-Kap121p complexes were immobilized on GT-Sepharose and then incubated with RanGTP, RanGDP, or GTP-loading buffer. RanGTP did not preferentially release Kap121p from the rg-NLS of Nop1p. Approximately 20% of the total amount of Kap121p bound to GST-Nop1p(aa1-

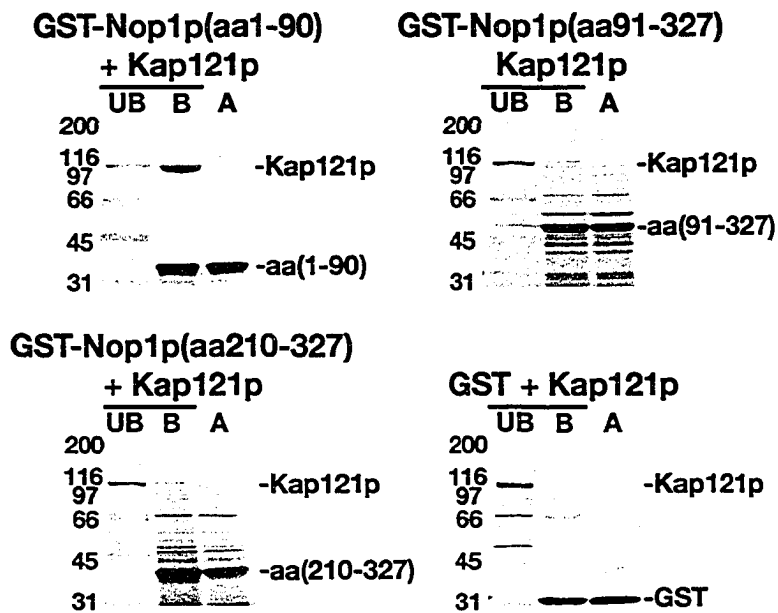
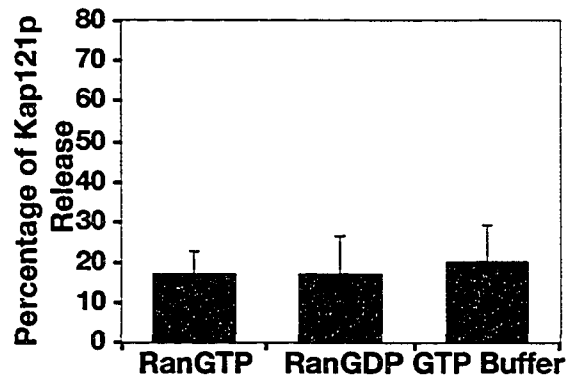
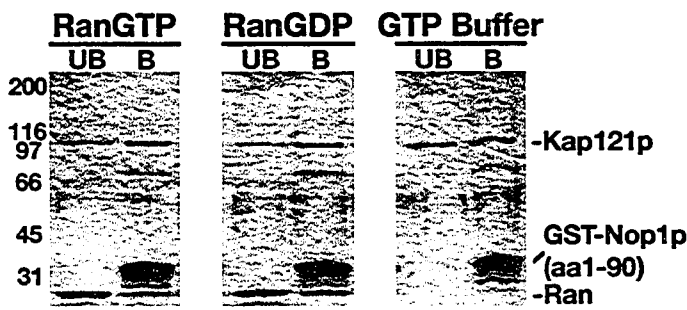


Figure 4.6.2: **Kap121p** interacts directly with the RGG-rich GAR domain of Nop1p. GST chimeras containing the deletion fragments of Nop1p (~400 ng) or GST alone were immobilized on GT-Sepharose and incubated with recombinant Kap121p (~300ng). Equal amounts of the unbound fractions (UB), bound fractions (B) and the GST-fusions alone (A) were analyzed by SDS-PAGE and Coomassie blue staining. Note, recombinant Kap121p interacts directly with GST-Nop1p(aa1-90).

90) was displaced from the protein complex upon incubation with RanGTP, RanGDP or GTP Buffer (Figure 4.7.1A). Studies have demonstrated that RanGTP alone is not always sufficient to induce nuclear import complex dissociation. This is true for many nucleic acid binding proteins, as researchers have demonstrated that a combination of RanGTP and nucleic acids are required to release these cargoes from their karyopherins (Lee and Aitchison, 1999; Pemberton *et al.*, 1999; Senger *et al.*, 1998). Therefore, it is possible that this is also the case for Kap121p. All of the previously identified Kap121p-specific import cargoes are transcription factors (see Chapter 3 and Chaves and Blobel, 2001; Delahodde *et al.*, 2001; Isoyama *et al.*, 2001; Kaffman *et al.*, 1998b; Ueta *et al.*, 2003), which by definition, are nucleic acid binding proteins. However, when tested, these Kap121p-cargo interactions were found to be sensitive to RanGTP (Figure 3.6.1; (Isoyama *et al.*, 2001; Kaffman *et al.*, 1998b; Ueta *et al.*, 2003)).

These findings suggested that Kap121p-Nop1p nuclear import complexes may, therefore, be insensitive to RanGTP for one of two reasons: 1. Kap121p not only imports Nop1p into the nucleus, but also mediates its intranuclear transport (and, possibly, that of other cargoes) to the nucleolus where the mutual binding of rRNA and RanGTP could lead to the dissociation of these import complexes; or 2. Kap121p-rg-NLS protein-protein interactions are specifically insensitive to RanGTP. Although, the NLS of Dbp9p has not been mapped, this protein does not contain a sequence similar to the rg-NLS of Nop1p. It does, however,

**A.**



**B.**

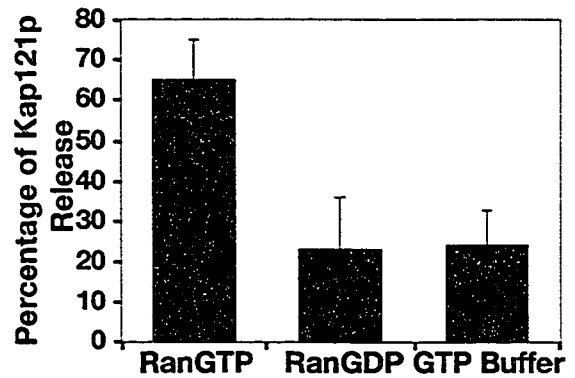
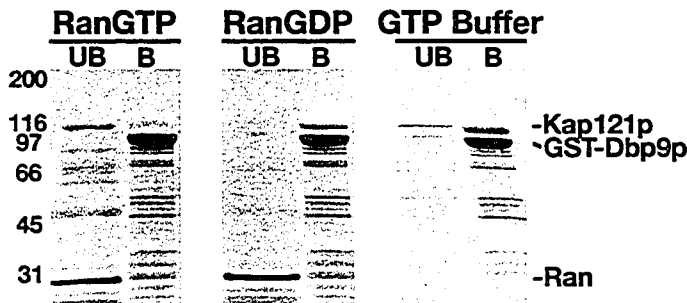


Figure 4.7.1: **RanGTP does not dissociate Kap121p-Nop1p import complexes.** GT-Sepharose immobilized protein complexes containing recombinant Kap121p bound to either GST-Nop1p(aa1-90) (*A*) or GST-Dbp9p (*B*) were incubated with Ran-GTP (~120 ng), Ran-GDP (~120 ng), or GTP-loading buffer, as indicated, for 30 min at room temperature. The unbound (UB) protein fractions were collected and after washing 1x SDS sample buffer was passed over the GT resin to release the bead-bound proteins (B). Equal amounts of each protein fraction were analyzed by SDS-PAGE and Coomassie blue staining (Left Panels). The results of three separate experiments were quantified as described in Materials and Methods (Right Panels). The graph represents the percentage of Kap121p that was released by each treatment. Note that when incubated with Ran-GTP Kap121p was preferentially released from GST-Dbp9p-Kap121p complexes, but not from GST-Nop1p(aa1-90)-Kap121p complexes. The standard deviations from the means were calculated from three separate experiments.

contain a lysine-rich domain similar to the NLSs of other Kap121p cargoes (Table 4-1), indicating that it likely represents a more typical Kap121p cargo. As Dbp9p also localizes to the nucleolus, it was used as a control to distinguish between these two hypotheses. Incubation with RanGTP specifically induced the release of Kap121p from immobilized GST-Dbp9p-Kap121p protein complexes (Figure 4.7.1B, left panel). By comparison when the complex was challenged with RanGDP or GTP-loading buffer, Kap121p remained predominantly bound to GST-Dbp9p. Quantification of the amount of Kap121p released in three separate experiments revealed that at least 2-fold more Kap121p dissociated from Dbp9p upon incubation with RanGTP when compared to that released upon incubation with either RanGDP or GTP-loading buffer (Figure 4.7.1B, right panel). The specific dissociation of the Kap121p-Dbp9p protein complex by RanGTP is similar to that of prototypical Kap121p-cargo interactions (Figure 3.6.1; (Isoyama *et al.*, 2001; Kaffman *et al.*, 1998b; Ueta *et al.*, 2003)). These findings implied that the insensitivity of Kap121p-Nop1p protein complexes to RanGTP was specific to Kap121p-rg-NLS interactions, not the intranuclear localization of this, or other, cargoes. As Nop1p represents a novel class of Kap121p cargoes, the remaining studies presented in this chapter focused on further analyzing Nop1p nuclear import and the molecular mechanisms that mediate its translocation.

#### **4.8 Kap121p is not able to bind lysine-rich NLS and rg-NLS containing cargoes simultaneously**

The data presented here, and previously (Chaves and Blobel, 2001; Delahodde *et al.*, 2001; Isoyama *et al.*, 2001; Kaffman *et al.*, 1998b; Mosammaparast *et al.*, 2001; Rout *et al.*, 1997) suggest that Kap121p can interact with two different types of NLSs. This raises the possibility that Kap121p might be capable of simultaneously interacting with two distinct NLSs. Therefore, *in vitro* competition assays were performed to determine whether Kap121p could form a single nuclear import complex containing both a lysine-rich NLS cargo and Nop1p (Figure 4.8.1). Nop1p-pA was purified from *NOP1-A* whole cell lysates and the interacting yeast proteins were removed by extensive washing with 1M MgCl<sub>2</sub>. The immobilized Nop1p-pA chimera was incubated with recombinant Kap121p to assemble Nop1p-pA-Kap121p import complexes. These heterodimers were then challenged with GST alone, GST-fusion proteins containing the Kap121p-specific NLS sequences of Nop1p (GST-Nop1p(aa1-90)), Ste12p (GST-Ste12p(aa494-688); Chapter 3), Pho4p (GST-Pho4p(aa140-166); (Kaffman *et al.*, 1998b)) or buffer alone. Under these conditions, challenging Kap121p-Nop1p protein complexes with an rg-NLS (GST-Nop1p(aa1-90)) or lysine-rich NLS sequences (GST-Ste12p(aa494-688) or GST-Pho4p(aa140-166)) displaced Kap121p from Nop1pA (Figure 4.8.1). These data suggest that, at least for the different NLSs tested here, Kap121p binds directly to only one cargo at a time.

#### **4.9 Kap104p mediates Nop1p nuclear import in the absence of Kap121p function**

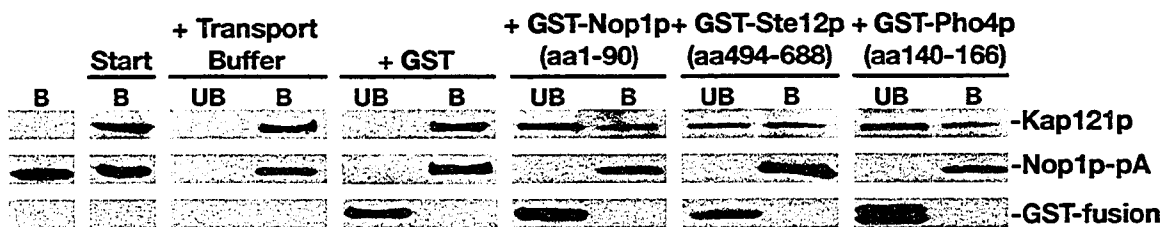
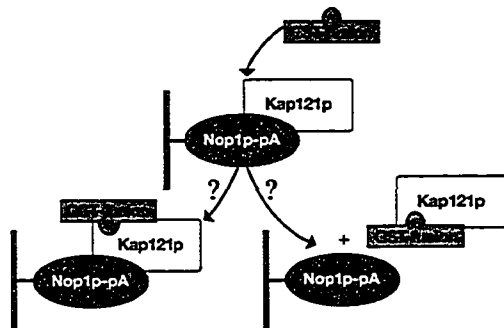


Figure 4.8.1: **Kap121p does not interact with cargoes containing lysine-rich NLSs and rg-NLSs concurrently.** Nop1p-pA was purified from *NOP1-A* whole cell lysates and the co-purifying proteins removed by washing with 1M MgCl<sub>2</sub> (far left panel). The immobilized pA-fusion was then incubated with recombinant Kap121p (~400ng), forming Kap121p-Nop1p-pA protein complexes (Start). These import complexes were then incubated with transport buffer, GST alone or GST-fusion proteins (~600-800ng) containing the Kap121p-specific NLS sequences of Nop1p (GST-Nop1p(aa 1-90)), Ste12p (GST-Ste12p(aa 494-688)) or Pho4p (GST-Pho4p(aa 140-166)). After washing, equal volumes of the unbound (UB) and bound (B) fractions were separated by SDS-PAGE, transferred to nitrocellulose and immunoblotted with  $\alpha$ -GST-Kap121p antibodies (which reacts with GST, protein A and Kap121p; Table 2-2). Note addition of the NLS sequences of Nop1p, Ste12p or Pho4p disrupted the Kap121p-Nop1p-pA import complexes.

**4.9.1 KAP104 and KAP121 are synthetically lethal** – The similarity between the rg-NLS sequences of Nop1p and those of the Kap104p cargoes Nab2p and Nab4p suggests possible overlap between the cargoes recognized by Kap121p and Kap104p. A synthetic lethal genetic assay was used to determine whether these two nuclear transport pathways functionally interact. A conditional *kap121::ura3::his3::LEU2*, *kap104::ura3::HIS3* double deletion haploid strain expressing a temperature-sensitive allele of *KAP121* (*kap121-34*) and a *URA3* selectable wild-type allele of *KAP104* was isolated (*kap121-34*,  $\Delta$ *kap104/pKAP104-URA3*). As a control, a *kap121-34*,  $\Delta$ *kap108/pKAP108-URA3* strain was also isolated. An equal number of cells from each culture were spotted in serial dilution on YEPD and 5-FOA-containing agar plates and incubated at 23°C (Figure 4.9.1). The double deletion strains grew equally well on rich medium. However, when these strains were grown on 5-FOA containing media (to select for cells lacking *pKAP104-URA3* or *pKAP108-URA3*) the *kap121-34*,  $\Delta$ *kap104/pKAP104-URA3* strains failed to grow, while the *kap121-34*,  $\Delta$ *kap108/pKAP108-URA3* grew as well as its parental strains. Thus, a wild-type copy of *KAP104* was required for growth of cells with compromised Kap121p function, suggesting that under such conditions Kap104p may mediate the import of essential Kap121p cargoes. By comparison, no synthetic lethal interaction between *kap121-34* and  $\Delta$ *kap108* was observed, suggesting a specific functional relationship between the Kap121p and Kap104p nuclear import pathways.

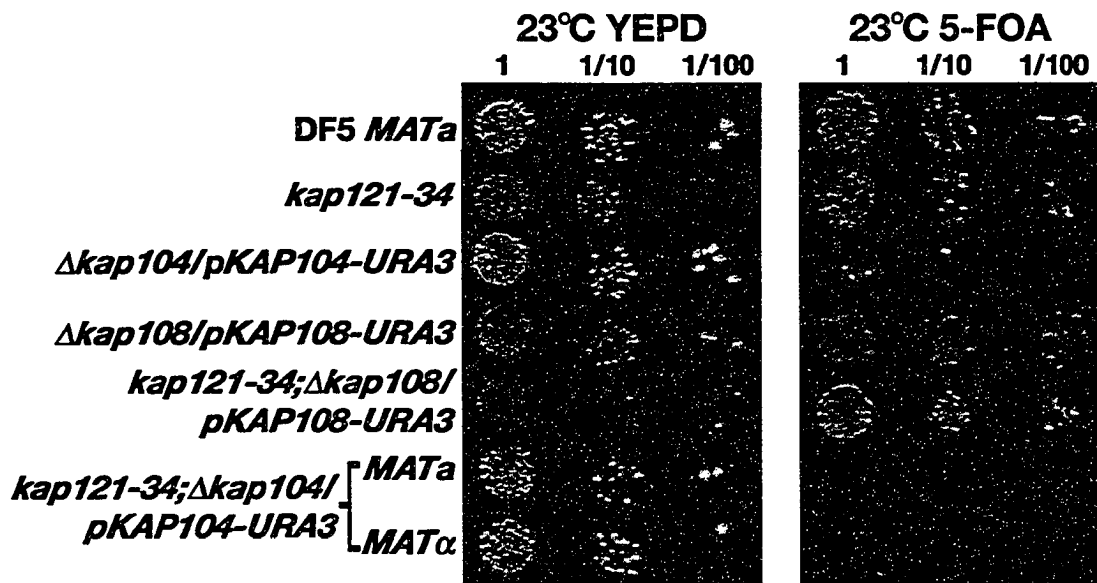


Figure 4.9.1: *kap121-34* and  $\Delta$ *kap104* are synthetically lethal in combination. The mutant strains shown were tested for their ability to withstand the loss of a wild-type copy of *KAP104* or *KAP108* at an otherwise permissive temperature. The indicated dilutions of actively growing cultures containing each strain were spotted onto YEPD or 5-FOA-containing (to select against cells containing p*KAP104-URA3* or p*KAP108-URA3*) agar plates and incubated at 23°C for 4 days. Note, *kap121-34*,  $\Delta$ *kap104* cells were unable to grow in the absence of wild-type *KAP104*.

**4.9.2 *Kap104p* imports *Nop1p* in the absence of functional *Kap121p*** – To directly test if *Kap104p* could supplant *Kap121p* activity, *KAP104* and *KAP108* were overexpressed in *kap121-34* cells expressing the galactose-inducible *NOP1GFP* gene fusion. Cultures were prepared as previously described and the localization of *GAL1-Nop1p-GFP* was determined by direct fluorescence microscopy (Figure 4.9.2A). Immunoblot analysis was used to confirm *KAP104* and *KAP108* overexpression in these cells (Figure 4.9.2B). *GAL1-Nop1p-GFP* localized to the nucleolus of *kap121-34* cells upon overexpression of *KAP104* but accumulated in the cytoplasm when *KAP108* was overexpressed in these cells (Figure 4.9.2A). These findings suggest that *Kap104p* is also capable of importing *Nop1p* into the nucleus. *Kap104p* thus likely contributes to the nuclear localization of *Nop1p* upon inactivation of *Kap121p*, and at least partially explains why it was necessary to regulate *Nop1p-GFP* expression to reveal its cytoplasmic accumulation in *kap121* mutant cells (Figure 4.4.3).

#### **4.10 *Kap121p*, and small amounts of *Kap104p*, co-immunopurify with *Nop1p***

The data presented in Sections 4.4.3 and 4.9.2 established that both *Kap121p* and *Kap104p* mediate the import of *Nop1p* *in vivo*. Co-immunopurification studies were used to investigate whether *Kap104p*, in addition to *Kap121p*, could interact with *Nop1p*. To this end, *Nop1p-pA* protein complexes were purified from a *NOP1-A* yeast whole cell lysate using rabbit IgG-conjugated magnetic beads. Bound proteins were eluted from the beads with

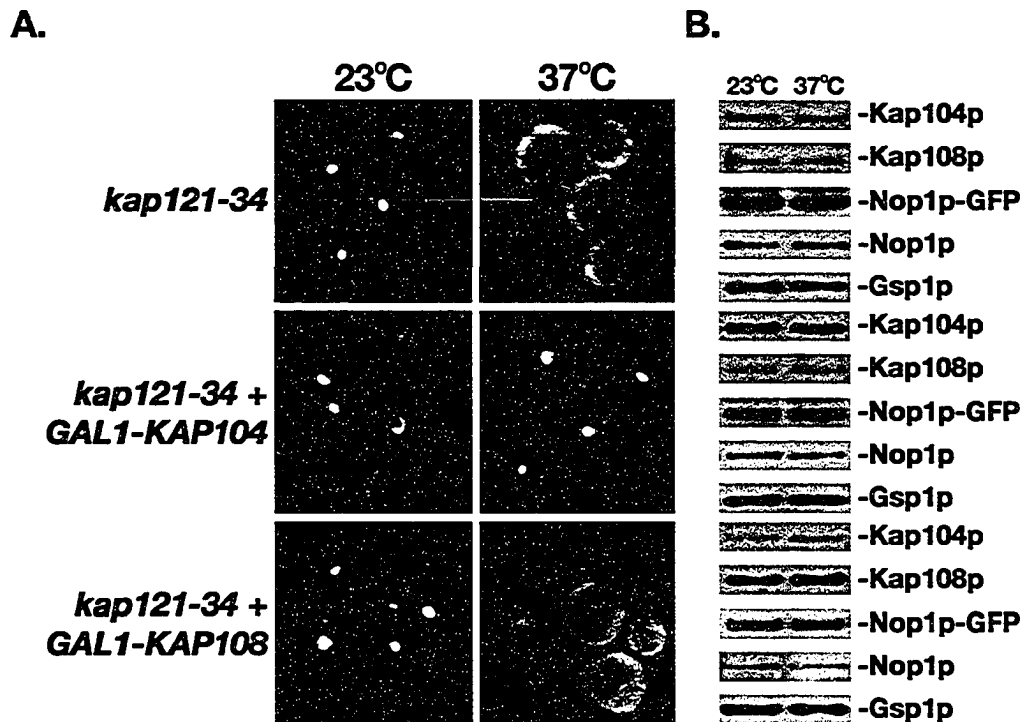


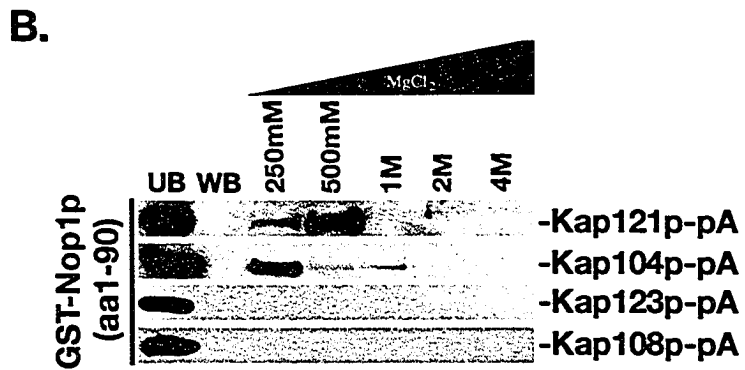
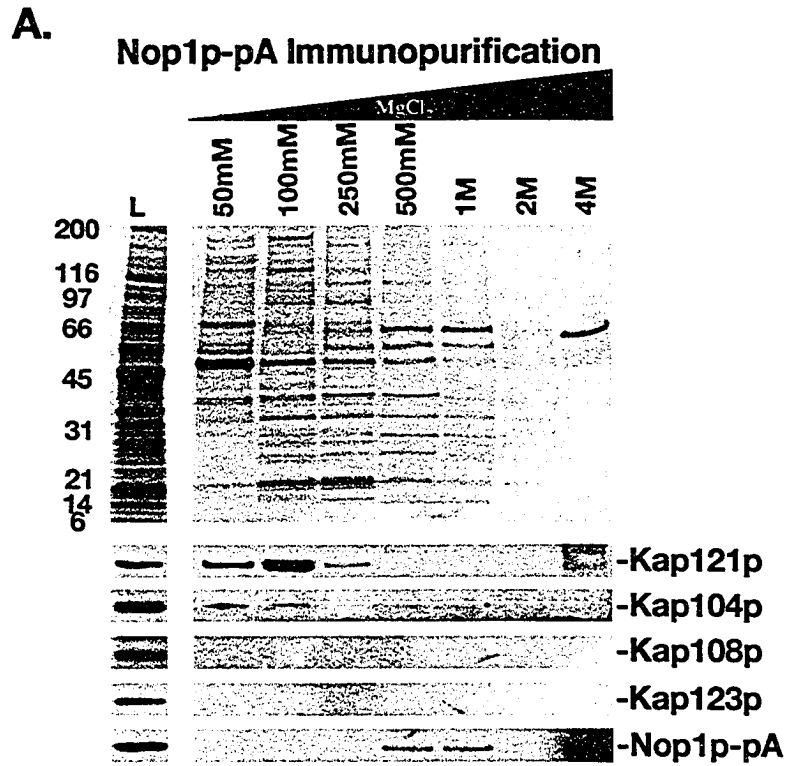
Figure 4.9.2: Overexpression of *KAP104* rescues the mislocalization of *GAL1-Nop1p-GFP* in *kap121-34* cells. *A.* *GAL1-KAP104* and *GAL1-KAP108* were induced in *kap121-34* cells containing *GAL1-Nop1p-GFP* (*pGAL1-NOP1GFP*) by shifting these cells to media containing galactose and incubating them at restrictive (37°C) or permissive (23°C) temperatures for 3 hours. Under these conditions, in the absence of additional Kap104p, Nop1p-GFP accumulates in the cytoplasm, but is nuclear upon co-induction of Kap104p. *B.* *kap121-34*, *kap121-34 + GAL1-KAP104* and *kap121-34 + GAL1-KAP108* whole cell lysates from the same cultures as those used for microscopy were probed with rabbit-polyclonal  $\alpha$ -Kap104p,  $\alpha$ -Kap108p,  $\alpha$ -Gsp1p and mouse-monoclonal  $\alpha$ -Nop1p (mAb D77 (Aris and Blobel, 1991)) antibodies (Table 2-2) (Right Panels). These western blots indicate the relative levels of Kap104p, Kap108p, Nop1p-GFP, endogenous Nop1p and Gsp1p (loading control).

increasing concentrations of  $MgCl_2$  and the fractions were analyzed by immunoblotting with four  $\beta$ -kap-specific polyclonal antibodies directed against Kap121p, Kap104p, Kap123p and Kap108p (Table 2-2). While inherent variations of antigen recognition for each  $\beta$ -kap-specific antibody precluded quantitative comparisons between these immunoblots, qualitative examination of these data suggested that of the  $\beta$ -kaps tested, only Kap121p and Kap104p interacted significantly with Nop1p-pA (Figure 4.10.1A). In parallel, GST-Nop1p(aa1-90) was immobilized on GT-Sepharose and incubated with lysates derived from yeast strains expressing pA-tagged copies of Kap121p, Kap104p, Kap123p and Kap108p. Immunoblot analysis was then used to determine which of the pA chimeras GST-Nop1p(aa1-90) bound. In agreement with the Nop1p-pA immunopurification studies, both Kap121p-pA and Kap104p-pA specifically enriched with GST-Nop1p(aa1-90), with Kap121p-pA appearing to bind this fragment of Nop1p with a higher affinity (Figure 4.10.1B). In contrast, neither Kap123p nor Kap108p enriched GST-Nop1p(aa1-90).

#### **4.11 Kap104p interacts directly with Nop1p**

Considering that previous studies demonstrated that Kap104p interacts directly with the rg-NLS sequences of Nab2p and Nab4p (Lee and Aitchison, 1999), we reasoned that Kap104p would also bind directly to the N-terminal rg-NLS of Nop1p. To address this, GST-Nop1p, GST-Nop1p(aa1-90), GST-Nop1p(aa91-327) and GST alone were immobilized on GT-Sepharose and incubated with recombinant Kap104p or Kap108p. In agreement with the

Figure 4.10.1: **Kap121p and Kap104p co-immunopurify with Nop1p.** *A.* Nop1p-pA was immunopurified from *NOP1-A* cells and the copurifying proteins were eluted with a step gradient of MgCl<sub>2</sub> as indicated. Equal volumes of the lysate (L) and eluate fractions were separated by SDS-PAGE and either stained with Coomassie blue (Top) or transferred to nitrocellulose for immunoblot analysis (Bottom) with the indicated kap-specific polyclonal antibodies and donkey  $\alpha$ -rabbit-HRP or donkey  $\alpha$ -mouse-HRP secondary antibodies (Table 2-2). The antigen-antibody complexes were then visualized using ECL reagents (Pierce). Nop1p-pA was also detected. *B.* Recombinant GST-Nop1p(aa1-90) was immobilized on GT-Sepharose and incubated with yeast whole cell lysates (1 mg/mL) from strains expressing Kap121p-pA, Kap104p-pA, Kap123p-pA and Kap108p-pA. Bound protein complexes were washed and eluted with a step gradient of MgCl<sub>2</sub> as indicated. Proteins from each eluate fraction, as well as the unbound (UB) and wash buffer (WB) fractions, were separated by SDS-PAGE and transferred to nitrocellulose membranes. Protein A (pA) chimeras were detected by immunoblotting using affinity-purified rabbit  $\alpha$ -mouse IgG and donkey  $\alpha$ -rabbit-HRP, and visualized as described above. Kap121p preferentially co-purified with both Nop1p-pA and GST-Nop1p (aa1-90), small amounts of Kap104p also co-purified with these Nop1p chimeras.



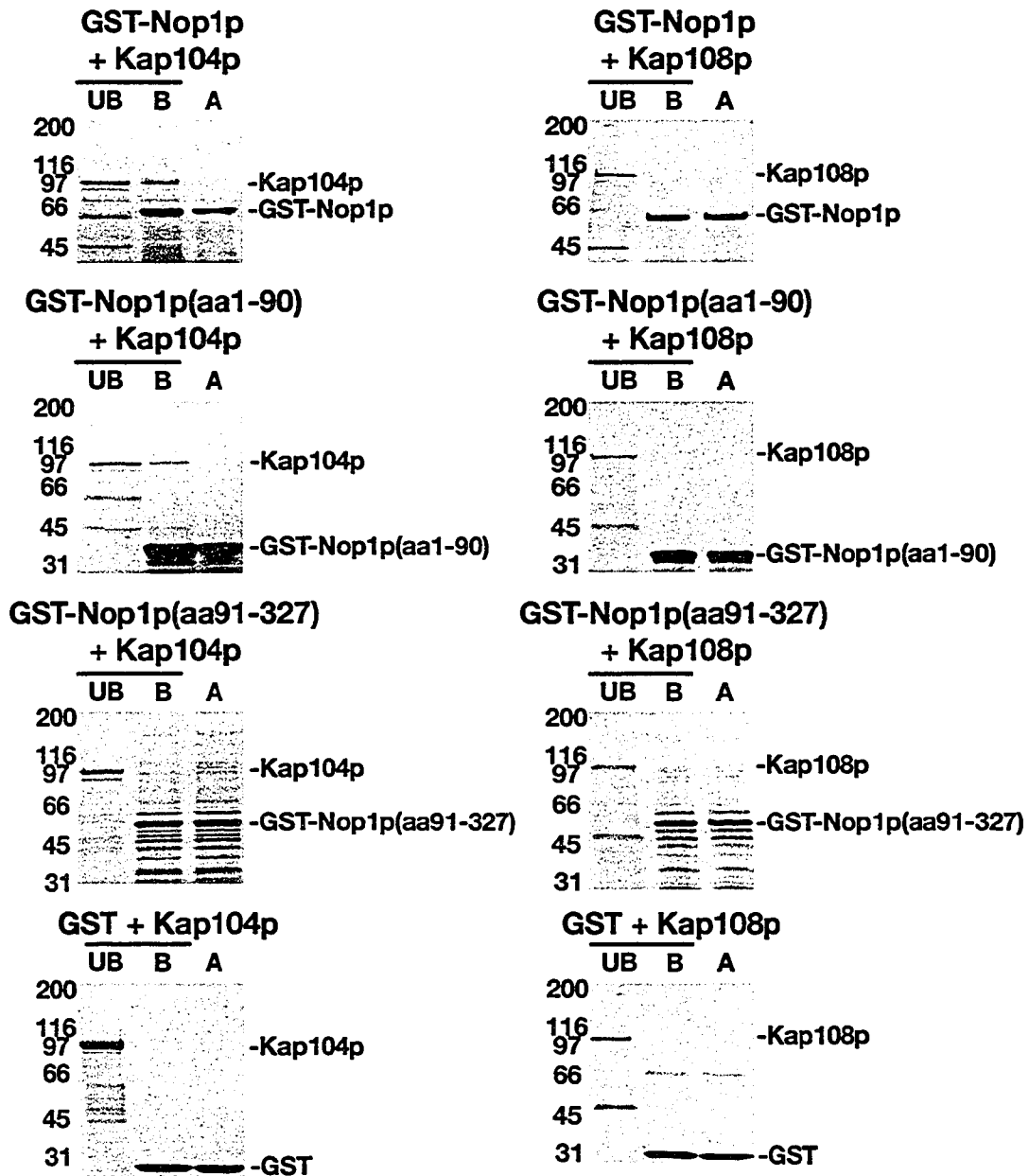


Figure 4.11.1: **Kap104p binds directly to Nop1p through its N-terminal, RGG-rich GAR domain.** GST-Nop1p (~400ng), GST-Nop1p(aa1-90) (~400ng), GST-Nop1p(aa91-327) (~400ng) and GST alone (~400ng) were immobilized on GT-Sepharose and incubated with recombinant Kap104p (~200ng) or Kap108p (~200ng) as indicated. Equal amounts of the unbound (UB), bound (B) and purified GST chimeras alone (A) were prepared and analyzed as described above. Kap104p interacted directly with both full-length Nop1p and the N-terminal, rg-NLS containing GAR domain of Nop1p.

immunopurification studies, Kap108p did not interact with these GST fusion proteins (Figure 4.11.1, Left). However, like Kap121p, Kap104p interacted directly with both full-length Nop1p and the rg-NLS-containing GAR domain of Nop1p (Figure 4.11.1, Right), but not with GST-Nop1p(aa91-327) or GST alone.

Collectively, these data suggest that the Kap104p and Kap121p transport pathways overlap in their cargo specificities. It is, thus, likely that Kap104p can supplant the activity of Kap121p upon its inactivation or disruption of its import activity (and *vice versa*). Nevertheless, as has been observed for other transport pathways, each  $\beta$ -kap appears to prefer its own cargo. Indeed, a significant change in the localization of Nop1p-GFP was not observed when its expression was induced in *kap104-16* cells (Aitchison *et al.*, 1996) at 37°C (Figure 4.11.2A) and the rg-NLS of Nab2p does not mislocalize in *kap121-34* cells at non-permissive temperatures. In addition, eNop1p-GFP did not dramatically mislocalize in a *kap121-34, kap104-16* double mutant strain that was shifted to the non-permissive temperature for 4 hours (Figure 4.11.2B). These findings were not unexpected as both Kap121p and Kap104p are functional in this strain at permissive temperature. Therefore, before the cells are shifted to 37°C both these  $\beta$ -kaps are able to import Nop1p. Because Nop1p is tethered in the nucleolus (Figures 4.4.1 and 4.4.2) any detectable signal in the cytoplasm would be attributable to new protein synthesis.

## 4.12 Discussion

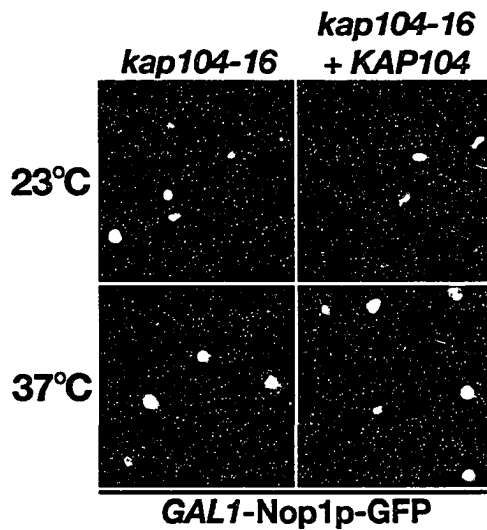
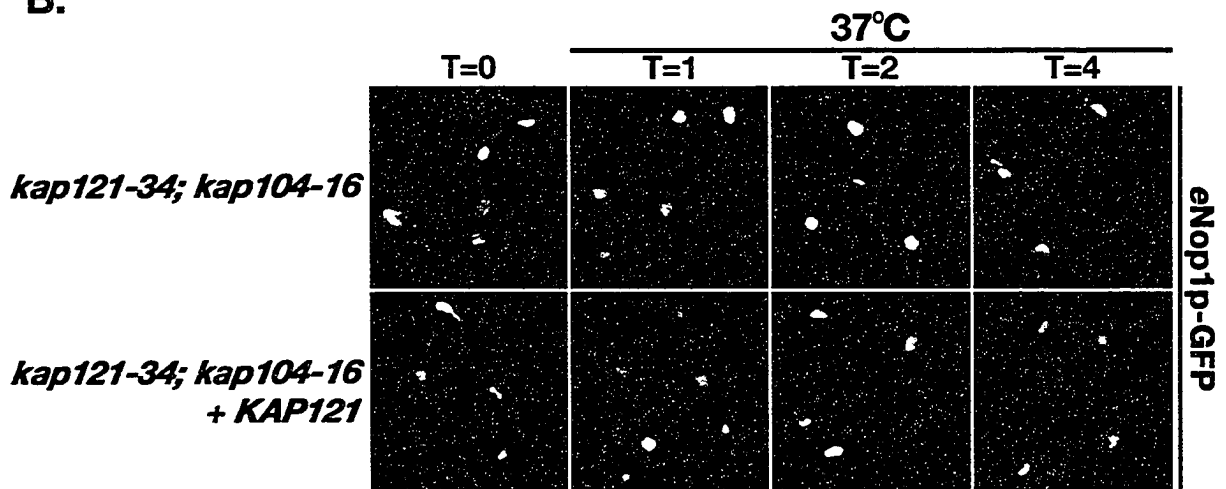
**A.****B.**

Figure 4.11.2: Nop1p is correctly localized to the nucleolus in *kap104-16* cells. *A.* The galactose-inducible *NOP1GFP* gene fusion (*GAL1-Nop1p-GFP*) was expressed in *kap104-16* cells in the presence or absence of wild-type *KAP104* at permissive (23°C) or restrictive (37°C) temperatures and visualized by direct fluorescence microscopy. Note there was no significant change in the localization of Nop1p in these strains at the non-permissive temperature. *B.* The *NOP1-GFP; kap121-34, kap104-16* strain was grown to mid-logarithmic phase at 23°C and *eNop1p-GFP* localized as described above (T=0). The culture was shifted to 37°C and the distribution of *eNop1p-GFP* monitored by direct fluorescence microscopy at the indicated time intervals. As a control, a wild-type copy of *KAP121* was added back this strain. Note, *eNop1p-GFP* remain exclusively nucleolar in *kap121-34* cells at the non-permissive temperature (37°C).

As described in Chapter 3, overlay blot assays probing a subset of nuclear proteins with cytosols from cells expressing Kap121p-pA identified many Kap121p-interacting proteins (Table 3-2, and Figures 3.3.1 and 4.2.1). Two of the most prominent Kap121p-interacting proteins identified were Nop1p and Dbp9p (Figure 4.2.1). Characterization of the Kap121p-Nop1p and Kap121p-Dbp9p interactions demonstrated that Nop1p and Dbp9p are *bona fide* import cargoes for Kap121p (Figure 4.4.3) and that Kap121p interacts directly with these cargoes (Figure 4.3.1).

As mentioned previously, several studies have identified the NLSs of Kap121p cargoes (Chaves and Blobel, 2001; Delahodde *et al.*, 2001; Kaffman *et al.*, 1998b; Mosammaparast *et al.*, 2002b; Mosammaparast *et al.*, 2001; Ueta *et al.*, 2003). While these sequences share little primary sequence similarities, they generally contain clusters of lysine residues (Table 1-2). Similarly, lysine-rich motifs were also found in Dbp9p and Nop1p (Table 4-1). However, Nop1p also contains an N-terminal RGG-rich GAR domain that shares significant sequence homology with NLS sequences recognized by another  $\beta$ -karyopherin, Kap104p (Figure 4.5.1). Studies analyzing Nop1p homologues have shown that this N-terminal GAR domain contains an NLS sequence that is required, but not always sufficient, for the efficient nuclear import of these homologues (Pih *et al.*, 2000; Snaar *et al.*, 2000). Nop1p has remained extremely well conserved, both structurally and functionally, throughout evolution (Aris and Blobel, 1991; Bachellerie *et al.*, 2002; Jansen *et al.*, 1991). Therefore, these findings

suggested that the RGG-rich GAR domain of Nop1p may contain a functional Kap121p NLS and indicated that Kap121p might recognize structurally distinct NLSs.

Moreover, Nop1p provides U3 and U14 snoRNP protein complexes with the methyltransferase activity required for the post-transcriptional modification of rRNA and, consequently, the flawless assembly of ribosome subunits is dependent on its function (Bachelierie *et al.*, 2002; Fatica and Tollervey, 2002; Venema and Tollervey, 1999). Therefore, comprehensively understanding ribosome biogenesis requires the characterization of all factors that contribute to the activity of proteins required for this process. In addition, researchers have demonstrated that Nop1p (fibrillarin) is an autoantigen in humans implicated in ~8% of the cases of the autoimmune disease scleroderma (Aris and Blobel, 1991; Lischwe *et al.*, 1985). The unique NLS characteristics of this putative Kap121p import substrate, the essential functions carried out by Nop1p and the potential extrapolation to vertebrates prompted further characterization of the Kap121p-Nop1p interaction.

A combination of *in vivo* fluorescence and *in vitro* binding studies established that Kap121p mediates Nop1p import by interacting directly with an rg-NLS present in the N-terminal GAR domain of this protein (Figures 4.6.1 and 4.6.2). Interestingly, the rg-NLS-containing fragment of Nop1p is 50 and 30 percent similar to the rg-NLS sequences of the Kap104p import cargoes Nab2p and Nab4p, respectively. This high degree of sequence similarity suggested that

these seemingly distinct nuclear transport pathways might converge and mediate the nuclear import of some common cargoes. Genetic studies demonstrated that mutations in both *KAP121* and *KAP104* are synthetically lethal (Figure 4.9.1), establishing a functional relationship between these two  $\beta$ -kaps and strongly implied that these two transport pathways overlap. Although rg-NLS sequences were originally characterized for Kap104p, and Kap104p can bind the rg-NLS of Nop1p *in vitro* (Figure 4.11.1), co-immunopurification demonstrated that Kap121p does so with higher affinity (Figure 4.10.1). In agreement with these findings, Nop1p-GFP was efficiently imported in *kap104-16* temperature-sensitive cells at all temperatures tested (Figure 4.11.2A), demonstrating that Kap121p is primarily responsible for its import. Nevertheless, overexpression of *KAP104* redirected Nop1p-GFP to nuclei of *kap121-34* cells at the restrictive temperature (Figure 4.9.2). Together, these data established that Kap104p provides an alternative transport route for Nop1p in the absence of Kap121p function.

As mentioned above, cargoes that are transported by the same  $\beta$ -kap typically contain related NLSs (reviewed in Mosammaparast and Pemberton, 2004; Talcott and Moore, 1999). However, this is not always the case, as indicated by the findings presented here and by similar studies with mammalian Kap  $\beta$ 1 (Cingolani *et al.*, 2002; Cingolani *et al.*, 1999; Lee *et al.*, 2003), and references within). Both Kap121p and Kap  $\beta$ 1 recognize, interact with, and transport cargoes containing unrelated NLSs. A recent study further characterizing mammalian Kap  $\beta$ 1-cargo interactions established that this  $\beta$ -kap

could simultaneously mediate the nuclear import of a fragment of Kap  $\alpha$  and nonclassical NLS-containing cargoes (Cingolani *et al.*, 2002). In contrast, *in vitro* competition assays demonstrated that Kap121p does not interact with lysine-rich NLSs of Kap121p cargoes and the rg-NLS of Nop1p at the same time (Figure 4.8.1). Based on these findings, it is feasible that Kap121p contains only one NLS binding pocket, or if two binding pockets are present, the occupation of one sterically, or allosterically, blocks cargo binding at the other site.

Interestingly, solution binding assays demonstrated that Kap121p-Nop1p import complexes are insensitive to RanGTP *in vitro* (Figure 4.7.1). Similarly, Lee and Aitchison (1999) demonstrated that *in vitro* RanGTP alone did not sufficiently displace Nab4p, a cargo whose rg-NLS is 30% similar to the rg-NLS-containing GAR domain of Nop1p (Figure 4.5.1), from Kap104p. In this case, a combination of RanGTP and RNA was required to dissociate Kap104p-Nab4p import complexes (Lee and Aitchison, 1999). Moreover, similar conditions were required to induce the dissociation of transport complexes containing nucleic acid binding proteins (Pemberton *et al.*, 1999; Senger *et al.*, 1998). To account for these findings researchers have suggested that  $\beta$ -kaps might mediate the intranuclear delivery of these cargoes to the subnuclear compartments where they function (like the nucleolus). However, most characterized Kap121p-specific import cargoes also bind nucleic acids and, when tested, transport complexes containing some of these substrates were also sensitive to RanGTP (Isoyama *et al.*, 2001; Kaffman *et al.*, 1998b; Ueta *et al.*, 2003).

This was also true for Dbp9p, a Kap121p cargo that like Nop1p interacts with rRNA and localizes to the nucleolus, but does not contain a GAR domain or a motif similar to the rg-NLS of Nop1p. Kap121p was specifically released from Dbp9p upon addition of RanGTP (Figure 4.7.1). In light of these findings, it appears as though Kap121p-rg-NLS interactions are insensitive to RanGTP and that nucleo-cytoplasmic transport can also be regulated in an NLS-specific manner. A transport mechanism such as this would promote cargo unloading under the appropriate conditions and/or in the presence of the correct cellular components. Additional experiments are required to identify the conditions and/or accessory factors that together with RanGTP induce the release of Nop1p from Kap121p.

It should also be noted that this study also describes the development of a regulated *in vivo* fluorescence nuclear import assay. Observing the cellular localization of constitutively expressed *NOP1-GFP* or *DBP9-GFP* demonstrated that these potential Kap121p transport cargoes did not behave in the same manner as other Kap121p substrates (Figures 4.4.1), which mislocalized to the cytoplasm upon Kap121p inactivation (Figure 3.2.2 and 3.4.1). Nop1p and Dbp9p, however, remained nucleolar under all conditions tested (Figures 4.4.1 and 4.4.2). This led me to conclude that their nucleolar concentrations were maintained by binding and retention mechanisms within this subnuclear domain. I, therefore, hypothesized that inducing the expression of Nop1p-GFP and Dbp9p-GFP after Kap121p inactivation would clarify whether this  $\beta$ -kap was

required for the nuclear import of these proteins. Indeed, under these conditions, both Nop1p and Dbp9p mislocalized to the cytoplasm of *kap121-34* cells at the non-permissive temperature (Figure 4.4.3). This assay was successfully used to identify the transport pathway that mediates the import of nucleolar proteins whose retention within this subnuclear domain made it technically impossible to characterize their transport routes using conventional nuclear import assays. This assay is generally useful to monitor the affect any conditional yeast mutant strain has on the cellular localization of insoluble nuclear proteins.

## Chapter 5 – Characterization of novel molecular mechanisms of Kap121p-mediated nuclear import<sup>15</sup>

### 5.1 Introduction

Numerous nuclear transport studies have demonstrated that a given karyopherin tends to transport cargoes involved in similar processes (Lee and Aitchison, 1999; Mosammaparast *et al.*, 2002a; Mosammaparast *et al.*, 2002b; Mosammaparast *et al.*, 2001; Rout *et al.*, 1997). These findings suggest that coordinating the nuclear import of these factors may serve as a means to regulate various cellular functions. Analysis of the Kap121p-interacting proteins identified in the overlay blot assays revealed that 8 out of 11 of these proteins are, or are predicted to be, *trans*-acting ribosome assembly factors (Table 3-2). Among these was Sof1p, which interacts both physically and functionally with Nop1p (Jansen *et al.*, 1993). Both Sof1p and Nop1p are essential members of the U3 box C/D snoRNP complex required for site-specific 2'-O-ribose methylation of pre-rRNA in the nucleolus (reviewed in Bachellerie *et al.*, 2002; Kressler *et al.*, 1999; Venema and Tollervey, 1999). However, unlike Nop1p, Sof1p does not contain an RGG-rich domain that could function as its NLS. Instead, visual analysis of the amino acid residue sequence of Sof1p identified a C-terminal lysine-rich domain (amino acid residues 411-450) more typical of the NLSs found in other Kap121p cargoes (Table 4-1; Figure 5.1.1). Presented with

---

<sup>15</sup> The data presented in this Chapter were published in Leslie, D.M., W. Zhang, B.L. Timney, B.T. Chait, M.P. Rout, R.W. Wozniak, and J.D. Aitchison. 2004. Characterization of karyopherin cargoes reveals unique mechanisms of Kap121p-mediated nuclear import. *Mol Cell Biol.* 24:8487-503.

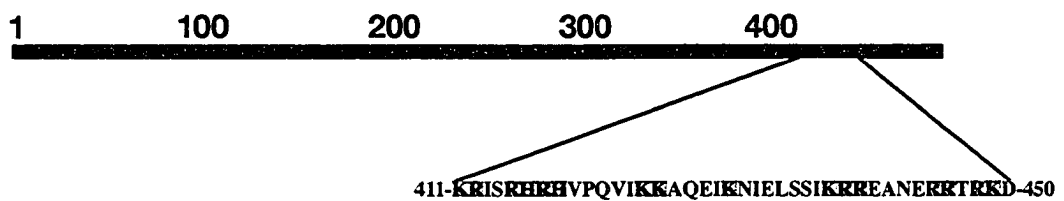


Figure 5.1.1: A **schematic diagram of Sof1p**. The gray segment represents a the lysine-rich region of Sof1p that is most similar to the NLS sequences of previously identified Kap121p cargoes.

the opportunity to study the import of two proteins carrying distinct NLSs that both physically interact and are functionally related, I chose to investigate the mechanism of Sof1p nuclear import. *In vivo* localization and solution binding studies established that Kap121p imports Sof1p by interacting directly with an NLS present between amino acid residues 381 and 489. Unexpectedly, this study also demonstrated that Sof1p nuclear import could be mediated by a “piggy-back” transport mechanism; with Nop1p bridging the interaction between Sof1p and Kap121p, revealing a novel molecular mechanism for Kap121p-mediated import.

## **5.2 Kap121p is required for the nuclear import of Sof1p**

*In vivo* fluorescence localization studies were used to determine whether Kap121p mediates the nuclear import of Sof1p. Endogenous Sof1p was C-terminally tagged with GFP and its localization in *kap121-34* cells was examined at both permissive (23°C) and non-permissive temperatures (37°C). Like Nop1p, eSof1p-GFP was retained in the nucleolus under these conditions (Figure 5.2.1). Consequently, the expression of a *SOF1GFP* gene fusion was placed under the control of a galactose-inducible promoter (*GAL1*) and its cellular localization was monitored after *kap121-34p* inactivation as described above. Under these conditions, *GAL1*-Sof1p-GFP accumulated in the cytoplasm of *kap121-34* cells at the non-permissive temperature (37°C) (Figure 5.2.1). Furthermore, this chimera remained nuclear at the permissive temperature (23°C) or when a wild-type copy of *KAP121* was present. These findings indicate that Kap121p function is

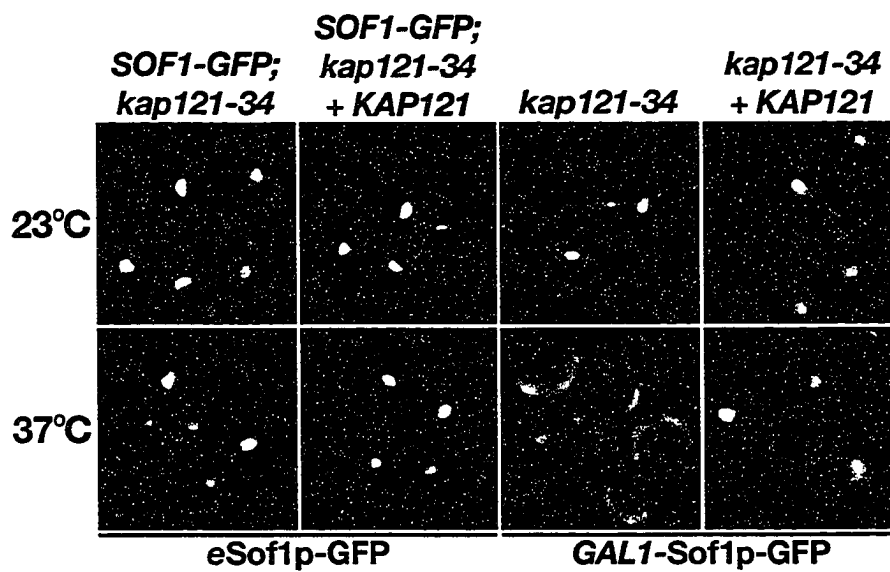


Figure 5.2.1: **Kap121p imports Sof1p.** Endogenously tagged *SOF1-GFP* (*eSof1p-GFP*) and a galactose-inducible *SOF1GFP* gene fusion (*GAL1-Sof1p-GFP*) were monitored by direct fluorescence microscopy in *kap121-34* cells at permissive (23°C) and non-permissive (37°C) temperatures as described previously. Note the cytoplasmic mislocalization of *GAL1-Sof1p-GFP* at 37°C.

required for the efficient nuclear import of Sof1p.

### **5.3 Both Kap121p and Nop1p co-immunopurify with, and interact directly with Sof1p**

Immunopurification studies were used to investigate whether Sof1p could interact with Kap121p. Following Sof1p-pA purification from a *SOF1-A* yeast whole cell lysate, immunoblot analysis with  $\alpha$ -Kap121p antibodies (Table 2-2) was used to determine if Kap121p co-purified with Sof1p. As previous studies have demonstrated that Sof1p and Nop1p interact (Jansen *et al.*, 1993),  $\alpha$ -Nop1p antibodies (Table 2-2 (Aris and Blobel, 1991)) were also used to follow the co-purification of this Sof1p-interacting protein. Both Kap121p and Nop1p co-enriched with Sof1p-pA, with the majority of Kap121p eluting in the 100 mM MgCl<sub>2</sub> fraction and Nop1p eluting in the 250 mM MgCl<sub>2</sub> fraction (Figure 5.3.1A).

Recombinant proteins and solution binding experiments were used in an attempt to reconstruct the Kap121p-Sof1p interaction *in vitro*. Sufficient quantities of full-length GST-Sof1p could not be synthesized using an *E. coli* expression system. Therefore, Sof1p-pA was isolated from yeast lysates and the copurifying yeast proteins were removed by repeated washes with 1M MgCl<sub>2</sub> (see Figure 5.3.1A). The resulting immobilized Sof1p-pA fusion was then incubated with recombinant Kap121p or GST-Nop1p (Figure 5.3.1B). As well as confirming the previously detected Sof1p-Nop1p interaction (Jansen *et al.*, 1993), these data also confirmed the interaction between Kap121p and Sof1p detected in the overlay blot assay (Figure 4.2.1).

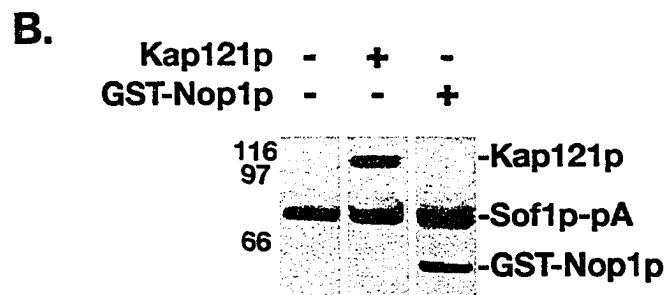
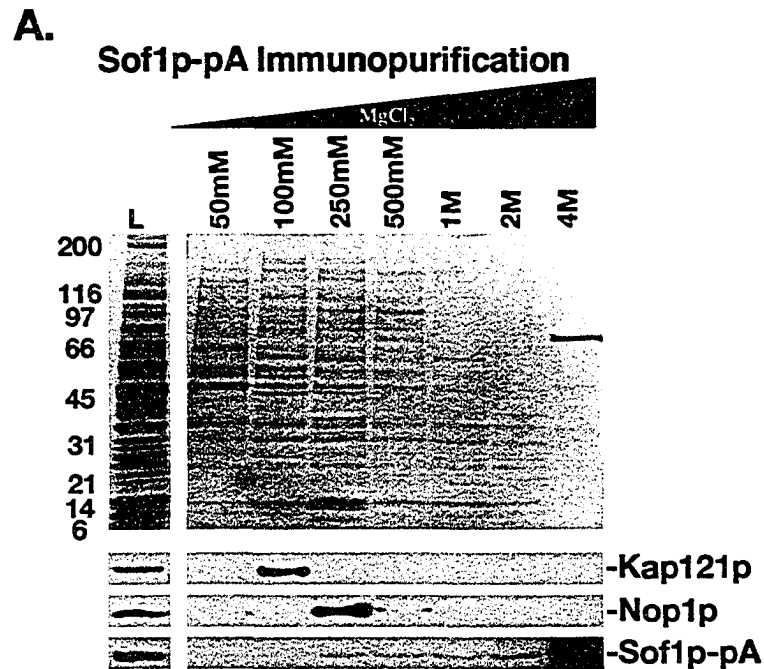


Figure 5.3.1: **Sof1p interacts directly with Kap121p and Nop1p.** *A.* Sof1p-pA protein complexes were purified from a *SOF1-A* whole cell lysate. The immobilized complexes were washed extensively and the bound proteins eluted with increasing concentrations of MgCl<sub>2</sub> as indicated. Equal volumes of the lysate (L) and eluate fractions were separated by SDS-PAGE and either stained with Coomassie blue (Top), or transferred to nitrocellulose and analyzed by immunoblotting with  $\alpha$ -Kap121p and  $\alpha$ -Nop1p (mAb D77 (Aris and Blobel, 1991)) antibodies (Table 2-2; Bottom). Note both Kap121p and Nop1p co-purified with Sof1p-pA. *B.* Sof1p-pA was purified as described above and the co-purifying proteins removed by washing with 1M MgCl<sub>2</sub> (Left panel). The beads were incubated with GST-Nop1p or recombinant Kap121p (Middle and Right panels, respectively) and equal volumes of each of the resulting bead-bound fractions were analyzed by immunoblotting with  $\alpha$ -Kap121p antibodies (which react with Kap121p, GST and pA (Marelli *et al.*, 1998)). Both Nop1p and Kap121p interacted directly with Sof1p.

## 5.4 Sof1p is imported by Kap121p using a lysine-rich NLS

**5.4.1 Kap121p binds amino acid residues 381 to 489 of Sof1p** – Visual analysis of the amino acid residue sequence of Sof1p identified a potential archetypal lysine-rich Kap121p NLS was identified within amino acid residues 411-450 of this protein (Figure 5.1.1). To determine if Kap121p is capable of interacting directly with Sof1p and if the interaction is mediated by this lysine-rich domain, GST fusion proteins containing amino acid residues 1-130, 131-380, 381-489 and 411-450 of Sof1p were constructed and synthesized in *E. coli*. These GST chimeras were immobilized on GT-Sepharose and incubated with recombinant Kap121p or Kap104p. Kap121p failed to bind either the N-terminal (aa1-130) or the central portion (aa131-380) of the protein, but interacted directly with both GST-Sof1p(aa381-489) and GST-Sof1p(aa411-450) (Figure 5.4.1). As these Kap121p-interacting fragments of Sof1p contain the above-mentioned sequence similar to previously identified Kap121p NLSs, this result suggests that this sequence may indeed function as the NLS for Sof1p. Interestingly, extending the Kap121p-interacting fragment of Sof1p from aa411-450 to aa381-489 significantly improved the observed Kap121p-Sof1p protein-protein interaction, indicating that these flanking sequences are required for optimal Kap121p binding. Kap104p did not interact with any of these GST fusion proteins nor was Kap123p found to interact with Sof1p in the overlay blot assay (Figures 3.3.1 and 4.2.1), suggesting that the observed Kap121p is specific.

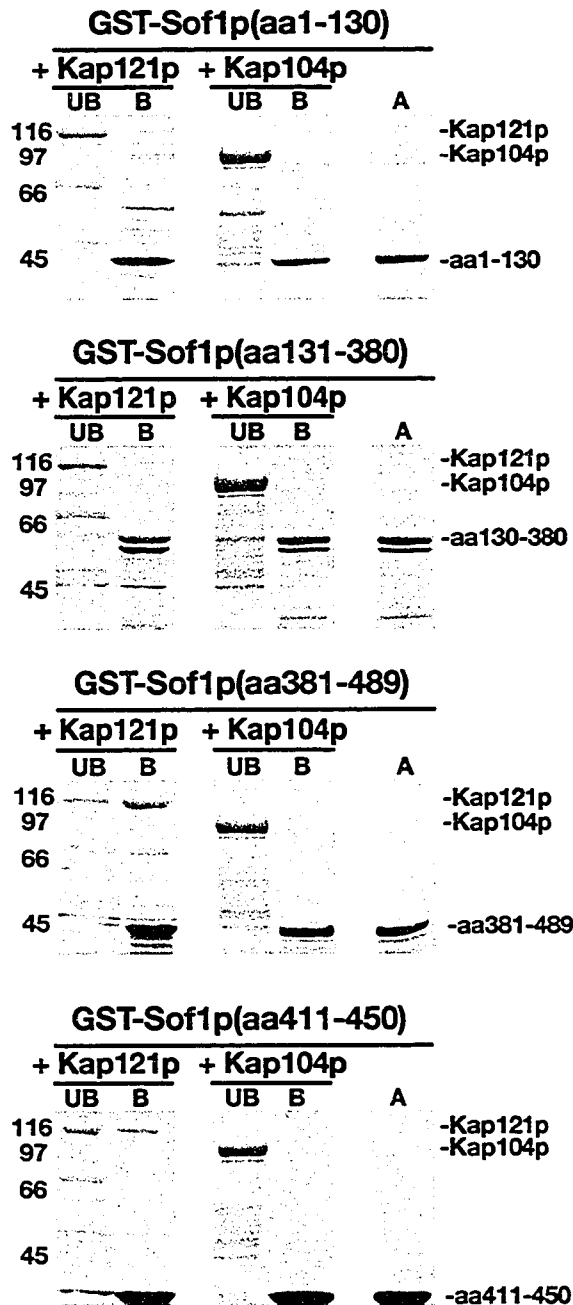


Figure 5.4.1: **Kap121p** interacts directly with amino acids 381-489 of **Sof1p**. GST chimeras containing fragments of **Sof1p** (~400 ng) were immobilized on GT-Sepharose and incubated with recombinant **Kap121p** (~200 ng) or **Kap104p** (~300 ng). Equal amounts of the unbound (UB) and bound (B) fractions, as well as the GST chimeric proteins alone (A), were analyzed by SDS-PAGE and Coomassie blue staining. Note that recombinant **Kap121p**, but not **Kap104p**, interacts strongly with **GST-Sof1p(aa381-498)** and weakly with **GST-Sof1p(aa411-450)**.

#### **5.4.2 Amino acid residues 381 to 489 of Sof1p contain a functional NLS –**

To evaluate the import potential of each fragment *in vivo*, the fragments described above were C-terminally fused to GFP and expressed from a galactose-inducible promoter (*GAL1*) in *kap121-34* cells. After overnight growth at 23°C under inducing conditions, their cellular localizations were monitored by fluorescence microscopy (Figure 5.4.2A). In agreement with the *in vitro* binding experiments, the Kap121p-interacting fragments (Sof1p(aa381-489)-GFP and Sof1p(aa411-450)-GFP) were targeted to the nucleus. The GFP chimeras containing amino acid residues 1 to 130 and 131 to 380 were found diffusely distributed throughout the cell. Furthermore, amino acid residues 381-489 exhibited a wild-type localization pattern; localizing the GFP reporter exclusively to the nucleolus. While the GFP chimera containing the smaller fragment of Sof1p(aa411-450) also concentrated in the nucleus its import was less efficient. Kap121p function was found to be required for the import of these NLS-containing reporters, as inactivation of Kap121p resulted in the mislocalization Sof1p(aa381-489)-GFP and Sof1p(aa411-450)-GFP (Figure 5.4.2B). Together, these data established that Kap121p interacts directly with Sof1p through a C-terminal, lysine-rich NLS that is both necessary and sufficient for its Kap121p-mediated import.

#### **5.5 Tertiary import complexes containing Kap121p, Nop1p and Sof1p assemble *in vitro***

The Sof1p-pA immunopurification studies presented above demonstrated

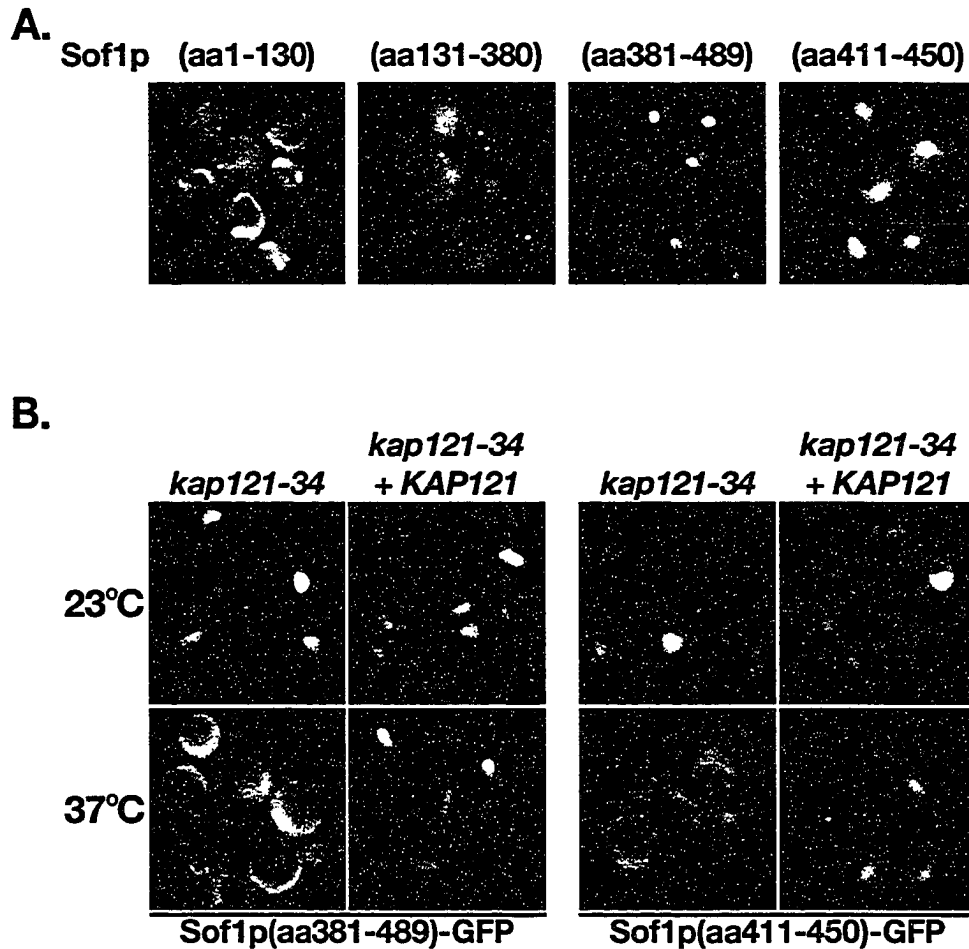


Figure 5.4.2: Amino acids 381-489 of Sof1p contain a functional NLS. *A.* Galactose-inducible GFP chimeric proteins containing the four fragments of Sof1p were synthesized at 23°C in *kap121-34* cells and analyzed by direct fluorescence microscopy. Note the nuclear localization of Sof1p(aa381-489)-GFP and Sof1p(aa411-450)-GFP. *B.* The cellular localizations of Sof1p(aa381-489)-GFP and Sof1p(aa411-450)-GFP were determined at both 23°C and 37°C in *kap121-34* and *kap121-34* cells containing p*KAP121-URA3* (*kap121-34* + *KAP121*). Note the nuclear import of these Sof1p fragments is dependent on Kap121p function.

that Nop1p eluted from Sof1p at a higher concentration of  $MgCl_2$  than that required to release Kap121p (Figure 5.3.1A). These data suggested that the protein-protein interaction between Nop1p and Sof1p was stronger than the Kap121p-Sof1p interaction. It was, therefore, reasoned that if Nop1p and Sof1p interact in the cytoplasm, then the cytoplasmic pool of Nop1p could inhibit the formation of Kap121p-Sof1p import complexes. In agreement with this idea, *in vitro* binding assays showed that when a Kap121p-Sof1p complex was preformed and Nop1p was added, Kap121p was displaced, and Nop1p, in turn, bound to Sof1p (Figure 5.5.1). These findings further suggest that, like the other NLSs examined (Figure 4.7.1), Kap121p cannot simultaneously interact with the lysine-rich NLS of Sof1p and the rg-NLS of Nop1p. However, when a complex between Nop1p and Sof1p was preformed and Kap121p was added subsequently, a tertiary complex was formed without displacing either component (Figure 5.5.1). These data demonstrate that Kap121p is capable of interacting with a protein complex containing both Nop1p and Sof1p and suggested that these proteins may be imported into the nucleus together.

## **5.6 Sof1p can be imported by a piggy-back transport mechanism**

Because addition of Nop1p to Kap121p-Sof1p heterodimers displaced Kap121p from Sof1p, we hypothesized that in such a scenario, the Nop1p rg-NLS would be engaged and Sof1p, in turn, would interact with Nop1p, and be carried piggy-back into the nucleus. To investigate this possibility, a cNLS from SV40 large T Antigen (Kalderon *et al.*, 1984b), which is recognized by

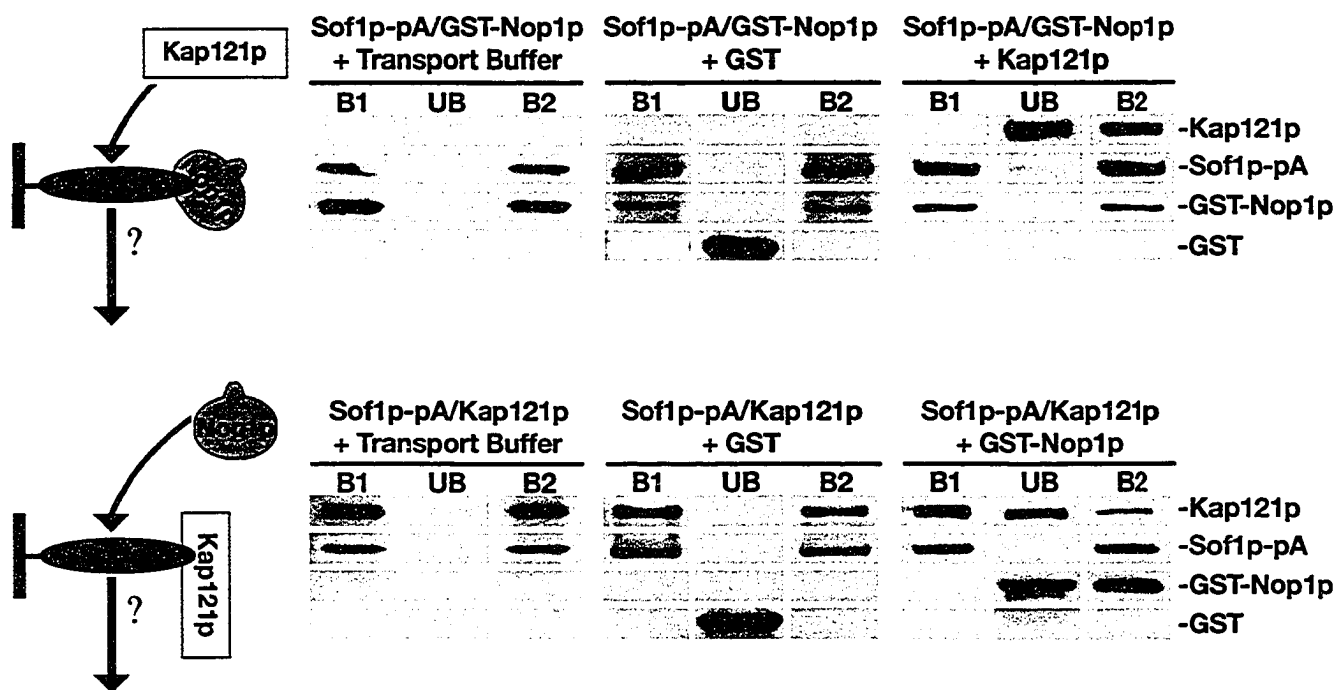


Figure 5.5.1: Heterotrimeric protein complexes containing Sof1p, Kap121p and Nop1p assemble *in vitro*. Sof1p-Nop1p (Sof1p-pA/GST-Nop1p) or Sof1p-Kap121p (Sof1p-pA/Kap121p) complexes were assembled as previously described (Figure 5.3.1) and incubated with recombinant Kap121p, GST-Nop1p, GST or transport buffer as indicated. After extensive washing, the initial complex (B1: Sof1p-pA/GST-Nop1p or Sof1p-pA/Kap121p), unbound (UB) and bound (B2) fractions were prepared for SDS-PAGE, separated, transferred to nitrocellulose and probed with  $\alpha$ -Kap121p antibodies (which react with GST, protein A and Kap121p). Note Nop1p dissociates Kap121p from Sof1p, while Kap121p interacts with the Sof1p-Nop1p protein complex without displacing Nop1p.

Kap95p/Kap60p, was appended to the C terminus of Nop1p; consequently bypassing the requirement of Kap121p for Nop1p nuclear import. If Nop1p and Sof1p can be imported as a single complex, this chimera should restore Sof1p nuclear import in *kap121-34* cells. *kap121-34* cells containing pGAL1-SOF1GFP were transformed with a single copy plasmid containing either *NOP1* or a *NOP1*cNLS. The expression of this GFP chimera was induced at 23°C and 37°C as described above, and its localization was monitored using direct fluorescence microscopy. Remarkably, the nuclear import of Sof1p-GFP was restored in the presence of *NOP1*cNLS, but remained mislocalized in *kap121-34* cells expressing *NOP1* alone (Figure 5.6.1A). Taken together, it appears that Sof1p can be imported as a complex with Nop1p, which in turn is bound to a  $\beta$ -kap.

Given that overexpression *KAP104* rescued the mislocalization of Nop1p-GFP in *kap121-34* cells (Figure 4.9.2), this condition should also rescue the mislocalization of Sof1p-GFP. Indeed, upon *KAP104* overexpression the nuclear import of Sof1p-GFP at the non-permissive temperature was restored in *kap121-34* cells (Figure 5.6.1A). This was not observed upon overexpression of the control  $\beta$ -kap, Kap108p, although immunoblotting of whole cell lysates from these cells confirmed that both *KAP104* and *KAP108* (Figure 5.6.1B) were induced to similar extents. Together these data show that Nop1p and Sof1p can be simultaneously imported by Kap104p, or if provided with a cNLS, by the Kap95p/Kap60p complex. In combination with the *in vitro* binding data, demonstrating that Kap104p does not interact with Sof1p (Figure 5.4.1), these

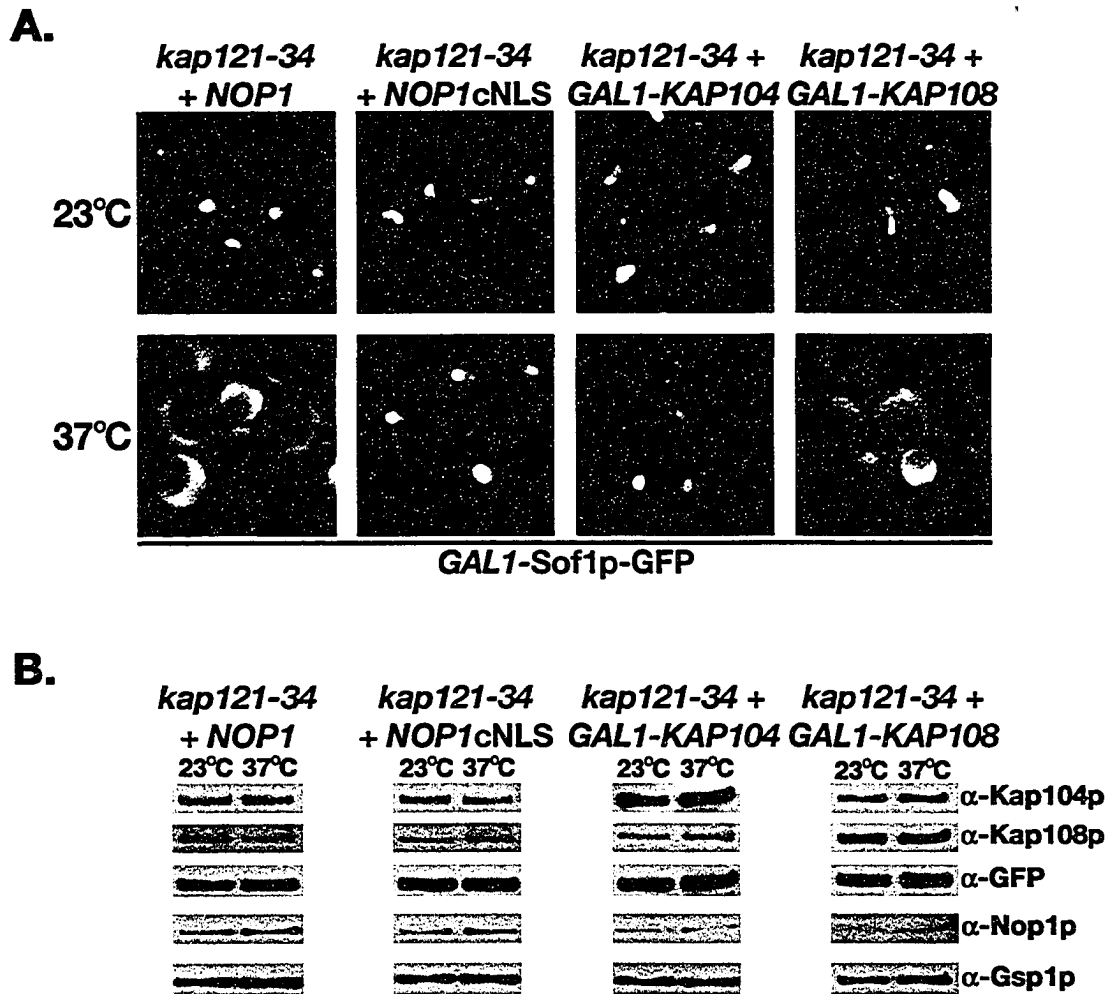


Figure 5.6.1: *Sof1p* can be imported by piggy-back. *A.* *Sof1p* is imported by interacting with *Nop1p* bound to a karyopherin. The galactose-inducible *SOF1GFP* gene fusion (*GAL1-Sof1p-GFP*) was expressed in *kap121-34* cells which contained a plasmid-linked copy of wild-type *NOP1* (*NOP1*), *NOP1* fused to a cNLS (*NOP1cNLS*), galactose-inducible *KAP104* (*GAL1-KAP104*) or galactose-inducible *KAP108* (*GAL1-KAP108*) at permissive (23°C) or restrictive (37°C) temperatures as previously described. Note that expression of *NOP1cNLS* or overexpression of *KAP104* rescued the cytoplasmic mislocalization of *Sof1p-GFP* at the non-permissive temperature (37°C). *B.* Whole cell lysates from the same cultures as those used for microscopy (as shown in panel *A*) were probed with  $\alpha$ -Kap104p,  $\alpha$ -Kap108p,  $\alpha$ -Gsp1p,  $\alpha$ -GFP and mouse-monoclonal  $\alpha$ -Nop1p (mAb D77 (Aris and Blobel, 1991)) antibodies (Table 2-2).

findings establish that Sof1p can be imported as a piggy-back complex with Nop1p and Kap121p or Kap104p.

## 5.7 Discussion

Studies have demonstrated that individual  $\beta$ -kaps frequently transport proteins that perform similar functions or function together (Aitchison *et al.*, 1996; Chaves and Blobel, 2001; Delahodde *et al.*, 2001; Jakel and Gorlich, 1998; Kaffman *et al.*, 1998b; Lee and Aitchison, 1999; Mosammaparast *et al.*, 2002b; Mosammaparast *et al.*, 2001; Muhlhauser *et al.*, 2001; Rout *et al.*, 1997; Sydorsky *et al.*, 2003; Ueta *et al.*, 2003). In agreement with these findings, most of the proteins that interacted specifically with Kap121p in the overlay blot assays are *trans*-acting protein factors required for ribosome biogenesis. These included Nop1p (Chapter 4), Kre31p, Kre32p, Sof1p, Dbp9p (Chapter 4), Imp4p, Nop12p and Rrp12p (Table 3-2). Along with Nop1p, three other components of the U3 C/D box snoRNP complex were also found: Kre31p, Sof1p and Imp4p. Of these Sof1p was unique, as it has been shown to be functionally related to Nop1p (Jansen *et al.*, 1993). Moreover, inspection of the amino acid residue sequence of Sof1p revealed that it does not contain an RGG-rich domain that could function as an rg-NLS, but does have a lysine-rich region similar to those found in most other Kap121p import cargoes. This presented me with the opportunity to dissect the nuclear import mechanisms of two ribosome assembly factors that physically interact and are functionally related, but carry different

types of NLSs. I, therefore, chose to further characterize the interaction between Kap121p and Sof1p.

*In vivo* fluorescence localization analysis and *in vitro* binding studies established that Kap121p could mediate the nuclear import of Sof1p through a C-terminal lysine-rich NLS (Figures 5.2.1, 5.4.1 and 5.4.2). Moreover, truncation analysis of Sof1p demonstrated that the lysine-rich region (amino acid residues 411-450) mentioned above provides the minimal signal required for Kap121p recognition, binding and subsequent import. However, amino acid residues 381 to 410 and 451 to 489 seem to provide additional contact points or adopt higher-order structural characteristics that reinforce the interaction between Kap121p and Sof1p. Furthermore, this fragment contains all of the information required for wild-type, nucleolar localization of Sof1p (Figures 5.4.1 and 5.4.2).

Interestingly, two nuclear import complexes containing Sof1p could be generated *in vitro*: Sof1p-Kap121p and Sof1p-Nop1p-Kap121p (Figure 5.3.1 and 5.5.1). These findings were intriguing as the *in vitro* competition assays demonstrated that Kap121p does not interact with lysine-rich and rg-NLS sequences at the same time (Figure 4.8.1). Nevertheless, these data indicate that Nop1p and Sof1p can be imported together by Kap121p. In this case, however, Nop1p and Sof1p form a complex that can be recognized by Kap121p, and the trimeric complex traverses the NPC. Indeed, both expression of *NOP1cNLS* chimera or overexpression of *KAP104* (which does not bind Sof1p

(Figure 5.4.1)) rescued the nuclear import defect of Sof1p-GFP in *kap121-34* cells (Figure 5.6.1).

Together, these findings established that Sof1p could be imported into the nucleus in two ways: by direct interaction with Kap121p via its C-terminal lysine-rich NLS or by a piggy-back transport mechanism where Nop1p bridges the interaction between Sof1p and a  $\beta$ -kap. But which one of these transport mechanisms acts as the primary import route and which one functions as the back-up? The immunopurification studies and solution binding assays demonstrated that under the conditions explored here, Kap121p appears to have a higher affinity for the rg-NLS of Nop1p than that present in Sof1p, and that Sof1p has a higher affinity for Nop1p than Kap121p (Figures 5.3.1 and 5.5.1). These findings suggest that *in vivo* the stronger interactions between Nop1p and Kap121p, and Nop1p and Sof1p would out compete the weaker Kap121p-Sof1p interaction, supporting the piggy-back transport mechanism as the primary import route for Sof1p. Moreover, the *in vivo* localization studies that re-directed the nuclear import pathway used by Nop1p in *kap121-34* cells completely restored the otherwise defective nuclear import of Sof1p-GFP in these cells. Based on these data, I suggest that Sof1p is primarily imported via the piggy-back transport mechanism and that the more typical Kap121p-Sof1p interaction provides an alternate means of transport into the nucleus. Alternatively, one could imagine that if the stoichiometric ratio of Sof1p:Nop1p present in U3 snoRNPs are not appropriate then both of these import mechanisms could be active *in vivo*. This

would ensure that the correct amount of each component (eg. 2 molecules of Sof1p:1 molecule of Nop1p) would be delivered to the nucleolus where U3 snoRNPs are assembled. To clearly determine which, if either, of these transport mechanisms dominates *in vivo*, additional experiments quantitatively assaying the nuclear import and determining the stoichiometric ratios of the proteins present in snoRNPs. Additionally, experiments analyzing how uncoupling the Nop1p-Sof1p interaction and disabling the activity of the NLS of Sof1p affect its import would also allow one to determine which import route prevails *in vivo*.

Importantly, these studies suggest that cellular factors that interact in the nucleus can assemble in the cytoplasm and be transported into the nucleus as pre-assembled complexes. A transport mechanism like this could be used by the cell to ensure that functionally related proteins are localized appropriately when required, while lessening the number of transport cycles required for a given cellular process. Moreover, this piggy-back transport mechanism might provide the cell with a back-up plan that would allow it to adapt to minor perturbations in an individual nuclear transport pathway.

## Chapter 6 – Perspectives

### 6.1 Summary

Cell biological, genetic and biochemical techniques were used to examine the molecular mechanisms that regulate the soluble phase of nucleo-cytoplasmic transport. Four novel nuclear import cargoes (Ste12p, Nop1p, Sof1p and Dbp9p) for the typical yeast  $\beta$ -karyopherin, Kap121p, were identified and the underlying kap-cargo interactions characterized. A direct connection was made between the phenotypes associated with *kap121-ts* mutants and the mislocalization of a cargo imported by this  $\beta$ -kap (Ste12p). Studies characterizing Nop1p nuclear import established that Kap121p could interact with and mediate the transport of, at least two classes of cargo: those containing lysine-rich NLSs and cargoes with rg-NLSs. This finding led to the discovery of a previously uncharacterized nucleo-cytoplasmic transport network in which the Kap121p and Kap104p nuclear import pathways transport some common cargoes. In addition, import  $\beta$ -kaps were found to be capable of transporting cytoplasmically pre-assembled protein complexes containing cellular factors that associate and function together in the nucleus (Nop1p and Sof1p). Together, these data have extended the repertoire of known kap-cargo interactions that facilitate nucleo-cytoplasmic exchange. Furthermore, the findings presented here highlight the numerous levels of redundancy and flexibility that are built into this transport system to ensure that many of the key components required for a given cellular process or response are localized to the appropriate compartment at the right time.

## 6.2 Perspectives on the regulation of nucleo-cytoplasmic transport

Nucleo-cytoplasmic transport pathways ferry numerous transcription factors, second messengers, housekeeping proteins and ribonucleoprotein (RNP) particles between the nucleus and cytoplasm. The cell's ability to remain viable, to maintain homeostasis, control growth, and to be able to effectively respond to external stimuli is dependent on an efficient nuclear transport system. The importance of DNA binding, *trans*-activation or repression, and protein interaction domains has been well documented in transcription factor function. However, data are accumulating which suggest that the nucleo-cytoplasmic transport of transcription factors and/or their co-regulators provides an additional level of regulation that controls gene expression (Fabbro and Henderson, 2003; Kau *et al.*, 2004; Schwartz and Madhani, 2004; Smith and Koopman, 2004; Xu and Massague, 2004).

Nuclear transport can be regulated on at least three levels: 1. cargo recognition; 2.  $\beta$ -kap activity; and 3. passage through the NPC.

**1. Cargo recognition** – All signal-mediated nuclear transport events are dependent on cargo recognition. Thus the activities of many transcription factors and their cofactors are often regulated by either masking or exposing their nuclear transport signals. For example, the NESs of NF-AT and PBX1/EXD are blocked by the binding of calcineurin and PREP1/HTH, respectively, thereby preventing  $\beta$ -kap recognition and facilitating their nuclear retention (Berthelsen *et al.*, 1999; Zhu and

McKeon, 1999). Similarly, the binding of I $\kappa$ B $\alpha$  to NF- $\kappa$ B in the cytoplasm inhibits its nuclear import by NLS masking (Chen and Greene, 2004). Altering the post-translational modification (PTM) state of a transcription factor or transcriptional coregulators can also be used to control their nuclear transport. For example, the NESs of BRCA1, p53 and INI1/hSNF5 are masked by phosphorylation (reviewed in Chen and Greene, 2004; Fabbro and Henderson, 2003; Kau *et al.*, 2004; Xu and Massague, 2004). Similarly, phosphorylation of Pho4p or dephosphorylation and ubiquitylation of p53 induce export by exposing their NESs (Kaffman *et al.*, 1998a; Kau *et al.*, 2004). In many of these cases, the proteins whose activities are regulated by PTMs and nuclear transport are tumour suppressors – gene encoding a protein that suppresses tumour formation. Thus, it is not surprising that mutations altering the manner in which their nuclear transport is regulated have been identified in various cancers (Fabbro and Henderson, 2003; Kau *et al.*, 2004). For example, a C-terminal truncation of INI1/hSNF5 associated with malignant rhabdoid tumours is found in the cytoplasm (Craig *et al.*, 2002). In normal cells its subcellular localization is tightly controlled by NES masking, which ensures that INI1/hSNF5 remains nuclear where it controls the G1-S cell cycle transition (Versteeg *et al.*, 2002). However, this truncation is thought to induce a conformational change that unmask its NES, thereby stimulating export and preventing INI1/hSNF5 induced

cell cycle arrest. Likewise, C-terminal truncations of the tumour suppressor BRCA1 impair its nuclear import in breast cancer cells, but do not alter its nuclear export (Chen *et al.*, 1995; Fabbro and Henderson, 2003; Taylor *et al.*, 1998); thus affecting its steady-state nuclear localization. This could affect one, or all, of the numerous cellular processes associated with BRCA1, which include cell cycle control, protein degradation, DNA damage repair and transcriptional regulation. Recent studies have also linked defects in nucleo-cytoplasmic shuttling with syndromes affecting organogenesis in humans (reviewed in Smith and Koopman, 2004). Mutations that deregulate the nuclear import and/or nuclear export of members of the SOX family of developmental transcription factors, including SRY (Li *et al.*, 2001), SOX9 (Gasca *et al.*, 2002; Preiss *et al.*, 2001) and SOX10 (Rehberg *et al.*, 2002), have been associated with human sex reversal syndromes.

**2.  $\beta$ -kap activity** –  $\beta$ -kap activity can also be regulated by PTMs and specific protein-protein interactions, which often occur consequent to the modification. For example, phosphorylated CAS/Cse1p is localized to the cytoplasm where it strongly associates with cytoplasmic microtubules, while the dephosphorylated form is found in the nucleus (Behrens *et al.*, 2003). Such dramatic changes in the localization of a  $\beta$ -kap are thought to affect its activity. Accordingly, it has been suggested that the cytoplasmic CAS/Cse1p tethering sites generate an inactive pool of CAS/Cse1p that

could affect its roles in apoptosis, proliferation and/or nuclear transport (Behrens *et al.*, 2003).

**3. Passage across the NPC** – Similarly, studies have established that the post-translational modification of an individual component of the NPC can specifically and dramatically alter the translocation of kap-cargo complexes through NPC. For example, Nup53p phosphorylation at certain stages of the cell cycle exposes a high affinity Kap121p binding site within this nup. Kap121p binding at this site specifically traps it at the NPC and, accordingly, inhibits the import of its cargoes (Makhnevych *et al.*, 2003).

Together, these findings demonstrate that specifically altering cargo recognition provides a means by which an isolated transport event can be regulated and that changing the activity of a  $\beta$ -kap and/or the rate at which transport complexes traverse the NPC can globally affect both regulated and constitutive nucleo-cytoplasmic exchange.

### **6.3 Perspectives on nucleo-cytoplasmic transport and cell physiology**

Nuclear transport pathways are extremely complex: a given  $\beta$ -kap mediates the transport of numerous cargoes with some transport events occurring continually and others only under certain conditions; the list of cargoes transported by each  $\beta$ -kap is incomplete; and mutations that alter the activity of  $\beta$ -kaps can change the nuclear:cytoplasmic distribution of numerous cellular factors. The mislocalization of any one of these factors, or combinations thereof, could lead to altered cellular phenotypes and disease. Therefore, precisely

relating a phenotype to the mislocalization of a specific protein can be very difficult.

For example, CAS/Cse1p (the export receptor for Kap  $\alpha$ ) is overexpressed, and often differentially localized, in some breast, colon and bladder cancers, as well as lymphoid neoplasms (Behrens *et al.*, 2001; Behrens *et al.*, 2003; Brinkmann, 1998; Wellmann *et al.*, 2001). Any change in the expression or steady-state localization of CAS could affect the import of Kap  $\beta$ 1/Kap  $\alpha$  cargoes, which include a number of transcription factors, tumour suppressors, oncoproteins and microtubule organizing proteins, or alter its ability to regulate mitosis, cell proliferation, and apoptosis (Behrens *et al.*, 2003; Brinkmann *et al.*, 1996; Ogryzko *et al.*, 1997; Scherf *et al.*, 1996). Furthermore, it is possible that in addition to Kap  $\alpha$ , CAS/Cse1p exports other cellular factors and that blocking their export may also result in the transformation of normal cells to cancerous cells. Therefore, the molecular nature of the association between CAS/Cse1p and cancer is unclear.

The study described in Chapter 3 provides a framework of experiments that could be used to determine precisely how perturbing CAS/Cse1p function causes cancer. We were faced with a similar problem in *S. cerevisiae*. Analysis of *kap121-ts* mutant strains revealed that these cells were unable to mate or grow invasively; cellular processes that were unrelated to those governed by known Kap121p cargoes. Proteomic studies were then used to initiate the identification of novel Kap121p cargoes. Among a number of potential Kap121p

cargoes was Ste12p, a transcription factor that regulates both of these differentiation programs. A role for Kap121p in Ste12p function was then highlighted by the data demonstrating that Kap121p imports Ste12p and that Ste12p-induced transcription was impaired in *kap121-ts* mutant cells. A direct relationship between these phenotypes and aberrant Ste12p import was then confirmed by the data demonstrating that changing the nuclear import pathway used by this cargo corrected the mating and invasive growth defects associated with *kap121-ts* mutants. Based on these findings, techniques such as those described here could be used to define the molecular interactions between  $\beta$ -kaps and their cargoes (or other cellular factors) that directly connect diseased states, including cancer, autoimmune diseases and aberrant embryo development, to a specific interaction or transport event.

Together, the data presented in Chapter 3 and the studies discussed here highlight the multiple ways nucleo-cytoplasmic transport pathways influence cell viability. However, we have only just begun to untangle the networks of interactions between karyopherins and their cargoes. Accordingly, a comprehensive inventory of kap-cargo interactions must be generated before we can truly begin to understand how these transport pathways influence normal cell growth and development. Once armed with this list, we can then begin to map the individual interactions or combinations of interactions that cause a particular phenotype and *vice versa*.

#### **6.4 Perspectives on nucleo-cytoplasmic transport networks**

Nucleo-cytoplasmic transport networks are groups of  $\beta$ -kaps that mediate the transport of some common cargoes. These networks provide cells with a mechanism that enables them to globally control specific classes of cellular factors at the level of nuclear transport. The experiments presented in Chapter 4, as well as previous studies, have begun to identify these networks. A synthetic lethal relationship between *KAP121* and *KAP104* was identified and subsequent experiments demonstrated that in the absence of Kap121p function, Kap104p provides an alternative transport route for Nop1p (a cargo that is primarily transported by Kap121p). Similarly, other yeast and mammalian  $\beta$ -kaps import overlapping groups of cargoes (Figure 1.4.2). For example, at least four  $\beta$ -kap transport pathways mediate the nuclear import of core histones and ribosomal proteins (Jakel and Gorlich, 1998; Mosammaparast *et al.*, 2002b; Mosammaparast *et al.*, 2001; Muhlhauser *et al.*, 2001; Rout *et al.*, 1997; Sydorsky *et al.*, 2003). The redundancies between nucleo-cytoplasmic transport pathways described here endow the cell with two mechanisms that allow it to carefully maintain the intricate balance of constitutive and regulated transport events.

**1. Fail-safes** – The yeast and mammalian nuclear transport networks that have been identified thus far mediate the import of housekeeping proteins that are required for basic cellular processes (e.g. ribosome biogenesis and chromatin organization). While numerous cargoes for each  $\beta$ -kap remain to be identified, it is doubtful that this trend is coincidental. The

data obtained from experiments overexpressing or reducing the expression of  $\beta$ -kaps suggests that their abundances are limited with respect to number and abundance of cargoes that need to be transported in the cell (Lund *et al.*, 2004; Rodriguez and Henderson, 2000; Yi *et al.*, 2003). Therefore, these transport networks are thought to provide fail-safes that ensure the timely delivery of essential cellular factors to the sites where they function.

**2. Globally regulating the transport cargo classes** - As mentioned above, Kap121p transport is specifically attenuated at certain stages of the cell cycle by the post-translational modification of Nup53p (Makhnevych *et al.*, 2003). Controlling nuclear transport in this manner has the potential to alter the import of numerous Kap121p cargoes, including those that could be required for cell cycle progression. However, the alternative kap-cargo associations described here create a situation where the loss of function of an individual karyopherin (either temporarily through regulation, or constitutively through genetic perturbation) would only affect the small number of cargoes that are specifically transported by that  $\beta$ -kap. A mechanism such as this would provide the cell with a means to shut down the transport of specific classes of molecules by modifying the  $\beta$ -kap (or a nup with which it specifically interacts) without affecting all of the cargoes normally transported by that karyopherin.

The presence of nucleo-cytoplasmic transport networks could explain why so few mutations in nuclear transport machinery have been associated with the transformation of normal cells into cancerous ones and aberrant embryonic development. As these networks provide cellular factors with multiple paths into nucleus, it is logical that mutations altering the active or inactive states of nuclear transport signals would be far more detrimental to the cell than mutations affecting the ability of a single karyopherin to recognize its cargo. Indeed, many of the mutations described above that affect the cellular localization of factors associated with abnormal growth constitutively unmask their nuclear transport signals. This negates that regulatory mechanisms that influence their alternate cellular localizations and, ultimately, control their activity (reviewed in Fabbro and Henderson, 2003; Smith and Koopman, 2004). As the  $\beta$ -kaps in a given transport network recognize a common NLS within their shared cargoes (see Chapter 4 and Mosammaparast *et al.*, 2002b; Mosammaparast *et al.*, 2001; Muhlhauser *et al.*, 2001; Rout *et al.*, 1997), transport networks would not provide the cell with an advantage in these instances.

Accordingly, mutations within nuclear transport receptors that have been identified in various cancer cells inhibit the function of kaps whose cargoes are not transported by other karyopherins (Kau *et al.*, 2004). Therefore, the lack of an alternative transport pathway for the tumour suppressors and oncoproteins that they translocate, which include p53, BRCA1, and RB (Behrens *et al.*, 2003), partially explains how these mutations manifest in uncontrolled cell growth and

cancer development. With these data in mind, it is imperative that researchers not only strive to generate a comprehensive list of cargoes for each member of the  $\beta$ -kap family but also globally characterize the molecular interactions that facilitate the transport of these cargoes. The techniques used in this study successfully identified a number of novel Kap121p cargoes, however these cargoes are likely among the most abundant in the cell. Therefore, we are still faced with the challenge of identifying low abundant cargoes and those that dynamically localize to the nucleus. High-throughput techniques, as well as *S. cerevisiae* deletion, TAP- and GFP-fusion strain libraries, have been developed since this study began and could now be used to identify these elusive cargoes. For example, large-scale localization studies in a series of *kap* mutant strains using automated microscopy coupled with protein chips, microfluidics and surface plasmon resonance (SPR) imaging would not only facilitate the rapid identification of transport cargoes but also measure the affinities of these interactions. Bioinformatics software tools could then be used to identify patterns within these large datasets, which could then be used to group cargoes into primary and secondary transport classes, identify additional and expand existing transport networks, and hypothesize how transport can be regulated on a systems level.

## **6.5 Perspectives on kap-cargo interactions**

Numerous studies have focused on characterizing kap-cargo interactions in an attempt to understand the molecular mechanisms that allow such a large

number of structurally diverse cargoes to be transported by a limited number of  $\beta$ -kaps. Individual  $\beta$ -kaps were originally thought to have high-affinities for only one type of NLS and weak-affinities for the NLSs of most other cargoes. However, studies characterizing the interactions between mammalian Kap  $\beta$ 1 and its cargoes revealed that this transport receptor recognizes and binds unrelated NLSs (either directly or indirectly via  $\alpha$ -kaps) (Chan *et al.*, 1998; Henderson and Percipalle, 1997; Lam *et al.*, 1999; Tiganis *et al.*, 1997). Similarly, the data presented in Chapter 4 demonstrated that Kap121p could also recognize and interact with two types of NLSs (lysine-rich NLSs and rg-NLSs). This raises the question: How can an individual  $\beta$ -kap recognize and interact with unrelated NLS sequences that likely adopt very different structural conformations?

A few studies analyzing the structure of mammalian Kap  $\beta$ 1 bound to different cargoes have begun to answer this question. As mentioned above, Cingolani *et al.* (2002) established that this  $\beta$ -kap contains two cargo-binding pockets and mediates the nuclear import of a fragment of Kap  $\alpha$  and non-classical NLS-containing cargoes simultaneously. However, the data presented in Chapter 4 demonstrated that Kap121p interacts with only one cargo at a time, suggesting that this might not be a common feature among  $\beta$ -kaps (Figure 4.8.1). As a result, we have not yet identified a universal molecular mechanism that can explain how a  $\beta$ -kap binds unrelated NLSs. A recent structural study by Lee *et al.* (2003) solved the crystal structure of Kap  $\beta$ 1 bound to SREBP-2 and

established that this  $\beta$ -kap adopts an SREBP-2 distinct conformation, which allows it to accommodate the bulky structural motifs of this cargo. Thus, it is possible that together these two characteristics, multiple NLS recognition and conformational flexibility, provide  $\beta$ -kaps with the mechanisms that enable them to transport a complex array of cellular factors.

This idea of  $\beta$ -kap conformational flexibility is further supported by the experiments presented in Chapters 3 and 5, as well as similar studies published by other groups (Chaves and Blobel, 2001; Delahodde *et al.*, 2001; Kaffman *et al.*, 1998b; Mosammaparast *et al.*, 2002b; Mosammaparast *et al.*, 2001; Rout *et al.*, 1997; Ueta *et al.*, 2003), characterizing the lysine-rich NLSs of Kap121p nuclear import cargoes. Beyond being basic in nature and, by definition, lysine-rich, these NLSs share little notable amino acid residue sequence similarities (Table 1-2). Moreover, exceptionally large karyopherin-interacting NLS domains have been identified (Chaves and Blobel, 2001), as well as multiple NLSs within a single cargo that function synergistically (Ueta *et al.*, 2003). For example, a 40 amino acid residue fragment of Sof1p (aa 411-450) was found to be import competent, but when this sequence was expanded to include an additional 69 amino acid residues (aa 381-489), its ability to interact with Kap121p improved markedly and this peptide displayed wild-type localization patterns. Together, these findings suggest that the similarities facilitating Kap121p NLS recognition lie, in part, in the higher-order structures adopted by these sequences.

With these findings in mind, I propose that the amino acid residue sequence similarities shared by the NLSs recognized by a given  $\beta$ -kap provide the backbone required for recognition. The secondary and tertiary structures adopted by these NLSs then solidify the interactions and prevent non-specific binding. Furthermore, it is likely that all members of the  $\beta$ -karyopherin family can adopt cargo specific conformations and use extensive interaction surfaces when binding cargoes. Together, these mechanisms would not only allow transport receptors to bind unrelated NLSs but also accommodate the various structural features of each cargo. This flexibility could also provide  $\beta$ -kaps with the characteristics that facilitate interactions with secondary transport substrates, thus permitting the import of alternative classes of cargo.

## **6.6 Perspectives on alternative mechanisms of nucleo-cytoplasmic transport**

The data presented in Chapter 5 characterizing the nuclear transport of Sof1p demonstrated that molecularly distinct mechanisms could mediate the nuclear import of a ribosome assembly factor. A typical kap-cargo interaction can be used, where Kap121p can recognize and bind a lysine-rich NLS present in the C terminus of this protein. Alternatively, Sof1p could be imported by a piggy-back import mechanism, where Nop1p was found to bridge the interaction between Sof1p and a  $\beta$ -kap (either Kap121p or Kap104p). While it is unclear which of these two mechanism functions as the primary mode of transport, this flexibility adds to the ever-growing list of redundancies that are built into the

nuclear transport system. These numerous contingency plans are reminiscent of the redundancies that are employed by viruses to ensure successful infection. For example, the nuclear import of the HIV preintegration complex (PIC) is facilitated by unique but redundant nuclear import signals. Recent studies have identified nuclear import signals in three different viral proteins (integrase, Matrix (MA), and VPR), as well as a “DNA flap” that is produced during reverse transcription (Sherman *et al.*, 2002). Based on the data currently available, researchers believe that HIV integrase plays the leading role in the nuclear import of HIV PICs, and that the signals present in MA, Vpr and the DNA flap increase infection efficiency (Sherman *et al.*, 2002).

Together, these data highlight the numerous ways a given cargo can gain access to the nucleus. But the techniques used to acquire these data are tied to the reductionist approach of examining individual components of an extremely complex system, therefore concluding how these redundant mechanisms function in the context of the cell is difficult. This complexity was underscored by the studies characterizing Sof1p. Truncation analysis of Sof1p suggested that its import could be mediated by a direct interaction between Kap121p and a C-terminal lysine-rich NLS. However, when its interacting partner Nop1p was added into the equation, the *in vitro*, *ex vivo* and *in vivo* studies overwhelmingly suggest that the piggy-back import complex (Kap121p-Nop1p-Sof1p) may prevail *in vivo*, with the Kap121p-Sof1p interaction functioning as a secondary transport route (see Section 5.7). Transport mechanisms such as these are exploited by

many types of viruses (e.g. HIV-1, influenza virus and SV40 (Sherman *et al.*, 2002) when infecting host cells, and by the cell when transporting RNPs. Transporting cargoes in this manner might reduce the number of transport cycles, and the amount of energy and resources required for a given process. But, more importantly, they would also ensure that essential, functionally dependent factors are properly localized, in appropriate molar ratios, to the subcellular compartments where they function. Thus, increasing the likelihood that the process they govern continues in a timely and flawless manner. It is possible that this piggy-back transport mechanism may also be used to mediate the concurrent transport of other cellular factors that function together in the nucleus, including ribosomal proteins, components of general transcription machinery complexes, transcriptional *trans*-activation and repression complexes. Moreover, I envision that like nuclear transport networks, piggy-back mechanisms may also provide the cell with an additional level of flexibility that could allow it to adapt to the loss of an individual nuclear transport pathway.

As discussed above and in Section 5.7, the presence of a NLS does not necessarily mean that it will act as the primary transport signal *in vivo*. The complex environment within the cell suggests that competition among transport cargoes, varying kap-NLS affinities and the presence of binding partners could all alter the activity of a particular NLS. To wholly appreciate how an individual nuclear transport pathway functions, researchers are now faced with the challenge of determining how this (and other) alternative transport mechanisms

are regulated with respect to classic mechanisms of transport and the cellular environment. To loosely paraphrase the Nobel Laureate Dr. Sydney Brenner – “The sum of the parts does not necessarily equal the whole...” – Nobel Lecture 2002 (<http://nobelprize.org/medicine/laureates/2002/brenner-lecture.html>).

## 6.7 Perspectives on cargo delivery

The small GTPase Ran is thought to provide nuclear transport complexes with directional cues. As mentioned above, nuclear import cycles are generally terminated upon translocation through the NPC, where RanGTP induces the dissociation of nuclear import complexes. However, studies have demonstrated that nucleic acids are occasionally required in addition to RanGTP to induce the dissociation of kap-cargo complexes containing nucleic binding proteins (Lee and Aitchison, 1999; Pemberton *et al.*, 1999; Senger *et al.*, 1998). Although the molecular mechanism that produces this cooperative effect is not known, researchers have hypothesized that Ran-insensitive  $\beta$ -kaps might have a relatively low affinity for RanGTP and that RNA binding could change the affinity of the  $\beta$ -kap for either the cargo or RanGTP (reviewed in Mosammaparast and Pemberton, 2004). In addition to RNA, transport cofactors have been shown to modulate the affinities of  $\beta$ -kaps for RanGTP. For example, the binding of the import cofactor Nap1p to Kap114p-cargo complexes containing histones H2A or H2B renders these complexes insensitive to RanGTP (Mosammaparast *et al.*, 2002a). As free histones are toxic to the cell, this is thought to inhibit their deposition and release within the nucleus until the appropriate target site is

encountered (Mosammaparast *et al.*, 2005; Mosammaparast *et al.*, 2002a). Based on these findings, it is likely that individual import events are terminated in a cargo type dependent manner.

The data presented in Chapters 3 and 4 support this hypothesis. Here we established that kap-cargo complex RanGTP sensitivity could be modified in an NLS dependent manner. Kap121p-lysine-rich NLS import complexes were found to be sensitive to RanGTP, while Kap121p-rg-NLS import complexes remained stable under the same condition. In this instance, it is possible that the conformation adopted by either the  $\beta$ -kap or the cargo upon import complex formation (in this case, rg-NLS cargoes and Kap121p) specifically obstructs RanGTP binding. This could promote the intranuclear movement of these kap-cargo complexes to the cargo's ultimate destination (e.g. nucleolus). Once delivered, accessory factors (a protein or RNA molecule) could interact with the cargo, stimulating a conformational change (either in the cargo or the  $\beta$ -kap) that exposes the  $\beta$ -kap's RanGTP binding pocket and induces cargo release.

Together, these data strongly indicate that  $\beta$ -kaps can function as transporters that not only deliver cargo to the proper cellular compartment, but also chaperone them to their distinct functional domains of the nucleus. Computational modeling of the Ran system indicates that the dissociation constant for RanGTP binding to several  $\beta$ -kaps is orders of magnitude higher than the levels of free RanGTP in the cell (Smith *et al.*, 2002). This suggests that, in addition to nucleic acids and accessory factors, the local RanGTP

concentration could be a critical factor that regulates kap-cargo dissociation by determining. In light of all of these data, insight into how nucleo-cytoplasmic transport is regulated demands a complete understanding of precisely how and where transport cycles are terminated, the influence cargo types have on this process and whether accessory factors are commonly used to alter kap-cargo complex stability.

## References

- Aitchison, J.D., G. Blobel, and M.P. Rout. 1996. Kap104p: a karyopherin involved in the nuclear transport of messenger RNA binding proteins. *Science*. 274:624-7.
- Aitchison, J.D., and M.P. Rout. 2000. The road to ribosomes. Filling potholes in the export pathway. *J Cell Biol*. 151:F23-6.
- Aitchison, J.D., M.P. Rout, M. Marelli, G. Blobel, and R.W. Wozniak. 1995. Two novel related yeast nucleoporins Nup170p and Nup157p: complementation with the vertebrate homologue Nup155p and functional interactions with the yeast nuclear pore-membrane protein Pom152p. *J Cell Biol*. 131:1133-48.
- Alberts, B., A. Johnson, J. Lewis, M. Raff, K. Roberts, and W. P. 2002. *Molecular Biology of the Cell*. Garland Science, New York, NY.
- Allen, T.D., J.M. Cronshaw, S. Bagley, E. Kiseleva, and M.W. Goldberg. 2000. The nuclear pore complex: mediator of translocation between nucleus and cytoplasm. *J Cell Sci*. 113:1651-9.
- Andrade, M.A., C. Petosa, S.I. O'Donoghue, C.W. Muller, and P. Bork. 2001. Comparison of ARM and HEAT protein repeats. *J Mol Biol*. 309:1-18.
- Aris, J.P., and G. Blobel. 1991. cDNA cloning and sequencing of human fibrillarin, a conserved nucleolar protein recognized by autoimmune antisera. *Proc Natl Acad Sci U S A*. 88:931-5.
- Ausubel, F.M., R. Brent, R.E. Kingston, D.D. Moore, J.G. Seidman, J.A. Smith, and K. Struhl. 1994. *Current Protocols in Molecular Biology*. Vol. 2. John Wiley & Sons, Ltd., Hoboken, NJ. 13.0.1-13.17.7.
- Bachelier, J.P., J. Cavaille, and A. Huttenhofer. 2002. The expanding snoRNA world. *Biochimie*. 84:775-90.
- Bardwell, L. 2004. A walk-through of the yeast mating pheromone response pathway. *Peptides*. 25:1465-76.
- Bastos, R., A. Lin, M. Enarson, and B. Burke. 1996. Targeting and function in mRNA export of nuclear pore complex protein Nup153. *J Cell Biol*. 134:1141-56.
- Bayliss, R., K. Ribbeck, D. Akin, H.M. Kent, C.M. Feldherr, D. Gorlich, and M. Stewart. 1999. Interaction between NTF2 and xFxFG-containing nucleoporins is required to mediate nuclear import of RanGDP. *J Mol Biol*. 293:579-93.
- Bednenko, J., G. Cingolani, and L. Gerace. 2003. Nucleocytoplasmic transport: navigating the channel. *Traffic*. 4:127-35.
- Behrens, P., U. Brinkmann, F. Fogt, N. Wernert, and A. Wellmann. 2001. Implication of the proliferation and apoptosis associated *CSE1L/CAS* gene for breast cancer development. *Anticancer Res*. 21:2413-7.
- Behrens, P., U. Brinkmann, and A. Wellmann. 2003. *CSE1L/CAS*: its role in proliferation and apoptosis. *Apoptosis*. 8:39-44.

- Ben-Efraim, I., and L. Gerace. 2001. Gradient of increasing affinity of importin beta for nucleoporins along the pathway of nuclear import. *J Cell Biol.* 152:411-7.
- Berthelsen, J., C. Kilstrup-Nielsen, F. Blasi, F. Mavilio, and V. Zappavigna. 1999. The subcellular localization of PBX1 and EXD proteins depends on nuclear import and export signals and is modulated by association with PREP1 and HTH. *Genes Dev.* 13:946-53.
- Bickel, T., and R. Bruinsma. 2002. The nuclear pore complex mystery and anomalous diffusion in reversible gels. *Biophys J.* 83:3079-87.
- Boeke, J.D., F. LaCrute, and G.R. Fink. 1984. A positive selection for mutants lacking orotidine-5'-phosphate decarboxylase activity in yeast: 5-fluoroorotic acid resistance. *Mol Gen Genet.* 197:345-6.
- Bogerd, H.P., R.E. Benson, R. Truant, A. Herold, M. Phingbodhipakkiya, and B.R. Cullen. 1999. Definition of a consensus transportin-specific nucleocytoplasmic transport signal. *J Biol Chem.* 274:9771-7.
- Bogerd, H.P., R.A. Fridell, R.E. Benson, J. Hua, and B.R. Cullen. 1996. Protein sequence requirements for function of the human T-cell leukemia virus type 1 Rex nuclear export signal delineated by a novel in vivo randomization-selection assay. *Mol Cell Biol.* 16:4207-14.
- Boustany, L.M., and M.S. Cyert. 2002. Calcineurin-dependent regulation of Crz1p nuclear export requires Msn5p and a conserved calcineurin docking site. *Genes Dev.* 16:608-19.
- Bradford, M.M. 1976. A rapid and sensitive method for the quantitation of microgram quantities of protein utilizing the principle of protein-dye binding. *Anal Biochem.* 72:248-54.
- Brinkmann, U. 1998. CAS, the human homologue of the yeast chromosome-segregation gene *CSE1*, in proliferation, apoptosis, and cancer. *Am J Hum Genet.* 62:509-13.
- Brinkmann, U., E. Brinkmann, M. Gallo, U. Scherf, and I. Pastan. 1996. Role of CAS, a human homologue to the yeast chromosome segregation gene *CSE1*, in toxin and tumor necrosis factor mediated apoptosis. *Biochemistry.* 35:6891-9.
- Burnette, W.N. 1981. "Western blotting": electrophoretic transfer of proteins from sodium dodecyl sulfate-polyacrylamide gels to unmodified nitrocellulose and radiographic detection with antibody and radioiodinated protein A. *Anal Biochem.* 112:195-203.
- Buss, F., H. Kent, M. Stewart, S.M. Bailer, and J.A. Hanover. 1994. Role of different domains in the self-association of rat nucleoporin p62. *J Cell Sci.* 107 ( Pt 2):631-8.
- Chaillan-Huntington, C., C.V. Braslavsky, J. Kuhlmann, and M. Stewart. 2000. Dissecting the interactions between NTF2, RanGDP, and the nucleoporin XFXFG repeats. *J Biol Chem.* 275:5874-9.
- Chan, C.K., S. Hubner, W. Hu, and D.A. Jans. 1998. Mutual exclusivity of DNA binding and nuclear localization signal recognition by the yeast

- transcription factor GAL4: implications for nonviral DNA delivery. *Gene Ther.* 5:1204-12.
- Chaves, S.R., and G. Blobel. 2001. Nuclear import of Spo12p, a protein essential for meiosis. *J Biol Chem.* 276:17712-7.
- Chen, L.F., and W.C. Greene. 2004. Shaping the nuclear action of NF-kappaB. *Nat Rev Mol Cell Biol.* 5:392-401.
- Chen, Y., C.F. Chen, D.J. Riley, D.C. Allred, P.L. Chen, D. Von Hoff, C.K. Osborne, and W.H. Lee. 1995. Aberrant subcellular localization of BRCA1 in breast cancer. *Science.* 270:789-91.
- Chook, Y.M., and G. Blobel. 2001. Karyopherins and nuclear import. *Curr Opin Struct Biol.* 11:703-15.
- Christianson, T.W., R.S. Sikorski, M. Dante, J.H. Shero, and P. Hieter. 1992. Multifunctional yeast high-copy-number shuttle vectors. *Gene.* 110:119-22.
- Cingolani, G., J. Bednenko, M.T. Gillespie, and L. Gerace. 2002. Molecular basis for the recognition of a nonclassical nuclear localization signal by importin beta. *Mol Cell.* 10:1345-53.
- Cingolani, G., C. Petosa, K. Weis, and C.W. Muller. 1999. Structure of importin-beta bound to the IBB domain of importin-alpha. *Nature.* 399:221-9.
- Clarke, P.R., and C. Zhang. 2001. Ran GTPase: a master regulator of nuclear structure and function during the eukaryotic cell division cycle? *Trends Cell Biol.* 11:366-71.
- Clontech Laboratories, I. 2001. Yeast Protocols Handbook. <http://www.bdbiosciences.com/clontech/techinfo/manuals/index.shtml>.
- Cole, C.N., and C.M. Hammell. 1998. Nucleocytoplasmic transport: driving and directing transport. *Curr Biol.* 8:R368-72.
- Craig, E., Z.K. Zhang, K.P. Davies, and G.V. Kalpana. 2002. A masked NES in INI1/hSNF5 mediates hCRM1-dependent nuclear export: implications for tumorigenesis. *Embo J.* 21:31-42.
- Cronshaw, J.M., A.N. Krutchinsky, W. Zhang, B.T. Chait, and M.J. Matunis. 2002. Proteomic analysis of the mammalian nuclear pore complex. *J Cell Biol.* 158:915-27.
- Cross, F.R. 1997. 'Marker swap' plasmids: convenient tools for budding yeast molecular genetics. *Yeast.* 13:647-53.
- Dargemont, C., M.S. Schmidt-Zachmann, and L.C. Kuhn. 1995. Direct interaction of nucleoporin p62 with mRNA during its export from the nucleus. *J Cell Sci.* 108 ( Pt 1):257-63.
- Daugeron, M.C., D. Kressler, and P. Linder. 2001. Dbp9p, a putative ATP-dependent RNA helicase involved in 60S-ribosomal-subunit biogenesis, functionally interacts with Dbp6p. *Rna.* 7:1317-34.
- Delahodde, A., R. Pandjaitan, M. Corral-Debrinski, and C. Jacq. 2001. Pse1/Kap121-dependent nuclear localization of the major yeast multidrug resistance (MDR) transcription factor Pdr1. *Mol Microbiol.* 39:304-12.

- Denning, D., B. Mykytka, N.P. Allen, L. Huang, B. Al, and M. Rexach. 2001. The nucleoporin Nup60p functions as a Gsp1p-GTP-sensitive tether for Nup2p at the nuclear pore complex. *J Cell Biol.* 154:937-50.
- Denning, D.P., S.S. Patel, V. Uversky, A.L. Fink, and M. Rexach. 2003. Disorder in the nuclear pore complex: the FG repeat regions of nucleoporins are natively unfolded. *Proc Natl Acad Sci U S A.* 100:2450-5.
- DeVit, M.J., and M. Johnston. 1999. The nuclear exportin Msn5 is required for nuclear export of the Mig1 glucose repressor of *Saccharomyces cerevisiae*. *Curr Biol.* 9:1231-41.
- Dickinson, J.R. 1996. 'Fusel' alcohols induce hyphal-like extensions and pseudohyphal formation in yeasts. *Microbiology.* 142 ( Pt 6):1391-7.
- Dietzel, C., and J. Kurjan. 1987. The yeast *SCG1* gene: a G alpha-like protein implicated in the  $\alpha$ - and  $\alpha$ -factor response pathway. *Cell.* 50:1001-10.
- Dilworth, D.J., A. Suprpto, J.C. Padovan, B.T. Chait, R.W. Wozniak, M.P. Rout, and J.D. Aitchison. 2001. Nup2p dynamically associates with the distal regions of the yeast nuclear pore complex. *J Cell Biol.* 153:1465-78.
- Dingwall, C., and R.A. Laskey. 1991. Nuclear targeting sequences--a consensus? *Trends Biochem Sci.* 16:478-81.
- Dingwall, C., S.V. Sharnick, and R.A. Laskey. 1982. A polypeptide domain that specifies migration of nucleoplasmin into the nucleus. *Cell.* 30:449-58.
- Dolan, J.W., and S. Fields. 1990. Overproduction of the yeast STE12 protein leads to constitutive transcriptional induction. *Genes Dev.* 4:492-502.
- Elion, E.A. 1998. Routing MAP kinase cascades. *Science.* 281:1625-6.
- Elion, E.A. 2000. Pheromone response, mating and cell biology. *Curr Opin Microbiol.* 3:573-81.
- Englmeier, L., M. Fornerod, F.R. Bischoff, C. Petosa, I.W. Mattaj, and U. Kutay. 2001. RanBP3 influences interactions between CRM1 and its nuclear protein export substrates. *EMBO Rep.* 2:926-32.
- Fabbro, M., and B.R. Henderson. 2003. Regulation of tumor suppressors by nuclear-cytoplasmic shuttling. *Exp Cell Res.* 282:59-69.
- Fabre, E., and E. Hurt. 1997. Yeast genetics to dissect the nuclear pore complex and nucleocytoplasmic trafficking. *Annu Rev Genet.* 31:277-313.
- Fahrenkrog, B., and U. Aebi. 2003. The nuclear pore complex: nucleocytoplasmic transport and beyond. *Nat Rev Mol Cell Biol.* 4:757-66.
- Fatica, A., and D. Tollervey. 2002. Making ribosomes. *Curr Opin Cell Biol.* 14:313-8.
- Fischer, U., J. Huber, W.C. Boelens, I.W. Mattaj, and R. Luhrmann. 1995. The HIV-1 Rev activation domain is a nuclear export signal that accesses an export pathway used by specific cellular RNAs. *Cell.* 82:475-83.
- Floer, M., and G. Blobel. 1999. Putative reaction intermediates in Crm1-mediated nuclear protein export. *J Biol Chem.* 274:16279-86.
- Fried, H., and U. Kutay. 2003. Nucleocytoplasmic transport: taking an inventory. *Cell Mol Life Sci.* 60:1659-88.

- Fukuhara, N., E. Fernandez, J. Ebert, E. Conti, and D. Svergun. 2004. Conformational variability of nucleo-cytoplasmic transport factors. *J Biol Chem.* 279:2176-81.
- Galardi, S., A. Fatica, A. Bachi, A. Scaloni, C. Presutti, and I. Bozzoni. 2002. Purified box C/D snoRNPs are able to reproduce site-specific 2'-O-methylation of target RNA in vitro. *Mol Cell Biol.* 22:6663-8.
- Gasca, S., J. Canizares, P. De Santa Barbara, C. Mejean, F. Poulat, P. Berta, and B. Boizet-Bonhoure. 2002. A nuclear export signal within the high mobility group domain regulates the nucleocytoplasmic translocation of SOX9 during sexual determination. *Proc Natl Acad Sci U S A.* 99:11199-204.
- Gerace, L. 1995. Nuclear export signals and the fast track to the cytoplasm. *Cell.* 82:341-4.
- Geymonat, M., A. Spanos, G.P. Wells, S.J. Smerdon, and S.G. Sedgwick. 2004. Clb6/Cdc28 and Cdc14 regulate phosphorylation status and cellular localization of Swi6. *Mol Cell Biol.* 24:2277-85.
- Goldfarb, D.S., J. Gariepy, G. Schoolnik, and R.D. Kornberg. 1986. Synthetic peptides as nuclear localization signals. *Nature.* 322:641-4.
- Gorner, W., E. Durchschlag, J. Wolf, E.L. Brown, G. Ammerer, H. Ruis, and C. Schuller. 2002. Acute glucose starvation activates the nuclear localization signal of a stress-specific yeast transcription factor. *Embo J.* 21:135-44.
- Guan, T., R.H. Kehlenbach, E.C. Schirmer, A. Kehlenbach, F. Fan, B.E. Clurman, N. Arnheim, and L. Gerace. 2000. Nup50, a nucleoplasmically oriented nucleoporin with a role in nuclear protein export. *Mol Cell Biol.* 20:5619-30.
- Gustin, M.C., J. Albertyn, M. Alexander, and K. Davenport. 1998. MAP kinase pathways in the yeast *Saccharomyces cerevisiae*. *Microbiol Mol Biol Rev.* 62:1264-300.
- Hagen, D.C., G. McCaffrey, and G.F. Sprague, Jr. 1991. Pheromone response elements are necessary and sufficient for basal and pheromone-induced transcription of the *FUS1* gene of *Saccharomyces cerevisiae*. *Mol Cell Biol.* 11:2952-61.
- Henderson, B.R., and P. Percipalle. 1997. Interactions between HIV Rev and nuclear import and export factors: the Rev nuclear localisation signal mediates specific binding to human importin-beta. *J Mol Biol.* 274:693-707.
- Hoh, J.H. 1998. Functional protein domains from the thermally driven motion of polypeptide chains: a proposal. *Proteins.* 32:223-8.
- Hung, W., K.A. Olson, A. Breitreutz, and I. Sadowski. 1997. Characterization of the basal and pheromone-stimulated phosphorylation states of Ste12p. *Eur J Biochem.* 245:241-51.
- Hurt, E., S. Hannus, B. Schmelzl, D. Lau, D. Tollervey, and G. Simos. 1999. A novel in vivo assay reveals inhibition of ribosomal nuclear export in ran-cycle and nucleoporin mutants. *J Cell Biol.* 144:389-401.

- Hurwitz, M.E., C. Strambio-de-Castillia, and G. Blobel. 1998. Two yeast nuclear pore complex proteins involved in mRNA export form a cytoplasmically oriented subcomplex. *Proc Natl Acad Sci U S A.* 95:11241-5.
- Iovine, M.K., J.L. Watkins, and S.R. Wentz. 1995. The GLFG repetitive region of the nucleoporin Nup116p interacts with Kap95p, an essential yeast nuclear import factor. *J Cell Biol.* 131:1699-713.
- Iovine, M.K., and S.R. Wentz. 1997. A nuclear export signal in Kap95p is required for both recycling the import factor and interaction with the nucleoporin GLFG repeat regions of Nup116p and Nup100p. *J Cell Biol.* 137:797-811.
- Isoyama, T., A. Murayama, A. Nomoto, and S. Kuge. 2001. Nuclear import of the yeast AP-1-like transcription factor Yap1p is mediated by transport receptor Pse1p, and this import step is not affected by oxidative stress. *J Biol Chem.* 276:21863-9.
- Jakel, S., and D. Gorlich. 1998. Importin beta, transportin, RanBP5 and RanBP7 mediate nuclear import of ribosomal proteins in mammalian cells. *Embo J.* 17:4491-502.
- Jansen, R., D. Tollervey, and E.C. Hurt. 1993. A U3 snoRNP protein with homology to splicing factor PRP4 and G beta domains is required for ribosomal RNA processing. *Embo J.* 12:2549-58.
- Jansen, R.P., E.C. Hurt, H. Kern, H. Lehtonen, M. Carmo-Fonseca, B. Lapeyre, and D. Tollervey. 1991. Evolutionary conservation of the human nucleolar protein fibrillarin and its functional expression in yeast. *J Cell Biol.* 113:715-29.
- Jaquenoud, M., F. van Drogen, and M. Peter. 2002. Cell cycle-dependent nuclear export of Cdh1p may contribute to the inactivation of APC/C(Cdh1). *Embo J.* 21:6515-26.
- Johnson, A.D. 1995. Molecular mechanisms of cell-type determination in budding yeast. [Review]. *Current Opinion in Genetics & Development.* 5:552-8.
- Kaffman, A., N.M. Rank, E.M. O'Neill, L.S. Huang, and E.K. O'Shea. 1998a. The receptor Msn5 exports the phosphorylated transcription factor Pho4 out of the nucleus. *Nature.* 396:482-6.
- Kaffman, A., N.M. Rank, and E.K. O'Shea. 1998b. Phosphorylation regulates association of the transcription factor Pho4 with its import receptor Pse1/Kap121. *Genes Dev.* 12:2673-83.
- Kalab, P., K. Weis, and R. Heald. 2002. Visualization of a Ran-GTP gradient in interphase and mitotic *Xenopus* egg extracts. *Science.* 295:2452-6.
- Kalderon, D., W.D. Richardson, A.F. Markham, and A.E. Smith. 1984a. Sequence requirements for nuclear location of simian virus 40 large-T antigen. *Nature.* 311:33-8.
- Kalderon, D., B.L. Roberts, W.D. Richardson, and A.E. Smith. 1984b. A short amino acid sequence able to specify nuclear location. *Cell.* 39:499-509.

- Kaplun, L., Y. Ivantsiv, A. Bakhrat, and D. Raveh. 2003. DNA damage response-mediated degradation of Ho endonuclease via the ubiquitin system involves its nuclear export. *J Biol Chem.* 278:48727-34.
- Kau, T.R., J.C. Way, and P.A. Silver. 2004. Nuclear transport and cancer: from mechanism to intervention. *Nat Rev Cancer.* 4:106-17.
- Kehlenbach, R.H., A. Dickmanns, A. Kehlenbach, T. Guan, and L. Gerace. 1999. A role for RanBP1 in the release of CRM1 from the nuclear pore complex in a terminal step of nuclear export. *J Cell Biol.* 145:645-57.
- Kikuma, T., M. Ohtsu, T. Utsugi, S. Koga, K. Okuhara, T. Eki, F. Fujimori, and Y. Murakami. 2004. Dbp9p, a member of the DEAD box protein family, exhibits DNA helicase activity. *J Biol Chem.* 279:20692-8.
- Kraemer, D., R.W. Wozniak, G. Blobel, and A. Radu. 1994. The human CAN protein, a putative oncogene product associated with myeloid leukemogenesis, is a nuclear pore complex protein that faces the cytoplasm. *Proc Natl Acad Sci U S A.* 91:1519-23.
- Kressler, D., P. Linder, and J. de La Cruz. 1999. Protein trans-acting factors involved in ribosome biogenesis in *Saccharomyces cerevisiae*. *Mol Cell Biol.* 19:7897-912.
- Kuersten, S., M. Ohno, and I.W. Mattaj. 2001. Nucleocytoplasmic transport: Ran, beta and beyond. *Trends Cell Biol.* 11:497-503.
- Kunzler, M., J. Trueheart, C. Sette, E. Hurt, and J. Thorner. 2001. Mutations in the *YRB1* gene encoding yeast ran-binding-protein-1 that impair nucleocytoplasmic transport and suppress yeast mating defects. *Genetics.* 157:1089-105.
- Lai, M.C., R.I. Lin, and W.Y. Tarn. 2001. Transportin-SR2 mediates nuclear import of phosphorylated SR proteins. *Proc Natl Acad Sci U S A.* 98:10154-9.
- Lam, M.H., L.J. Briggs, W. Hu, T.J. Martin, M.T. Gillespie, and D.A. Jans. 1999. Importin beta recognizes parathyroid hormone-related protein with high affinity and mediates its nuclear import in the absence of importin alpha. *J Biol Chem.* 274:7391-8.
- Lee, D.C., and J.D. Aitchison. 1999. Kap104p-mediated nuclear import. Nuclear localization signals in mRNA-binding proteins and the role of Ran and Rna. *J Biol Chem.* 274:29031-7.
- Lee, S.J., T. Sekimoto, E. Yamashita, E. Nagoshi, A. Nakagawa, N. Imamoto, M. Yoshimura, H. Sakai, K.T. Chong, T. Tsukihara, and Y. Yoneda. 2003. The structure of importin-beta bound to SREBP-2: nuclear import of a transcription factor. *Science.* 302:1571-5.
- Leslie, D.M., B. Grill, M.P. Rout, R.W. Wozniak, and J.D. Aitchison. 2002. Kap121p-mediated nuclear import is required for mating and cellular differentiation in yeast. *Mol Cell Biol.* 22:2544-55.
- Leslie, D.M., W. Zhang, B.L. Timney, B.T. Chait, M.P. Rout, R.W. Wozniak, and J.D. Aitchison. 2004. Characterization of karyopherin cargoes reveals

- unique mechanisms of Kap121p-mediated nuclear import. *Mol Cell Biol.* 24:8487-503.
- Li, B., W. Zhang, G. Chan, A. Jancso-Radek, S. Liu, and M.A. Weiss. 2001. Human sex reversal due to impaired nuclear localization of SRY. A clinical correlation. *J Biol Chem.* 276:46480-4.
- Li, M., C.L. Brooks, F. Wu-Baer, D. Chen, R. Baer, and W. Gu. 2003. Mono- versus polyubiquitination: differential control of p53 fate by Mdm2. *Science.* 302:1972-5.
- Lindsay, M.E., J.M. Holaska, K. Welch, B.M. Paschal, and I.G. Macara. 2001. Ran-binding protein 3 is a cofactor for Crm1-mediated nuclear protein export. *J Cell Biol.* 153:1391-402.
- Lindsay, M.E., K. Plafker, A.E. Smith, B.E. Clurman, and I.G. Macara. 2002. Npap60/Nup50 is a tri-stable switch that stimulates importin-alpha:beta-mediated nuclear protein import. *Cell.* 110:349-60.
- Lischwe, M.A., R.L. Ochs, R. Reddy, R.G. Cook, L.C. Yeoman, E.M. Tan, M. Reichlin, and H. Busch. 1985. Purification and partial characterization of a nucleolar scleroderma antigen (Mr = 34,000; pI, 8.5) rich in NG,NG-dimethylarginine. *J Biol Chem.* 260:14304-10.
- Liu, H., C.A. Styles, and G.R. Fink. 1993. Elements of the yeast pheromone response pathway required for filamentous growth of diploids. *Science.* 262:1741-4.
- Lodish, H., A. Berk, S.L. Zipursky, P. Matsudaira, D. Baltimore, and J. Darnell. 1999. *Molecular Cell Biology.* W. H. Freeman and Company.
- Lorenz, M.C., N.S. Cutler, and J. Heitman. 2000. Characterization of alcohol-induced filamentous growth in *Saccharomyces cerevisiae*. *Mol Biol Cell.* 11:183-99.
- Lorenz, M.C., and J. Heitman. 1997. Yeast pseudohyphal growth is regulated by GPA2, a G protein alpha homolog. *Embo J.* 16:7008-18.
- Lorsch, J.R., and D. Herschlag. 1998a. The DEAD box protein eIF4A. 1. A minimal kinetic and thermodynamic framework reveals coupled binding of RNA and nucleotide. *Biochemistry.* 37:2180-93.
- Lorsch, J.R., and D. Herschlag. 1998b. The DEAD box protein eIF4A. 2. A cycle of nucleotide and RNA-dependent conformational changes. *Biochemistry.* 37:2194-206.
- Lund, E., S. Guttinger, A. Calado, J.E. Dahlberg, and U. Kutay. 2004. Nuclear export of microRNA precursors. *Science.* 303:95-8.
- Lusk, C.P., T. Makhnevych, M. Marelli, J.D. Aitchison, and R.W. Wozniak. 2002. Karyopherins in nuclear pore biogenesis: a role for Kap121p in the assembly of Nup53p into nuclear pore complexes. *J Cell Biol.* 159:267-78.
- Lydall, D., Y. Nikolsky, D.K. Bishop, and T. Weinert. 1996. A meiotic recombination checkpoint controlled by mitotic checkpoint genes. *Nature.* 383:840-3.
- Macara, I.G. 2001. Transport into and out of the Nucleus. *Microbiol Mol Biol Rev.* 65:570-94.

- Madhani, H.D., and G.R. Fink. 1997. Combinatorial control required for the specificity of yeast MAPK signaling. *Science*. 275:1314-7.
- Makhnevych, T., C.P. Lusk, A.M. Anderson, J.D. Aitchison, and R.W. Wozniak. 2003. Cell cycle regulated transport controlled by alterations in the nuclear pore complex. *Cell*. 115:813-23.
- Maniatis, T., E.F. Fritsch, and J. Sambrook. 1982. Molecular cloning: A laboratory manual. Cold Spring Harbor Laboratory, Cold Spring Harbor.
- Marelli, M., J.D. Aitchison, and R.W. Wozniak. 1998. Specific binding of the karyopherin Kap121p to a subunit of the nuclear pore complex containing Nup53p, Nup59p, and Nup170p. *J Cell Biol*. 143:1813-30.
- Mattaj, I.W., and L. Englmeier. 1998. Nucleocytoplasmic transport: the soluble phase. *Annu Rev Biochem*. 67:265-306.
- Matunis, M.J., E. Coutavas, and G. Blobel. 1996. A novel ubiquitin-like modification modulates the partitioning of the Ran-GTPase-activating protein RanGAP1 between the cytosol and the nuclear pore complex. *J Cell Biol*. 135:1457-70.
- Matunis, M.J., J. Wu, and G. Blobel. 1998. SUMO-1 modification and its role in targeting the Ran GTPase-activating protein, RanGAP1, to the nuclear pore complex. *J Cell Biol*. 140:499-509.
- McKinsey, T.A., C.L. Zhang, J. Lu, and E.N. Olson. 2000. Signal-dependent nuclear export of a histone deacetylase regulates muscle differentiation. *Nature*. 408:106-11.
- Mead, J., A.R. Bruning, M.K. Gill, A.M. Steiner, T.B. Acton, and A.K. Vershon. 2002. Interactions of the Mcm1 MADS box protein with cofactors that regulate mating in yeast. *Mol Cell Biol*. 22:4607-21.
- Moore, M.S. 1998. Ran and nuclear transport. *J Biol Chem*. 273:22857-60.
- Mosammaparast, N., B.C. Del Rosario, and L.F. Pemberton. 2005. Modulation of histone deposition by the karyopherin Kap114. *Mol Cell Biol*. 25:1764-78.
- Mosammaparast, N., C.S. Ewart, and L.F. Pemberton. 2002a. A role for nucleosome assembly protein 1 in the nuclear transport of histones H2A and H2B. *Embo J*. 21:6527-38.
- Mosammaparast, N., Y. Guo, J. Shabanowitz, D.F. Hunt, and L.F. Pemberton. 2002b. Pathways mediating the nuclear import of histones H3 and H4 in yeast. *J Biol Chem*. 277:862-8.
- Mosammaparast, N., K.R. Jackson, Y. Guo, C.J. Brame, J. Shabanowitz, D.F. Hunt, and L.F. Pemberton. 2001. Nuclear import of histone H2A and H2B is mediated by a network of karyopherins. *J Cell Biol*. 153:251-62.
- Mosammaparast, N., and L.F. Pemberton. 2004. Karyopherins: from nuclear-transport mediators to nuclear-function regulators. *Trends Cell Biol*. 14:547-56.
- Mosch, H.U., and G.R. Fink. 1997. Dissection of filamentous growth by transposon mutagenesis in *Saccharomyces cerevisiae*. *Genetics*. 145:671-84.

- Moy, T.I., and P.A. Silver. 1999. Nuclear export of the small ribosomal subunit requires the ran-GTPase cycle and certain nucleoporins. *Genes Dev.* 13:2118-33.
- Muhlhauser, P., E.C. Muller, A. Otto, and U. Kutay. 2001. Multiple pathways contribute to nuclear import of core histones. *EMBO Rep.* 2:690-6.
- Muhlrad, D., R. Hunter, and R. Parker. 1992. A rapid method for localized mutagenesis of yeast genes. *Yeast.* 8:79-82.
- Newmeyer, D.D., D.R. Finlay, and D.J. Forbes. 1986. In vitro transport of a fluorescent nuclear protein and exclusion of non-nuclear proteins. *J Cell Biol.* 103:2091-102.
- Ogryzko, V.V., E. Brinkmann, B.H. Howard, I. Pastan, and U. Brinkmann. 1997. Antisense inhibition of *CAS*, the human homologue of the yeast chromosome segregation gene *CSE1*, interferes with mitosis in HeLa cells. *Biochemistry.* 36:9493-500.
- Olson, K.A., C. Nelson, G. Tai, W. Hung, C. Yong, C. Astell, and I. Sadowski. 2000. Two regulators of Ste12p inhibit pheromone-responsive transcription by separate mechanisms. *Mol Cell Biol.* 20:4199-209.
- Pan, X., T. Harashima, and J. Heitman. 2000. Signal transduction cascades regulating pseudohyphal differentiation of *Saccharomyces cerevisiae*. *Curr Opin Microbiol.* 3:567-72.
- Pemberton, L.F., J.S. Rosenblum, and G. Blobel. 1999. Nuclear import of the TATA-binding protein: mediation by the karyopherin Kap114p and a possible mechanism for intranuclear targeting. *J Cell Biol.* 145:1407-17.
- Pi, H., C.T. Chien, and S. Fields. 1997. Transcriptional activation upon pheromone stimulation mediated by a small domain of *Saccharomyces cerevisiae* Ste12p. *Mol Cell Biol.* 17:6410-8.
- Pichler, A., A. Gast, J.S. Seeler, A. Dejean, and F. Melchior. 2002. The nucleoporin RanBP2 has SUMO1 E3 ligase activity. *Cell.* 108:109-20.
- Pih, K.T., M.J. Yi, Y.S. Liang, B.J. Shin, M.J. Cho, I. Hwang, and D. Son. 2000. Molecular cloning and targeting of a fibrillarlin homolog from *Arabidopsis*. *Plant Physiol.* 123:51-8.
- Preiss, S., A. Argentaro, A. Clayton, A. John, D.A. Jans, T. Ogata, T. Nagai, I. Barroso, A.J. Schafer, and V.R. Harley. 2001. Compound effects of point mutations causing campomelic dysplasia/autosomal sex reversal upon SOX9 structure, nuclear transport, DNA binding, and transcriptional activation. *J Biol Chem.* 276:27864-72.
- Prinz, S., I. Avila-Campillo, C. Aldridge, A. Srinivasan, K. Dimitrov, A.F. Siegel, and T. Galitski. 2004. Control of yeast filamentous-form growth by modules in an integrated molecular network. *Genome Res.* 14:380-90.
- Qin, J., D. Fenyo, Y. Zhao, W.W. Hall, D.M. Chao, C.J. Wilson, R.A. Young, and B.T. Chait. 1997. A strategy for rapid, high-confidence protein identification. *Anal Chem.* 69:3995-4001.
- Quimby, B.B., and M. Dasso. 2003. The small GTPase Ran: interpreting the signs. *Curr Opin Cell Biol.* 15:338-44.

- Radu, A., G. Blobel, and M.S. Moore. 1995. Identification of a protein complex that is required for nuclear protein import and mediates docking of import substrate to distinct nucleoporins. *Proc Natl Acad Sci U S A.* 92:1769-73.
- Rehberg, S., P. Lischka, G. Glaser, T. Stamminger, M. Wegner, and O. Rosorius. 2002. Sox10 is an active nucleocytoplasmic shuttle protein, and shuttling is crucial for Sox10-mediated transactivation. *Mol Cell Biol.* 22:5826-34.
- Reid, B.J., and L.H. Hartwell. 1977. Regulation of mating in the cell cycle of *Saccharomyces cerevisiae*. *J Cell Biol.* 75:355-65.
- Rexach, M., and G. Blobel. 1995. Protein import into nuclei: association and dissociation reactions involving transport substrate, transport factors, and nucleoporins. *Cell.* 83:683-92.
- Ribbeck, K., and D. Gorlich. 2001. Kinetic analysis of translocation through nuclear pore complexes. *Embo J.* 20:1320-30.
- Ribbeck, K., and D. Gorlich. 2002. The permeability barrier of nuclear pore complexes appears to operate via hydrophobic exclusion. *Embo J.* 21:2664-71.
- Ribbeck, K., G. Lipowsky, H.M. Kent, M. Stewart, and D. Gorlich. 1998. NTF2 mediates nuclear import of Ran. *Embo J.* 17:6587-98.
- Robbins, J., S.M. Dilworth, R.A. Laskey, and C. Dingwall. 1991. Two interdependent basic domains in nucleoplasmin nuclear targeting sequence: identification of a class of bipartite nuclear targeting sequence. *Cell.* 64:615-23.
- Roberts, C.J., B. Nelson, M.J. Marton, R. Stoughton, M.R. Meyer, H.A. Bennett, Y.D. He, H. Dai, W.L. Walker, T.R. Hughes, M. Tyers, C. Boone, and S.H. Friend. 2000. Signaling and circuitry of multiple MAPK pathways revealed by a matrix of global gene expression profiles. *Science.* 287:873-80.
- Roberts, R.L., and G.R. Fink. 1994. Elements of a single MAP kinase cascade in *Saccharomyces cerevisiae* mediate two developmental programs in the same cell type: mating and invasive growth. *Genes Dev.* 8:2974-85.
- Rodriguez, J.A., and B.R. Henderson. 2000. Identification of a functional nuclear export sequence in BRCA1. *J Biol Chem.* 275:38589-96.
- Rosenblum, J.S., L.F. Pemberton, N. Bonifaci, and G. Blobel. 1998. Nuclear import and the evolution of a multifunctional RNA-binding protein. *J Cell Biol.* 143:887-99.
- Rothstein, R. 1991. Targeting, disruption, replacement, and allele rescue: integrative DNA transformation in yeast. *Methods Enzymol.* 194:281-301.
- Rout, M.P., and J.D. Aitchison. 2000. Pore relations: nuclear pore complexes and nucleocytoplasmic exchange. *Essays Biochem.* 36:75-88.
- Rout, M.P., and J.D. Aitchison. 2001. The nuclear pore complex as a transport machine. *J Biol Chem.* 29:29.
- Rout, M.P., J.D. Aitchison, M.O. Magnasco, and B.T. Chait. 2003. Virtual gating and nuclear transport: the hole picture. *Trends Cell Biol.* 13:622-8.

- Rout, M.P., J.D. Aitchison, A. Suprapto, K. Hjertaas, Y. Zhao, and B.T. Chait. 2000. The yeast nuclear pore complex: composition, architecture, and transport mechanism. *J Cell Biol.* 148:635-51.
- Rout, M.P., and G. Blobel. 1993. Isolation of the yeast nuclear pore complex. *J Cell Biol.* 123:771-83.
- Rout, M.P., G. Blobel, and J.D. Aitchison. 1997. A distinct nuclear import pathway used by ribosomal proteins. *Cell.* 89:715-25.
- Rout, M.P., and S.R. Wentz. 1994. Pores for thought: nuclear pore complex proteins. *Trends Cell Biol.* 4:357-65.
- Sanger, F., S. Nicklen, and A.R. Coulson. 1977. DNA sequencing with chain-terminating inhibitors. *Proc Natl Acad Sci U S A.* 74:5463-7.
- Scherf, U., I. Pastan, M.C. Willingham, and U. Brinkmann. 1996. The human CAS protein which is homologous to the CSE1 yeast chromosome segregation gene product is associated with microtubules and mitotic spindle. *Proc Natl Acad Sci U S A.* 93:2670-4.
- Schlenstedt, G., E. Smirnova, R. Deane, J. Solsbacher, U. Kutay, D. Gorlich, H. Ponstingl, and F.R. Bischoff. 1997. Yrb4p, a yeast ran-GTP-binding protein involved in import of ribosomal protein L25 into the nucleus. *Embo J.* 16:6237-49.
- Schrick, K., B. Garvik, and L.H. Hartwell. 1997. Mating in *Saccharomyces cerevisiae*: the role of the pheromone signal transduction pathway in the chemotropic response to pheromone. *Genetics.* 147:19-32.
- Schwartz, M.A., and H.D. Madhani. 2004. Principles of map kinase signaling specificity in *Saccharomyces cerevisiae*. *Annu Rev Genet.* 38:725-48.
- Schwoebel, E.D., T.H. Ho, and M.S. Moore. 2002. The mechanism of inhibition of Ran-dependent nuclear transport by cellular ATP depletion. *J Cell Biol.* 157:963-74.
- Seedorf, M., and P.A. Silver. 1997. Importin/karyopherin protein family members required for mRNA export from the nucleus. *Proc Natl Acad Sci U S A.* 94:8590-5.
- Senger, B., G. Simos, F.R. Bischoff, A. Podtelejnikov, M. Mann, and E. Hurt. 1998. Mtr10p functions as a nuclear import receptor for the mRNA-binding protein Npl3p. *Embo J.* 17:2196-207.
- Sherman, M.P., C.M. De Noronha, S.A. Williams, and W.C. Greene. 2002. Insights into the biology of HIV-1 viral protein R. *DNA Cell Biol.* 21:679-88.
- Shulga, N., and D.S. Goldfarb. 2003. Binding dynamics of structural nucleoporins govern nuclear pore complex permeability and may mediate channel gating. *Mol Cell Biol.* 23:534-42.
- Shulga, N., P. Roberts, Z. Gu, L. Spitz, M.M. Tabb, M. Nomura, and D.S. Goldfarb. 1996. In vivo nuclear transport kinetics in *Saccharomyces cerevisiae*: a role for heat shock protein 70 during targeting and translocation. *J Cell Biol.* 135:329-39.

- Sikorski, R.S., and P. Hieter. 1989. A system of shuttle vectors and yeast host strains designed for efficient manipulation of DNA in *Saccharomyces cerevisiae*. *Genetics*. 122:19-27.
- Siomi, H., and G. Dreyfuss. 1995. A nuclear localization domain in the hnRNP A1 protein. *J Cell Biol*. 129:551-60.
- Smillie, D.A., A.J. Llinas, J.T. Ryan, G.D. Kemp, and J. Sommerville. 2004. Nuclear import and activity of histone deacetylase in *Xenopus* oocytes is regulated by phosphorylation. *J Cell Sci*. 117:1857-66.
- Smith, A., A. Brownawell, and I.G. Macara. 1998. Nuclear import of Ran is mediated by the transport factor NTF2. *Curr Biol*. 8:1403-6.
- Smith, A.E., B.M. Slepchenko, J.C. Schaff, L.M. Loew, and I.G. Macara. 2002. Systems analysis of Ran transport. *Science*. 295:488-91.
- Smith, J.M., and P.A. Koopman. 2004. The ins and outs of transcriptional control: nucleocytoplasmic shuttling in development and disease. *Trends Genet*. 20:4-8.
- Smith, W.A., B.T. Schurter, F. Wong-Staal, and M. David. 2004. Arginine methylation of RNA helicase a determines its subcellular localization. *J Biol Chem*. 279:22795-8.
- Snaar, S., K. Wiesmeijer, A.G. Jochemsen, H.J. Tanke, and R.W. Dirks. 2000. Mutational analysis of fibrillarin and its mobility in living human cells. *J Cell Biol*. 151:653-62.
- Sprague, G.F., Jr. 1991. Assay of Yeast Mating Reaction. Academic Press, Inc., San Diego. 77-93 pp.
- Stade, K., C.S. Ford, C. Guthrie, and K. Weis. 1997. Exportin 1 (Crm1p) is an essential nuclear export factor. *Cell*. 90:1041-50.
- Stoffler, D., B. Fahrenkrog, and U. Aebi. 1999. The nuclear pore complex: from molecular architecture to functional dynamics. *Curr Opin Cell Biol*. 11:391-401.
- Strambio-de-Castillia, C., G. Blobel, and M.P. Rout. 1995. Isolation and characterization of nuclear envelopes from the yeast *Saccharomyces*. *J Cell Biol*. 131:19-31.
- Strawn, L.A., T. Shen, N. Shulga, D.S. Goldfarb, and S.R. Wentz. 2004. Minimal nuclear pore complexes define FG repeat domains essential for transport. *Nat Cell Biol*. 6:197-206.
- Strawn, L.A., T. Shen, and S.R. Wentz. 2001. The GLFG regions of Nup116p and Nup100p serve as binding sites for both Kap95p and Mex67p at the nuclear pore complex. *J Biol Chem*. 276:6445-52.
- Strom, A.C., and K. Weis. 2001. Importin-beta-like nuclear transport receptors. *Genome Biol*. 2:3008.
- Suntharalingam, M., and S.R. Wentz. 2003. Peering through the pore: nuclear pore complex structure, assembly, and function. *Dev Cell*. 4:775-89.
- Sydorsky, Y., D.J. Dilworth, E.C. Yi, D.R. Goodlett, R.W. Wozniak, and J.D. Aitchison. 2003. Intersection of the Kap123p-mediated nuclear import and ribosome export pathways. *Mol Cell Biol*. 23:2042-54.

- Talcott, B., and M.S. Moore. 1999. Getting across the nuclear pore complex. *Trends Cell Biol.* 9:312-8.
- Taylor, J., M. Lymboura, P.E. Pace, P. A'Hern R, A.J. Desai, S. Shousha, R.C. Coombes, and S. Ali. 1998. An important role for BRCA1 in breast cancer progression is indicated by its loss in a large proportion of non-familial breast cancers. *Int J Cancer.* 79:334-42.
- Tiganis, T., A.J. Flint, S.A. Adam, and N.K. Tonks. 1997. Association of the T-cell protein tyrosine phosphatase with nuclear import factor p97. *J Biol Chem.* 272:21548-57.
- Tollervey, D., H. Lehtonen, R. Jansen, H. Kern, and E.C. Hurt. 1993. Temperature-sensitive mutations demonstrate roles for yeast fibrillarin in pre-rRNA processing, pre-rRNA methylation, and ribosome assembly. *Cell.* 72:443-57.
- Towbin, H., T. Staehelin, and J. Gordon. 1979. Electrophoretic transfer of proteins from polyacrylamide gels to nitrocellulose sheets: procedure and some applications. *Proc Natl Acad Sci U S A.* 76:4350-4.
- Treisman, R. 1996. Regulation of transcription by MAP kinase cascades. *Curr Opin Cell Biol.* 8:205-15.
- Trueheart, J., J.D. Boeke, and G.R. Fink. 1987. Two genes required for cell fusion during yeast conjugation: evidence for a pheromone-induced surface protein. *Mol Cell Biol.* 7:2316-28.
- Ueta, R., A. Fukunaka, and Y. Yamaguchi-Iwai. 2003. Pse1p mediates the nuclear import of the iron-responsive transcription factor Aft1p in *Saccharomyces cerevisiae*. *J Biol Chem.* 278:50120-7.
- van Deursen, J., J. Boer, L. Kasper, and G. Grosveld. 1996. G2 arrest and impaired nucleocytoplasmic transport in mouse embryos lacking the proto-oncogene CAN/Nup214. *Embo J.* 15:5574-83.
- Vassileva, M.T., and M.J. Matunis. 2004. SUMO modification of heterogeneous nuclear ribonucleoproteins. *Mol Cell Biol.* 24:3623-32.
- Venema, J., and D. Tollervey. 1999. Ribosome synthesis in *Saccharomyces cerevisiae*. *Annu Rev Genet.* 33:261-311.
- Versteeg, I., S. Medjkane, D. Rouillard, and O. Delattre. 2002. A key role of the hSNF5/IN11 tumour suppressor in the control of the G1-S transition of the cell cycle. *Oncogene.* 21:6403-12.
- Warner, J.R. 1999. The economics of ribosome biosynthesis in yeast. *Trends Biochem Sci.* 24:437-40.
- Weis, K. 2003. Regulating access to the genome: nucleocytoplasmic transport throughout the cell cycle. *Cell.* 112:441-51.
- Wellmann, A., P. Flemming, P. Behrens, K. Wuppermann, H. Lang, K. Oldhafer, I. Pastan, and U. Brinkmann. 2001. High expression of the proliferation and apoptosis associated *CSE1L/CAS* gene in hepatitis and liver neoplasms: correlation with tumor progression. *Int J Mol Med.* 7:489-94.
- Whiteway, M., L. Hougan, D. Dignard, L. Bell, G. Saari, F. Grant, P. O'Hara, V.L. MacKay, and D.Y. Thomas. 1988. Function of the STE4 and STE18 genes

- in mating pheromone signal transduction in *Saccharomyces cerevisiae*. *Cold Spring Harb Symp Quant Biol.* 53 Pt 2:585-90.
- Whiteway, M., L. Hougan, D. Dignard, D.Y. Thomas, L. Bell, G.C. Saari, F.J. Grant, P. O'Hara, and V.L. MacKay. 1989. The *STE4* and *STE18* genes of yeast encode potential beta and gamma subunits of the mating factor receptor-coupled G protein. *Cell.* 56:467-77.
- Wozniak, R.W., G. Blobel, and M.P. Rout. 1994. POM152 is an integral protein of the pore membrane domain of the yeast nuclear envelope. *J Cell Biol.* 125:31-42.
- Wu, J., M.J. Matunis, D. Kraemer, G. Blobel, and E. Coutavas. 1995. Nup358, a cytoplasmically exposed nucleoporin with peptide repeats, Ran-GTP binding sites, zinc fingers, a cyclophilin A homologous domain, and a leucine-rich region. *J Biol Chem.* 270:14209-13.
- Wu, X., L.H. Kasper, R.T. Mantcheva, G.T. Mantchev, M.J. Springett, and J.M. van Deursen. 2001. Disruption of the FG nucleoporin NUP98 causes selective changes in nuclear pore complex stoichiometry and function. *Proc Natl Acad Sci U S A.* 98:3191-6.
- Xu, L., and J. Massague. 2004. Nucleocytoplasmic shuttling of signal transducers. *Nat Rev Mol Cell Biol.* 5:209-19.
- Yi, R., Y. Qin, I.G. Macara, and B.R. Cullen. 2003. Exportin-5 mediates the nuclear export of pre-microRNAs and short hairpin RNAs. *Genes Dev.* 17:3011-6.
- Yuan, Y.L., and S. Fields. 1991. Properties of the DNA-binding domain of the *Saccharomyces cerevisiae* STE12 protein. *Mol Cell Biol.* 11:5910-8.
- Zasloff, M. 1983. tRNA transport from the nucleus in a eukaryotic cell: carrier-mediated translocation process. *Proc Natl Acad Sci U S A.* 80:6436-40.
- Zhang, H., H. Saitoh, and M.J. Matunis. 2002. Enzymes of the SUMO modification pathway localize to filaments of the nuclear pore complex. *Mol Cell Biol.* 22:6498-508.
- Zhang, W., and B.T. Chait. 2000. ProFound: an expert system for protein identification using mass spectrometric peptide mapping information. *Anal Chem.* 72:2482-9.
- Zhu, J., and F. McKeon. 1999. NF-AT activation requires suppression of Crm1-dependent export by calcineurin. *Nature.* 398:256-60.